Injection Moulded Short Hemp Fibre Polypropylene Composites

A dissertation submitted by

Amir Etaati

BEng *Amirkabir Uni Tech*
MEng *KN Toosi UTech*

For the award of

DOCTOR OF PHILOSOPHY

2015

ABSTRACT

Natural fibre reinforced polymer composites are attracting the attention of various industrial fields due to both their environmental and economic advantages. Bio-composites, which refer to composites that combine natural fibres with either biodegradable or non-biodegradable, provide numerous benefits. The natural fibres in the bio-composites could be kenaf, jute, hemp or sisal.

Investigations on the use of hemp fibres as reinforcement, to increase polypropylene performance, have introduced many applications for hemp fibre polypropylene composites in automotive and construction industries.

The aim of this project was to utilise cheap waste hemp fibres (noil) to produce short fibre polypropylene composites and to carry out detailed investigations into the various parameters that contribute to composite performance characteristics.

The microstructural, chemical and tensile characterizations of noil hemp fibre and normal hemp fibres were first studied using scanning electron microscopy (SEM), fourier transform infrared analysis (FTIR) and Dynamic Mechanical Analyser (DMA). Noil hemp fibre reinforced polypropylene composite samples with different noil fibre contents (10-60 wt%) were fabricated using an intermixer/extrusion and injection moulding machines. Maleic anhydride grafted polypropylene (MAPP) and maleic anhydride grafted polyethylene octane (MAPOE) were used as coupling agents for modifying the matrices.

X-ray micro-tomography, image analysis and Weibull statistical methods were employed to characterise the size distributions of noil hemp fibres in the

polypropylene matrices. X-ray micro-tomography provided direct observations and accurate measurements of length and width of noil hemp fibres within the hemp-polypropylene composites. The effects of the weight content of the noil hemp fibre and the addition of compatibilisers on the fibre breakage, due to the manufacturing process of the composites, were studied using X-ray micro-tomography in this project.

Tensile, impact and flexural tests were carried out to study the mechanical properties of samples. Free vibration testing and dynamic mechanical analysis methods were also used to study the damping and thermo mechanical properties of the composites. Furthermore, the influence of fibre content and compatibiliser addition on interfacial shear strengths (IFSS) was evaluated by means of the modified Bowyer and Bader model. Finally, the influence of the type and initial length of the hemp fibre (0.2, 0.5, 1 and 2 mm) on mechanical properties of the composites was studied.

The results indicated that the tensile strength of the noil hemp fibre reinforced composites without the coupling agents was lower than that of pure polypropylene. High noil hemp fibre content caused more fibre breakage due to the fibre-fibre interaction mechanism.

The addition of coupling agents improved the tensile strength of the composites by the enhanced fibre/matrix interfacial adhesion. This was confirmed by SEM observations. It was also shown that the addition of MAPP reduced the fibre breakage due to the better dispersion of fibres.

DMA revealed no noticeable changes in the α-transition temperature when the fibre content increased or coupling agents were added. The composites revealed better temperature resistance at higher fibre content. However, the increase in storage

modulus was negligible in composites reinforced with more than 40 wt% hemp fibres due to the agglomeration of the fibres. The results of the damping ratio analysis revealed that higher interfacial bonding was achieved by the addition of MAPP coupling agent in comparison with the addition of MAPOE coupling agent. The storage modulus of the composites increased with the increase in hemp fibre content. However, the maximum damping ratio was obtained from the composite with 30 wt% noil hemp fibre. The addition of coupling agents reduced the damping capacity of all composites. However, 30 wt% noil hemp fibre reinforced polypropylene coupled with 2.5 wt% MAPOE revealed the highest damping ratio among coupled composites.

Finally, the noil hemp fibre composites indicated slightly lower tensile properties than the alkali-treated ones. However, the difference was not significant. The analysis of the tensile, flexural and impact results indicated the optimum initial fibre length of 0.2 mm produced the ideal composites due to better dispersion of fibres (powders). This test methodology can be extended to different types of natural fibres.

CERTIFICATION OF DISSERTATION

I certify that the ideas, experimental work, results, analysis and conclusions reported in this dissertation are entirely my own effort, except where otherwise acknowledged. I also certify that the work is original and has not been previously submitted for any award, except where otherwise acknowledged.

---------- / / ---------- / /

Signature of Candidate Date

Endorsed:

---------- / / ---------- / /

Signature of Principal Supervisor Date

---------- / / ---------- / /

Signature of Associate supervisor Date

ACKNOWLEDGMENTS

In the first place, I wish to thank my principle supervisor Professor Hao Wang, leader of the Biomass Composites Program at Centre for Excellence in Engineered Fibre Composites (CEEFC), USQ. I appreciate all his contributions of time and ideas to put together my PhD experience productive and motivating. He has supported me not only by providing a research assistantship over almost three years, but also academically and emotionally through the rough journey from the day I applied for getting admission at USQ to the day I finished this PhD thesis. He helped me come up with the thesis topic; provided me with instruments, facilities I needed to do the experiments and then he gave me the moral support and the autonomy I needed to move on.

I am grateful to A/Prof. Selvan Pather, whom I worked with as my associate supervisor, for his constructive comments and suggestions during tough times in the PhD pursuit. He always has been a source of good advice and collaboration. A/Prof. Pather guided me in the journey of technical papers writing.

Couple of other people have helped, contributed and taught me immensely in my personal and professional time at University of Southern Queensland (USQ). A special acknowledgement goes to Dr. Fransisco Cardona for his help and training of various laboratory instruments throughout.

Furthermore, I really praise Mr. Wayne Crowell who has been supportive in performing the mechanical experiments of the projects. I also would like to thank Dr. Zili Yan for sharing some of his profound expert knowledge with me.

I wish to thank Dr. Ahmad Sharifian-Barforoush who has been an inspiration on how to act perfectly as well as Peter Penfold for his amazing support all this time. They gave me the precious opportunities to teach some courses and workshops at USQ.

A special group that deserves its own part is PARTEC Institute and the Composites Training Centre. Thanks to the director, Mr. Roger Cater and the staff of the PARTEC especially Mr. Paddy O'Sullivan and Mr. Keith Chairman, those who helped with the injection moulding and producing essential relevant samples in the project. Also, thanks to Dr. Michael Heitzmann and Ms Angelica Legras at University of Queensland (UQ) who have helped me fabricating some extruded pellets using their lab-scale extrusion machine.

Besides, I wish to acknowledge all staff of Adelaide Microscopy centre at University of Adelaide and JKMRC at the University of Queensland where I carried out the x-ray micro-tomography analysis. The studies discussed in this dissertation would not have been possible without the precious help of Adelaide Microscopy staff especially Ms Ruth Williams.

Also, I would like to thank Mr. Joshua Peauril at SKJ International Company for proof reading of the dissertation. He improved the language of this thesis by correcting spelling and grammatical errors.

The last but not the least, I would like to thank my family for all their cares and encouragements all through my life. It was my parents who propped me up to further my education to PhD. Moreover, the supportive presence of my wife here during the most critical stages of this PhD pursuit is highly appreciated.

PUBLICATIONS

Journal Papers:

Etaati, A., Rahman, M., Wang, H (2015). Ground hemp fibres as filler/Reinforcement for thermoplastic biocomposites, Advances in Materials Science and Engineering, Article ID 513590, 11 pages, 2015. doi:10.1155/2015/513590

Etaati, A., Pather, S., Cardona, F., Wang, H (2014). Injection Moulded noil Hemp Fibre Composites: Interfacial Shear Strength, Fibre Strength And Aspect Ratio. Polymer Composites, published online, DOI: 10.1002/pc.23172

Etaati, A., Pather, S., Fang, Z., Wang, H. (2014). The Study Of Fibre/Matrix Bond Strength In Short Hemp Polypropylene Composites From Dynamic Mechanical Analysis. Composites Part B: Engineering, 62, 19–28

Etaati, A., Abdanan Mehdizadeh, S., Wang, H., Pather, S. (2014). Vibration damping characteristics of short hemp fibre thermoplastic composites. Journal of Reinforced Plastics and Composites, 33, 330–341

Etaati, A., Wang, H., Pather, S., Yan, Z., Abdanan Mehdizadeh, S. (2013). 3D X-Ray Microtomography Study On Fibre Breakage In noil Hemp Fibre Reinforced Polypropylene Composites. Composites Part B: Engineering, 50, 239–246.

Refereed Conferences:

Etaati, A., Wang, H. (2014). Influence Of The Type And Initial Length Of Hemp Fibre On Tensile Properties Of Short Hemp Fibre Polypropylene Bio-Composites. ACCM-9: 9th Asian-Australasian Conference on Composite Materials. 15-17 October, Suzhou, China

Etaati, A., Selvan, P., Hao W. (2014), Performance Of Short noil Hemp Fibre Polypropylene Composites. ACMSM23: 23rd Australasian Conference on the Mechanics of Structures and Materials, 9-12 December, Byron Bay, Australia

TABLE OF CONTENTS

LIST OF FIGURES

LIST OF TABLES

Symbols

D	Average fibre diameter
E	Young's modulus
E"	Loss modulus
E′	Storage modulus
E_a	Absorbed energy
E_C	Young's modulus of the composite
E_f	Young's modulus of the fibre
E_g'	Storage modulus in the glassy region
E_i	Impact energy
E_m	Maximum impact energy
E_r	Rebounded energy
E_r'	Storage modulus in the rubbery region
F_m	Impact force
L_c	Critical fibre length
l_i	Sub-critical fibre length
l_j	Super-critical fibre length
L_ε	Critical fibre length
R^2	Correlation factor
S_c	Critical fibre aspect ratio
tan δ	Loss factor
V_f	Volume fraction of fibre
V_i	Volume fractions of the sub-critical fibre
V_j	Volume fractions of the super-critical fibre
V_m	Volume fraction of matrix
W_f	Fibre weight fraction
α	Shape parameter
β	Scale parameter
ε_c	Strain at failure of the composite
ε_f	Strain at failure of the fibre
εm	Strain at failure of the matrix
η	Fibre orientations factor
ρ_f	Fibre density
ρ_m	Matrix density
σ_c	Composite strength

σ_f	Fibre strength
σ_m	Tensile strength of matrix
τ	Interfacial shear strength
ζ	damping ratio

Abbreviations

CDF	Cumulative distribution functions
CMC	Ceramic Matrix Composites
DD	Damage degree
DMA	Dynamic Mechanical Analysis
DSC	Differential Scanning Calorimetry
EIHA	European Industrial Hemp Association
FFT	Fast Fourier transformation
FRP	Fibre reinforced polymer
FTIR	Fourier Transform Infrared Analysis
GFRP	Glass fibre reinforced plastics
GPa	Gigapascal
HDPE	High-density polyethylene
IFSS	Interfacial shear strength
LDPE	Low-density polyethylene
MA	Maleic anhydride
MAPOE	Maleic anhydride grafted Poly (ethylene octane)
MAPP	Maleic anhydride grafted polypropylene
MFA	Microfibrils angle
MFD	Mould flow direction
MMC	Metal Matrix Composites
MPa	Megapascal
NFRC	Natural fibre reinforced composites
PDF	Probability density functions
PMC	Polymer Matrix Composites
PP	Polypropylene
PVC	Polyvinyl chloride
ROM	Rule of mixtures
rpm	Revolutions per minute
SEM	Scanning Electron Microscopy
TGA	Thermogravimetric Analysis

wt%	Weight percentage

1. Introduction

1.1 Background

Composites date back to prehistoric times. Chopped straws were used to reinforce clay for construction of buildings in many parts of Persia. Early Mongolians also used a combination of bullock tendon, horn, bamboo strips, silk and pine resin to make and strengthen archery bows. Although composites have been used in numerous forms throughout the history of human kind, modern composites are considered as the most promising and dominant emerging materials in transportation, aerospace, military, sport, medical and other related industries since the 1950's.

The matrix is used to classify composites into three groups: Metal Matrix Composites (MMC), Ceramic Matrix Composites (CMC) and Polymer Matrix Composites (PMC). The most commonly used matrix material is polymers. The strength and stiffness of polymer composites are lower than metal and ceramic composites. A major advantage is that the processing of polymer matrix composites does not need high temperatures and the equipment required for the manufacture of polymer matrix composites is simpler. The reinforcing effects of other materials can overcome the low mechanical properties of the polymer matrix.

A specific type of two-component composites, consisting of high strength fibres embedded in a polymer matrix, is called fibre reinforced polymers (FRP) (Panigrahy et al., 2006). The conventional reinforcements in fibre reinforced polymer composites are mostly synthetic fibres. The most common fibres being used for fabricating high performance FRP are carbon and aramid. Carbon and aramid fibres are very stiff and

lightweight, but expensive. Hence, they are only used for specific applications where exceptional strength, high stiffness and low density are required.

A cheaper alternative reinforcement for use in general applications is glass fibres. Considerable attention has been given to glass fibre reinforced polymers (GFRP) in construction, automotive and aerospace industries due to their high specific strength, fairly high specific stiffness, corrosion and fatigue resistance, ease of handling and ease of fabrication.

On the other hand, there are serious issues regarding the use of glass fibres. Glass fibres tend to be abrasive, which makes them hazardous for workers as well as for equipment and machinery. Moreover, fossil fuel provide the energy for fabrication of glass fibres. Glass fibre fabrication releases large amounts of CO_2, which is believed to be the main cause of the greenhouse effect and climatic changes. Natural fibres are CO_2-neutral because they absorb carbon dioxide when they grow. Also, natural fibres require much less energy to produce and they can be incinerated at the end of their lifecycle for energy recovery (Wambua et al., 2003).

One of the main applications of fibre composites is in the automotive industry. The automotive industry has utilised glass fibre plastic composites in order to reduce the weight of their vehicles and thus increase vehicle's fuel efficiency. In July 2002, the European Union Council of Ministers approved the EU end-of-life vehicle directive. The directive states that from 2015, all new vehicles should be 85 wt% reusable and recyclable, 10 wt% can be used for energy recovery and only 5 wt% can be disposed of in landfills (Karus and Kaup, 2002). Hence, most major European vehicle

manufacturers are now utilising natural fibre based composite components such as seat backs, door panels, door inserts, parcel trays, etc.

Therefore, there is an increasing demand for environmentally friendly natural fibres to replace the existing synthetic fibres as reinforcement in various applications in automotive industry. As a result of such attempts, bio-composites have been developed that combine natural fibres such as kenaf, jute, hemp and sisal with either biodegradable or non-biodegradable polymers (Lee et al., 2009, Mohanty et al., 2002).

1.2 Thesis overview

As aforementioned, there is an increased urgency for developing and commercializing new composites, which are low cost and more environmentally friendly. One of the new research focuses in this field is the combination of natural fibres with thermoplastics. Hemp fibre reinforced polypropylene composite studied in this project. Hemp, unlike other types of bast fibres, has been chosen in this project because it is a renewable source that can be cultivated in many different countries and climatic environments, especially in Australia. Hemp appears to be more free of pests than other crops. It grows very fast (needs only 100 days to be 4 meters tall and be ready for processing) and is itself a great soil improver. It is biodegradable, sustainable and it has a high specific tensile strength (Roulson et al., 2006, Shubhra et al., 2010, Ku et al., 2011). Thus, hemp fibres are a promising alternative for glass fibres in many composite applications especially in the automotive industries. In addition, the outcomes from this project would be valuable for applications of other types of natural fibres that have similar chemical compositions and properties to hemp fibre. Polypropylene has been selected as the thermoplastic matrix in this project since

it has the lowest density among the thermoplastic polymers and water absorption along with acceptable tensile strength, low cost and a reliable market.

Compression moulding currently is a common processing method in the manufacturing of natural fibre composites, which is used mainly in the automotive sector (Vogt, 2010). The major disadvantage of this process is that it cannot fabricate complex shapes. However, the process of injection moulding can produce high quality complex parts, which is evident from the mass production of plastic parts with complex shapes used in the construction, furniture, appliance and automotive industries. As a method for composite manufacture, the long natural fibres need to be chopped to produce injection-moulded parts. Noil hemp fibres, which are by-products of hemp fibres used in the textile industry, are 80% cheaper and originally short fibres and hence are more economical to be used for extrusion or injection moulding.

The main objectives of the current project were:

- To reinforce polypropylene with the waste of hemp fibres (noil) from textile industries and to investigate the effects of fibre content, addition of compatibilisers and its content on the mechanical properties of injection moulded noil hemp fibre reinforced polypropylene composites.
- To compare characteristics of normal hemp and noil hemp fibres to determine whether noil fibres require further chemical treatment or not.
- To provide the microstructure-tensile property relationships for Noil hemp fibre reinforced polypropylene composites.

- Using available micro-mechanical models, predict the tensile properties of the final composite based on the aspect ratio.
- To improve the fibre-matrix interfacial bonding, thermal and mechanical properties of the composites.

Thesis Outline

This thesis is composed of nine chapters.

Chapter 1 introduces natural fibre composites, project objectives and outlines.

Chapter 2 delivers a literature review of the most related topics about natural fibres, polymers and natural fibre composites. This chapter also includes a market study and challenges facing the production and development of natural fibre composites.

Chapter 3 states all raw materials and experimental methods used in the conduct of this research. It details the type of fibres, matrices and compatibilisers used, the composite preparation and fabrication methods utilised, and characterization methods and testing procedures performed for analysing of either fibres or composites.

Chapter 4 investigates the chemical, thermal, morphological and mechanical properties of the normal and noil hemp fibres.

Chapter 5 covers the microstructure of the noil hemp fibre reinforced composites; focusing on the fibre breakage and fibre agglomerations.

Chapter 6 studies the mechanical and thermo mechanical performance of the noil hemp fibre composites including tensile properties, vibration/damping characteristics and dynamic mechanical performances.

Chapter 7 uses the normal (not waste) and noil hemp fibres to fabricate sample composites. Instead of short fibres, ground fibres were used to make the composites, and the influences of initial length (0.2, 0.5, 1, and 2 mm) on tensile, flexural and impact properties of the composites were studied.

Chapter 8 concludes this research thesis by presenting a comprehensive conclusion, and future work to continue the further development of this research.

2. Literature Review

2.1 Natural Fibres

2.1.1 Classification

Natural fibres can be classified as plant and animal based fibres. Animal-based fibres include wool, hair and silk. Plant based natural fibres may be classified in two broad categories of non-wood and wood fibres. The examples of wood fibres are soft and hard woods. Non-wood fibres include seed (cotton), bast (flax, hemp, jute and kenaf), leaf (sisal, abaca) and fruit (coir). Among these, the bast fibres (hemp, flax) are the most promising candidates for the replacement of glass fibres as the reinforcement in composites due to their high tensile strength and Young's modulus (Shubhra et al., 2010, Koronis et al., 2013). Compared to those of other natural fibres, this difference could be attributed to the different morphological characteristics of the bast fibres.

2.1.2 Morphology of Bast Fibres

The stems of plants where bast fibres include pith, xylem (core), cambium, phloem, cortex and the epidermis, from the inside to the outside (Figure 2.1). The phloem is the layer that contains the bast fibre bundles. These bundles form a ring in the outer part of the stem, with the fibre cells joined through the middle lamella. The xylem layer, occupying two third of the stem volume, provides stiffness to the hemp stem. While the phloem gives tensile and flexural strength, accounts for the other one third of the volume. The responsibility of the thin epidermis layer is to protect the stem from parasites.

The bast fibres in the phloem can be categorised into two fibre cell types: primary and secondary fibre cells. Primary fibre cells are long with compact cell walls and small lumen. The secondary fibre cells are much thinner, shorter and with higher lignin content (Garcia-Jaldon et al., 1998, Vignon and Garciajaldon, 1994).

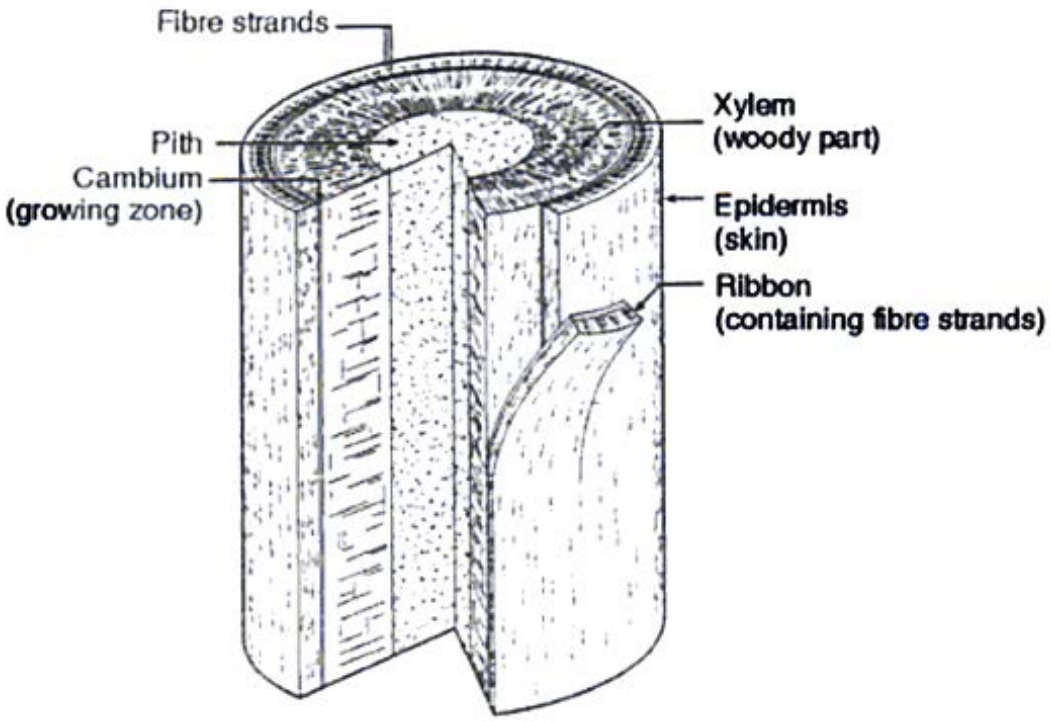

Figure 2.1: Diagram of the anatomy of a bast fibre (Jarman, 1998).

It should be noted that only primary fibres are valued for their strength and length, while the secondary fibres are believed to cause undesired coarseness and inhomogeneity. The primary hemp fibre is well known for its high tensile strength and stiffness and its application as reinforcement in composites. However, several researchers recently studied the potential and capability of core (xylem) for reinforcing polymers (Lips et al., 2009, Mutje et al., 2007).

Figure 2.2a illustrates the schematic structure of a natural fibre from stem to micro fibril. Figure 2.2b shows that the fibre bundles are in the cortex as a ring in the phloem parenchyma (Nykter et al., 2008). The middle lamella links fibre cells together. The cell wall forms most of the fibre diameter and it is divided into the thin primary cell wall and the secondary cell wall. The walls consist of several layers of fibrils that are linked together by lignin. Hemicelluloses, on the other hand, is responsible to link micro fibrils together in the secondary wall. The secondary wall can be sub-divided into S1, S2and S3- which differ in the orientation, or direction, of the cellulose microfibrils

2.1.3 Chemical Composition of Natural Fibres

Chemical composition of natural fibres differs depending on the type and species of the fibre itself and the environmental and climate conditions under which the fibre is grown. However, they have similar compositions, as seen in Table 2.1, The plant fibres consist of mainly four constituents as below:

2.1.3.1 Cellulose

Cellulose is a linear polymer of D-glucose molecules (poly [β-1, 4-D-anhydroglucopyranose], ($C_{6n}H_{10n}+2O_{5n+1}$), in which two adjacent glucose units are linked by elimination of one water molecule between their hydroxyl groups at carbon atoms 1 and 4. Figure 2.3 illustrates that the hydrogen bonds can be formed either within its own chain (intra-molecular) or with neighbouring chains (inter-molecular). The hydrogen bonding forms the linear crystalline structure and provides strength and rigidity to cellulosic materials.

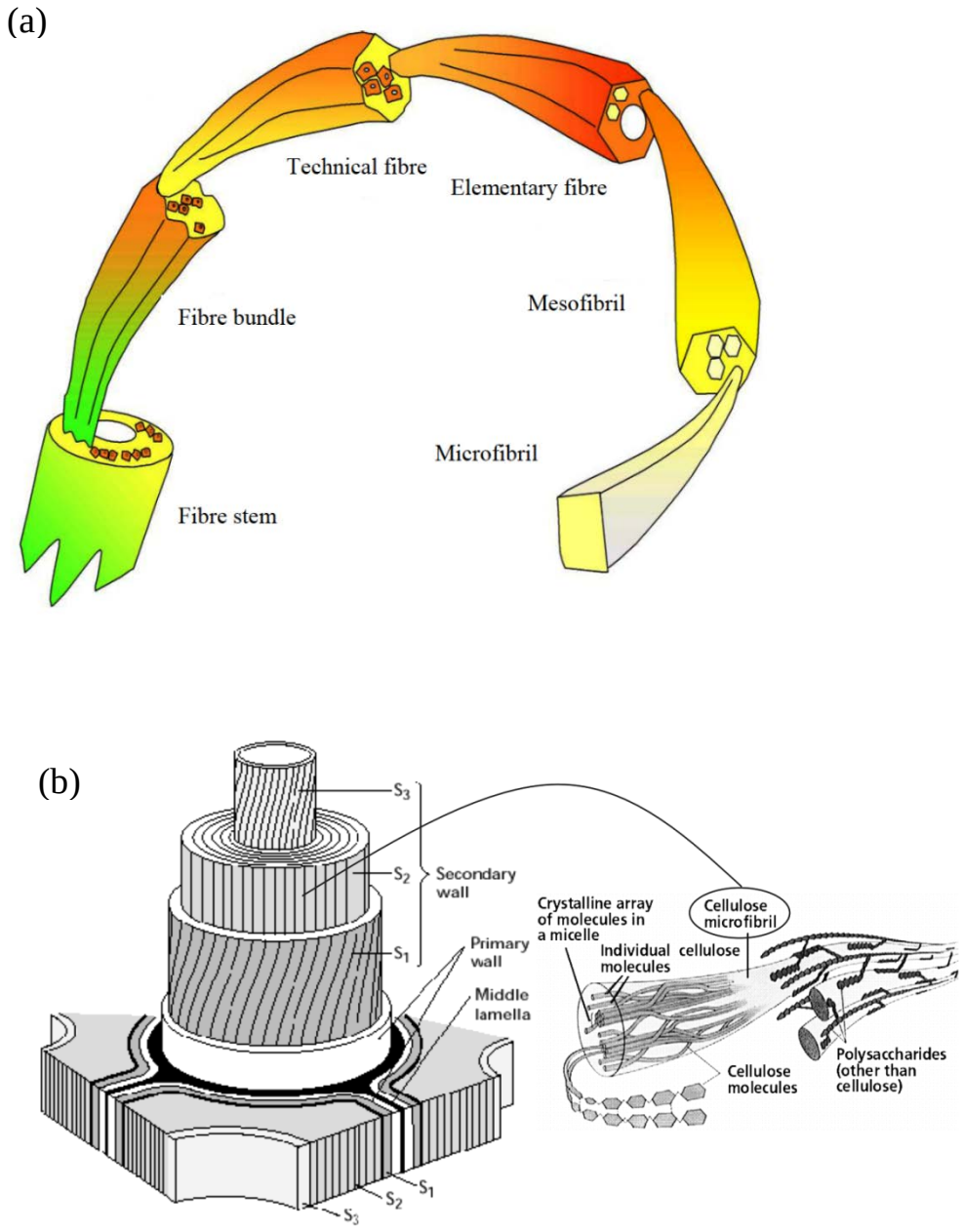

Figure 2.2: (a) Schematic representation of a natural fibre from stem to micro fibril (Kasuga et al., 2001), (b) Schematic representation of the elementary fibre (Kontturi, 2005).

Table 2.1: Chemical composition and microfibrillar angle of several cellulosic fibres (Sedan et al., 2007, Panigrahy, 2006, Ku et al., 2011, Malkapuram et al., 2009)

Fibre	Cellulose (Wt%)	Hemicellulose (Wt%)	Lignin (Wt%)	Pectin (Wt%)	Wax (Wt%)	Microfibrillar angle
Hemp	70.2-74.1	17.9-22.4	3.7-5.7	0.9	0.8	
Flax	71	18.6-20.6	2.2	2.3	1.7	10˚
Jute	61-71.5	13.6-20.4	12-13	0.4	0.5	
Ramie	68.6-76.2	13.1-16.7	0.6-0.7	1.9	0.3	
Sisal	67-78	10-14.2	8-11	10	2	20˚
Kenaf	31-39	21.5	15-19	-	-	
Cotton	82.7	5.7	-	-	0.6	
PALF	70-82	50-12	-	-	-	14˚
Henequen	77.6	4-8	13.1	-	-	
Coir	36-43	10-20	41-45	3-4	-	41˚-45 ˚

The degree of polymerisation (n or DP) is defined as the number of glucose units in the chain. The degree of polymerisation is around 4400 in cotton, 2100 in pine pulp and 7000 in modified raw hemp fibres (Thygesen et al., 2005, Evans et al., 1989).

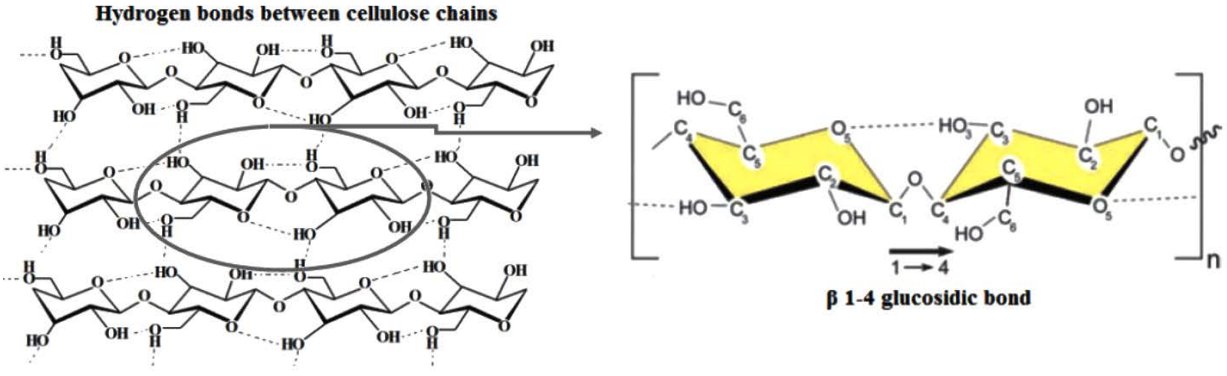

Figure 2.3: Schematic cellulose structure, representing that the β1-4 glucosidic bond and the intrachain hydrogen bonding and hydrogen bonds are formed within its own chain and also with neighbouring chains (Poletto et al., 2013).

A lack of adequate inter-molecular hydrogen bonding (amorphous cellulose structure), introduces accessible hydroxyl groups for bonding with water molecules. Thus, it is more hydrophilic compared with crystalline cellulose. It is reported that most plant-derived cellulose has 80% crystalline structure although crystallinity may be increased by rearrangement of amorphous cellulose chains by chemical treatments (Thygesen et al., 2005, Evans et al., 1989).

It is worth mentioning that the crystal structure of the formed cellulose is called cellulose Iβ that technically is a centre-based monoclinic unit cell as shown in Figure 2.4.

2.1.3.2 Hemicellulose

An elementary natural fibre itself can be considered as a composite, i.e. a network of ultrafine cellulose fibrils embedded in a matrix of hemicelluloses and lignin. The hemicellulose consists of a collection of polysaccharides. Unlike cellulose, hemicellulose contains many different sugar monomers such as xylose, mannose, galactose, rhamnose and arabinose and, in comparison with cellulose, the degree of polymerisation is much lower (20 - 300).

Hemicellulose is deposited as the amorphous and none-oriented cell-wall constituent, which occupy spaces between the fibrils in both primary and secondary walls. They are primarily hydrogen-bonded to cellulose. Because of this linkage, hemicellulose degradation leads to a separation of fibre bundles into cellulose micro fibrils

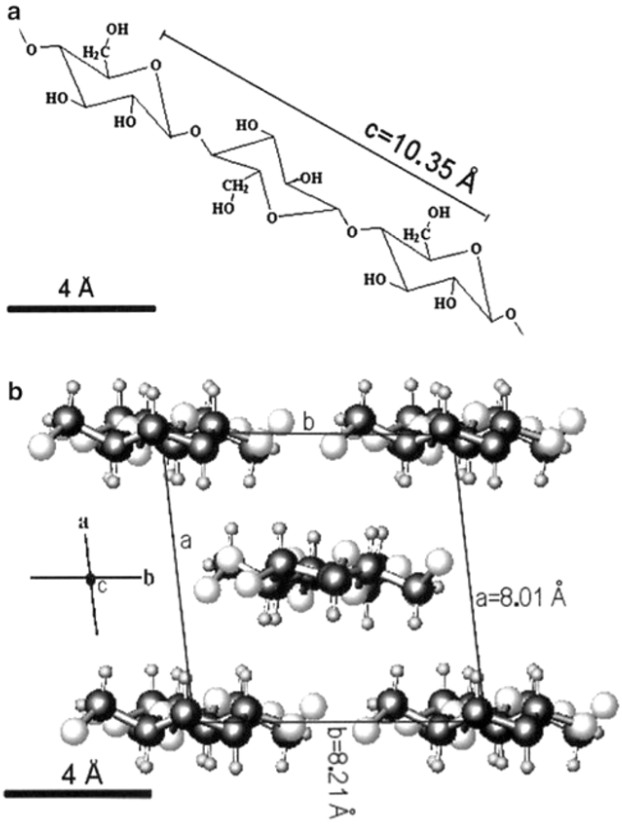

Figure 2.4: (a) Cellulose unit cell in c-axis, (b) cellulose Iβ structure showing unit cell in a-axis and b-axis (Thygesen et al., 2005).

2.1.3.3 Lignin

Lignin is a three-dimensional amorphous natural polymer composed of phenyl propane units with carbonyl, hydroxyl and methoxyl substitutions. Lignin acts as a stabiliser against mechanical, biochemical and environmental stresses and gives compression strength to plants by gluing the fibres together (Gregorová et al., 2006).

Cellulose is the main constituent of wood, responsible for its firm structure and lignin is the glue, which binds the wood cells together and, together with hemicelluloses, controls the water content within the cell wall. Lignin is distributed in primary, secondary walls and the middle lamella. Thus, degradation of lignin in the middle

lamella leads to fibre separation while degradation of those in cell walls reduces fibre tensile strength slightly (Gibson, 2012, Credou and Berthelot, 2014).

2.1.4 Properties of Natural Fibres

Mechanical, chemical and physical properties of natural fibres are affected by the structure, chemical composition, microfibrillar angle and cell dimension defects of the fibres. Climatic conditions, age and the digestion process of natural fibres influence the chemical composition and subsequently final mechanical properties. Microfibrillar angle of the cellulosic fibres are defined as the angle between the axis and the microfibril of the fibre. The smaller angle, the higher mechanical properties and the higher ductility of the fibres (Malkapuram et al., 2009). Table 2.2 shows mechanical properties of different types of natural fibres.

Table 2.2: Mechanical properties of several cellulosic fibres (Sedan et al., 2007, Panigrahy, 2006, Ku et al., 2011, Malkapuram et al., 2009, Koronis et al., 2013)

Fibre	Density (g/cm^3)	Tensile strength (MPa)	Young's modulus (GPa)	Elongation at Break (%)
Hemp	1.47	550–900	38–70	1.6–4
Flax	1.5	345-1500	27–39	2.7-3.2
Jute	1.3-1.45	393–800	13-26.5	1.16-1.5
Ramie	1.5–1.6	400-938	61.4-128	1.2-3.8
Sisal	1.45	468–700	9.4–22	3-7
Kenaf	1.5–1.6	350–930	40–53	1.6
Cotton	1.5-1.6	287-800	5.5-12.6	7-8
Coir	1.15	131-175	4-6	15-40

From table 2.2, it can be seen that the strongest fibres are hemp, jute, Ramie and flax. hemp, Ramie and flax having the highest values for Young's modulus. As

reinforcement fibres for composite materials, the most suitable cones are therefore hemp, Ramie flax. unlike others, hemp can be cultivated in many different countries and climatic environments, especially in Australia. Hemp grows very fast and is itself a great soil improver. Hemp has dvantage of being extremely disease and pest resistant. This provides another advantage over other natural fibres where restrictions on herbicide use is prevalent.

2.2 Polymers

A polymer is an organic compound composed of long-chain molecules consisting of smaller repeated units called monomers. The function of the polymer matrix in a composite is responsible to bind the fibres together, to separate and diffuse fibres within the composite, to protect the fibres from abrasion and environmental degradation, and to transfer forces between the individual fibres. The matrix should be chemically and thermally compatible with the fibres (Taj et al., 2007, Panigrahy, 2006). General speaking, polymer matrices have been divided into two categories: Thermosets and Thermoplastics.

2.2.1 Thermosets

The most common thermosets used as matrices for natural fibre composites are epoxy resin, unsaturated polyester and vinyl ester (Aziz et al., 2005, Ataollahi et al., 2012, Yan et al., 2012). Most of the thermosets are in a liquid state at room temperature. This gives the ability to rapidly manufacture products by means of vacuum or positive pressure pump. Thermoseting resins are resistant to solvents and corrosive media, heat and high temperature and fatigue.

In thermoset polymers, molecules are interlinked by covalent bonds and possess a 3D network structure. Thus, thermosets do not soften when they are heated. This makes thermosets impossible or very difficult to recycle (Cervenka, 1999, Panigrahy et al., 2006).

2.2.2 Thermoplastics

Unlike thermosets, thermoplastics do not have a network structure but linear or branched molecular chains which are linked together mainly with van der Waals forces or hydrogen bonding. This is the reason why thermoplastics can be recycled many times with almost no changes in bonding between the chains of the polymer. Since they can be processed many times, these materials are the backbone of the plastics recycling industry (Panigrahy et al., 2006). Table 2.3 presents properties of common thermoplastics.

Table 2.3: Properties of some common thermoplastics (Beadle, 1971, Panigrahy et al., 2006).

Polymer	Density (g/cm^3)	Water Absorption 24 hours (wt%)	Tg (°C)	Tm (°C)	Tensile Strength (MPa)	Elastic Modulus (GPa)	Elongation (%)
PP	0.899–0.920	<0.01	–10 to 0	160–176	26–41.4	0.95–1.77	15–700
LDPE	0.910–0.925	<0.015	–125	105–116	40–78	0.055–0.38	90–800
HDPE	0.94–0.96	0.01–0.2	–133 to –100	120–140	14.5–38	0.4–1.5	2.0–130
PVC	1.49-1.58	0.04-0.4	-	80	51.8-62.1	3-3.3	50-80
Nylon 6	1.12–1.14	1.3–1.8	48	215	56–80	43–79	2.9
Nylon 6,6	1.13-1.15	1.0–1.6	80	250–269	12.4–94	2.5–3.9	35–300
PS	1.04–1.06	0.03–0.10	-	110–135	25–69	4–5	1–2.5

There are some factors that should be considered for the selection of a thermoplastic polymer among all types of thermoplastics. The first criterion that restricts selection

of thermoplastics is thermal degradation of natural fibres. Moreover, water absorption, density and tensile properties of thermoplastics are of great importance for the selection of a thermoplastic polymer.

Unlike synthetic fibres (carbon, glass), the behaviour of plant-based fibres depends strongly on temperature (Davies and Bruce, 1998). Degradation initiates from 170-220˚C depending on the plant types and species (190-220˚C for dry wood, 150-180˚C for hemp and 170˚C for flax). Nevertheless, it was reported that (Davies and Bruce, 1998) flax fibre bundles, which were subjected to this temperature (170˚C) during composite processing, did not show significant effects on their tensile properties if this temperature was maintained for less than 1 hour. However, major damage could occur after an exposure time of four minutes at a temperature above 240˚C.

On the other hand, the temperature of composite processing should be above the melting temperature of polymer matrix. Otherwise, the matrix cannot wet the fibres and fill the mould properly. Thus, referring to Table 2.3, PP, LDPE, HDPE and PVC polymers have potential to be matrices for natural fibres. PVC has high mechanical properties. However, it has the highest density. This restricts its application in weight sensitive applications.

Among thermoplastics, which are suitable to be used as a matrix for natural fibre composites, polypropylene has the lowest density and water absorption along with an acceptable tensile strength, cheap price and a reliable market. This leads PP as the most suitable thermoplastic to be used for the fabrication of natural fibre composites.

It is worth mentioning that PP already has a high global demand in the market. Global Business Intelligence (http://www.gbiresearch.com/) says that global PP demand, from 26.6 million tons in 2000, grew at a Compound Annual Growth Rate (CAGR) of 3.6% until 2009, to 36.5 million tons. The global polypropylene demand is expected to grow at a CAGR of 4.6% from 2009 to 2020, estimated to reach 59.6 million tons in 2020.

Referring to GBI research, global polypropylene demand in 2009 was 36.5 million tons, with the packaging industry holding the largest share at 54% and automotive industry with a share of 15.6%. As mentioned previously, low density of polypropylene makes it suitable for automotive industries since it reduces the weight of the vehicles, improves fuel efficiency, and significantly reduces cost.

2.3 Natural Fibre Reinforced Thermoplastics

Synthetic fibres have been the dominant fibres in composites in all industries for decades. Recently natural fibres are attracting high attention and interest. This is due to natural fibre's low cost, low density, comparable specific tensile properties, non-abrasive to the equipment, non-irritant to the skin and reduction of energy consumption. Besides, they are biodegradable, renewable, commercially viable, and environmentally acceptable, hence sustainable, (Ku et al., 2011, Mohanty et al., 2002)..

2.3.1 Challenges and Issues

In spite of the mentioned positive properties of natural fibres, natural fibre reinforced thermoplastic composites have shown undesirable properties, which include:

2.3.1.1 Poor Interfacial Adhesion

The main components of natural fibres are cellulose, hemicellulose, lignin and pectin. Lignin is much less hydrophilic than pectin, cellulose and hemicellulose, and has the least water absorption of the natural fibre components. They have hydroxyl (OH) groups in their structure, which make them polar and hydrophilic materials while most of the polymers are non-polar and hydrophobic. It has been reported that the main reason of poor interfacial adhesion is attributed to the hydrophilic nature of natural fibres which is incompatible with the hydrophobic thermoplastic matrices. Thus, weak interface bonding occurs due to this incompatibility of the polar hydrophilic fibres and non-polar hydrophobic polymer matrices. This phenomenon leads to poor mechanical properties of a composite material. It should be noted that modification of the surface of the hemp fibres is more critical rather than other natural fibres since it has been found that hemp fibres are more hydrophilic in nature than other plant fibres (Beckermann and Pickering, 2008, Herrera-Franco and Valadez-González, 2005).

2.3.1.2 Defects in Natural Fibres

It is the nature of plant-based fibres to have non-uniform geometry and defects, either kink bands or micro cracks. Kink band defects happen where the microfibril angle of one cell wall differs from the angle of the neighbour cell wall, which results in misalignment of the crystalline orientation. Not only do these defects decrease the strength of the fibres, they also result in property variations.

Moreover, as a result of defects, stress concentration occurs in the matrix when load is applied and retards the mechanical properties of natural fibre reinforced composites (Thygesen et al., 2007).

2.3.1.3 Limited Thermal Stability

Natural fibres include cellulose, hemicellulose, lignin, pectin, waxes and water-soluble substances. These chemicals are not thermally stable. They tend to degrade at relatively low temperatures. Therefore, the thermal degradation of the fibres is a major issue that must be considered when choosing natural fibres as reinforcements for a polymer matrix (Tajvidi and Takemura, 2010, Rachini et al., 2009).

If the mixing temperature of the fibres and the thermoplastic is too low, an acceptable fibre dispersion cannot be achieved. In addition, the mixture may not fill the mould completely. On the other hand, if the temperature is too high, fibre degradation can occur during processing. Hence, an optimum mixing temperature should be selected.

A Thermogravimetric analysis carried out by Ramiah (Ramiah, 1970) under vacuum condition showed that among cellulose, hemicellulose and lignin components, lignin is the most thermally resistant; cellulose intermediate and the hemicellulose is the least stable.

2.3.1.4 Moisture Absorption

A further problem regarding lignocellulosic fibres is that they have a high moisture absorption characteristic, due to their hydrophilic chemical structure. The moisture absorption results in swelling of fibres and dimensional changes in the composite, reduction in the adhesion between the fibre and the matrix, and consequently reduction in the mechanical properties of the composite.

Although a number of efforts have been carried out to address this issue, moisture absorption of composites is still of great concern especially for outdoor applications (Wang et al., 2006, Stark, 2001, Rangaraj and Smith, 2000).

2.3.1.5 Fibre Agglomeration

Another issue associated with the difference between the polarity of thermoplastic matrices and natural fibres is the poor fibre dispersion. The combination of the polar hydrophilic fibres with non-polar hydrophobic matrix results in clumping and agglomeration of fibres, which must be minimised to have a homogenous structure. Fibre agglomeration in the matrix makes the final product very sensitive to micro cracking which subsequently leads to inferior mechanical behaviour. In order to achieve good mechanical properties, it is necessary to have separated fibres and good fibre distribution within the matrix. Insufficient fibre dispersion causes agglomeration of the fibre in the matrix which results in an inhomogeneous microstructure (Rowel et al., 1997).

2.3.2 Fibre and Matrix Modifications

Poor interfacial adhesion, thermal degradability, moisture absorption and fibre agglomeration are commonly associated with the incompatibility of the hydrophilic fibres and the hydrophobic thermoplastics.

The hydrophilic nature of plant-based fibres is due to the presence of hydroxyl groups (OH) in the structure of the fibres. The crystalline cellulose is closely packed and most of its OH positions are inaccessible because they are used for inter-chain bonding of the cellulose. On the other hand, non-cellulosic amorphous constituents

(hemicellulose, pectin and waxes) are highly hydrophilic. Thus, hydrophobicity of natural fibres can be increased by chemically treating the fibres. Chemical treatments can partially or completely remove the non-cellulosic materials. However, other treatment methods using biological (retting), physical (steam explosion (Jacquet et al., 2011), plasma treatment (Morshed et al., 2010, Sinha and Panigrahi, 2009, Luciu et al., 2008) and mechanical (ball milling (Prasad et al., 2005)) have also been studied by various researchers. All these methods aim to remove the cementing non-cellulosic materials and/or increase the roughness of the fibre surface. Removal of cementing materials results in increase of the crystallinity of fibres. Consequently, this improves interfacial bonding of fibres and matrix. The increase in fibre surface roughness also increases interlocking bonds between fibres and the matrix. The two important chemical treatments that were applied in this project are detailed below.

- Alkali Treatment

Alkaline treatment has been found to be one of the best chemical treatments for natural fibre reinforced thermoplastics and thermosets. The Alkalization rule is to disrupt hydrogen bonding in the network structure and subsequently increase surface roughness. It also removes a certain amount of pectin, lignin, hemicellulose and wax from the external surface of the fibre cell wall (Mohanty et al., 2001) .

The type of alkali treatment, such as KOH, LiOH, NaOH and its concentration influence the cellulosic fibril, the degree of polymerisation and the extraction of lignin and hemicellulose compounds (Li et al., 2007). The reaction that takes place during this treatment is shown below:

$$\text{Fibre-OH} + \text{NaOH} \rightarrow \text{Fibre-O-Na} + H_2O \quad (2.1)$$

Thus, the addition of aqueous sodium hydroxide (NaOH) to natural fibre provides the ionisation of the hydroxyl group to the alkoxide (Agrawal et al., 2000).

Jacob et al. (Jacob et al., 2004), investigated the effects of NaOH with different concentrations (0.5, 1, 2, 4 and 10%) for treating sisal fibre reinforced composites and, concluded that the maximum tensile strength resulted from the 4% NaOH treatment at room temperature. In another research work (Mishra et al., 2003), it was reported that 5% NaOH treated sisal fibre reinforced polyester composites had better tensile strength than that of 10% NaOH treated composites due to the fibre damage occurring at higher alkali concentrations.

- Maleation

Maleic anhydride (MA) is an applicable interface modifier to improve composite strength. Maleic anhydride is not only used to modify fibre surface but also the PP matrix to achieve better interfacial bonding and mechanical properties in composites.

During grafting, maleic anhydride reacts with the hydroxyl groups in the amorphous region of fibre and removes them from the fibre. Treatment also produces a brush-like long chain polymer coating on the fibre surface and reduces the hydrophilic tendency. Additionally, the treatment of cellulose fibres with hot MA copolymers provides covalent bonds across the interface. This covalent bonding between the fibre surface and matrix provide balanced properties to make a bridge interface (fibre-matrix) for efficient interlocking (Li et al., 2007, Bledzki et al., 1996). The mechanism of reaction

can be divided into two steps (Figure 2.5); I: The Activation of the copolymer by heating (T = 170˚C) (before fibre treatment) and II: The Esterification of cellulose

It is reported that mechanical properties like Young's modulus, flexural modulus and impact strength of plant fibre reinforced composites increased after maleic anhydride treatment (Beckermann and Pickering, 2009, Beckermann and Pickering, 2008, Mutje et al., 2007, Pickering et al., 2007a).

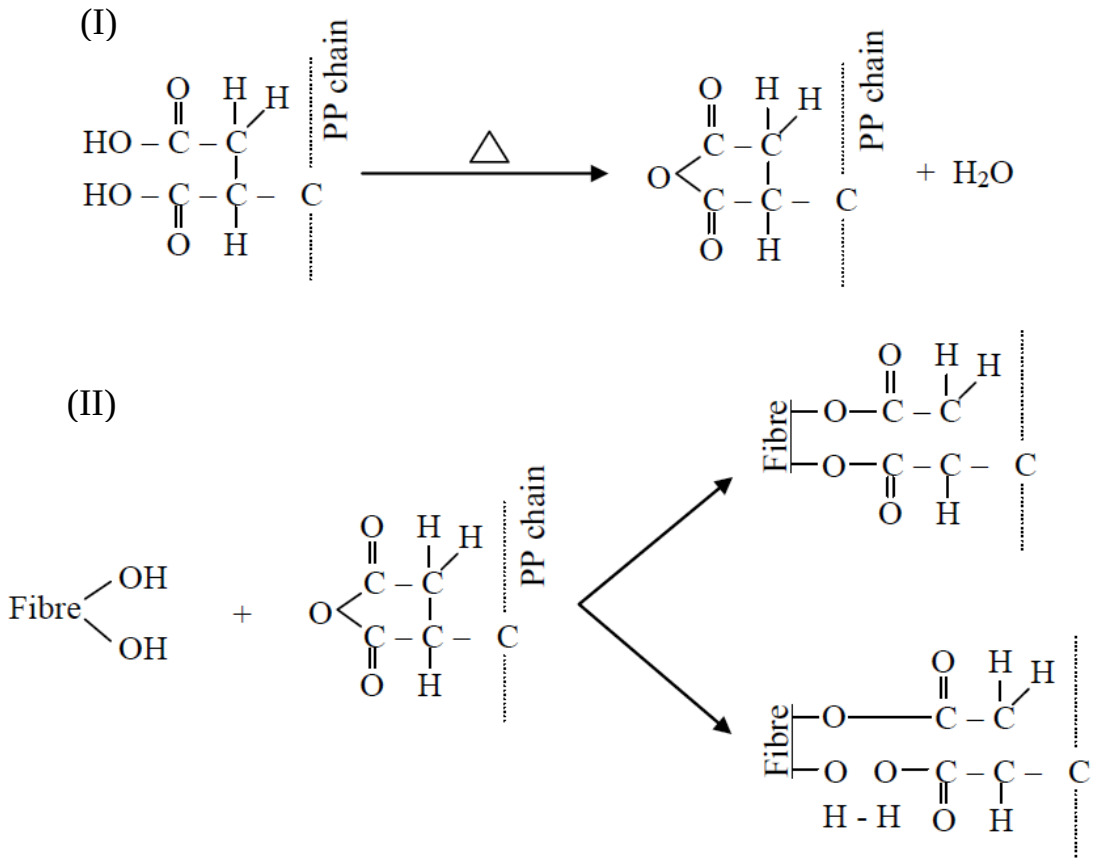

Figure 2.5: The reaction of cellulose fibres with MAPP copolymers (Bledzki et al., 1996).

Beside the aforementioned treatments, a number of other chemical treatments of natural fibre have also been reported such as acetylation, silane, Benzoylation treatment, Acrylation treatment, Peroxide treatment, Isocyanate treatment, Stearic

Acid treatment, Sodium Chlorite etc. The above studies conclude that chemical treatment of natural fibres can improve wetting and bonding between fibre and matrix, resulting in improvement of composite properties (George et al., 2001, Beckermann and Pickering, 2008, Bledzki et al., 1996, Li et al., 2007, Panigrahy et al., 2006, Sawpan et al., 2011).

2.3.3 Processing Methods

Fibre reinforced thermoplastic composites can be produced by a wide variety of methods. Natural fibre reinforced thermoplastic composites can also be manufactured with the same techniques. However, the most commonly used methods for producing natural fibre reinforced thermoplastics are compression and injection moulding techniques. Also, melt mixing, solution mixing and extrusion are common methods to make mixtures (granules) of natural fibres and thermoplastics.

2.3.3.1 Melt Mixing

In melt mixing (internal mixing), the fibres are added to a melt of thermoplastic and mixing is performed using a mixer at a specified temperature, speed and time. The mixture then can be rolled and chopped into granules. (Thomas and Pothan 2009)

2.3.3.2 Solution Mixing

In the solution mixing method, the fibres are added to a viscous solution of thermoplastic in a solvent. The temperature is maintained for some time and the mixture transferred to a flat tray and kept in a vacuum oven to remove the solvent. The solution mixing procedure avoids fibre damage that normally occurs during blending of fibre and thermoplastic by melt mixing (Thomas and Pothan 2009).

2.3.3.3 Extrusion

Extrusion is the most fundamental and most widely used unit operation in melt processing. An extruder is a device that pressurises a melt in order to force it through a shaping die or some other units. The polymer (flakes, chips, or pellets) and short fibres are fed in a single screw or two rotating screws where melting and mixing take place. Then, it is conveyed forward by the screw, becoming molten by the time it reaches the metering section. Pressure builds up in the flow direction until the end of the screw, where the compound is forced through a shaping die. Twin screws are very effective mixing devices and they are commonly used for compounding blends and composites (Denn, 2008).

2.3.3.4 Compression Moulding

Compression moulding can be used for both thermoplastic and thermoset polymers. In the case of thermoplastic polymers, first, granules or aligned fibre mats along with thermoplastic sheets are placed into the bottom half of a preheated mould cavity. Then the top half of the mould is lowered at a constant rate until melting of the thermoplastic matrix and consolidation of the composite occur. At the end of the process, the composite is cooled down and removed from the mould (Denn, 2008).

2.3.3.5 Injection Moulding

Injection moulding is the technique suitable for manufacturing of short-fibre reinforced thermoplastics. Short fibres with thermoplastic can be a granulated mixture or a physical mixture. The mixture is fed into the hopper and transferred into the heated barrel (Figure 2.6). The material softens by the heat transfer from the barrel wall. At the same time, the screw rotates to apply high-shear stress to provide further

heat and to fill the barrel. The molten material is collected in front of the screw by the rotation of the screw and then injected with a high pressure into the mould cavity through the runner and the gate. The mould is then cooled below the solidification temperature of the thermoplastic.

During injection moulding, extensive fibre damage occurs due to the intensive mixing with high-shear and passage through a narrow gate. Therefore, injection moulding is only suitable for short fibres. The important processing parameters are time, temperature, pressure and flow rate. These variables have different values at different points in the process and depend on the thermoplastic, fibre types, fibre length and fibre concentration and etc. (Thomason, 2002, Fara and Pavan, 2004).

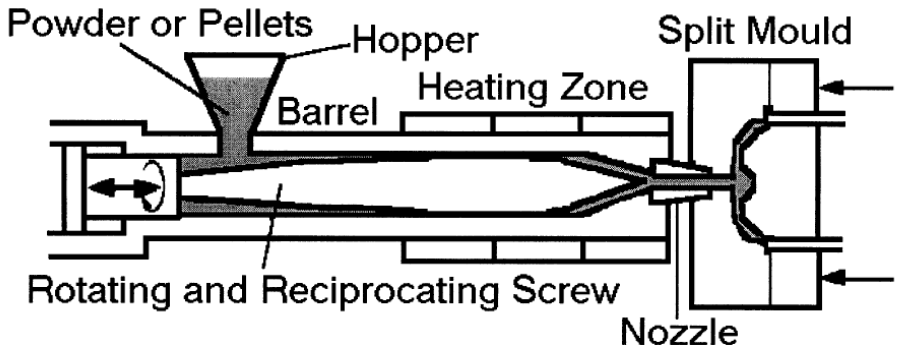

Figure 2.6: Schematic of injection moulding machine(Bull et al., 2000).

2.4 Performance of the Natural Fibre Composites

The performance of a composite material is determined by its properties and behaviour under tensile, flexural, compressive, shear and other static or dynamic loading conditions. Composites properties can be evaluated by conducting standard mechanical and physical tests under monitored laboratory conditions.

There are several parameters that can affect the performance of natural fibre reinforced composites. Apart from the individual properties of the constituents (fibre and matrix), the performance of the natural fibre reinforced composites can also be influenced by fibre/filler content, fibre/matrix interfacial interaction. Another important factor that significantly influences the properties of the natural fibre composites is the processing and manufacturing parameters used in composites production. Appropriate processing techniques must be selected to achieve the optimum composite performances. All these parameters can affect the tensile, flexural, impact, damping and vibration properties of the composites.

In this section, the performance of natural fibre reinforced polymer composites was briefly reviewed with an emphasis on the impacts of above mentioned parameters in their properties and behaviour.

2.4.1 Tensile Properties

Tensile properties of a material are the basic design data in most of engineering applications. In general, the tensile properties of a polymer are significantly enhanced by the addition of fibres to a polymer matrix as fibres have much higher strength and stiffness values than those of the matrices (Ku et al., 2011). Many researchers (Facca et al., 2006, Hargitai et al., 2008, X Li et al., 2006) have reported that the values of the tensile strength of natural fibre reinforced composites increased with fibre content up to a peak value where it then decreased. On the other hand, the Young's Moduli of fibre reinforced composites were observed to have increased gradually with increasing fibre content. In addition, a higher fibre/matrix interfacial adhesion can improve the tensile strengths of the composites. Various chemical modifications such

as fibre treatments, coupling agents and graft co-polymerization have been used to improve the tensile properties of the composites (Kabir et al., 2012b, Lee et al., 2009, Panigrahy et al., 2006, Li et al., 2007).

Another critical factor that significantly influences the tensile properties of the composites is the processing parameters such as barrel temperature, mixing time and screw speed in the compounding/injection moulding methods. Optimum parameters have been suggested by researchers for different composite systems (Medina et al., 2009, Joseph et al., 1999, Ku et al., 2011). A temperature of 180-190°C was recommended for better quality natural fibre polypropylene composites. Lower mixing temperatures lead to inconsistent melting of the matrix that can lead to non-uniform dispersion of the fibres in the composites, which finally decrease the tensile strength of the composites. The injection temperature should not be lower than 160°C in order to ensure acceptable melting of the matrix. On the other hand, very high temperatures result in fibre thermal degradation and then lower fibre reinforcing effects. A very high screw speed leads to shorter mixing times, non-uniform dispersion of fibres, high porosity, high fibre breakage and consequently lower tensile strengths. As the mixing time is increased, melting of the matrix becomes extensive and results in better fibre distribution. When mixing time is too long, fibre breakage and degradation would happen, resulting in a significant decrease in tensile properties of the composites (Medina et al., 2009, Joseph et al., 1999, Ku et al., 2011).

Several mathematical models have been developed to predict the tensile strength of the fibre reinforced composites. Most of the recent predictions are based on the assumption that fibres are continuous and/or aligned completely to the applied load.

The strength prediction of short and randomly orientated fibres is more complex than that of continuous and aligned composites.

- ***Rule of Mixtures***

The simplest available model that can be used to predict the tensile strength of a composite material is the rule of mixtures (ROM) (Beckermann and Pickering, 2009, Raabe and Hangen, 1995).

For unidirectional, continuous fibres, it is assumed that that both the matrix and fibre experience the same strain. So, the average composite tensile strength σ_c is determined by a force balance which weights the average fibre (σ_f) and matrix (σ_m) by their corresponding volume fractions V_f and V_m respectively, giving the following equation:

$$\sigma_c = V_f \sigma_f + V_m \sigma_m \quad (2.2)$$

At low strains, where both fibre and matrix behave completely elastically, the composite modulus E_C is as below:

$$E_c = V_f E_f + V_m E_m \quad (2.3)$$

On the other hand, the elastic modulus of the composite in the transverse direction is determined by assuming that the applied stress is equal in both the fibre and the matrix. As a result, E_C is determined by an inverse rule of mixtures equation that is given as:

$$\frac{1}{E_c} = \frac{V_f}{E_f} + \frac{V_m}{E_m} \quad (2.4)$$

When the composite strain is increased more than its yield point, the ROM equation (Eq. 2.2) is not applicable because composite failure is generally characterised by a critical local event rather than by average phenomena as assumed in the elastic region. In other words, failure of the brittle continuous fibres triggers composite failure. So, considering that $\varepsilon_c = \varepsilon_f$, then the tensile strength of a composite is as below:

$$\sigma_c = V_f \sigma_f + V_m E_m \frac{\sigma_f}{E_f} \quad (2.5)$$

- ***Kelly-Tyson model***

Eq. 2.5 was based on the assumption that the fibres were continuous and aligned in the direction of the applied stress. While the reinforcing efficiency of short fibres may be reduced due to their low aspect ratio of fibres.

Kelly and Tyson developed a model to predict the tensile strength of axially aligned discontinuous fibre composites taking into account whether the average fibre length (L) is greater than the critical fibre length ($L > L_c$) or less than the critical fibre length ($L < L_c$).

Referring to this model, the tensile strength (σ_c) of the composites containing fibres with an average length of L is given by:

$$\sigma_c = K_2 V_f \sigma_f + V_m E_m \frac{\sigma_f}{E_f} \quad (2.6)$$

where

$$K_2 = \frac{L}{2L_c} \qquad \text{For } L < L_C \quad (2.7)$$

$$K_2 = 1 - \frac{L_c}{2L} \qquad \text{For } L \geq L_C \tag{2.8}$$

Also, the minimum or critical fibre aspect ratio (S_c), which determines if there is sufficient fibre surface area for the fibres to break during composite loading, is found using the Kelly and Tyson model.

$$S_c = \frac{L_c}{D} = \frac{\sigma_f}{2\,\tau_i} \tag{2.9}$$

where L_c, D and τ_i are the critical length, fibre diameter and interfacial shear stress, respectively (Li et al., 2000).

- ***Bowyer-Bader Model***

The Kelly-Tyson model (Li et al., 2000) can be considered only for composites having short fibres, which are completely aligned to the loading direction. Kelly-Tyson model cannot be integrated to give a factor, which accounts for the complex fibre orientations in many moulded thermoplastic composites.

In randomly oriented fibre reinforced composites, it was necessary to consider the fibre orientation factor for modelling the tensile strength of the composite. A simple numerical fibre orientation factor (K_1) can be added to the Rule of Mixtures equation.

$$\sigma_c = K_1 K_2 V_f \sigma_f + V_m \sigma_m \tag{2.10}$$

Also, in Bowyer-Bader Model, instead of average fibre length, the effect of fibre length distribution can be considered for modelling the composite yield stress as below:

$$\sigma_c = K_1 \left\{ \sum_i \left[\frac{V_i \sigma_f L_i}{2L_c} \right] + \sum_i \left[V_j \sigma_f \left(1 - \frac{L_c}{2L_j} \right) \right] \right\} + V_m \sigma_m \tag{2.11}$$

where V_i and V_j are the volume fractions of the sub-critical and super-critical fibre lengths, respectively; and L_i and L_j are the sub-critical and super-critical fibre lengths, respectively. Subscripts i and j refer to the sub-critical and super-critical lengths, respectively (Li et al., 2000).

Due to the inconsistency of the hemp fibre diameters, fibre orientations cannot be measured using conventional methods. For example with glass fibres, fibre orientation can be measured by observing the cross section of the composite using an optical microscope. In this method since the diameter of glass fibre is consistent, the observed surface area of glass fibre is applied to calculate the orientation of the fibres.

2.4.2 Flexural Properties

The flexural strength of a composite is its capability to bend without undergoing any major malformations and failures. Three-point tests or four-point tests can be used to determine a composite's flexural properties, such as its flexural strength and flexural modulus. The flexural strength of the composite is evaluated based on the amount of load that collapses the composite, the distance between the platforms and the width and thickness of the specimen. The flexural strength of a composite usually relates with its tensile strength because when it is bent, it is also somewhat stretched locally.

Many studies have been carried out to investigate the effects of different factors on the flexural properties of natural fibre composites. (Lu and Oza, 2013) have reported a strong correlation between tensile and flexural strengths of hemp fibre reinforced virgin or recycled high density polyethylene composites. Many researchers have reported the effects of various chemical treatments (alkali, silane and acetylation

treatment) (Kabir et al., 2012a, Kabir, 2012) and coupling addition (Panaitescu et al., 2015) on flexural properties of hemp fibre reinforced composites. It was observed that the flexural properties of hemp fibre composites were highly improved by chemical treatments (alkali, silane and acetylation treatment) and/or matrix modifications.

2.4.3 Impact Strength

The impact properties of materials represent their capacity to absorb and dissipate energy under impact loading. The impact condition may range from the accidental dropping of hand tools to high-speed collisions and the reaction of a structure may be partial damage or entire breakdown. The fracture modes in impact conditions can be quite different from those observed in static tests such as tensile or flexural (Mallick, 2007).

The impact strength of natural fibre composites is of important concern because they exhibit lower impact strengths and smaller elongation at break than the polymer matrices.

In addition, referring to the literature, unlike tensile strength, improvement of fibre/matrix adhesion did not lead to any significant improvement in impact strengths of the composites. It has been reported that the addition of maleic anhydride grafted polypropylene (MAPP) coupling agent increased yield strength but lowered impact strength. While the addition of rubber or elastomer improved the impact strength but resulted in an unsatisfactory yield strength compared to unmodified composites (Niu et al., 2011, Tasdemir et al., 2009, Khoathane et al., 2008).

Impact strength of the composite is more critical in the presence of short fibres in the matrices. It has been reported that short fibre composites tend to display lower impact properties in most circumstances when compared to long fibre composites (Aji et al., 2009). Thus, as compounding/injection moulding composite fabrication methods result in very short fibres, study of impact strengths of composites are expected to be investigated in this project.

2.4.4 Damping of the Natural Fibre Composites

Damping is one of the important parameters associated with the dynamic behaviour of a material because of its impact on system performance, safety and reliability (Khan et al., 2011). Vibration may generate high noise levels, stress fatigue failure, premature wear and unsafe operating conditions. Structures can experience excessive vibrations when the dynamic loading creates vibrations at the natural frequency of a composite material. This type of vibration can cause catastrophic failure of the structure (Haldar et al., 2011). Therefore, understanding of complete vibration response of a composite material is essential to the effective design and use of this composite.

Polymers exhibit viscoelastic behaviour, which results in higher damping properties than metallic materials. Extensive studies have been carried out on the mechanism of vibration damping in polymers (Sperling, 1990, Song et al., 2001, Povolo and Goyanes, 1996, Sun et al., 1992, Fitzgerald et al., 1999). However, damping mechanisms in fibre reinforced polymer materials differ entirely from those in conventional polymers. In case of composite materials, the presence of fillers or reinforcing agents creates complex internal structures in the material. In such cases,

the damping behaviours depend not only on properties of individual materials but also on many other factors, e.g. the volume fraction of the fillers, the quality of the interface, loading direction and plasticisation of the polymer matrix. There are different energy dissipation mechanisms in fibre reinforced composites such as: the viscoelastic nature of the matrix and/or fibre materials; the friction generated from the slip in the matrix/fibre interface; the energy dissipation at cracks and delamination produced at damaged locations; and viscoplastic and thermoelastic damping (Chandra et al., 1999, Chauhan et al., 2009). Synthetic fibre reinforced polymers often suffer from the threat of vibrations during their normal operations (Khan et al., 2011), whereas the presence of natural fibres in the thermoplastic material has been reported to improve the damping properties (Di Landro and Lorenzi, 2009b, Di Landro and Lorenzi, 2009a). It has been shown that natural fibre composites have damping properties that are comparable and sometimes superior to glass fibre composites (Di Landro and Lorenzi, 2009b, Haldar et al., 2011, Genc et al., 2012, Di Landro and Lorenzi, 2009a).

The ability of natural fibre reinforced composites (NFRC) to reduce noise and vibrations is a characteristic which provide a distinctive advantage over glass fibre composites, especially for automotive applications. It has been reported that short discontinuous fibres make the composites theoretically more suitable to optimise the damping properties (Haldar et al., 2011). NFRC can replace glass fibres as reinforcement in interior or/and exterior parts of cars and commercial vehicles such as doors and instrumental panels, glove boxes, arm rests, seat backs, engine covers, packing trays and other parts where the materials are exposed to vibration excitation and where vibration absorption is of great importance.

Unlike synthetic fibres, the natural fibres are composed of pectin, lignin, hemicellulose and cellulose and they can be considered as viscoelastic materials. Many researchers have studied the behaviour of cellulose and lingo-cellulosic materials (Montes et al., 1997, Roig et al., 2011, Placet, 2009). Referring to the literature (Kelley et al., 1987, Jafarpour et al., 2008, Obataya et al., 2001, Placet, 2009), four transition modes have been reported for the hemp fibre so far with increasing the temperature. Two transition modes (γ and β) were observed below 0°C while the rest (α_1 and α_2) were observed above 0°C. The γ-relaxation mode is associated with methyl (RCH_3) and hydroxyl (OH) groups motions of plant amorphous regions (cellulose, hemicelluloses). The β-relaxation mode is associated to the localised movements of the β_1–4 glycosidic bonds of semicrystalline regions (cellulose). The α_1 and α_2 modes are associated to the main transition involving polymer chain cooperative movements of lignin and amorphous carbohydrate components (hemicelluloses and cellulose), respectively (Kelley et al., 1987, Jafarpour et al., 2008, Obataya et al., 2001, Placet, 2009) .

Wang et al. (Wang et al., 2012) stated that the cantilever beam vibration method is a cost-efficient and time-saving technique to study the damping behaviour of a material. This method was employed to measure dynamic modulus of elasticity and damping ratio values of three commercial wood-based composites, i.e. plywood, high-density fibreboard and oriented strand board. The dynamic modulus of elasticity and damping ratio values were determined from the spectral analysis of light on the first natural frequency and the first and fifth amplitudes of vibration in the vertical direction. Yan (Yan, 2012) studied the effect of alkali treatment on the compressive, in-plane shear, impact properties and vibration characteristics of flax and linen-fabric reinforced

epoxy composites. The results showed that, after the treatment, the damping ratio of the flax and linen composites decreased. In another research, Naghipour et al. (Naghipour et al., 2005) measured the damping ratio values of five kinds of three-layer glued laminated timber beams reinforced with three lay-ups of glass fibre reinforced polymer (GFRP) sheets. These GFRP sheets of the lay-ups varied in thickness, orientation and location. The timber samples were from the group of spruce–pine–fir timbers. The logarithmic decrement analysis technique was used to determine the damping ratio via the frequency response function. Their results showed that the average damping ratio values of the reinforced beams were close to or about 12% higher than that of the beams without GFRP reinforcement. The largest average damping ratio value of the GFRP reinforced beams was about 0.07.

2.4.5 Dynamic Mechanical Performance

Dynamic Mechanical Analysis (DMA) has become a widely used method for determining the viscoelastic behaviour and the interfacial characteristics of heterogeneous polymeric systems (Ray et al., 2002). The dynamic properties of polymeric materials are of great significance if it is investigated over a range of temperatures and frequencies. The DMA method can evaluate storage modulus (E′), loss modulus (E") and loss factor (tan δ) of the materials. DMA analysis is an efficient way to calculate the effectiveness of reinforcement on the moduli of the composites. Moreover, because of molecular motion involving chain segments, DMA also provides precise information for the evaluation of relaxation or transition processes (Romanzini et al., 2012). It can provide information about the relaxation peaks of PP.

Polypropylene (PP) has been commonly utilised as matrix in natural fibre composites for the last decade. It can be extended to extrusion and injection techniques for moulding composite parts with short natural fibres (Lee and Cho, 2008). Referring to the literature, two relaxation peaks were observed in the tan δ curve of polypropylene at ranges of 5-10˚C (β) and 60-100˚C (α) (John and Anandjiwala, 2009, Zugenmaier, 2006, Tajvidi et al., 2006, Tajvidi et al., 2010). The β-transition corresponds to the glass transition temperature and is related to relaxation of unrestricted amorphous chains of polypropylene. The α-transition is associated to the relaxation of the restricted crystalline phase of polypropylene and can be attributed to molecular chain rotation in the crystalline phase (John and Anandjiwala, 2009).

DMA also provides precise information about the influence of fibre incorporation in a matrix. An increase in the storage modulus or stiffness of the composite has been reported due to the incorporation of the fibres. In addition, it has been reported that the storage modulus of the materials decreases at transition temperatures as they transfer from glassy to rubbery regions. (Romanzini et al., 2012, Mohanty et al., 2006).

Using DMA analysis, the reinforcing effects of fibres in different temperatures can be evaluated by effectiveness coefficient C. The effectiveness coefficient C is the ratio between the composite storage modulus (E′) in the glassy and rubbery regions in relation to the neat resin and can be calculated using Eq. 2.12:

$$C = \frac{{E'_g}/{E'_r}\ composite}{{E'_g}/{E'_r}\ resin} \tag{2.12}$$

where E_g' and E_r' are the storage moduli in the glassy and rubbery regions, respectively. The higher the value of the constant C, the lower the effectiveness of the filler (Romanzini et al., 2012, Idicula et al., 2005).

2.5 Market Study

Figure 2.7 illustrates the share of different processing technology in the German automotive industry in 2005 (Karus et al., 2006). The share of injection moulding in the German automotive industry for fabrication of bio-composites was very low (only 2%) in 2005 while press moulding was the dominant processing technique.

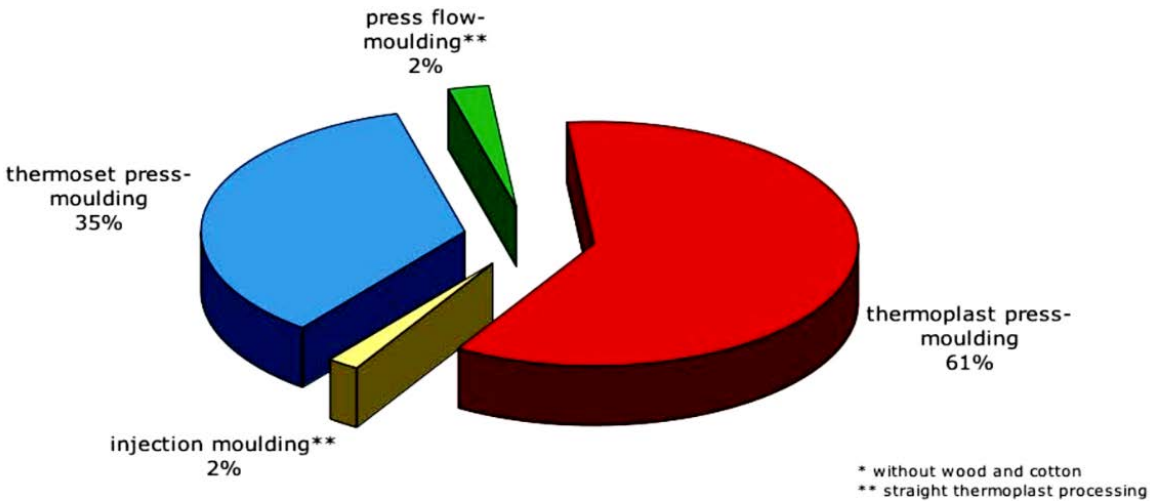

Figure 2.7: Share of different processing technology in German automotive industry in 2005 (Karus et al., 2006).

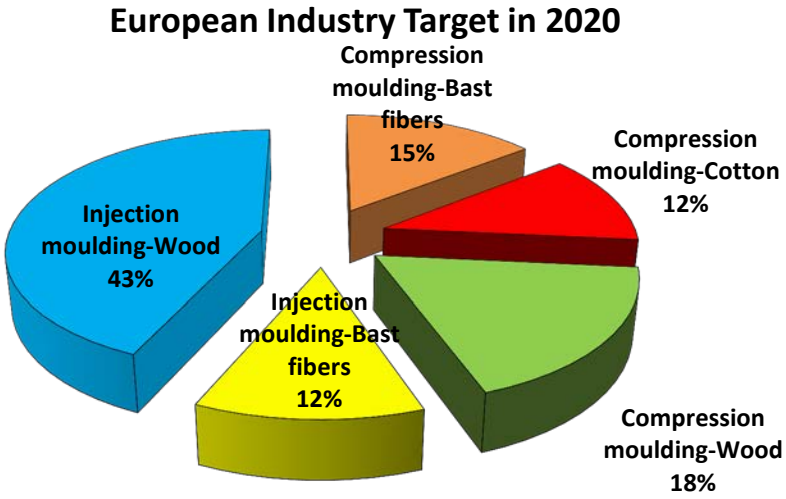

Figure 2.8: Target of European industries for fabrication of bio based- thermoplastic composites in 2020 (Source: nova-Institut 2010).

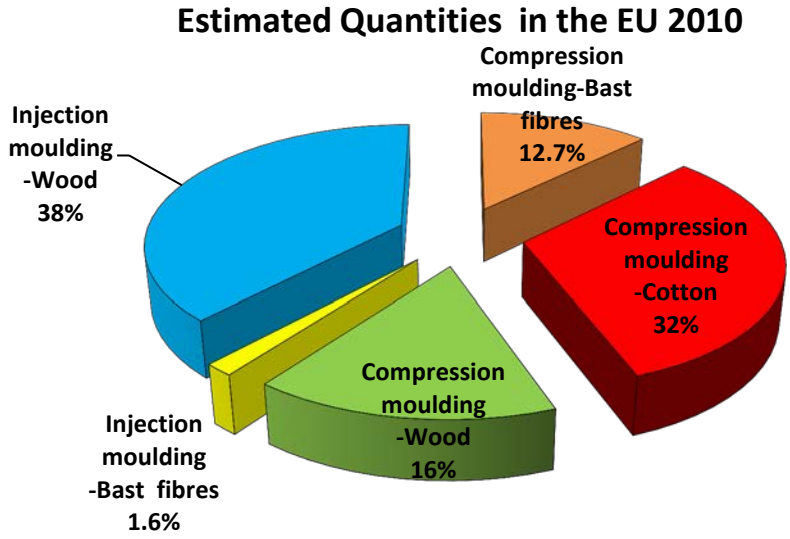

Figure 2.9: Share of injection and compression mouldings for fabrication of bio-based thermoplastic composites in 2010 in European industries (Source: nova-Institut 2010).

The European Industrial Hemp Association (EIHA) has reported European market targets for bio-based composites and natural fibres (Figure 2.8). Referring to this report, from a total 2.4 million tons thermoplastic-based composite, at least 315,000 tons were reinforced by natural fibres, mainly in the automotive and construction

sectors in 2010 (Figure 2.9). By 2020, this quantity should reach 830,000 tons and total composite production (glass, carbon and natural fibre reinforced plastics) is estimated to be 3 million tons by 2020. Most of the natural fibres used as reinforcement in polymers are short randomly oriented fibres because most natural fibres are processed from agricultural sources, crops or waste, which are already chopped into smaller sizes. Besides, it is much easier to introduce short fibres to an inexpensive technique such as injection moulding (Fotouh et al., 2014). Contrary to the potential of injection moulding, injected thermoplastics reinforced by bast fibres (flax, hemp, jute, kenaf, sisal, cork) was 5000 tons in 2010, as shown in Figure 2.9, which formed only 1.6% of total bio-composites in construction, furniture, automotive, consumer goods applications. The low share of the injection moulding method for bast fibre-thermoplastic composites in both 2005 and 2010 implies that there are some critical issues in the injection moulding method. However, the assigned target for injected thermoplastic composites reinforced by bast fibres for European Industries in 2020 is 100,000 tons. This shows a dramatic increase from 5000 tons to 100,000 tons (20 times) which will make 12% of total bio-composites in 2020. This target will not be achieved unless the current technical issues regarding injection moulding of bast fibre thermoplastic composites are identified and resolved. So, this is an area where the natural fibres still have not made a market breakthrough.

2.6 The Challenges of Injection Moulding

In spite of a number of advantages of natural fibres such as low density, high specific strength, recyclability, availability, reduced abrasion to processing machinery and CO_2 neutrality, injected short natural fibre reinforced thermoplastic composites have not satisfied industries yet.

Several drawbacks have been associated with the natural fibres such as incompatibility with classical hydrophobic polyolefins, tendency to form aggregates, poor thermal stability and poor resistance to moisture. Other factors, which affect the properties of the final product, are morphological characteristics: fibre composition, presence and location of defects depend on fibre type, growth conditions and extraction methods. These factors make the mechanical prediction of composite properties complicated (Duc et al., 2011).

Some drawbacks have been associated with the injection moulding method. The injection moulding process can be more problematic because of the intensive thermal and mechanical stresses being applied to the fibres. This introduces more complexity to the hemp/polypropylene system. Parameters, such as fibre orientation and final fibres aspect ratio, are critical as these determine the final properties of the composite.

2.6.1 Fibre Orientation

Fibre orientation has a great impact on the mechanical properties of fibre reinforced composites. It is reported (Ku et al., 2011) that the maximum composite strength occurs when the reinforcing fibres are completely aligned parallel to the direction of the applied load, while in injection moulding, fibres are oriented randomly within matrix.

For a simple mould geometry, three different layers can be identified after injection moulding; skin, shell and core layers.

When the melt mixture enters a mould cavity during injection moulding, mould walls affect the orientation of fibres since the melt polymer close to mould wall is prone to

shear stresses, which tend to position the fibres parallel to the mould flow direction (MFD). However, in the middle zone, fibres tend to orientate perpendicular to the MFD because the shear stresses vanish in this area and extensional flow prevails. A third, very thin skin, layer exists at the surface, with random fibre orientation, where the melt polymer touches the colder mould walls and freezes without any orientation effect on fibres (Bernasconi et al., 2007). The schematic injection-moulded short fibre composite is presented in Figure 2.10, which shows different orientations of the short fibres in skin, shell and core layers.

All accurate composite strength predications need precise knowledge of fibre orientations although investigation on the fibre orientations is not simple because fibres are concealed by thermoplastic and they do not have uniform geometry.

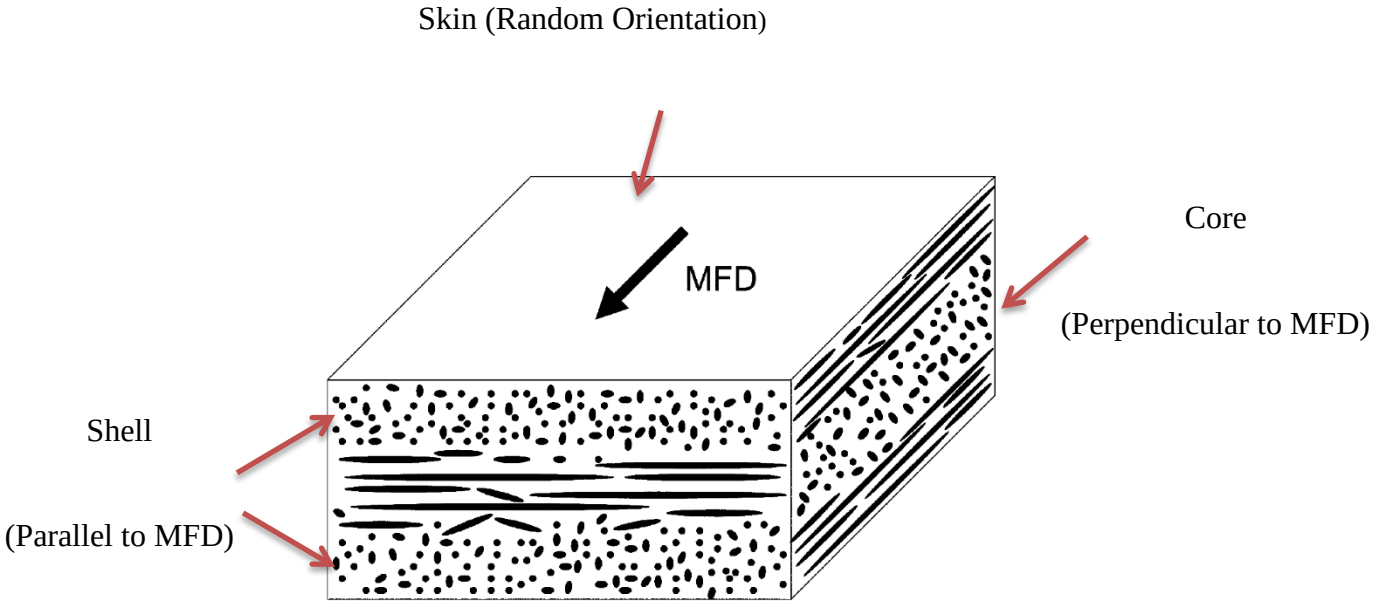

Figure 2.10: Different orientations of the short fibres in skin, shell and core layers of an injection moulded plate (Bernasconi et al., 2007) .

2.6.2 Fibre Aspect Ratio

Another important parameter that should be considered strongly in the injection moulding process is the fibre aspect ratio. There is a critical fibre aspect ratio for each composite depending on fibre, matrix and fibre-matrix interface quality. Figure 2.11: Damage modes observed in short fibre composites during failure: (1) yielding of matrix, (2) fibre debonding, (3) fibre debonding and pullout and (4) fibre fracture. (Nystrom et al., 2007). If fibre length is less than a critical value then the fibre will be debonded and/or pulled out of the matrix before it can be fractured. Therefore, a higher fibre aspect ratio is desired. However, if the fibre aspect ratio is too high, the fibres may be entangled during mixing resulting in poor fibre dispersion.

In the conventional method, fibre size measurements are done by parallel sectioning of the composite or fibre extraction based on chemical dissolution of the polymer matrix followed by image analysis using a light microscope or scanning technique. However, these techniques have technical difficulties and may cause fragmentation of fibres. Also very short fibres can be lost during screening of extracted fibres from the solution. (Bos et al., 2006). In this project fibre size measurements was done by X-ray microtomography.

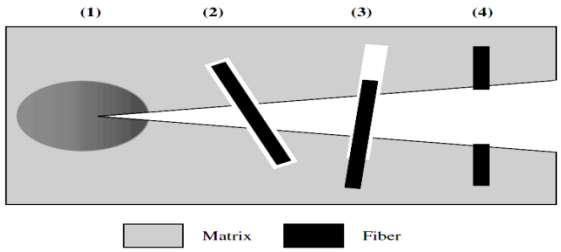

Figure 2.11: Damage modes observed in short fibre composites during failure: (1) yielding of matrix, (2) fibre debonding, (3) fibre debonding and pullout and (4) fibre fracture. (Nystrom et al., 2007). If fibre length is less than a critical value then the fibre will be debonded and/or pulled out of the matrix before it can be fractured.

2.6.2.1 X-ray microtomography

Conventional microstructural characterization techniques such as optical microscopy, scanning electron microscopy, transmission electron microscopy and atomic force microscopy are generally limited to observe the surface or a localised portion of the sample volume. In addition, they often require sample preparations, or they are complex in terms of data interpretation. Lately, the technique of X-ray microtomography has been developed, which offers the capability of observing the internal structure of materials in micron scale (Pakzad et al., 2011).

X-ray microtomography, as a radiographic imaging technique, can provide 3D images of an internal structure of a material at a spatial resolution better than 1 micrometre. This technique does not require sample preparations. It can be a non-destructive method allowing many scans to be made of the same specimen under different conditions. X-ray microtomography is frequently called a micro CT scan because it has been developed based on Computerised Axial Tomography (CAT or CT) scans that have been used for medical imaging for 40 years (Landis and Keane, 2010).

CT scans were an extension of conventional projection radiography, a technique that 2D images can be extracted which presents the internal structure of the sample. For example, cracked bones can easily be recognised due to the variations in X-ray absorption between bone and the surrounding tissues. However, a 2D image cannot show the position of a feature of interest such as Tumour. Also, a 2D radiograph image can only present us with the average X-ray absorption through the sample's out-of-plane dimension. Then a feature can be completely missed because it overlaps with other competing features through the depth (Landis and Keane, 2010).

These problems can be resolved by the utilization of CT scans which combine data from a series of 2D X-ray absorption images recorded while the object is rotated around a single axis. Using mathematical principles of tomography, a series of images are reconstructed to create a 3D digital image. Each voxel (volume element or 3D pixel) is associated to the X-ray absorption at that point. Therefore, the 3D structure of the sample can be depicted due to the relationship between X-ray absorption and material density. Finally, internal features can be uniquely observed and analysed (Herman, 1980). A significant development in microtomographic methods was the use of synchrotron radiation as an X-ray source. It brought noteworthy enhancements to the micro CT images. It should be noted that in order to realise most of the advantages of synchrotron X-ray sources, imaging is typically limited to relatively small specimens, typically 5–10 mm (Landis and Keane, 2010).

In summary, a tomographic reconstruction of projection images provides with a 3D map of X-ray absorption. Because different material features and phases often have different X-ray absorption properties, the different features from these images can be easily recognise.

3D images are particularly effective for qualitative evaluation of spatial relationships. While these images have significant qualitative value, another useful aspect of them is the digital nature of the 3D images. Quantitative measurements on internal structure of the samples is also applicable using digital image processing. . Generate 3D objects (fibres) and then can be used to measure the dimensions. Also, The quantitative measurements can include relatively simple characteristics such as phase volume

fractions to more complicated measurements such as distributions, orientations, alignment and connectivity of a microstructural feature (Landis and Keane, 2010).

X-ray microtomography has numerous practical applications in different fields of research. In polymer composite materials, specifically, applications of X-ray micro CT include but are not limited to: characterization of fibres (Requena et al., 2009), void volume fraction and dispersion and size measurements of fibres in polymer composites (Landis and Keane, 2010, Laiarinandrasana et al., 2010). Just recently, its applications extended to composites reinforced with natural and cellulosic fibres, including paper, wood and hemp (Alemdar et al., 2008, Tanaka et al., 2007).

3. Materials and Methods

3.1 Raw Materials

3.1.1 Fibres

Two types of hemp fibres were used in this project as can be seen in Figure 3.1

1. China-Hemp Industrial Investments and Holding Co. Ltd. supplied noil hemp fibres. It is an overly degummed hemp fibre, a by-product of hemp fibre production for textile purposes, with a length shorter than the requirement for textile industry and average diameter of 20–30μm. It is 80 % cheaper than normal industrial hemp fibre. It consists of cellulose (91.9 wt%), lignin (1.7 wt%), hemicellulose (3.5 wt%) and pectin (1.2 wt%) (Yan et al., 2013). Later on in this thesis, it is referred to as noil hemp fibre.
2. Normal hemp fibres were obtained from Ecofibre Industries. The fibres were first washed and dried. This type was used only for fabricating the composites in Chapter 7.

3.1.2 Thermoplastics

Two types of random copolymers polypropylene thermoplastics were used in this project. The first was M800E polypropylene supplied by Sinopec Shanghai petrochemical Co. Ltd., China with a melt flow index of 8.0 g/10min which was used as the matrix. The second was Moplen EP203N polypropylene supplied by Basell Australia with a density of 0.9 gr/cm^3 and a melt flow index of 11 g/10min (Appendix 2). The second PP was used only for fabricating the composites in Chapter 7.

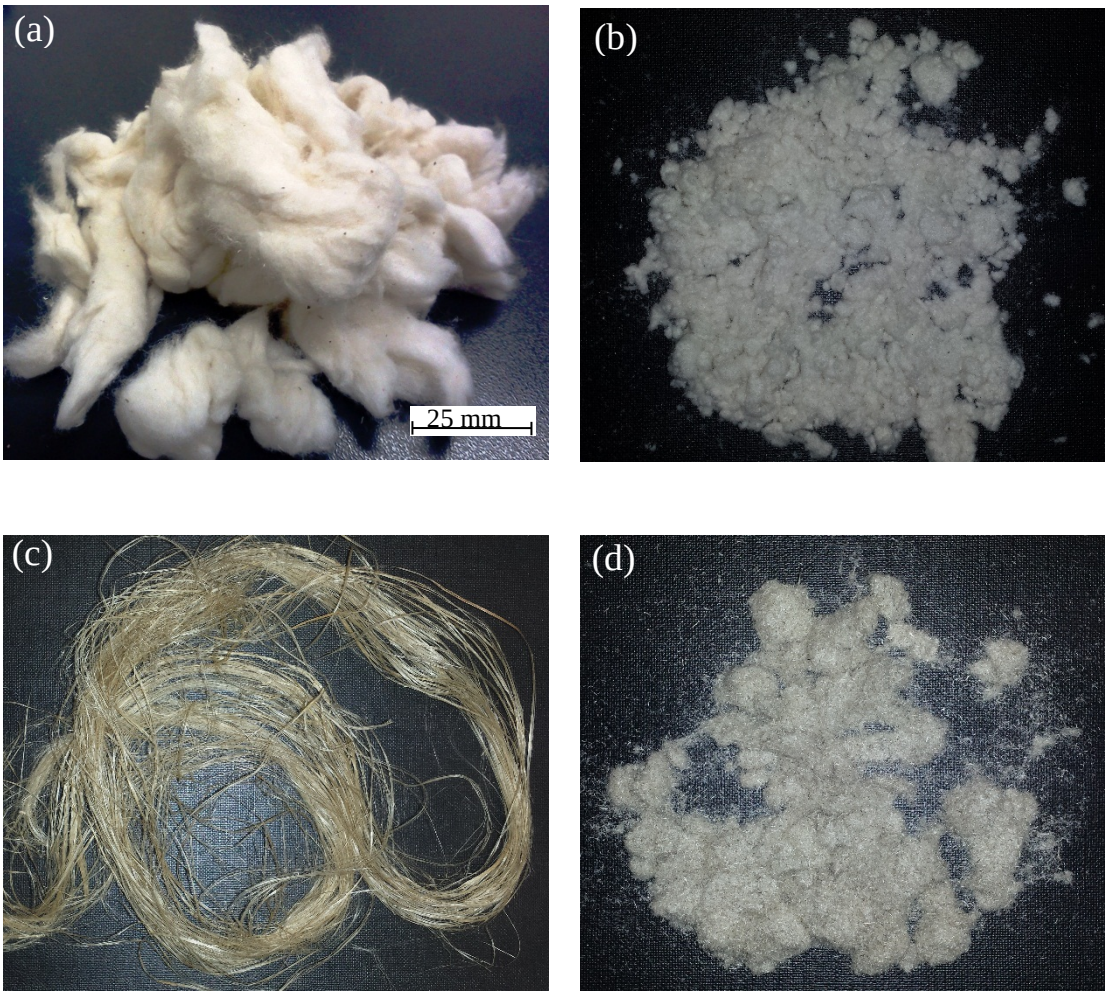

Figure 3.1: (a) as-received noil hemp bundles (b) ground noil fibres, (c) as-received normal hemp fibres and (d) treated ground hemp fibres.

3.1.3 Compatibilisers and Additives

The compatibilisers used in this research were maleic anhydride grafted polypropylene (MAPP) and maleic anhydride grafted poly ethylene octane (MAPOE). MAPP with an MA content of 1.0 wt% supplied from Bondyram1001, Polyram Ram-On Industries, Israel, was used as the compatibiliser to the PP matrix. MAPOE brand 8999 was supplied by Dupont Dow Elastomers LLC. In addition, 0.3 wt% Irganox 1010 was used as on antioxidant to the composites, which was supplied by BASF Corporation, Germany.

3.2 Composite Fabrication

Two sets of different methods were used to fabricate the composites: Firstly, melt mixing and injection moulding in Chapters of 4, 5 and 6; and secondly, extrusion and injection moulding in chapter 7.

3.2.1 Melt Mixing and Injection Moulding

The composites were fabricated with a hemp fibre content range of 0-60 wt% using melt mixing and injection moulding machines. The compatibilisers used in this research were maleic anhydride grafted polypropylene (MAPP) and maleic anhydride grafted poly ethylene octane (MAPOE). Different contents of 0, 2.5 and 5 wt% of a compatibiliser were used to fabricate the samples. The sample compositions are shown in Table 3.1. For fabrication, the coupling agent was mixed with the PP at 170–180˚C in the intermixer, Figure 3.2(a), (XH-409, Dongguan City Xihua Testing Machine Co. Ltd., China) for 15 min before the addition of the hemp fibres. The fibres were held in an oven for 24 hours at 80 °C before mixing.

Oven-dried noil hemp fibres were mixed in the intermixer at 180˚C for another 15 min. The mixture was then rolled using a roll mixer (XH-401B, Dongguan City Xihua Testing Machine Co. Ltd., China), Figure 3.2(b) and then crushed into granules with the size of 5-7 mm using a crusher (RPC-180, Shanghai Runpin Industry & Trade Co. Ltd., China). The compounded and dried granules were placed in an injection moulding machine (MJ 55, Chen Hsong Group and China), Figure 3.2(c), and the specimens were injection moulded.

The fibre volume fraction (V_f) of each composite was calculated from the fibre weight fraction (W_f) using the Eq. 3.1 .

$$V_f = (1 + \frac{\rho_f}{\rho_m} \frac{1-W_f}{W_f})^{-1} \quad (3.1)$$

where ρ_f is the hemp fibre density and ρ_m is the matrix density.

Table 3.1: Composition of fabricated composite samples via melt mixing and injection moulding.

Samples	Hemp (wt%)	PP (wt%)	MAPP (wt%)	MAPOE (wt%)
PP	0	100	0	0
10H	10	90	0	0
20H	20	80	0	0
30H	30	70	0	0
40H	40	60	0	0
50H	50	50	0	0
60H	60	40	0	0
30H2.5MAPP	30	67.5	2.5	0
40H2.5MAPP	40	57.5	2.5	0
30H5MAPP	30	65	5	0
40H5MAPP	40	55	5	0
30H2.5MAPOE	30	67.5	0	2.5
40H2.5MAPOE	40	57.5	0	2.5
30H5MAPOE	30	65	0	5
40H5MAPOE	40	55	0	5

(a)

(b)

(c)

Figure 3.2: (a) Intermixer, (b) roll mixer and (c) injection moulding,

3.2.2 Extrusion and Injection Moulding

Normal hemp fibres were immersed in NaOH solutions with a concentration of 5wt% at ambient temperature holding for 3 hours. After treatment, fibres were washed several times with 40˚C water until their PH reached 7. Then they were oven-dried for 24 hours at 80˚C. Then both noil fibres and treated hemp fibres were chopped into 0.2, 0.5, 1 and 2 mm lengths and dried at 80˚C for 24 h. The 40 wt% chopped fibre; 5wt% MAPP and polypropylene were compounded in a EuroLab 16XL twin-screw extruder (Figure 3.3a) operated at 100 revolutions per minute (rpm).

Figure 3.3: (a) Extrusion and (b) Injection moulding machines.

The extruder barrel consists of six heating zones, which were set at 180˚C. After cooling in air, the extruded composite material was granulated in an industrial granulator to produce composite pellets with a length around 5 mm. The composite pellets were then dried at 80˚C for 3 h before being injection moulded (Figure 3.3b) into tensile test specimens.

3.3 Microstructural Observations

3.3.1 Optical Microscopy

Individual noil hemp fibres were first separated from their bundles by hand and a photographic image was captured with a MOTIC SMZ-168 series stereo zoom microscope equipped with a CC12 Soft Imaging System. The average diameter of fibres was obtained by measuring the diameter at 5 locations along the fibre length under the same microscope via calibrated software. A typical image of an elementary fibre is shown in Figure 3.4.

3.3.2 Scanning Electron Microscopy

Fracture surfaces of the composite tensile test specimens and the surfaces of the chemically treated and untreated fibres were examined by scanning electron microscope (JEOL 7800F SEM) operated at 5 kV to investigate the effects of the coupling agent addition on fibre–matrix interface adhesion. Samples were mounted onto aluminium stubs with carbon tape and then sputter coated with platinum for 120 seconds to make them conductive prior to SEM observation.

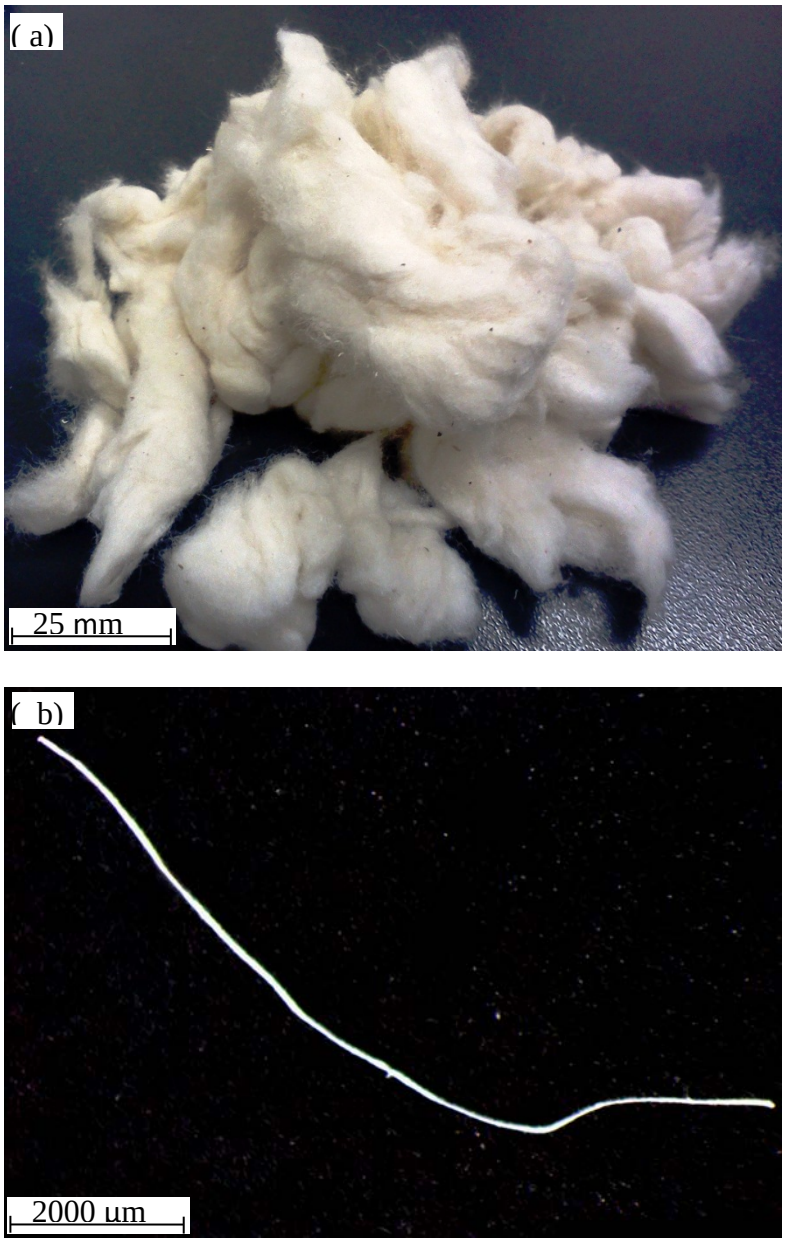

Figure 3.4: (a) Noil hemp bundles and (b) a separated elementary fibre.

3.3.3 X-ray Micro-Tomography

3.3.3.1 Experimental Set-up

In this project, X-ray microtomograph (SkyScan-1072 high-resolution desk-top micro-CT system) was used to measure fibre aspect ratio and to observe fibre agglomerations in the composites. In order to get the resolution necessary for accurate

analysis (2.4 μm), small x-ray micro-tomography samples were cut and then scanned using a cone beam x-ray source with a rotation angle of 0.4˚. A CCD camera with resolution of 1024x1024 pixels took pictures of 450 projections to cover a 180˚ scan.

The scanning time taken was about half an hour. The voltage and amperage used were 48 kV and 146 μA respectively. The projection images were constructed according to the different x-ray absorption of the fibres and the matrix. After scanning, X-ray projection images were reconstructed using NRECON reconstruction software provided by SKYSCAN. A schematic presentation of X-ray micro-tomography acquisition and reconstruction steps is shown in Figure 3.5.

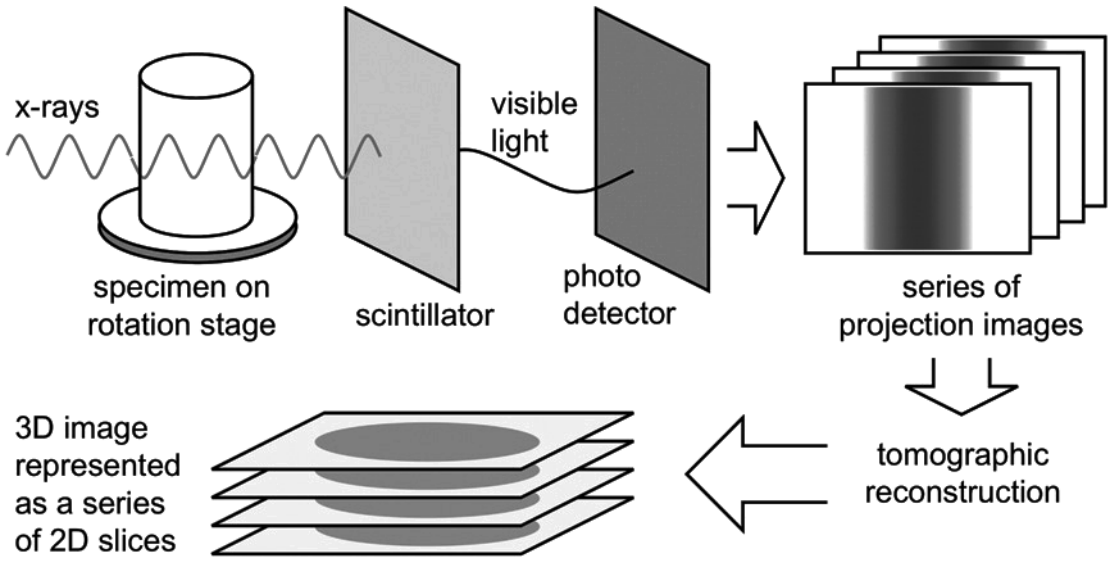

Figure 3.5: Schematic illustration of X-ray micro-tomography acquisition and reconstruction steps (Landis and Keane, 2010).

3.3.3.2 Image Analysis

Afterwards, using the FIJI software package and its plugins (Schindelin et al., 2012, Iannuccelli et al., 2010, Bolte and CordeliÈRes, 2006), a stack of these reconstructed images were then added together to form a 3D view of the sample. Then, the aspect ratio, length and width of each fibre were measured using the FIJI software package

and its 3D plugins by selecting an appropriate threshold due to the different X-ray absorptions of the fibres and the matrix. Finally, utilizing appropriate thresholds and brightness, fibre agglomerations were extracted and analysed from the 3D views. In addition, the FIJI software package and its plugins enabled the measurement of the length and width of the fibres after injection moulding. For further information, please browse http://fiji.sc/Documentation. For sure, this method is not completely perfect and includes some errors such as other methods.

3.4 Fourier transform infrared analysis

Fourier transform infrared analysis (FTIR) was used to study the chemical structure of the normal and noil hemp fibres. FTIR analysis was examined using a Thermo Nicolet FTIR Spectrometer model Nexus, Figure 3.6, using a Perking-Elmer spectrometer and the standard KBr pellet technique. Approximately 3 mg of Hemp fibres were crushed into fine particles and mixed with about 15 mg KBr and then pressed into a pellet for FTIR measurement. The effects of fibre treatment on chemical composition of the hemp fibres were investigated.

Figure 3.6: FTIR used in this project.

3.5 Thermal Analysis

Thermal analysis of untreated and alkali treated hemp fibres were performed using Thermogravimetric Analysis (TGA) and Differential Scanning Calorimetry (DSC) experiments. TGA-Model Q500, Figure 3.7(a), was used to carry out thermogravimetric analysis of the fibres at a constant heating rate of ˚C/min from 25˚C to 430˚C under nitrogen flow rate of 60 mL/min. 10 - 20 mg fibres were taken for analysis.

The differential scanning calorimetry carried out via a DSC instrument, Model Q100, Figure 3.7(b). Firstly, the samples were heated up from 10˚C to 500˚C at a heating rate of 10˚C / min under nitrogen atmosphere at a flow rate of 80 mL/min.

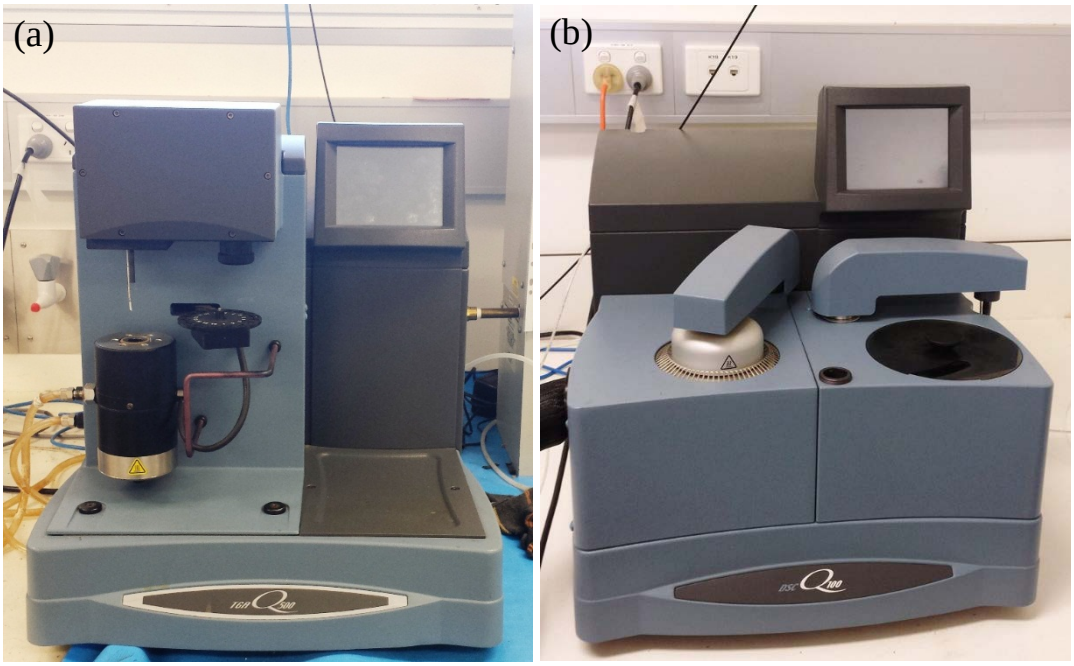

Figure 3.7: (a)TGA and (b) DSC used in this research.

3.6 Mechanical Experiments

3.6.1 Single Fibre Tensile Test

A Dynamic Mechanical Analyser (DMA Q800 V5.1, Figure 3.8) was used at ambient temperature to investigate the tensile properties of the noil hemp fibres according to ASTM D 3822-01. Noil hemp fibres were separated and then mounted on cardboards with 7, 12 and 20 mm holes as gauge lengths.

Fibres were observed under a MOTIC SMZ-168 series stereo zoom microscope equipped with a CC12 Soft Imaging System to measure the diameter of the fibres (taking the average of 5 randomly measured diameters). The mounted fibres were then placed in the holders and the supporting sides of the mounting cards were cut. The fibres were then tensile tested to failure at rate of 1 mm/min.

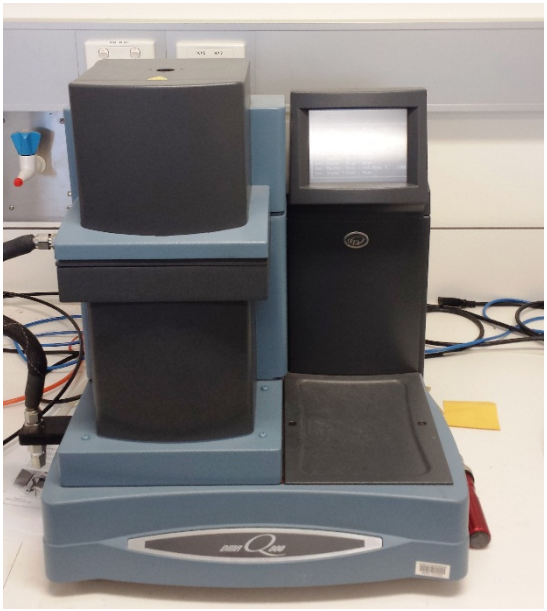

Figure 3.8: DMA Q800 V5.1 DMA equipment.

3.6.2 Tensile Test

After composites fabrication, the tensile strength of the specimens (Figure 3.9a) were evaluated using a multifunctional tensile machine (Figure 3.10) (AG-2000A, Shimadzu Corp., Japan) according to the ASTM D638-91 at the specified rate of 10 mm/min. The composite specimens were tested to failure (Figure 3.9b&c) and the average value from 10 tensile-tested specimens was reported for each sample. However, only in Chapter 7 , a 10 kN MTS testing machine was used to measure the tensile strength of the specimens. Figure 3.11 shows stress- strain curves of 10 wt% hemp fibre reinforced polypropylene composites.

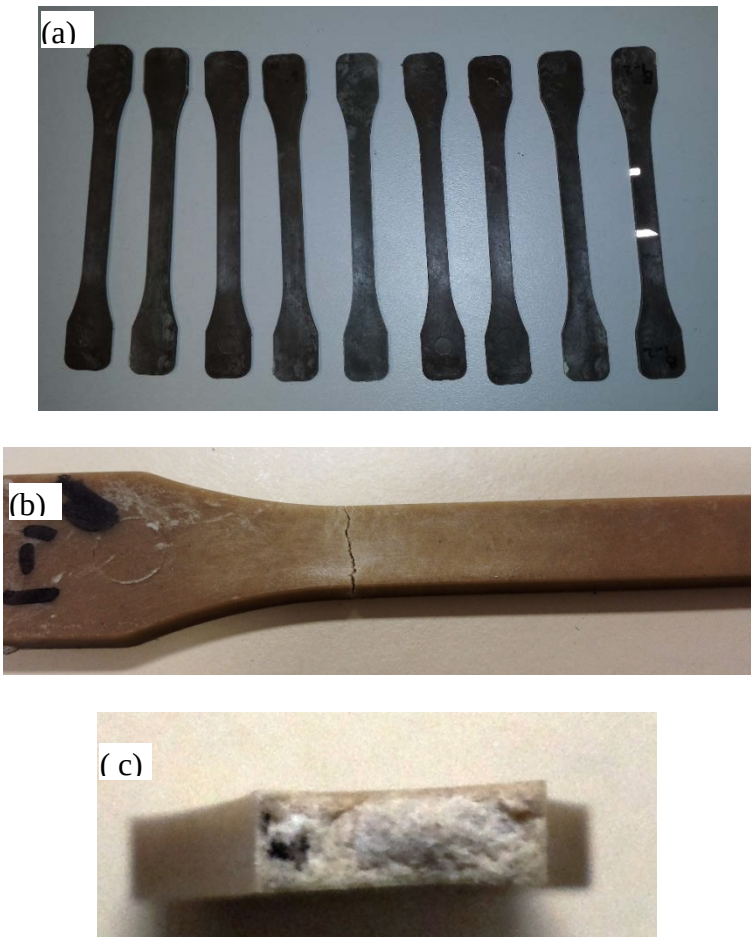

Figure 3.9: (a) Injection moulded tensile specimens, (b) a tensile specimen after failure and (c) cross section of the specimen after failure

Figure 3.10: 10 KN MTS testing machine.

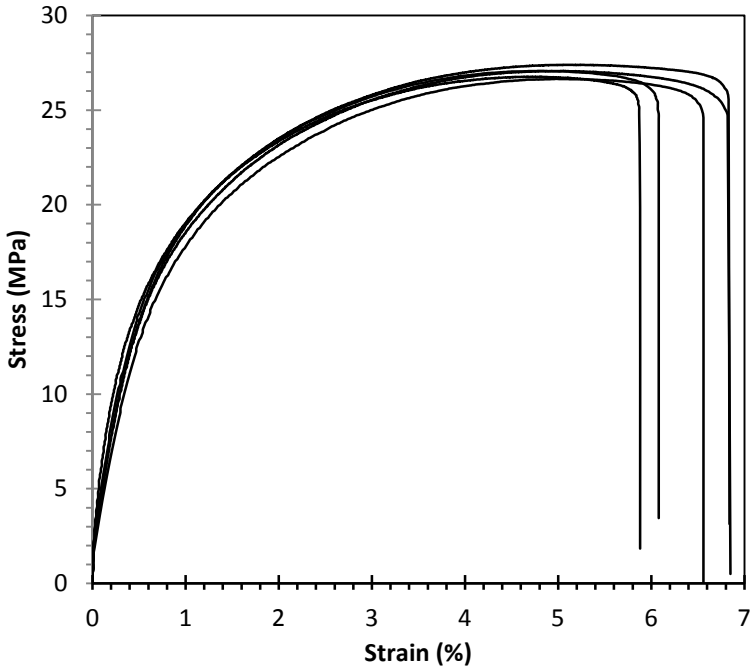

Figure 3.11: Stress- strain curves of 10 wt% hemp fibre reinforced polypropylene composites.

3.6.3 Flexural test

3-point flexural testing of the pure polypropylene and normal hemp fibre polypropylene composites were carried out by means of a 10 kN MTS testing machine according to the ISO 178 at a standard rate of 5 mm/min. The average from 5 specimens with cross sections of 4 mm x 10 mm was reported for each sample. The span was set at approx. 16 times of the thickness.

The specimens were first simply mounted in the testing machine as shown in Figure 3.12 and then load was applied at middle of the span. The load and specimen deflection were recorded up to failure of the specimens. Figure 3.13 shows a typical sample of flexural stress vs. strain curves of the matrix and normal hemp fibre composites.

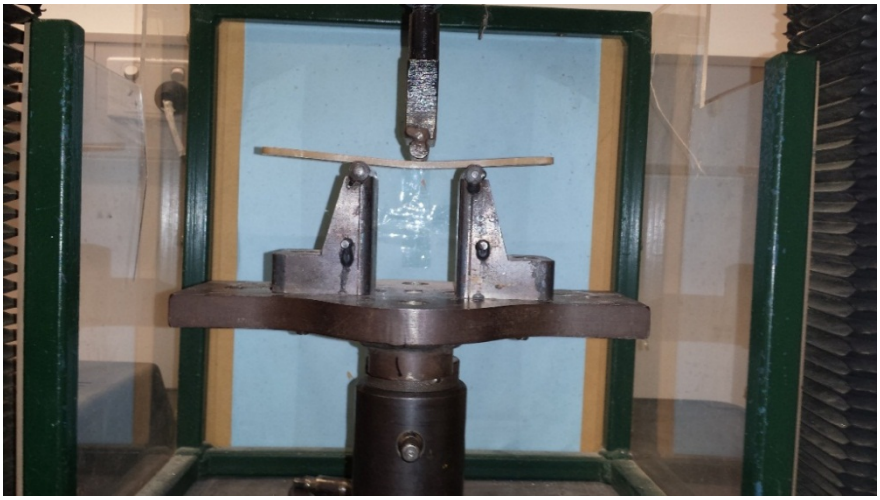

Figure 3.12: Flexural test setup.

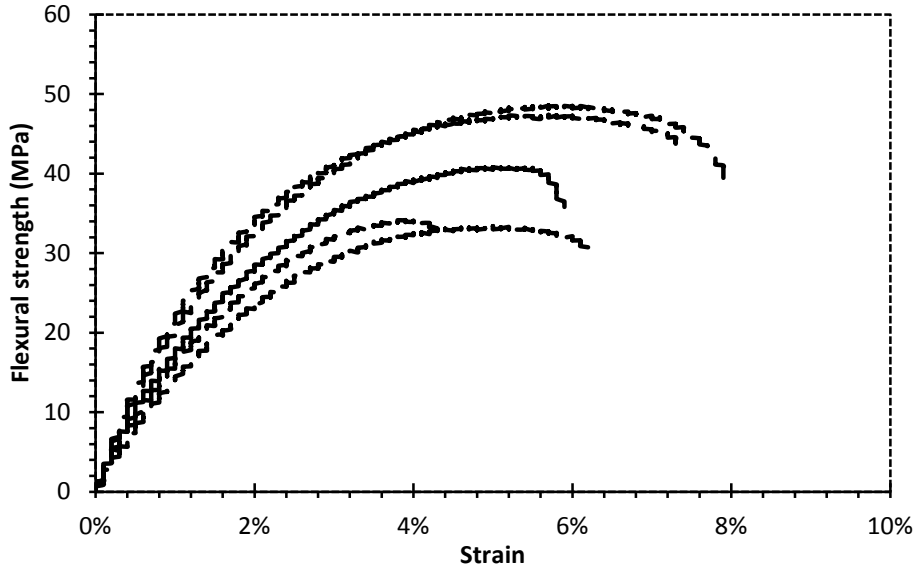

Figure 3.13: Typical flexural stress-strain curves of hemp fibre reinforced polypropylene composites.

3.6.4 Impact test

To investigate the impact performance of the composites, an un-notched Charpy impact test was carried out according to ASTM-D256, using an Instron Dynatup drop weight impact tester shown Figure 3.14. The Instron impact test was used to characterise the impact performance of composites with varying original fibre length. Sample dimensions were 160 mm x 10 mm x 4 mm for impact testing. A total of 5 specimens per compositions were used to determine the impact properties of the composites. Appendix 1 shows a summary of mechanical property results. .

3.6.5 Free Vibration-Damping Testing

To perform free vibration damping tests, specimens were held as a cantilever beam. The free-end of each sample attached to an accelerometer and the vibration was triggered using a rubber hammer. Figure 3.15 gives a schematic view of the vibration system set-up.

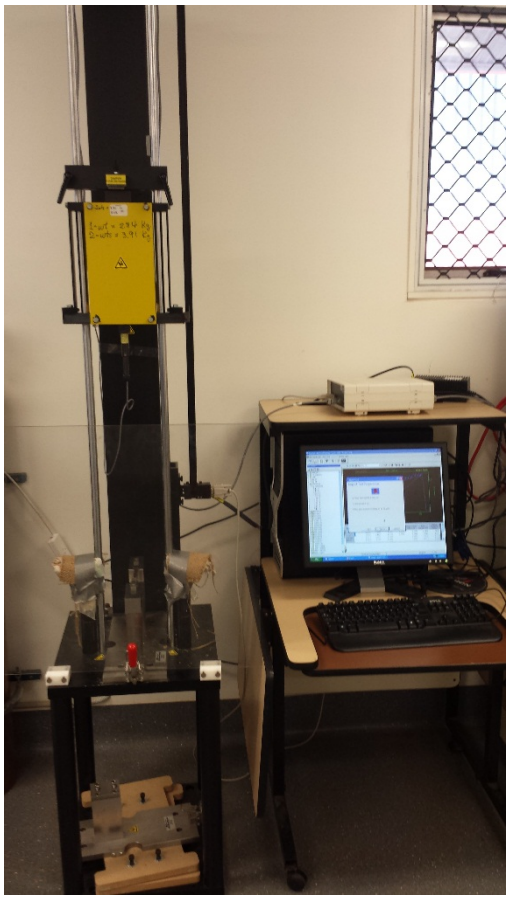

Figure 3.14: Instron Dynatup Model 8200 drop weight impact testing instrument.

Three specimens of each composition with the size of 17 mm × 10 mm × 4 mm were used for the vibration test and the cantilever beam length was kept at 16 mm for all specimens. The vibration acceleration time histories were recorded by a data acquisition program. The logarithmic decrement was used for calculating the damping ratio ξ of the cantilever beam from the recorded acceleration time histories based on the following equation (Yan, 2012).

$$\xi = \frac{1}{2\pi j} \ln\left(\frac{x_i}{x_{i+j}}\right) \tag{3.2}$$

where x_i is the peak acceleration of the i^{th} peak, x_{i+j} is the peak acceleration of the peak j cycles after i^{th} peak.

The vibration frequency spectrum was obtained from the measured time-histories according to the fast Fourier transformation (FFT). The first main peak corresponds to the natural frequency of the composite. The average damping ratio and average natural frequency from three specimens of each composite were reported.

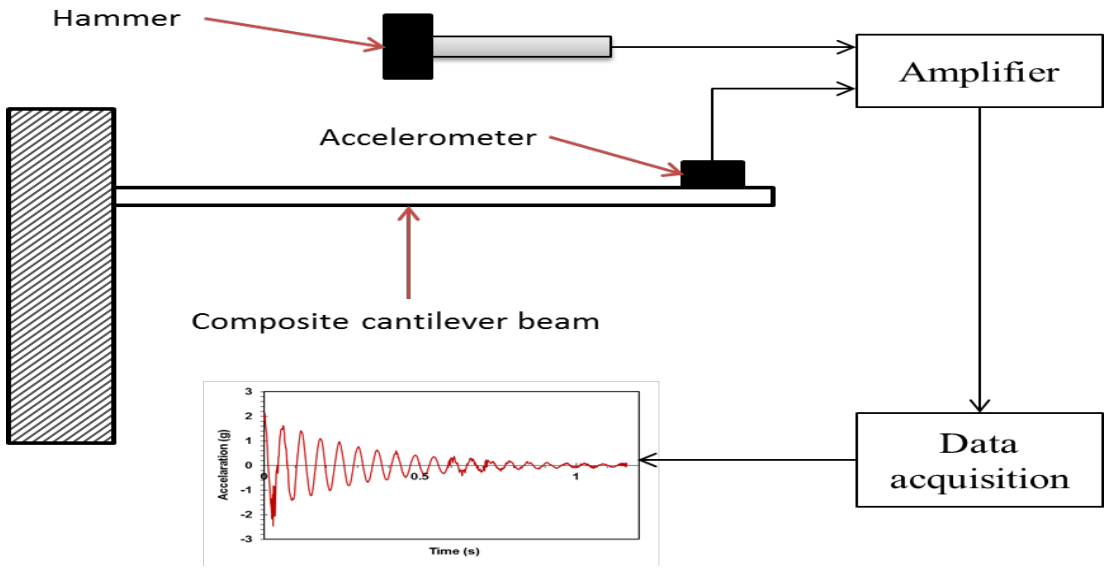

Figure 3.15: Schematic view of free vibration testing setup.

3.6.6 Dynamic Mechanical Analysis (DMA)

Dynamic mechanical analysis was performed using a DMA Q800, TA Instrument with a heating rate of 3˚C/min. A single cantilever mode and a low strain amplitude (20) were selected and the composites were scanned over a temperature range of 25-150˚C under different frequencies of 1, 10 and 100 Hz. The storage modulus (E′), loss modulus (E") and mechanical loss factor (tan δ) of the composite specimens were plotted vs. temperature at different frequencies. Dynamic mechanical analysis was

also carried out as a function of frequency, ranging from one to 200 Hz, at a fixed temperature of 25˚C. It should be noted that the cantilever length was 35 mm and the specimens cross-sections were 10 mm × 4 mm.

4. Hemp fibre Characterizations

4.1 Chemical Structure of the Fibres

Fourier Transform Infrared Analysis (FTIR) was used to indicate the influence of chemical treatment on variations of hemp fibre composition. Infrared spectra of un-treated hemp, treated hemp and noil hemp fibres are plotted in Figure 4.1. Table 4.1 summarises the major peaks observed in the FTIR spectra along with their possible sources.

In Figure 4.1, one of the most noticeable changes caused by alkali treatment is the disappearance of the peak at 1732 cm^{-1}. Referring to the literature, this can be attributed to the C=O carbonyl stretching in carboxylic groups that occur in the branched chain hemicelluloses and also in esterified and carboxylic groups in pectin. (Korte and Staiger, 2008, Sonia and Dasan, 2013). Therefore, the disappearance of the mentioned peak indicates the removal of pectin and hemicellulose from surface of the fibre.

The peak located at 1505 cm^{-1}, which originates from lignin, can be seen in the spectra before and after alkali treatment. Nevertheless, another peak associated with lignin (peak at 1246 cm^{-1}) was broadened after alkali treatment. It appears to indicate that the alkali can partially remove the lignin from the hemp fibre's surface.

As aforementioned, lignin is distributed in primary and secondary walls and within the middle lamella. In order to have a better fibre dispersion, it is required to remove

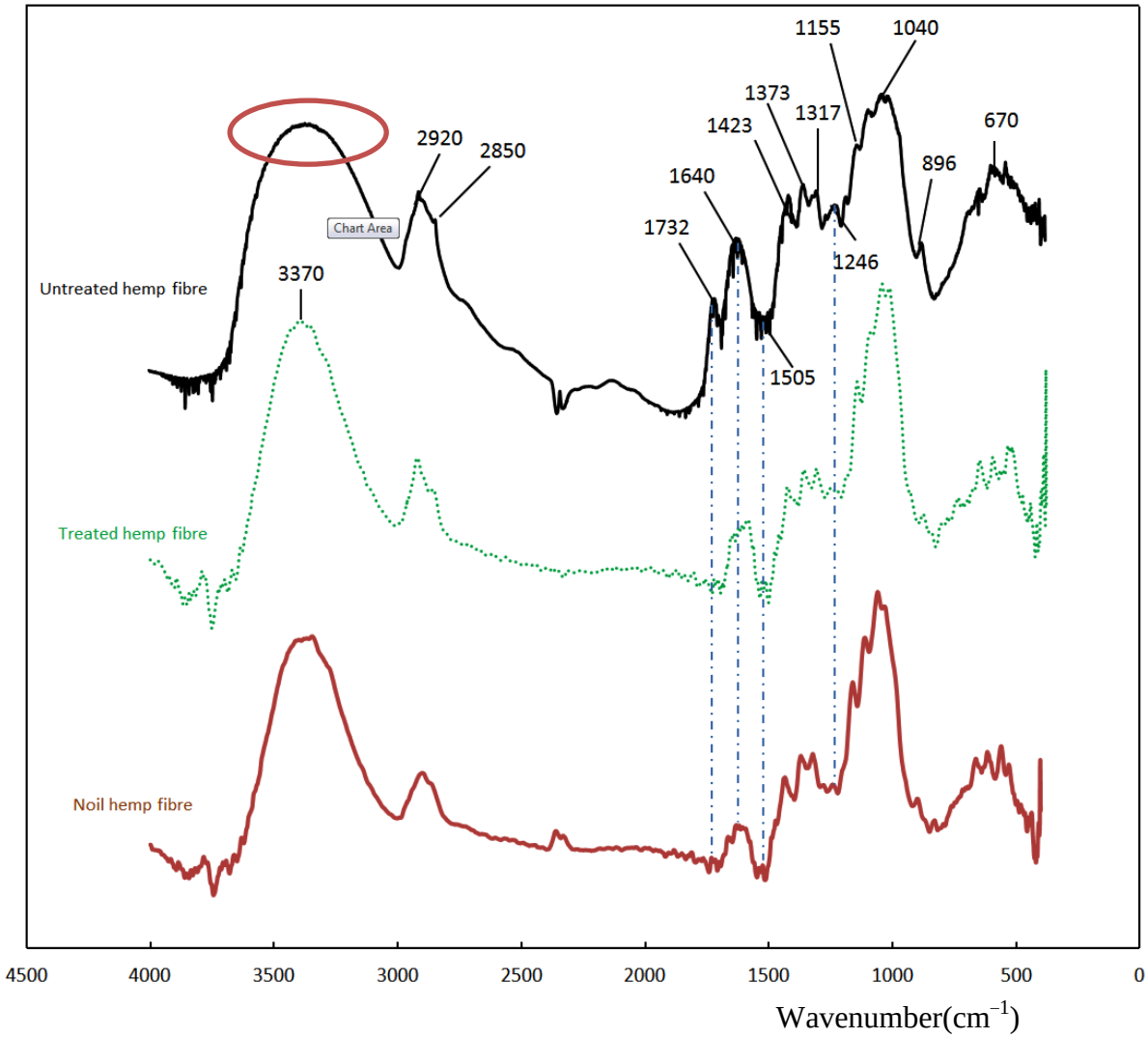

Figure 4.1: Infrared spectra of untreated, treated hemp and noil hemp fibres.

lignin from middle lamella because its degradation in the cell wall can reduce fibre tensile strength.

A blunt peak can be seen in FTIR spectra of untreated fibre in the region of 3250-3550 cm^{-1}. This peak is associated with the stretching vibration of the hydrogen bonding of the hydroxyl group. It is not sharp due to interfering contributions from a variety of stretching modes in the amorphous regions (Sonia and Dasan, 2013). However, after removal of the amorphous materials (hemicellulose, pectin and lignin), the peak becomes sharper at 3370 cm^{-1}. Besides this, there is another sharp peak in the FTIR spectrum of untreated fibres around 1640 cm^{-1}, which is associated with the OH bending of absorbed water. This peak broadened after alkali treatment. Thus, treating the fibres reduced the moisture absorbance of the fibres by removal of hydrophilic lignocellulosic materials which include accessible hydroxyl groups.

It is worth mentioning that FTIR spectrum of the noil hemp fibre was very similar to the FTIR spectra of the treated fibre. Noil hemp fibre contains almost the same type of chemical components as treated hemp fibres.

Table 4.1: The major peaks observed in the FTIR spectra and their possible source (Dai and Fan, 2010, Liu et al., 2013, Sedan et al., 2007, Le Troedec et al., 2009)

Wavenumber (cm^{-1})	Vibration	Sources
670	C-OH out-of-plane bending	Cellulose
896	COC,CCO and CCH deformation and stretching	Cellulose
1040	C-C, C-OH, C-H ring and side group vibrations	Cellulose, Hemicellulose
1155	C-O-C asymmetrical stretching	Cellulose, Hemicellulose
1246	C–O aryl group	Lignin
1317	CH_2 rocking vibration	Cellulose
1373	In-the-plane CH bending	Cellulose, Hemicellulose
1423	HCH and OCH in-plane bending vibration	Pectin, lignin, hemicellulose and calcium pectates
1505	C=C aromatic symmetrical stretching	Lignin
1640	OH bending of absorbed water	Water
1732	C=O stretching	Xylans (hemicelluloses)
	Esterified and carboxylic groups	Pectin
2850	CH_2 symmetrical stretching	Wax
2920	C–H symmetrical stretching	Cellulose
3370	O–H linked shearing	Polysaccharides

4.2 Fibre Morphology Analysis

The morphology of the fibres was studied by scanning electron microscope (SEM). SEM micrographs of the fibre surfaces can be seen from Figure 4.2 to Figure 4.5. Figure 4.2 reveals the SEM micrographs of an untreated hemp bundle with a diameter of approx. 75 µm and the fibre surface is covered by the gummy polysaccharides of

pectin and hemicellulose. These materials are partially or completely removed after alkali treatment, as can be seen in Figure 4.3. Removal of the lignin, pectin and hemicellulose alters the morphology of the hemp fibre. The fibres can partially or completely be separated into elementary fibres after alkali treatment. The separation lines, which show continuous elementary fibres, can be viewed in this figure. The elementary fibres are aligned along with the fibre axis with a diameter of approximately 10 µm. In comparison with the untreated fibre, the treated fibres are clean but rough. The roughness enhances mechanical interlocking bonding mechanisms between fibre and the matrix and the clean surfaces are supposed to create stronger bonding between OH groups of the fibre and the matrix by the coupling agent. This observation clearly indicated that alkali treatments could remove the hemicellulose and lignin coverings from the fibre surfaces. Figure 4.4 shows the SEM micrographs of a noil hemp fibre. As can be seen in this figure, the fibre surfaces are completely clean of gummy polysaccharides. The elementary fibres are more separated and their diameter is approximately 10 µm. The low thickness of the noil hemp fibre bundle (Technical fibre) and its cleanness imply that cementing materials are already removed during the degumming processes in the textile industry. Thus, in correlation with FTIR analysis, noil hemp does not require any treatments to remove the non-cellulosic materials (pectin, lignin and hemicellulose).

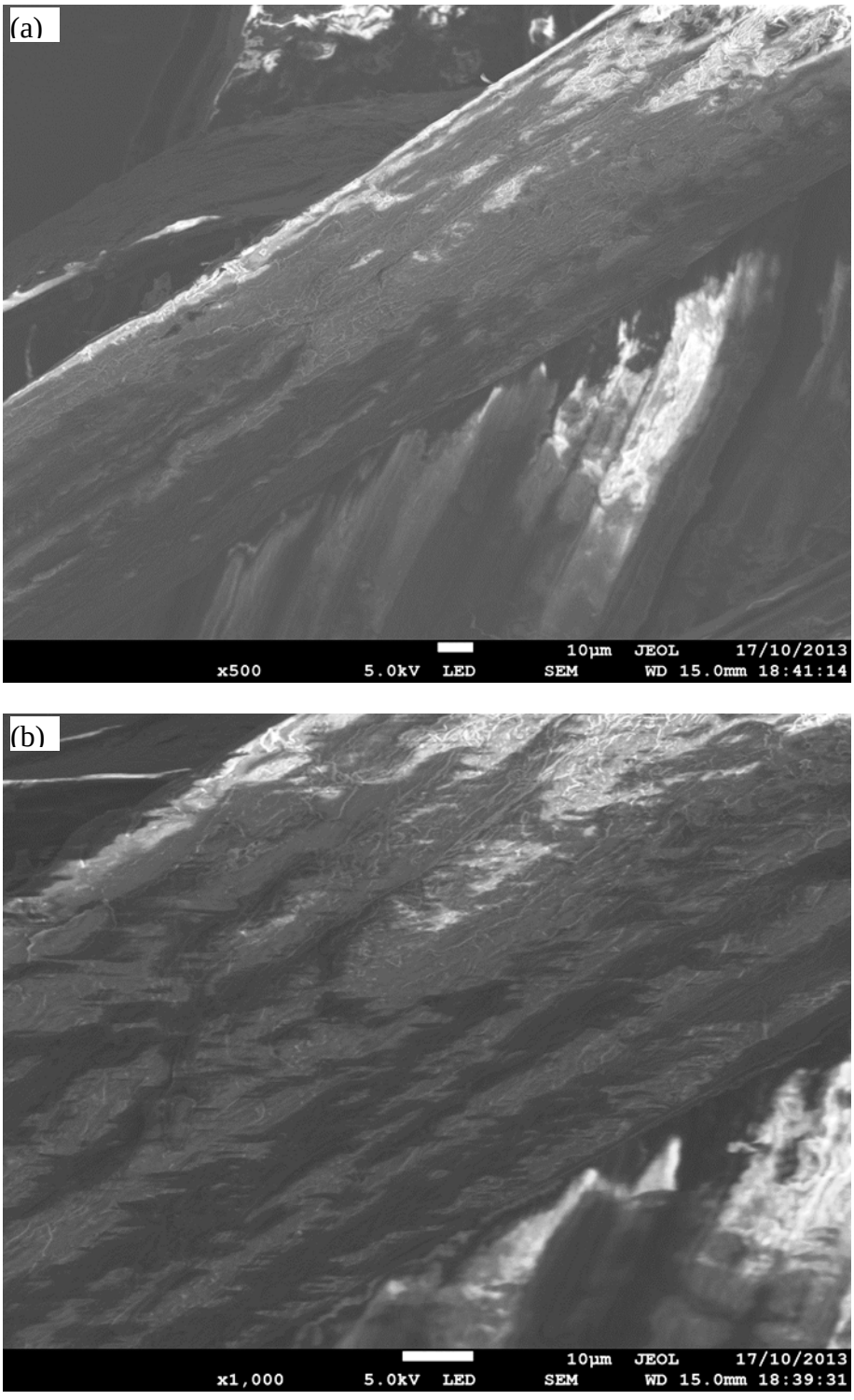

Figure 4.2: (a) x500 and (b) x1000 of SEM micrographs of an untreated hemp bundle (the surface is covered by the gummy polysaccharides)

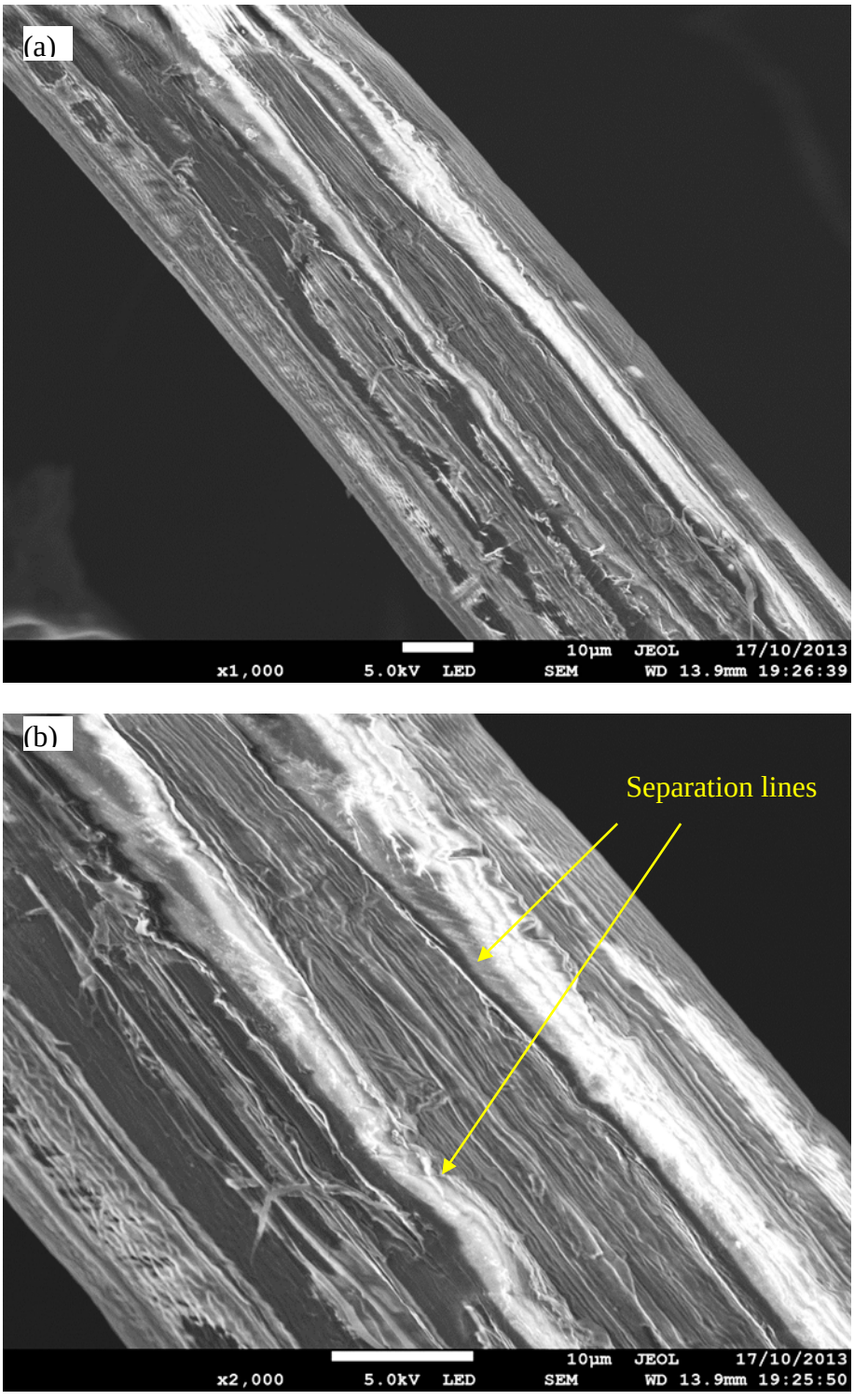

Figure 4.3: SEM micrographs of a treated hemp fibre, (a) x1000 and (b) x2000

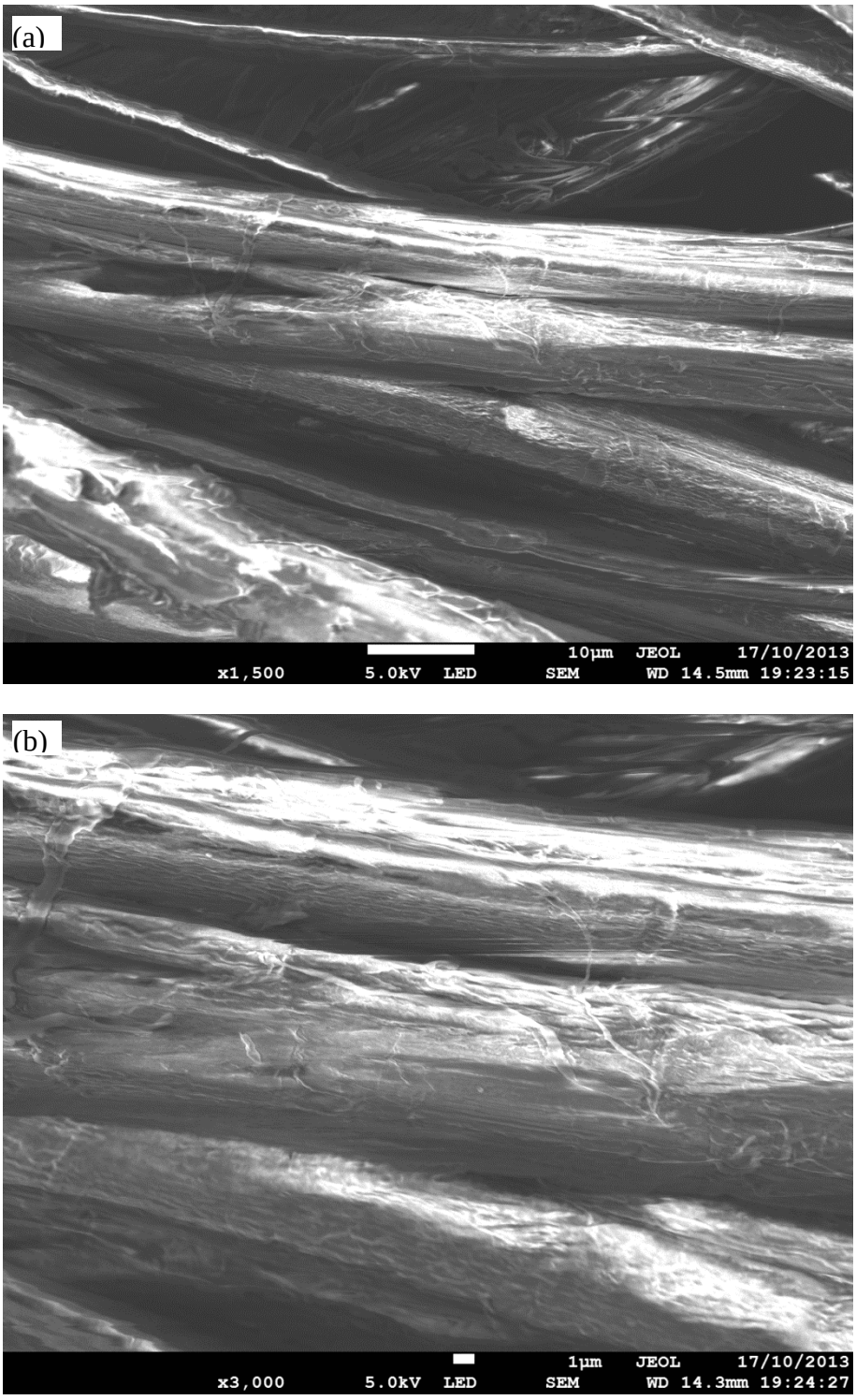

Figure 4.4: SEM micrographs of the noil hemp fibre (elementary fibres are already separated) (a): x1500 and (b) x3000.

Two main types of defects, which are expected to be found in the cell walls of the natural fibres, are known as kink bands and micro cracks. Figure 4.5 shows the kink band observed in SEM micrographs of noil hemp fibres. At the kink band regions, the angle of the micro fibrils relative to the fibre axis differs from the angle of the surrounding cell wall, which corresponds to a change in the crystalline orientation. It has been reported that the kink bands suggest a lower strength and they are the most likely area to break during the tensile tests of fibres (Baley, 2004, Symington et al., 2011). Figure 4.6 shows SEM micrographs of noil hemp fibres including micro-cracks in fibre cell wall along the fibre length. Micro cracks lead to stress concentrations when fibres are under load. Not only do these defects cause variability in fibre properties but they also reduce fibre strength considerably.

These defects in natural fibres arise from two main sources: (1) during growth and (2) during processing of fibres. More defects (micro-cracks) were observed in noil hemp fibres because they are highly processed during textile manufacturing. Thus, it can be expected that noil hemp fibres have lower tensile strength than normal hemp fibres.

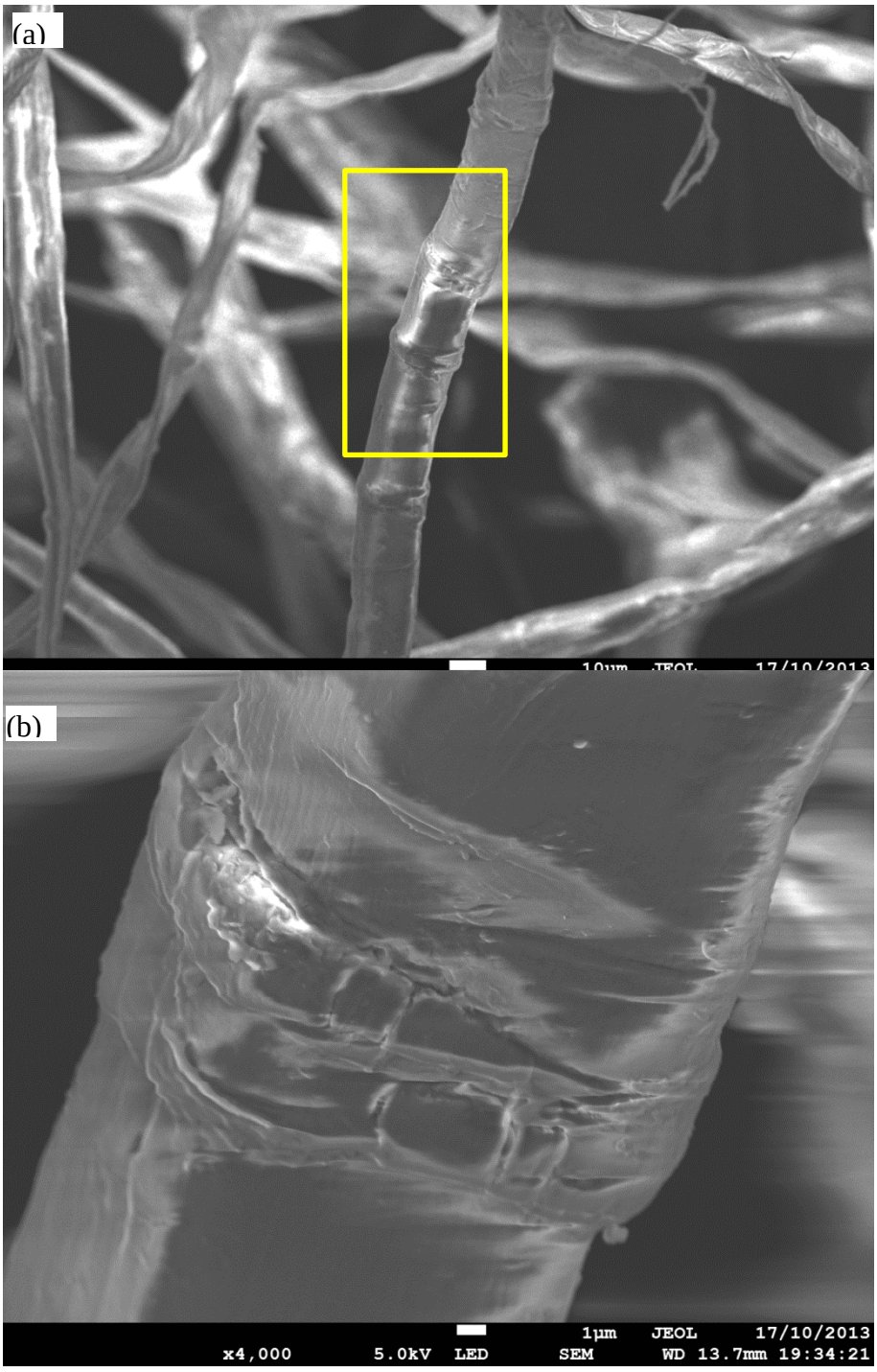

Figure 4.5: SEM micrographs of noil hemp fibres presenting the kink band clearly observed in noil hemp fibres, (a) x500 and (b) x4000.

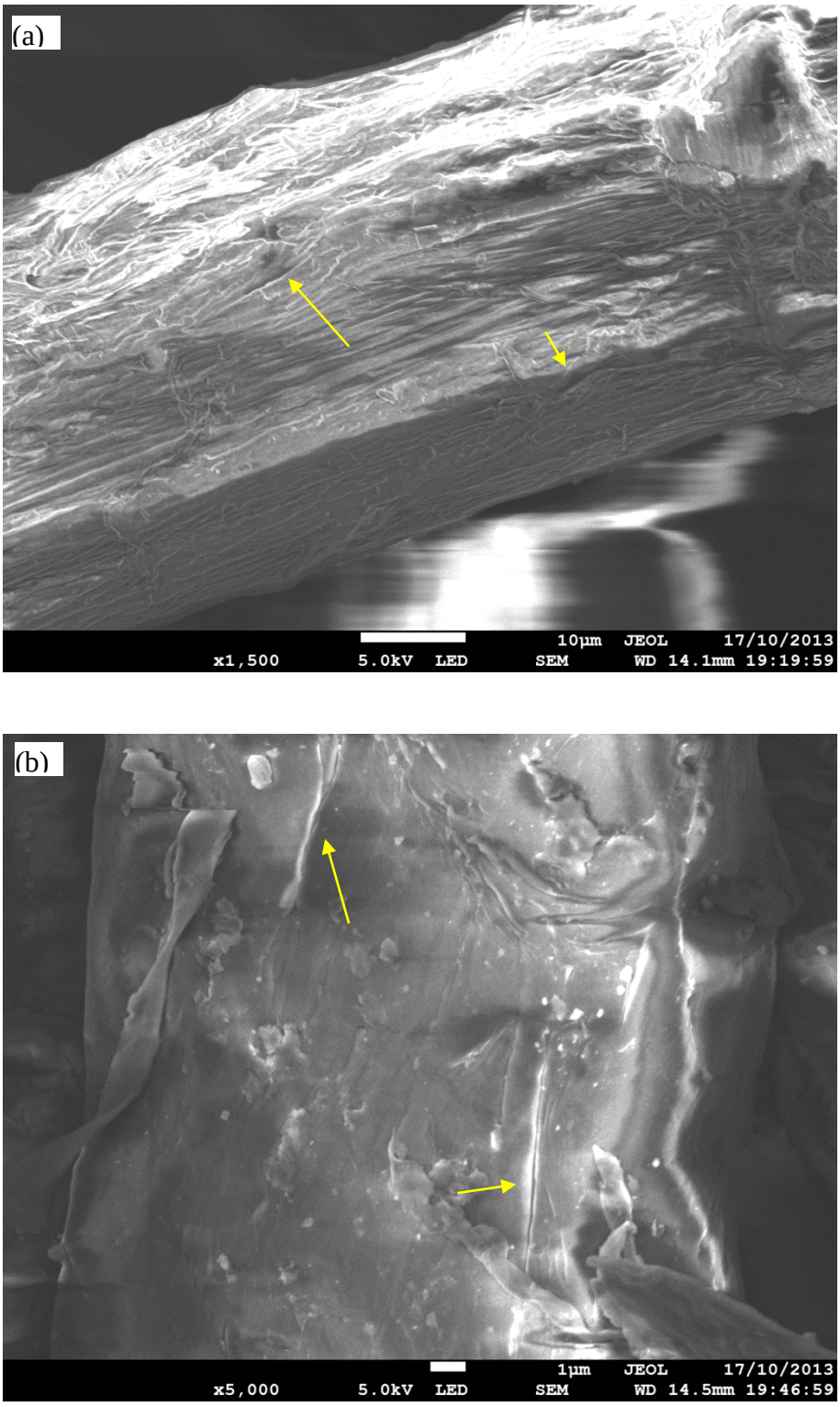

Figure 4.6: SEM micrographs of noil hemp fibres presenting the micro cracks, (a) x1500 and (b) x5000.

4.3 Thermal Degradation of the Fibres

Thermal analysis of untreated, alkali treated and noil hemp fibres was conducted via Differential Scanning Calorimetric (DSC) and Thermogravimetric Analysis (TGA) according to the procedure mentioned in section 3.5.

4.3.1 Thermogravimetric Analysis (TGA)

Figure 4.7 presents TGA and derivative thermogravimetric (DTG) plots of untreated hemp fibres. Four different stages can be recognised in the degradation behaviour of the untreated hemp fibre as shown in Figure 4.7. At the 1st stage, when the temperature was below 100˚C, the gradual decrease in TGA curve can be observed due to the evaporation of residual moisture (free water) in hemp fibre. The 2nd stage was almost a steady state although small weight loss can be seen, which is associated with the loss of carbon-dioxide or other low molecular weight organic compounds. The 3rd stage starts around 200˚C and finishes around 400˚C. The main weight loss occurred in this stage (62%). This stage can be divided into two further separated steps. Weight decrease is lower in the first step than in the second step. The first step occurs because of degradation of cementing materials mostly pectin and hemicellulose while, the sharp drop happens due to the decomposition of cellulose structure. Decomposition of the cellulosic part results in formation of levoglucosan and other volatile products. Therefore, in the last stage, more weight loss was observed because of volatilization of mentioned products when temperature increased above 400˚C .

Figure 4.8 compares the TGA plots of untreated, alkali treated and noil hemp fibres. It can be seen that significant thermal degradation of untreated, alkali treated and noil hemp fibres begins at approx. 200^{o}C, 220^{o}C and 225^{o}C respectively.

The first step of the third stage can be observed for untreated fibre while it was almost non-existent for treated fibres and noil hemp fibres. This implies that thermal degradation of untreated fibre at lower temperatures is due to the presence of thermally unstable fibre constituents such as pectin and hemicellulose. On the other hand, a fibre is more thermally stable (by approx. 20°C) after the removal of the cementing materials (Kabir et al., 2013).

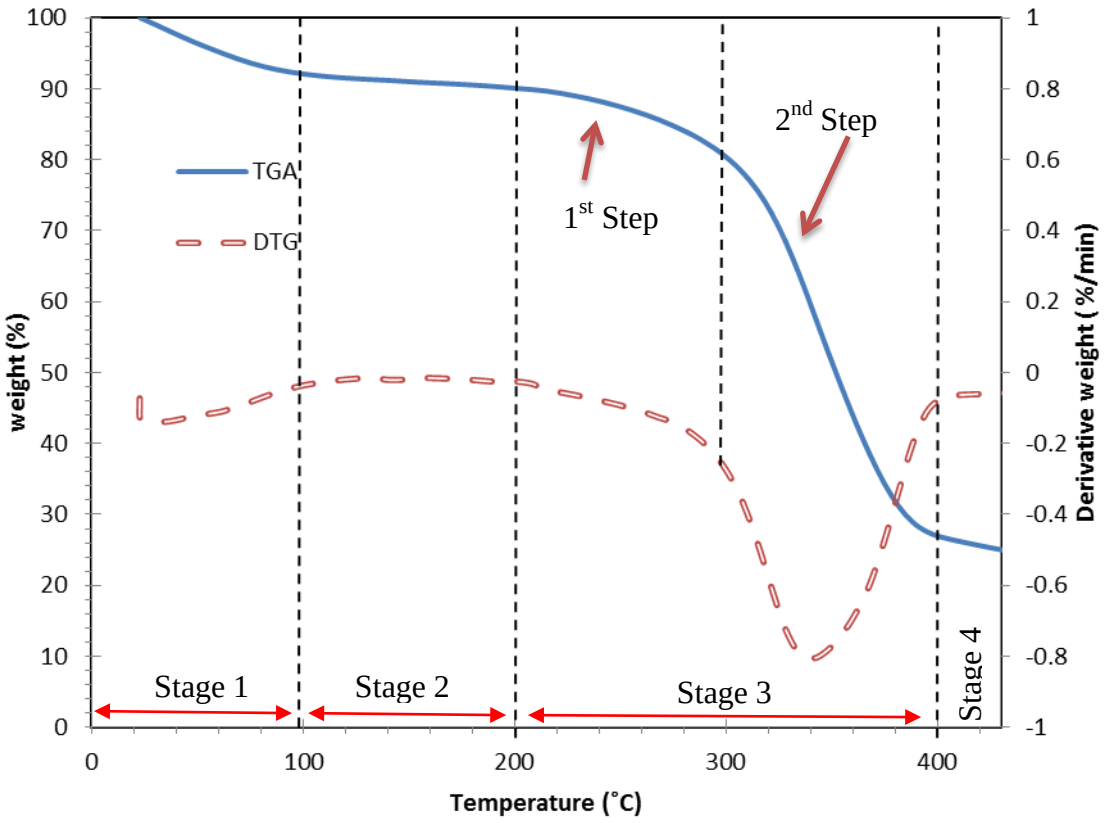

Figure 4.7: TGA and DTG curves of untreated hemp fibre.

Table 4.2 provides the weight loss and the onset of thermal degradation at different stages. Referring to Figure 4.8 and Table 4.2, unlike the untreated fibre, treated and noil fibres show similar thermal behaviour due to the removal of cementing materials. It should be noted that the third stage for untreated fibre started at 205˚C while at least 20˚C raise was observed in the onset temperatures for thermal degradation of treated fibres in this stage.

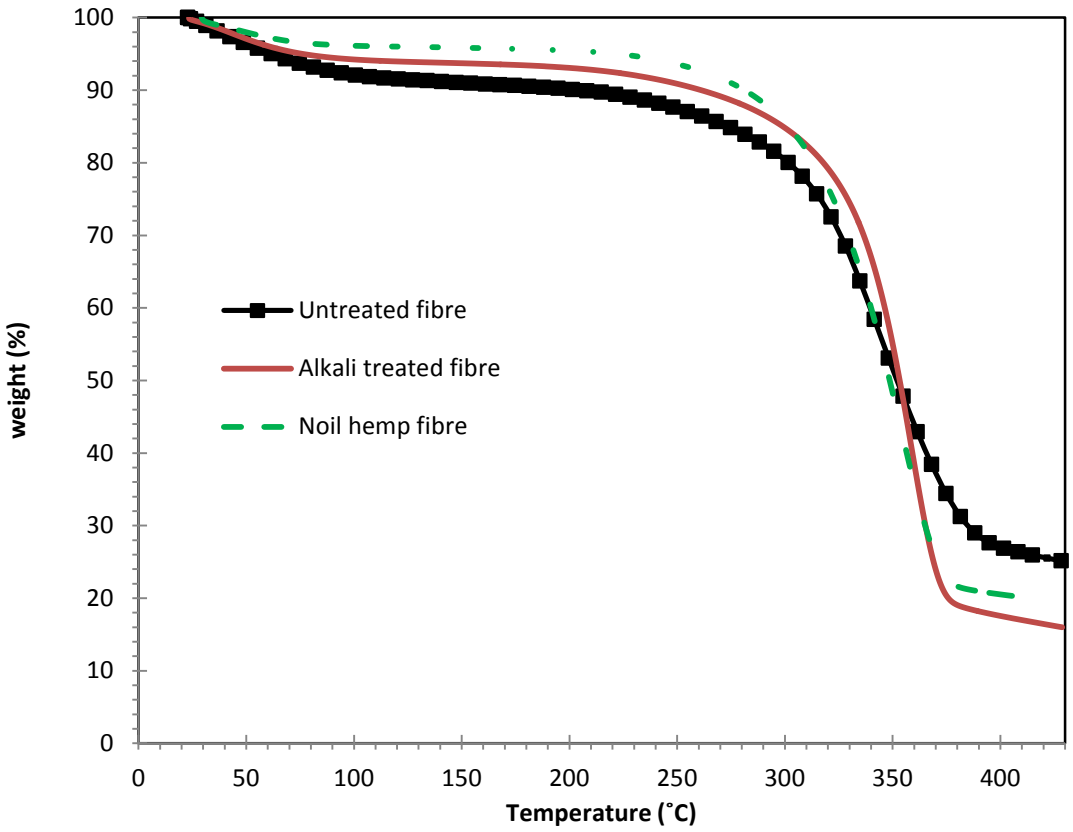

Figure 4.8: TGA curves of untreated, alkali treated and noil hemp fibres.

It is also worth mentioning that the maximum weight loss in first stage was determined as 8% for untreated fibre, referring to Table 4.2. As mentioned previously, the weight loss in the first stage is related to evaporation of moisture. Therefore, it can be concluded that existence of more cementing materials (pectin, lignin and

hemicellulose) indicates untreated fibres have more potential for moisture absorption when compared to the treated and noil hemp fibres.

Table 4.2: Temperature ranges and weight loss percentage of untreated and treated hemp fibres at different stages

Samples	Stage 1		Stage 2		Stage 3		Stage 4	
	Temp. range (˚C)	Weight loss (%)	Temp. range(˚C)	Weight loss (%)	Temp. range(˚C)	Weight loss (%)	Temp. range(˚C)	Weight loss (%)
Untreated	25-100	8.00	100-200	2.00	200-395	62.46	395-430	2.85
Alkali treated	25-100	5.77	100-220	1.95	220-375	71.97	375-430	4.33
noil hemp fibre	25-100	3.87	100-225	1.21	225-375	71.33	375-430	3.21

4.3.2 Differential Scanning Calorimetry

In order to study the thermal properties of untreated, treated and noil hemp fibres, Differential Scanning Calorimetric (DSC) analysis was utilised. The DSC curves of the fibres are presented in Figure 4.9.

There is an initial endothermic peak (peak#1) that can be observed between 50 and 150˚C, which is attributed to the evaporation of the moisture, including the free water and physisorbed water. DSC results show higher moisture absorption of untreated hemp than that of treated hemps.

There are different peaks that can be seen in the DSC curves in Figure 4.9. Analysis of these peaks requires understanding of the thermal behaviour of hemp fibre ingredients.

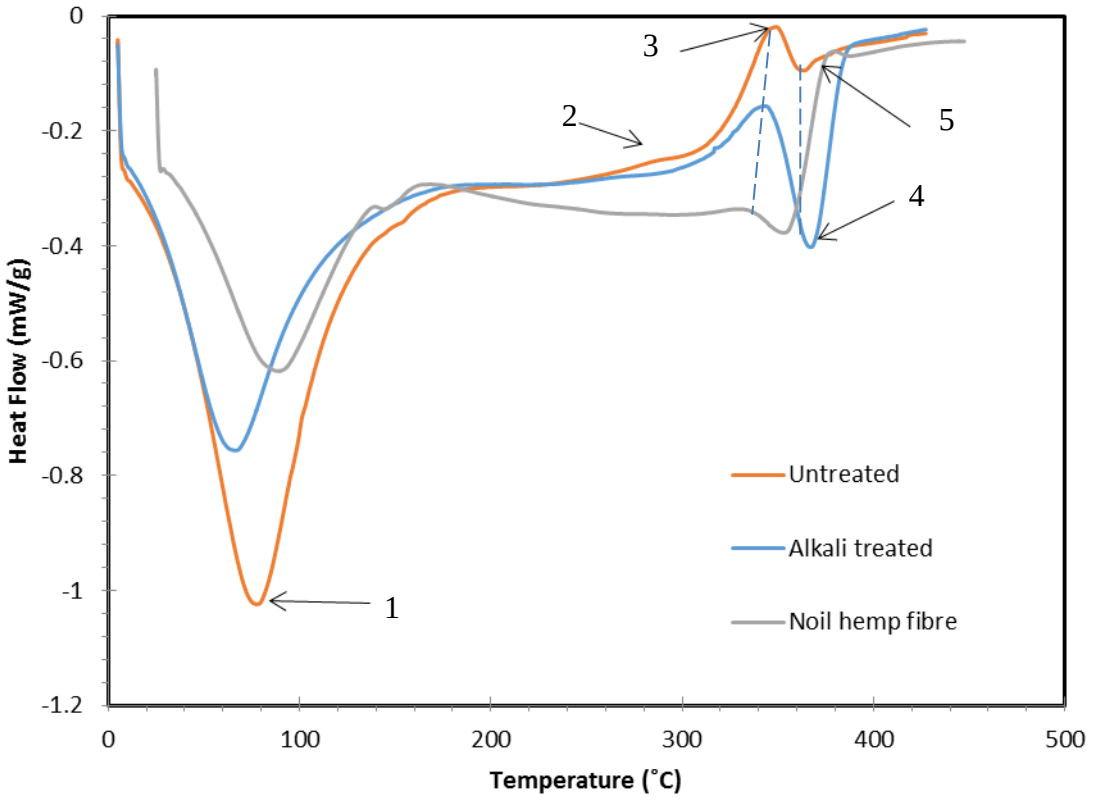

Figure 4.9: DSC curves of untreated, alkali treated and noil hemp fibres.

Referring to the literature, (Rachini et al., 2009, Yang et al., 2007, Kifani-Sahban et al., 1997), pectin thermal degradation causes an endothermic peak at 224˚C. Also, hemicellulose degradation occurs between 200˚C and 315˚C with an exothermic peak at 235˚C. DSC testing of cellulose extracted from hemp fibres shows a broad endothermic behaviour in the temperature range of 315-360°C and a small exothermic event at around 360°C. In the endothermic event, depolymerisation of cellulose occurs with the formation of volatiles. The depolymerisation process also generates cellulose char residue via exothermic reactions (Kim and Eom, 2001). Lignin degrades in a wide range of temperatures from 280˚C to 500˚C with an exothermic reaction (Kifani-Sahban et al., 1997).

Therefore, there were three outcomes of simultaneous thermal depolymerisation of hemicellulose, pectin and a portion of lignin components. These were:

1. A slight increase in heat flow (thermal degradation) of untreated hemp fibre from 200 ˚C

2. A small exothermic peak (peak #2) at the temperature range of 250-290°C

3. An exothermic peak at around 340˚C (peak#3).

The small exothermic peak (peak#2) disappeared and the sharp peak (peak#3) reduced for the treated and noil hemp fibres due to the removal of pectin and hemicellulose from the external surface of hemp fibres.

The reaction of lignin and cellulose at the same temperature range caused a small endothermic peak at 360˚C (peak#4) for untreated fibres. Due to the removal of lignin partially in the treated hemp fibre and noil hemp fibres, another exothermic peak associated with the cellulose degradation observed at approximately 380˚C while this peak was not significant.

To conclude, thermal analysis of investigated fibres revealed that alkali treatments could improve the thermal stability of treated hemp fibres by removing the cementing materials especially hemicellulose and pectin. In addition, treated hemp fibres and noil hemp fibres are thermally more stable than untreated fibre since high amount of lingo-cellulosic materials have been removed from the fibres during textile manufacturing.

4.4 Strength of the Fibres

Single fibre tensile tests were first established to measure the tensile strength and modulus of synthetic fibres. In order to measure the strength of the fibres, a cross-sectional area of the fibres must be found. The cross-section area was assumed consistent and cylindrical for synthetic fibres. However, this assumption cannot be true for natural fibres because natural fibres consist of a bundle of elementary fibres, which results in an irregular shape. Moreover, the elementary fibre cannot be assumed perfectly cylindrical too. Therefore, measuring the cross-sectional area is one of the most controversial challenges associated with all types of natural fibres.

Three methods suggested measuring the cross section area of natural fibres. In one method, a fibre is assumed cylindrical and the average fibre diameter from five different random locations is obtained to determine the cross section area of the fibre. In another method, the minimum diameter of a fibre is considered for determining cross-section area of the fibre. There is no certainty that the natural fibre's failure during tensile testings will occur at the smallest cross-section area because failure is most likely to take place where a defect is situated (Davies and Bruce, 1998, Arbelaiz et al., 2005). It is also reported that the probability of fibre break at minimum diameter is in the range of 40–60% (Yu et al., 2003). In another method proposed by Wei Hu et. al. (Hu et al., 2010b, Hu et al., 2010a), an accurate cross-sectional area could be obtained from the SEM observation of a flat and clear fractured end surface. Although this method requires a reasonable number of test specimens (six specimens), there are still some issues relating to this method. Sample preparation is time-consuming and an SEM Machine is necessary for observing the cross section of

fibres. So, in the current project, the first conventional method was utilised for measuring fibre diameter and the calculation of cross-sectional area.

The average diameter of untreated, alkali treated and noil hemp fibres is illustrated in Figure 4.10. 20-30 replicates for each type of fibre were involved. As can be seen in this figure, alkalization had an impact in the reduction of hemp fibre diameter due to the removal of adhesives from the fibre cell wall. In other words, alkalization was responsible for removing pectin, lignin and hemicellulose from surface of the fibres. It can also be seen that noil hemp fibres have even smaller diameters than alkali treated hemp fibres due to the higher removal of cementing materials from surface of the fibres.

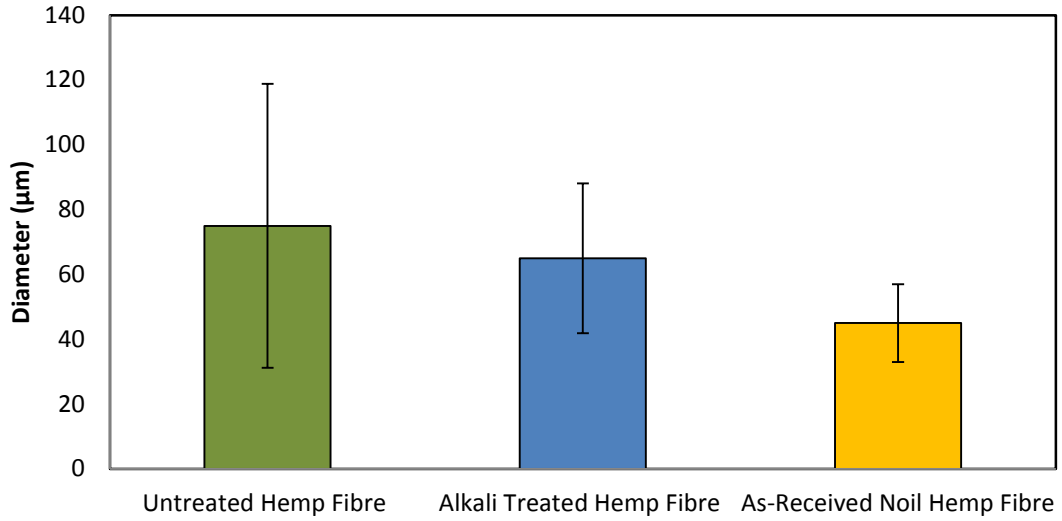

Figure 4.10: A comparison of average diameter of untreated, alkali treated and noil hemp technical fibres.

The tensile properties of single hemp fibres were evaluated according to section 3.6.1 for all fibres. Figure 4.11a and Figure 4.11b show the typical stress-strain curves of single noil hemp fibres and the average tensile strength values of untreated, treated and noil hemp fibres, respectively.

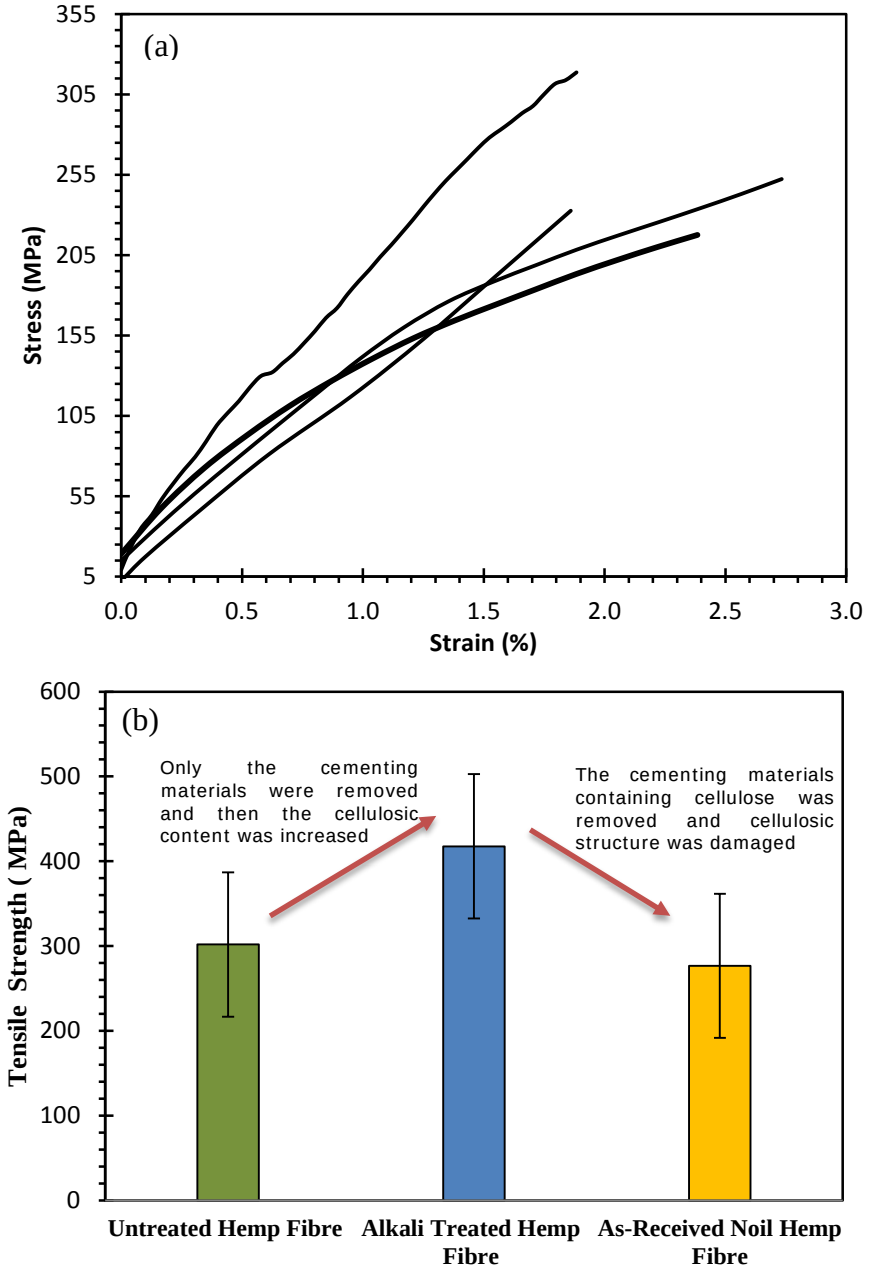

Figure 4.11: (a) Typical stress-strain curves of single noil hemp fibre at gauge length of 12 mm and (b) Tensile strength of the untreated, alkali treated and noil hemp fibres at the same gauge length.

It can be seen that the stress-strain curves were almost linear until fracture of the fibre occurred. The results also show that the tensile strength of the 5 wt% alkali treated fibre is almost 40% higher than that of the untreated fibre. The increase in tensile strength of the treated fibre was due to removal of some cementing materials (non-strength materials), which resulted in smaller cross-sections of fibres in single fibre tensile testing. Besides this, removal of cementing materials (i.e. pectin, lignin and hemicellulose) may have improved the cellulose chain packing order (Clemons et al., 1999). On the other hand, noil hemp fibres showed 8% lower tensile strength compared with untreated fibre.

As mentioned previously, the transversal cross section of hemp is not cylindrical and there are many defects that can exist along the fibre's length. Thus, this great deviation is inevitable in studying the characteristics of hemp fibres.

Although the standard deviation of the data is high, it can be concluded that tensile strength of noil hemp fibres were significantly lower than those of normal hemp fibres. In other words, the noil hemp fibres have lower mechanical properties than even untreated hemp fibres. Significant reduction in mechanical properties of noil fibres is more likely due to the cellulose degradation (fibre defects) caused from over-degumming treatment in textile processing. Figure 4.12 presents micro-cracks, which can degrade the mechanical properties of the fibres, especially the tensile strength. It is believed that stress concentrations around micro-cracks can act as sites for the initiation of fibre matrix debonding, leading to fracture of the hemp fibre.

A significant reduction in hemp fibre strength has also been reported (Pickering et al., 2007b) as a result of cellulose degradation in alkali treatment due to the use of high NaOH concentration (10 wt%).

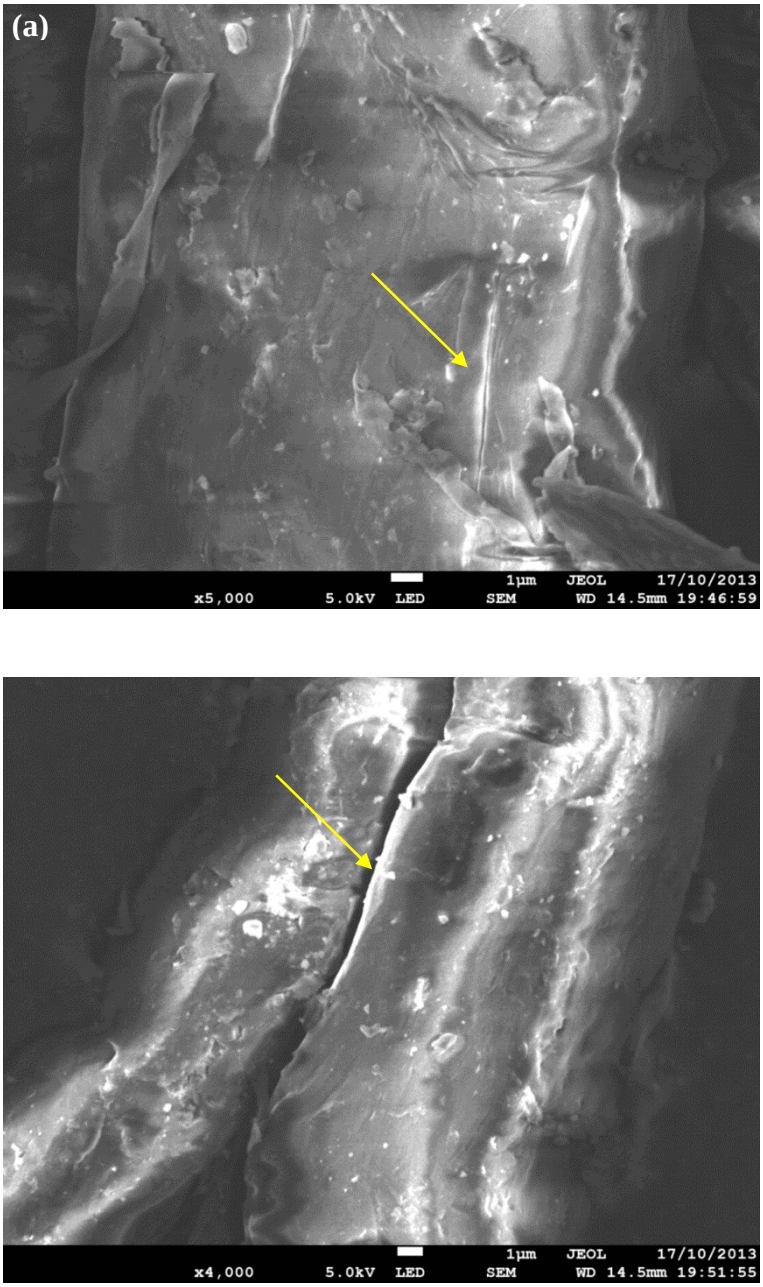

Figure 4.12: micro-cracks, which occurred due to the degumming process in noil hemp fibres in different investigate fibres.

It has been found that the initial cracks of hemp fibres under tension starts from the primary cell wall and then proceed into the secondary cell wall (Dai and Fan, 2010). The microfibril angle (MFA) in the inner part of the S2 layer is about 2.65° with respect to the fibre axis, while the MFA in the outer part of S2 layer ranges from 23° to 30°. This means that the strength of the inner part of the S2 layer should be higher than that of the outer part of the S2 layers. Therefore, cracks proceed into the secondary wall of hemp fibre, giving a breaking order of: S1 layer to the outer part of the S2 layer to the inner part of the S2 layer (Dai and Fan, 2010).

To conclude this chapter, Alkali treatments improved the thermal stability and strength of treated hemp fibres by removing the cementing materials especially hemicellulose and pectin. Referring to the thermal analysis, treated hemp fibres and noil hemp fibres are thermally more stable than untreated fibre since high amount of lingo-cellulosic materials have been removed from the fibres during textile manufacturing. Also, due to the cellulose degradation (fibre defects) caused from over-degumming treatment, tensile strength of noil hemp fibres were significantly lower than those of normal hemp fibres.

5. Microstructural Investigation

5.1 Fibre agglomeration

A typical projection image of the x-ray micro-tomography and a typical reconstructed cross section of the 20H sample are shown in Figure 5.1. A series of X-ray projection images was acquired and reconstructed to produce the 3D visualization of each sample. Figure 5.2 shows 3D views of 10H sample using the FIJI software package. Also, its 3D plug-ins (Schindelin et al., 2012, Iannuccelli et al., 2010, Bolte and CordeliÈRes, 2006) were used to improve the contrast and quality of the 3D visualization.

Figure 5.3 shows how fibre agglomerations (primary fibres that have tangled up together) can be extracted from the 3D model of the composites by utilizing increased levels of the threshold filter. Figure 5.4 compares fibre agglomeration of the composites with different fibre contents in a 2D view. As can be observed, a few agglomerations of fibres can be observed in the 10H sample. The amount of agglomerations was slightly increased with the increase in fibre content from 10 wt% to 30 wt% due to the limited compatibility between the cellulose fibres and the matrix. This results in poor dispersion of the fibres in the composite. Poor fibre dispersion means agglomeration of the fibres, which consequently creates an inhomogeneous microstructure.

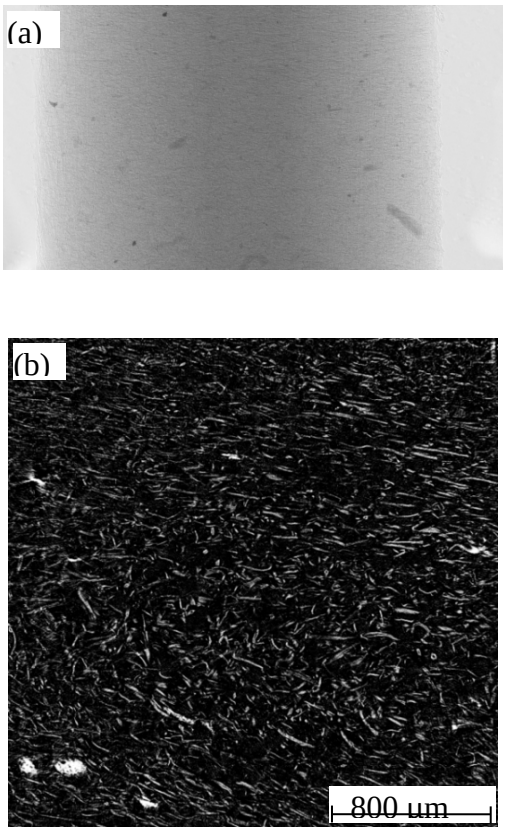

Figure 5.1: (a) a typical projection image and (b) a typical reconstructed cross section of a noil hemp fibre composite.

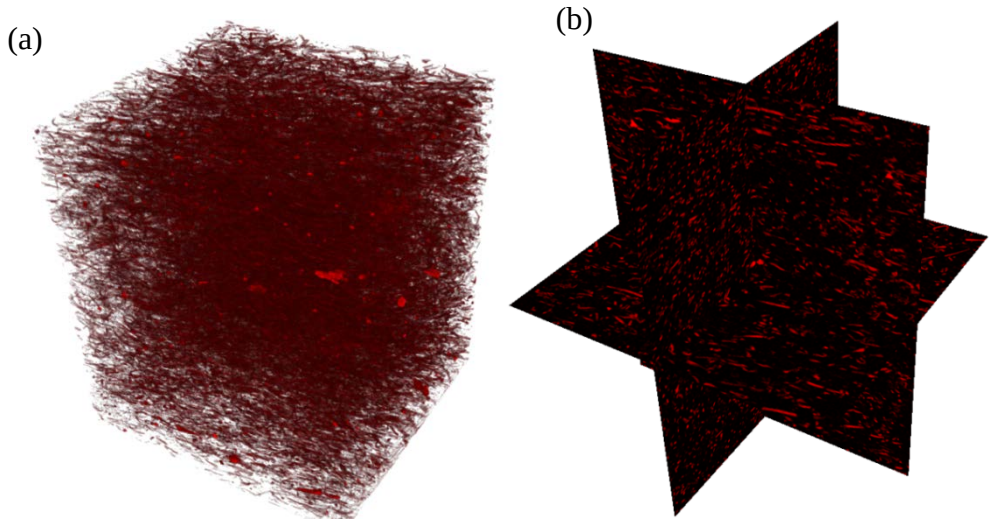

Figure 5.2: Reconstructed 3D view of 10H sample: (a) Volume view, (b) Orthoslice view

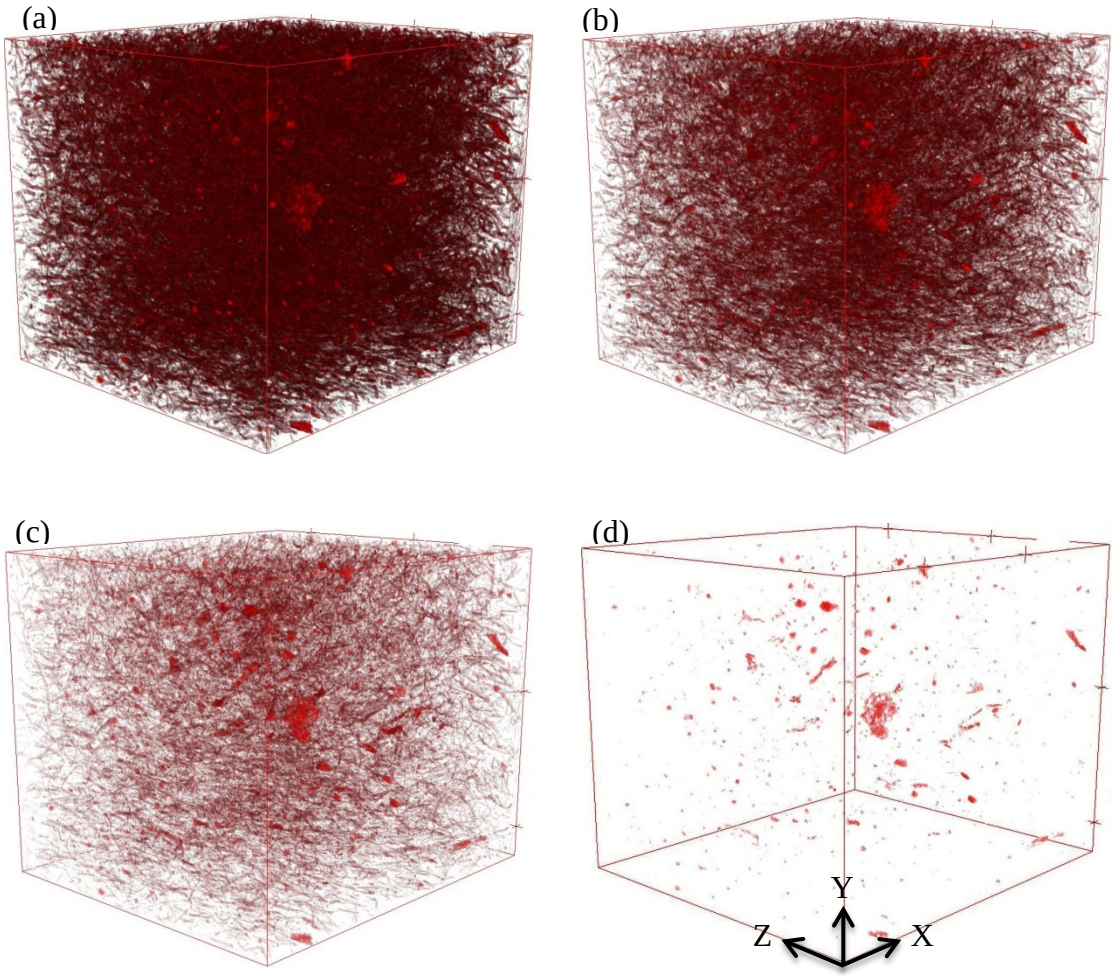

Figure 5.3: Extraction of the fibre agglomerations from 3D views of 10H sample using FIJI software package.

The fibre agglomeration in the composites with 40 wt%, 50 wt% and 60 wt% hemp fibre is significantly higher as can be seen in Figure 5.4. This concludes that in composites with fibre contents higher than 40 wt%, noil hemp fibres cannot be evenly dispersed in the matrix and hence extensive agglomeration of the fibres occurs, reducing the reinforcing effects of the fibres.

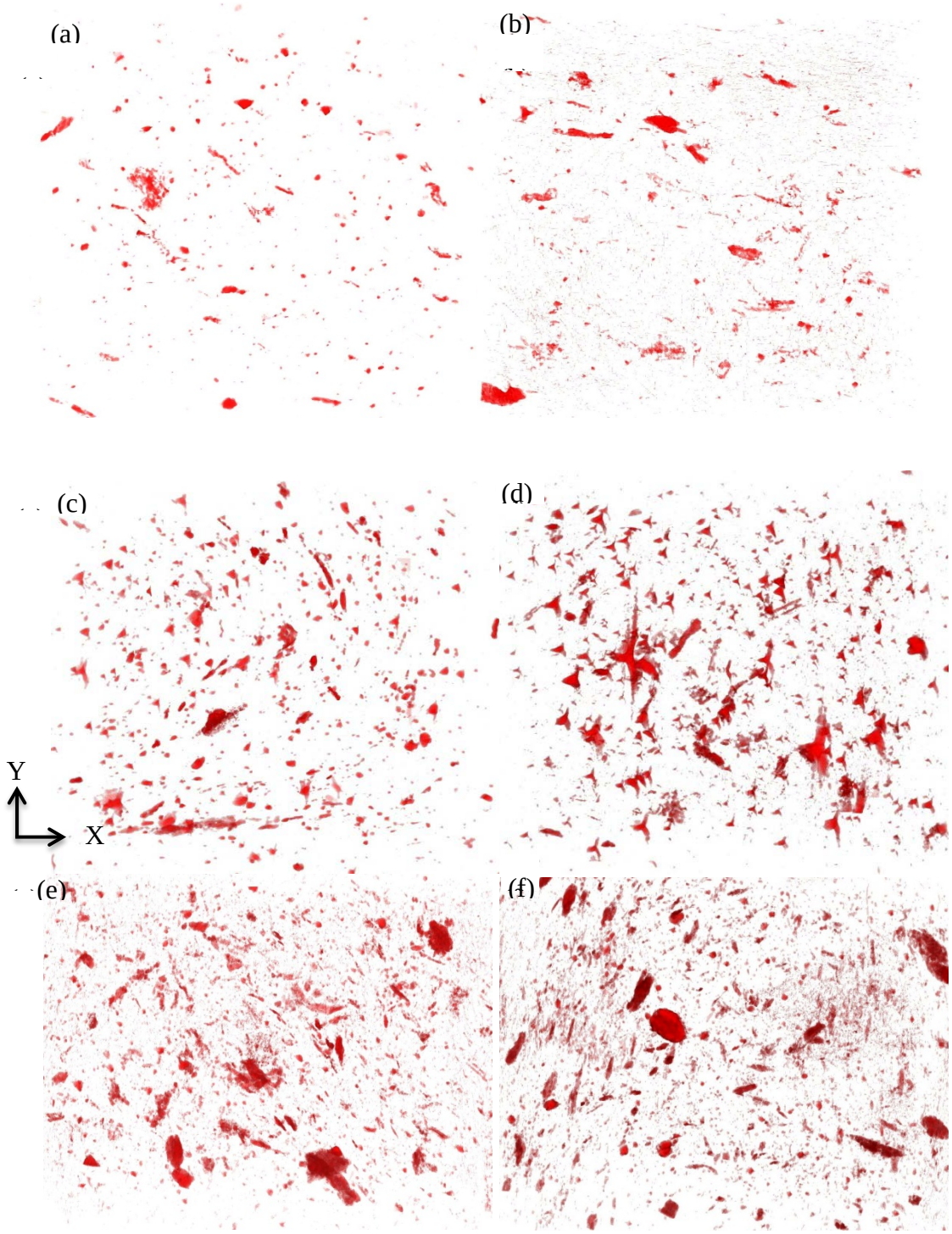

Figure 5.4: Extracted fibre agglomerations for the composites with (a) 10%, (b) 20%, (c) 30%, (d) 40%, (e) 50% and (f) 60% hemp fibre, seen in the z-axis. Figures were all done with the same filter levels

The effects of compatibiliser (MAPP) addition on dispersion of fibres in the composites can be observed in Figure 5.5 (30 wt% hemp fibre) and Figure 5.6 (40 wt% hemp fibres). It can be observed that the addition of 5 wt% MAPP resulted in better dispersion of fibres. The better fibre dispersion is attributed to the fact that the addition of coupling agents to the matrix improves the wettability of the matrix by reducing the contact angle, which ultimately results in a more homogenous structure (Zhou et al., 2013).

5.2 Fibre size analysis

A two-parameter Weibull distribution was employed to describe fibre size distribution of initial feedstock fibres and the fibres in the composite products. The Weibull distribution density function is given by (Bhattacharya, 2011):

$$f(x) = \frac{\alpha}{\beta}\left(\frac{x}{\beta}\right)^{\alpha-1} \exp\left\{-\left(\frac{x}{\beta}\right)^{\alpha}\right\},\ x > 0,\ \alpha > 0\ and\ \beta > 0 \tag{5.1}$$

Moreover, the cumulative Weibull distribution function is given by:

$$F(x) = 1 - \exp\left\{-\left(\frac{x}{\beta}\right)^{\alpha}\right\} \tag{5.2}$$

where α is the shape parameter and β is the scale parameter. In order to determine the shape and scale parameter of each sample, the Maximum Likelihood Estimator method was used and the Eq. 5.3 was solved.

$$\frac{\sum_{i=1}^{n} x_i^{\alpha}\ ln\, x_i}{\sum_{i=1}^{n} x_i^{\alpha}} - \frac{1}{\alpha} - \frac{\sum_{i=1}^{n} x_i^{\alpha}}{n} = 0 \tag{5.3}$$

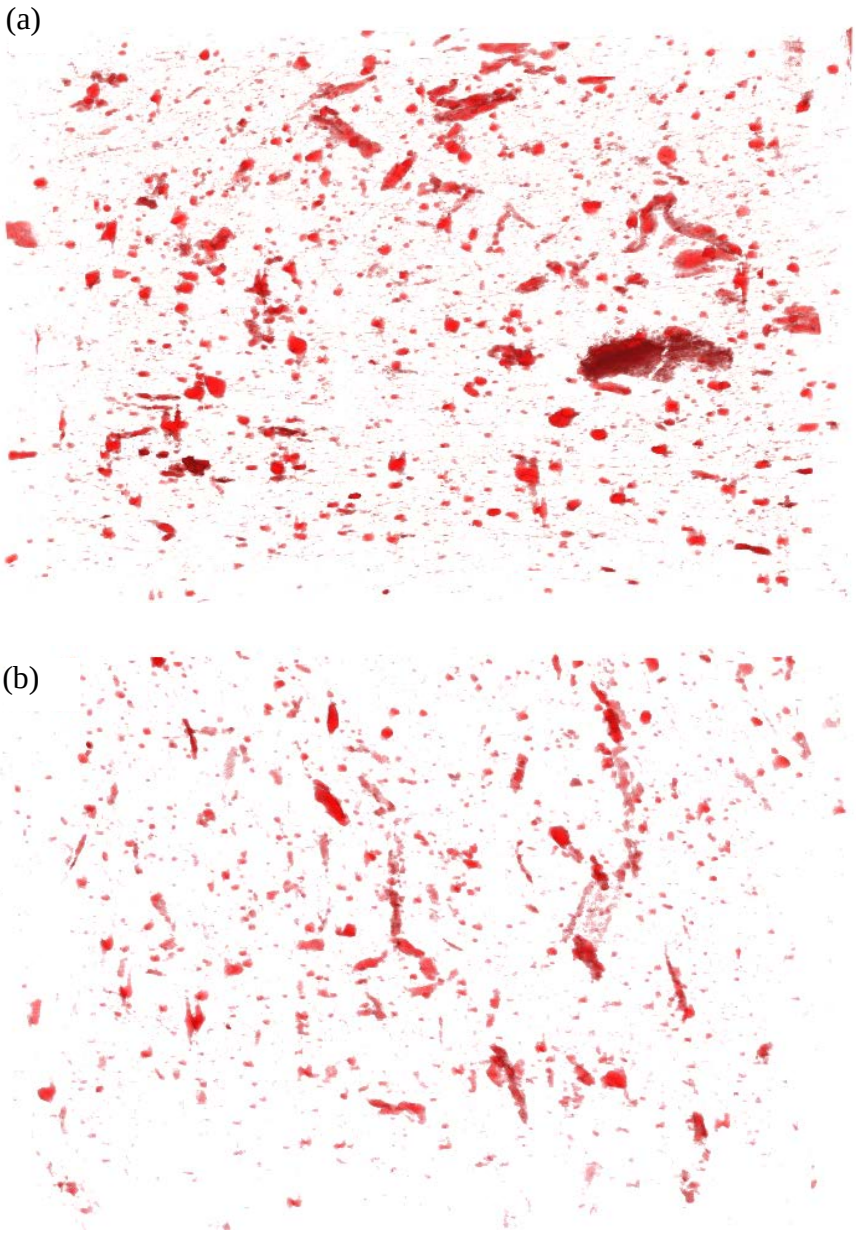

Figure 5.5: Noil hemp fibre agglomerations in a polypropylene matrix: (a) 30H and (b) 30H5MAPP.

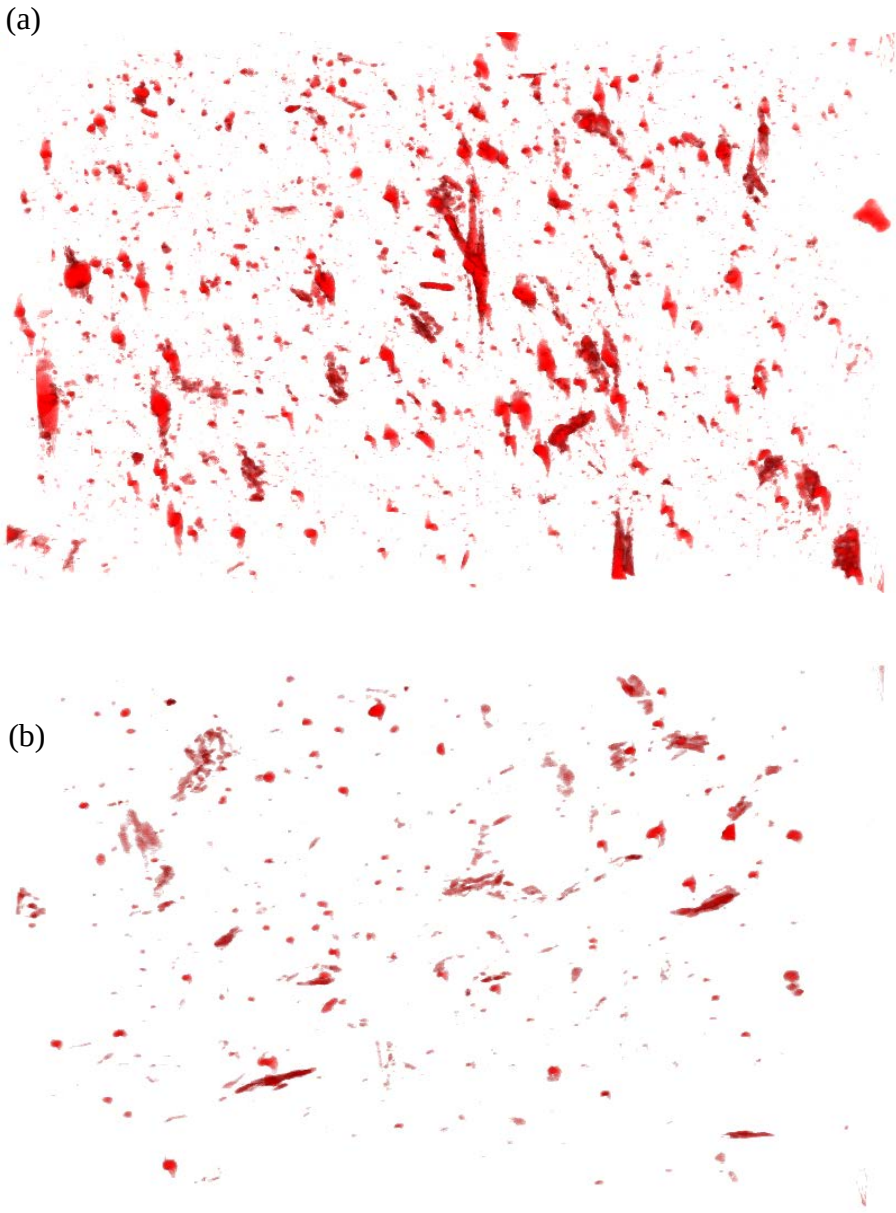

Figure 5.6: Noil hemp Fibre agglomerations in a polypropylene matrix: (a) 40H and (b) 40H5MAPP.

where n is the number of random variables (x). This equation was solved using Newton-Raphson method for each sample. Once α was determined, β would be estimated using Eq. 5.4 as:

$$\beta = \frac{\sum_{i=1}^{n} x_i^{\alpha}}{n} \tag{5.4}$$

Figure 5.8 to Figure 5.10 represent probability density functions (PDF) and cumulative distribution functions (CDF), calculated using shape (α) and scale (β) parameters as shown in Table 5.1.

Table 5.1: Average values and Weibull parameters calculated for length and width of the noil hemp fibres

Samples	Length			Width		
	Average (µm)	α	β	Average (µm)	α	β
As-received	13230.00	0.96	1.31	43.87	3.65	48.43
10H	186.67	3.62	205.66	36.41	5.56	39.04
20H	162.54	2.83	181.45	37.09	7.01	39.51
30H	107.94	1.78	122.25	22.83	1.83	25.86
40H	105.22	2.08	119.19	22.02	2.20	24.86
30H5MAPP	144.90	1.71	163.87	31.87	1.72	36.07
40H5MAPP	128.04	1.85	145.13	28.63	1.88	32.47

To measure the size of an as-received fibre, an optical microscopic image was first taken and then the image was analysed using Matlab software. More than 100 as-received fibres were analysed and then the average length of as-received fibres was measured to be about 13 mm.

X-ray micro-tomography results show that after the fabrication of hemp fibre reinforced polypropylene composites, the fibre length was significantly decreased to 187, 163, 108 and 105 μm for 10H, 20H, 30H and 40H samples respectively.

Although the fibre length analysis, obtained from x-ray micro-tomography method, is in correlation with the literature (Guo et al., 2010, Alemdar et al., 2008), some optical microscopic images (Figure 5.7) have been taken from within the composite samples and parallel to injection moulding direction, to confirm the x-ray microtomographic results. It can be seen from Figure 5.7 that the maximum length of the fibres are in correlation with the x-ray microtomography results (Figure 5.8 to Figure 5.10). The shortening of the fibres was most likely caused by fibre breakage during compounding and injection moulding processes.

5.2.1 Influence of fibre content

Figure 5.8 is the plot of hemp weight content against length distribution of fibres. It shows that the decline in fibre length which was more severe in the composites having 30 wt% and 40 wt% noil hemp fibre compared with the composites having 10 wt% and 20 wt% noil hemp fibre.

Fibres can be broken into shorter lengths due to three mechanisms: fibre–fibre interaction, fibre-polymer interaction and fibre-wall interaction (Rezadoust and Esfandeh, 2005). Considering the fibre-polymer interaction mechanism, the melt mixture with higher fibre weight content can increase the applied shear forces on the fibres due to the higher viscosity of the melt mixture. Thus, the viscosity and pseudo-

plasticity of the melt matrix play the most important roles in the fibre-matrix interaction mechanism.

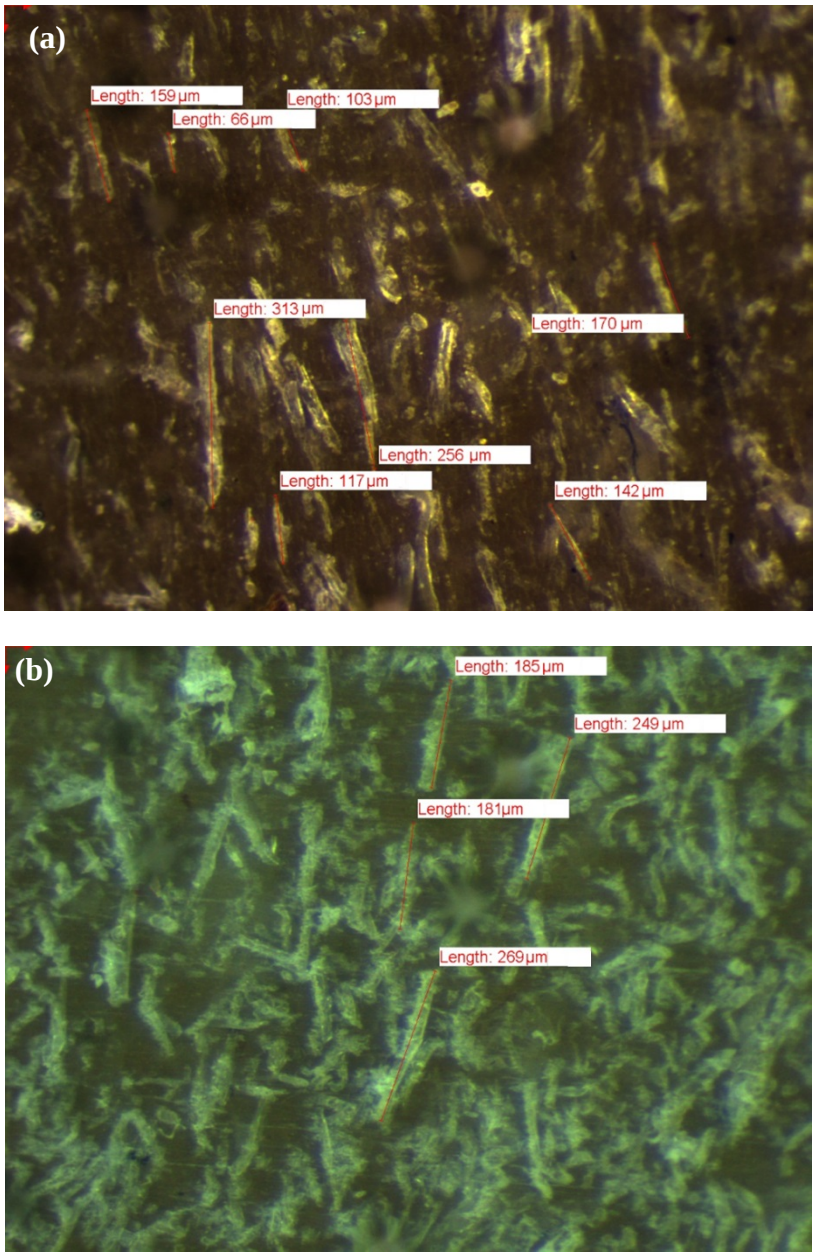

Figure 5.7: Optical microscopic images of the noil hemp fibre composites with (a) 20 wt% noil hemp fibre and (b) 40 wt% noil hemp fibre.

A fibre, preferentially aligned in the direction of the molten flow, is unlikely to be exposed to breakage. It is more likely that the fibres were not aligned in the melt flow direction due to the “fountain flow” phenomena. This occurs during the injection moulding process, where the lower melt velocity near the walls and the higher melt velocity at the centre of the channel results in a fountain flow effect that causes the central material to splay outwards at the flow front. In addition, rotating fibres experience deforming stresses that result in the bending of fibres

Fibre breakage occurs when the critical shear stress is reached and the fibre collapses (Yamamoto and Matsuoka, 1995). In research carried out by Guo, it was concluded that after just 1 injection moulding all studied natural fibre types were reduced to fibre lengths of approximately 250 μm (Guo et al., 2010). This is in correlation with the current project’s results.

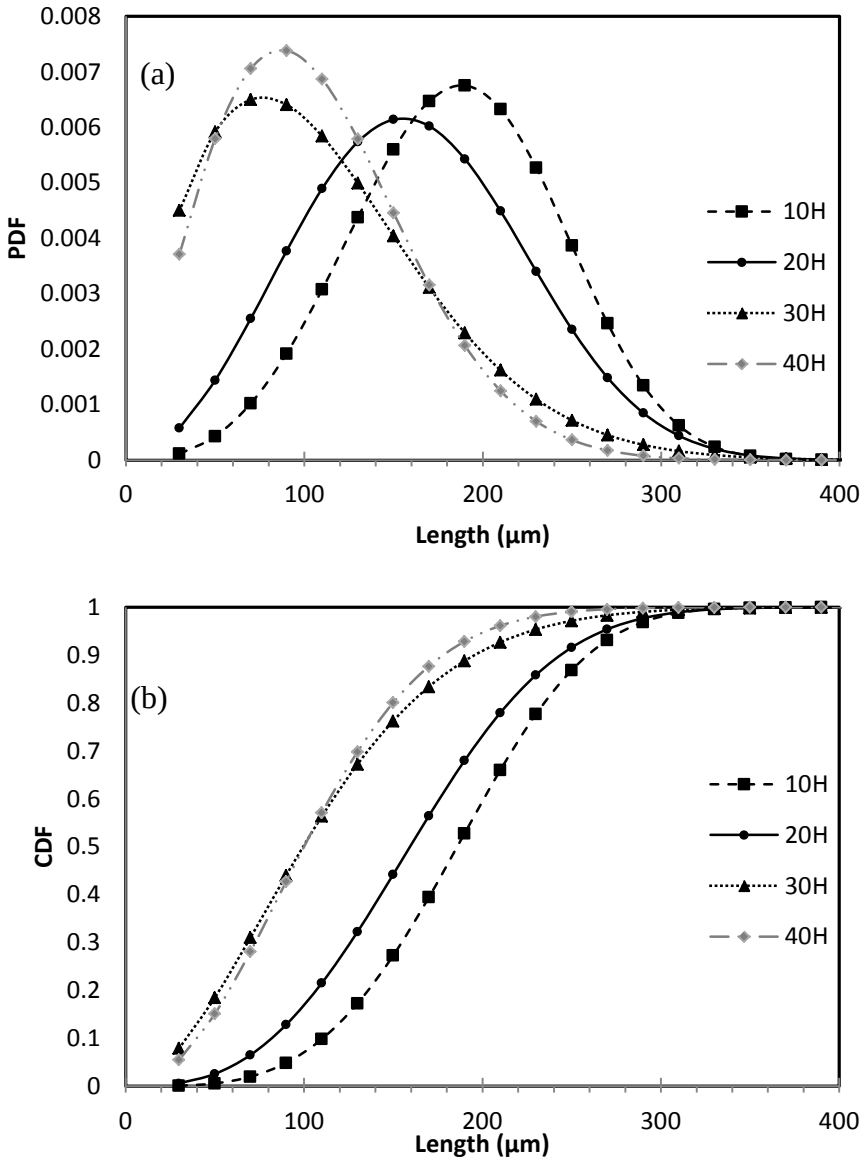

Figure 5.8: The influence of hemp weight content on the length distribution of fibres: (a) Probability Density Functions (PDF) and (b) Cumulative Distribution Functions (CDF).

Figure 5.9 also shows that fibre widths of 30H and 40H samples were considerably lower than the 10H and 20H samples. The 30H and 40H samples showed almost the same width distribution, while the 10H and 20H samples have similar trends with each other.

It might be due to the fibre-fibre interaction mechanism occurring in the mixture with higher fibre weight content. When the fibre weight content is high, overlap and agglomeration of fibres cause abrasion and erosion between fibres. However, abrasion between fibres should not have significant impact on width reduction of the fibres. Another possibility, which might have reduced the fibre width, is the longitudinal division of elementary fibres from technical fibres. As mentioned earlier in section 4.2, the diameter of as-received noil fibre was approximately 45 µm and the elementary fibre observed was approximately 10 µm. Therefore, width reduction from approximately 45 µm for the as-received noil fibre to approximately 22 µm for the 40H sample might have occurred because of abrasion between fibres and splitting technical fibres into two.

Fibre width reduction can make the fibres more susceptible to bending. Bending stresses introduced into the fibres can cause stress concentrations which lead to strength reduction in the fibres. Therefore, the fibre-fibre interaction mechanism can accelerate the shortening of the fibres for 30H and 40H samples during processing.

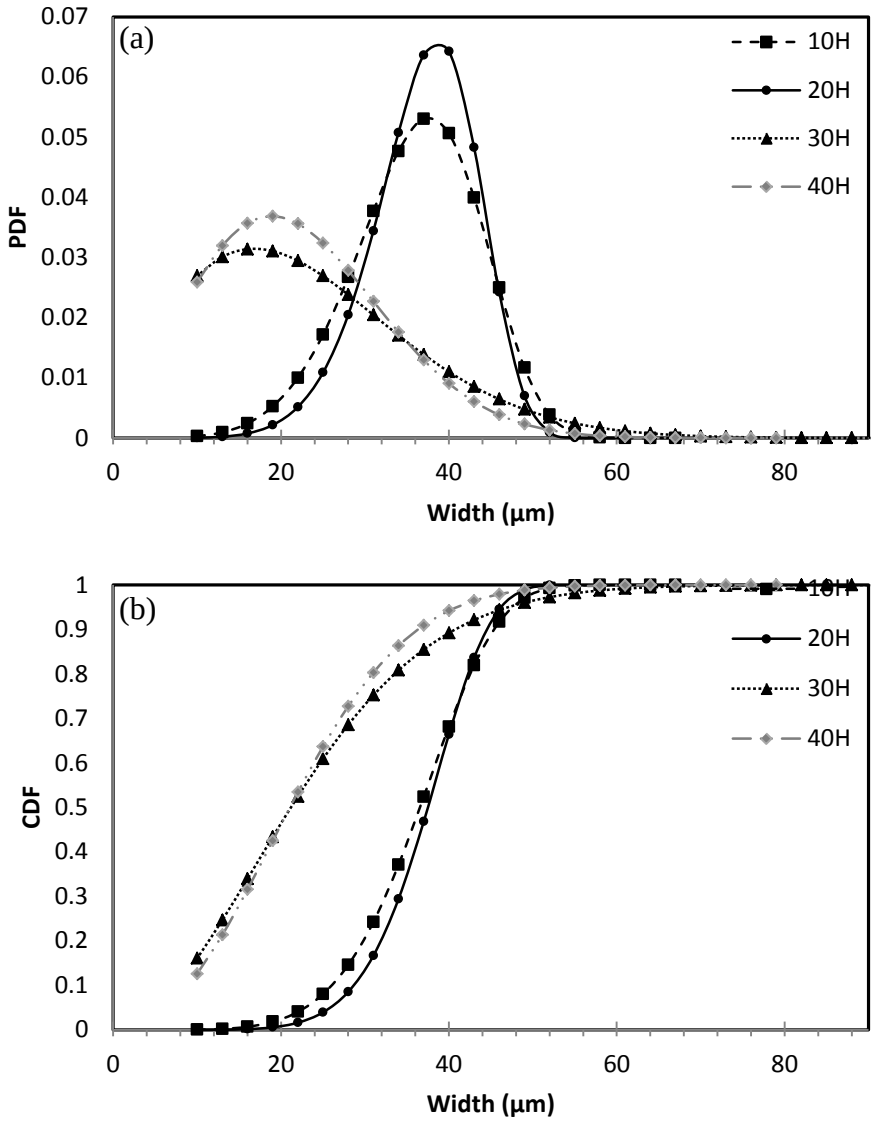

Figure 5.9: The influence of hemp weight content on the width distribution of fibres: (a) Probability Density Functions (PDF) and (b) Cumulative Distribution Functions (CDF).

5.2.2 Influence of MAPP

Figure 5.10a provides a comparison between the Weibull length distributions of composites having 30 wt% and 40 wt% hemp fibres with and without the coupling agents. The results clearly show that the noil hemp fibres in compatibilised matrices were relatively longer than those in uncoupled matrices. It would appear that the coupling agents act as a lubricant in the polypropylene and consequently reduce the shear stresses during processing. However, in order to fully understand the effects of the coupling agents on fibre breakage, it is essential to understand the effects of the coupling agent on the fibre breakage mechanisms, i.e., fibre–fibre and fibre-matrix interactions.

In studies undertaken by Bengtsoon *et al*., it was reported that the addition of 3 wt% MAPP coupling agent reduced the average fibre length of both bleached sulphite cellulose fibre reinforced polypropylene and bleached kraft cellulose fibre reinforced polypropylene composites (Bengtsson et al., 2007) . Contrary to this report, Alemdar *et al*. observed an increase in average fibre length of wood fibre reinforced polypropylene with the addition of MAPP (Alemdar et al., 2008). Since neither of these studies provides adequate evidence, this section aims to investigate the effects of compatibiliser addition on fibre length distribution.

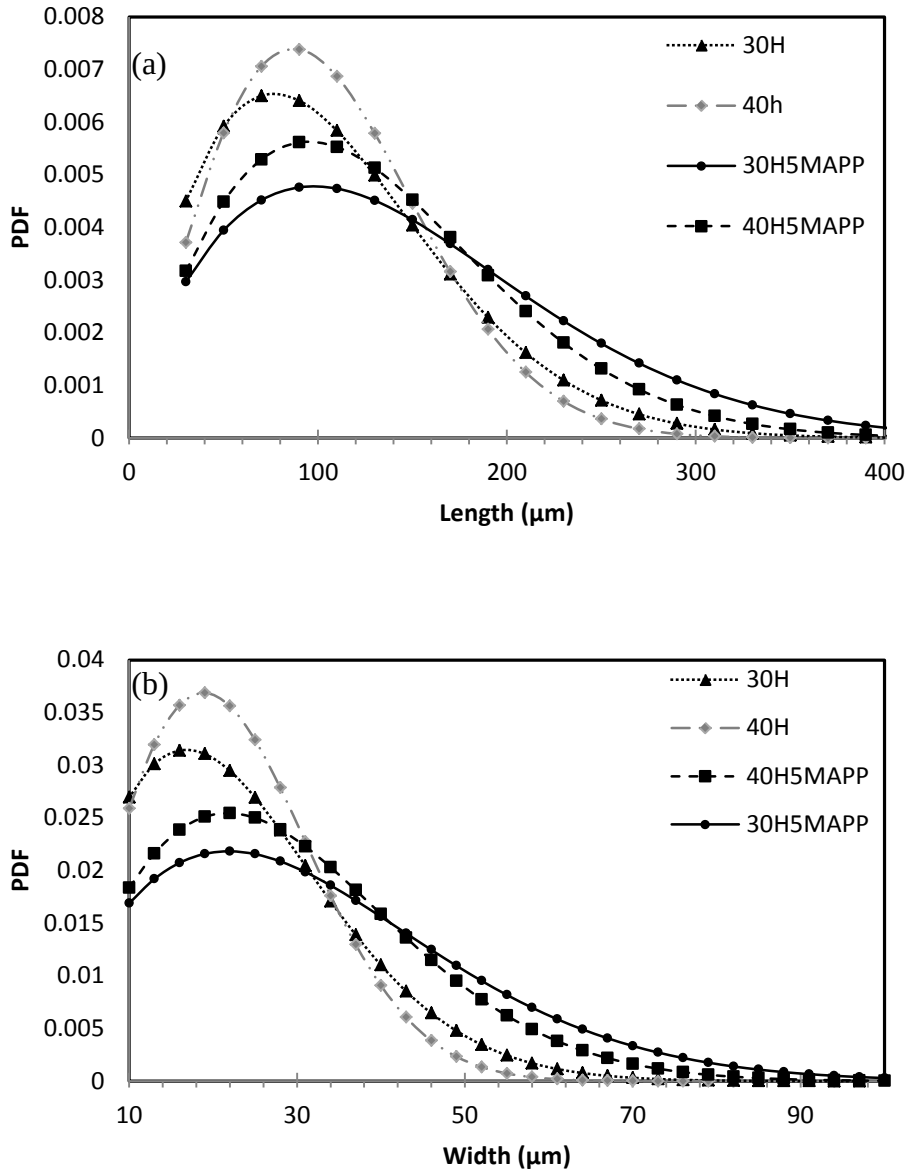

Figure 5.10: The influence of compatibiliser addition on: (a) fibre length distribution and (b) fibre width distribution.

An increase of MAPP content can decrease pseudoplasticity and viscosity of the melt blend (Moghaddam, 2008, Li et al., 1999a). This may be effective in decreasing the shear stresses in the matrix and thereby reducing the occurrence of fibre breakage. However, it is only at low shear rates or rotation speeds that the addition of MAPP can significantly reduce the dynamic viscosity of melted PP (Li et al., 1999b, Byung S et al., 2007, Tessier et al., 2012). In processing techniques such as extrusion, melt mixing or injection moulding, where high shear rates or rotation speeds are applied, the decrease in melt viscosity and consequently decrease in shear stresses may not be substantial. Thus, it is more likely that increase in fibre length as a result of MAPP addition was not associated to the fibre-matrix interaction.

The fibre-fibre interaction is one of the three main mechanisms which cause fibre breakage during processing. For the same volume fraction, this mechanism is more critical in shorter fibres. Because, a higher number of fibres are introduced into short fibre composites which can contribute to higher collisions, compared with long fibres. Therefore, in order to reduce fibre-fibre interactions, good fibre dispersion is more essential in short fibres than in long ones.

Figure 5.10b shows an increase in the width of the fibres in 30H5MAPP and 40H5MAPP samples compared with 30H and 40H samples. It implies that less fibre abrasions/fibre-fibre interactions have occurred with the addition of MAPP. As observed in Figure 5.5 and Figure 5.6, the addition of MAPP enhanced the wettability of the matrix and improved the homogeneity of composite microstructures. Therefore, the fibre-fibre interaction was reduced due to the better fibre dispersion that was the subsequent to MAPP addition.

6. Performance of the Composites

In this chapter, the influence of noil hemp fibre content and coupling agent addition on performance of short noil hemp fibre composites is investigated. In this regard, tensile properties, vibration damping characteristics and dynamic mechanical analysis of the composites are discussed elaborately.

6.1 Tensile Properties of the Composites

Tensile tests of the noil hemp fibre composites were carried out according to the procedure described in chapter 3.6.2. Tensile strength and Young's modulus of the pure PP and the composites with different noil hemp fibre content and coupling agents are listed in Table 6.1.

6.1.1 Effects of the fibre Content

The tensile strength of the composites as a function of fibre weight content is illustrated in Figure 6.1. Referring to the literature, it was expected to observe an initial increase from pure PP then a subsequent decline in tensile strength with an increase in fibre content (Ku et al., 2011). Although higher fibre content is generally preferred for achieving better mechanical properties of short fibre reinforced polymer composites (Ahmad et al., 2006), Figure 6.1 indicates that increase in fibre content resulted in a decrease in tensile strength of all composites without a compatibiliser. The tensile strength was reduced from 31 MPa for the pure PP to 27 MPa for the composite with 10 wt% hemp fibre (10H sample).

Table 6.1: Tensile strength of the fabricated composite samples

Samples	Tensile strength (MPa)	Elastic Modulus (GPa)
PP	31.1 (±2.2)	1.3 (±0.2)
10H	26.7 (±0.7)	1.6 (±0.1)
20H	28.9 (±0.9)	2.3 (±0.2)
30H	28 (±1.5)	2.8 (±0.2)
40H	28.1 (±0.6)	3.6 (±0.2)
50H	29.3 (±2.4)	4.4 (±0.2)
60H	24.8 (±4.0)	3.6 (±0.4)
30H 2.5MAPP	39.7 (±2.0)	4.0 (±0.2)
30H 5MAPP	39.3 (±2.3)	3.3 (±0.2)
40H 2.5MAPP	36.5 (±3.0)	3.0 ±0.2)
40H 5MAPP	40.8 (±3.3)	4.3 (±0.2)
30H 2.5MAPOE	34.5 (±0.8)	3.2(±0.4)
30H 5MAPOE	39.0 (±1.8)	3.0(±0.1)
40H 2.5MAPOE	35.6 (±3.5)	3.2(±0.3)
40H 5MAPOE	37.0 (±0.9)	2.7(±0.1)

Tensile strengths of 20H, 30H, 40H and 50H samples were, on average, 28 MPa and below the tensile strength of pure PP. This phenomenon is symptomatic of poor interfacial adhesion between the hemp fibres and the polypropylene matrices as can be seen in the SEM micrographs of fractured surfaces without a coupling agent. Figure 6.2 to Figure 6.4 reveal a number of holes and fibres with clean and smooth surfaces, which are evidence of fibre pull-out. In addition, gaps can be observed

between the fibres and the matrix because of fibre debonding. Debonded/pulled out fibres implies poor interfacial bonding between the fibres and the matrix.

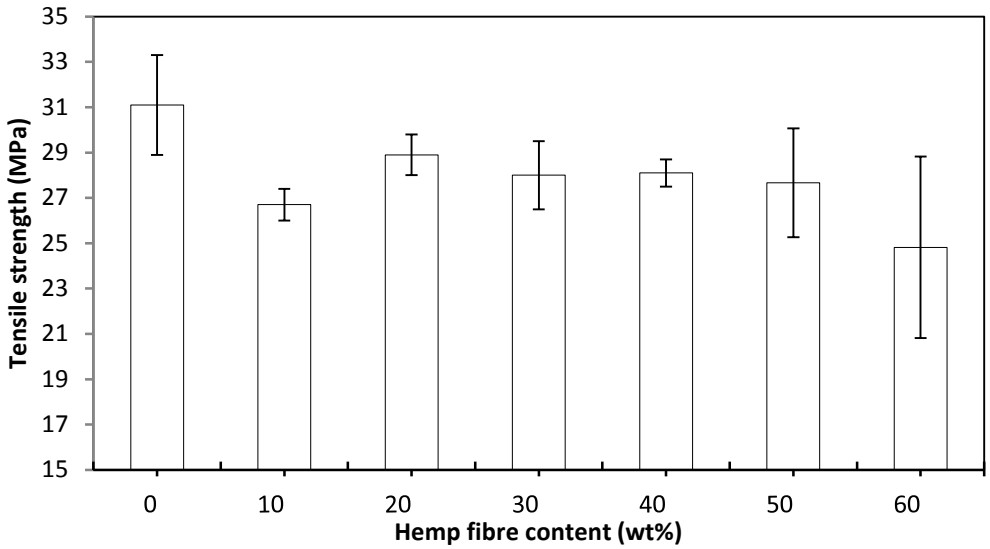

Figure 6.1: The influence of the fibre weight content on tensile strength of the noil hemp fibre reinforced polypropylene composites.

Referring to Figure 6.1, it also can be noted that the tensile strengths of 30H, 40H, 50H and 60H composite samples were even lower than that of the 20H sample. It implies that the reinforcing effect of the fibres declined at higher fibre content. In order to take full advantage of the reinforcing effect of the fibres, the fibres' length must be greater than the critical value. As elaborated previously in section 5.2.1, higher level of fibre breakage occurs during the processing of higher fibre content composites (Etaati et al., 2013).

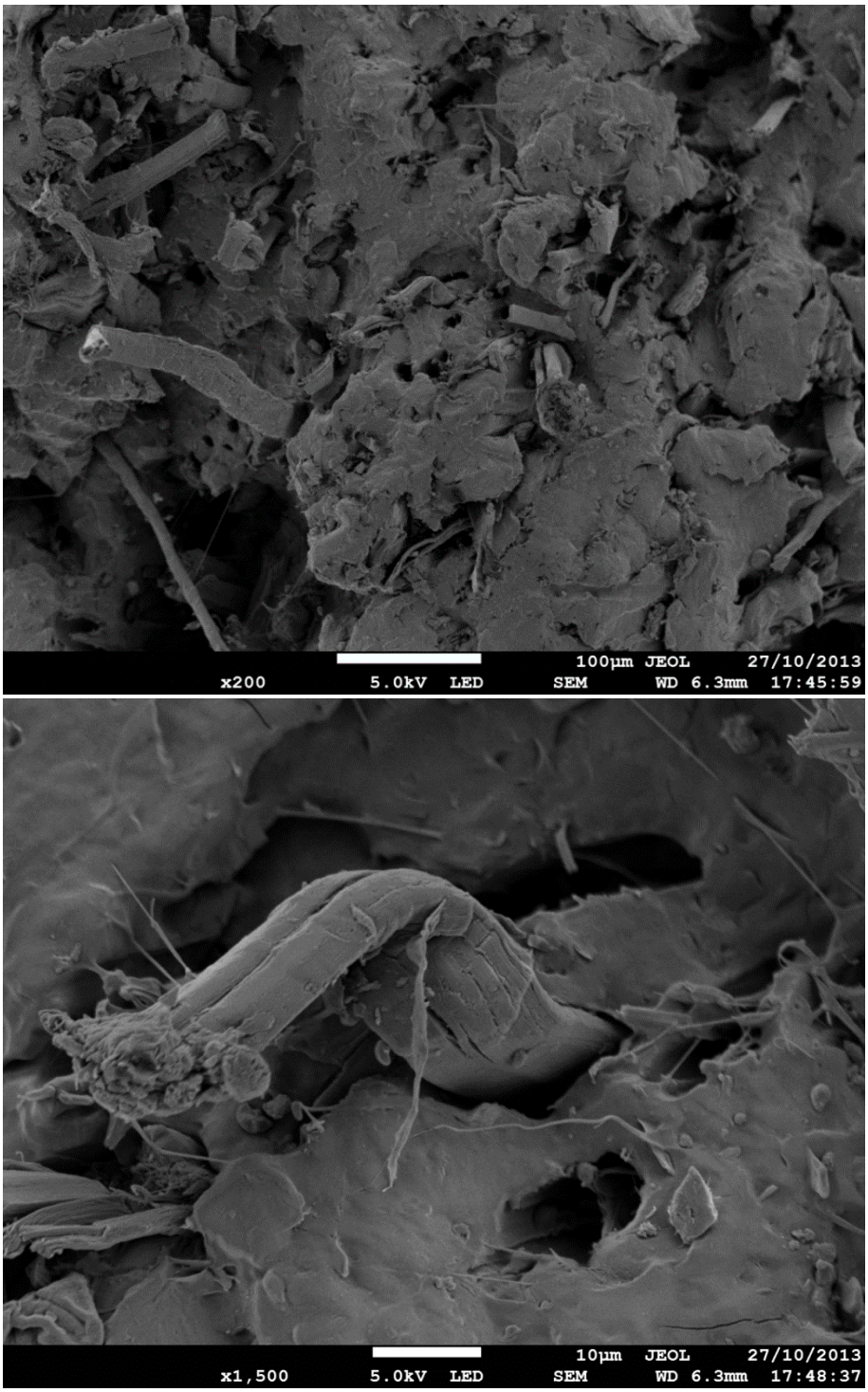

Figure 6.2: SEM micrographs of fractured surface for the 10 wt% hemp fibre polypropylene composite without a coupling agent.

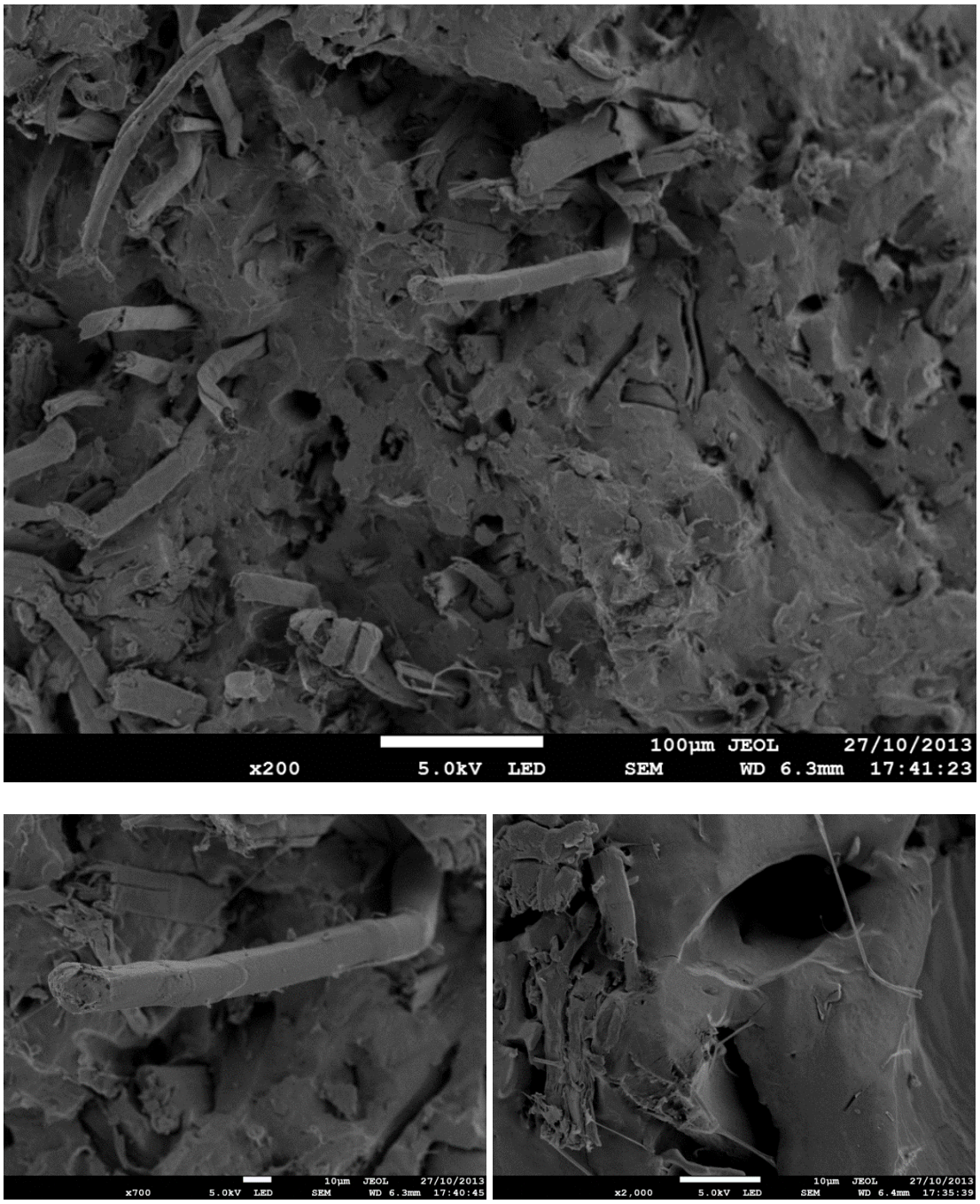

Figure 6.2 (continued)

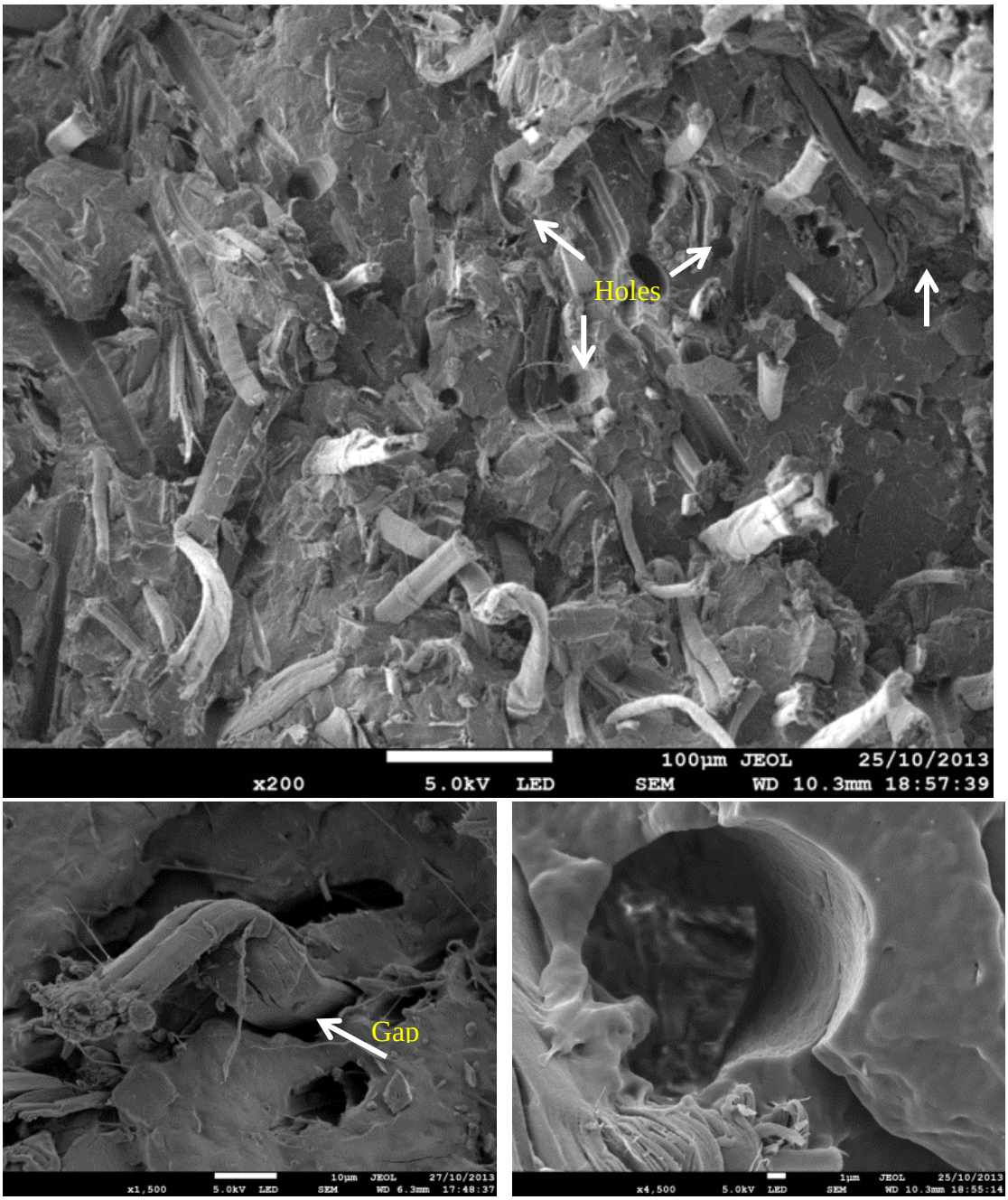

Figure 6.3: SEM micrographs of fractured surface for the 20 wt% hemp fibre polypropylene composite without a coupling agent.

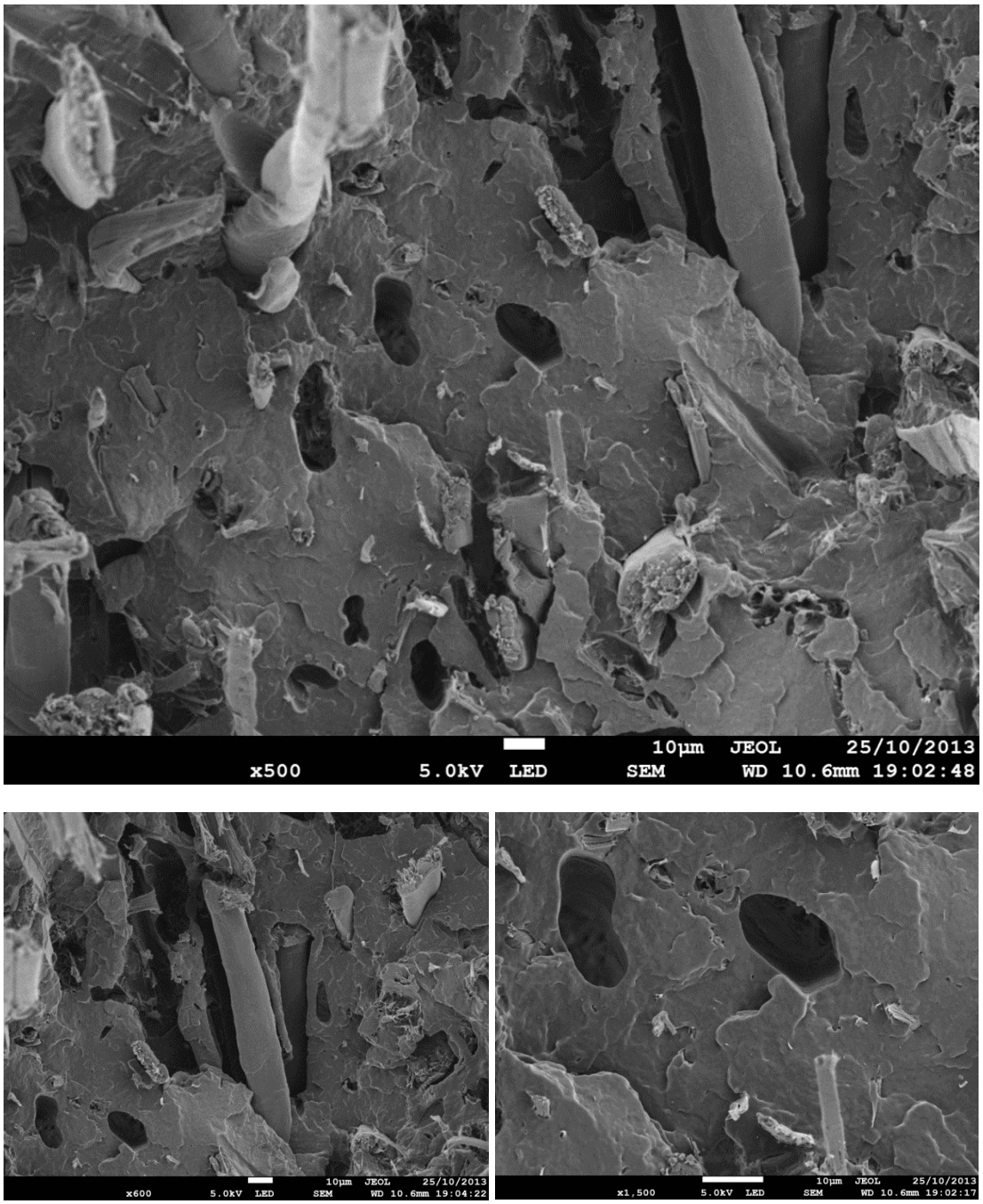

Figure 6.3 (continued)

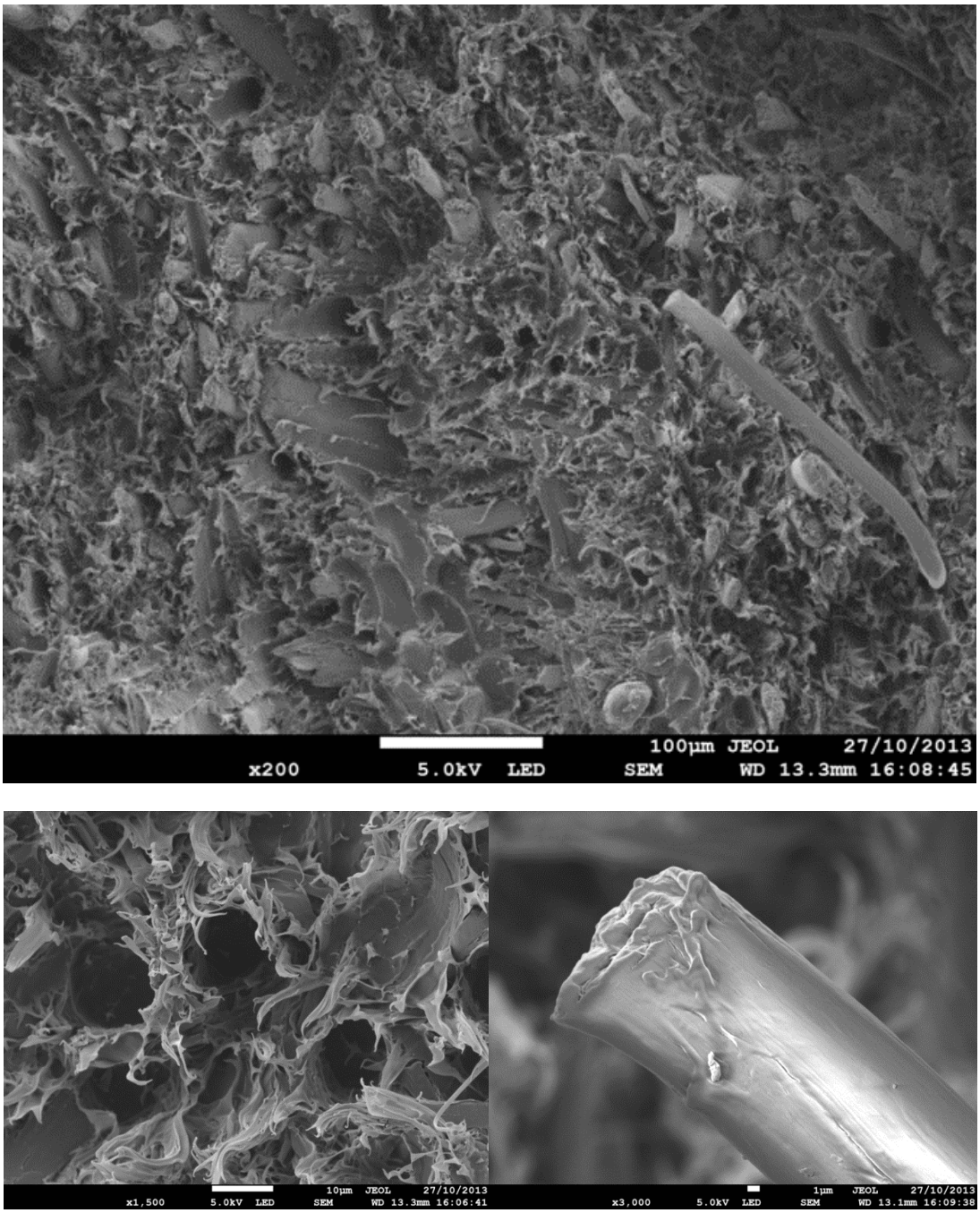

Figure 6.4: SEM micrographs of fractured surface for the 60 wt% hemp fibre polypropylene composite without a coupling agent.

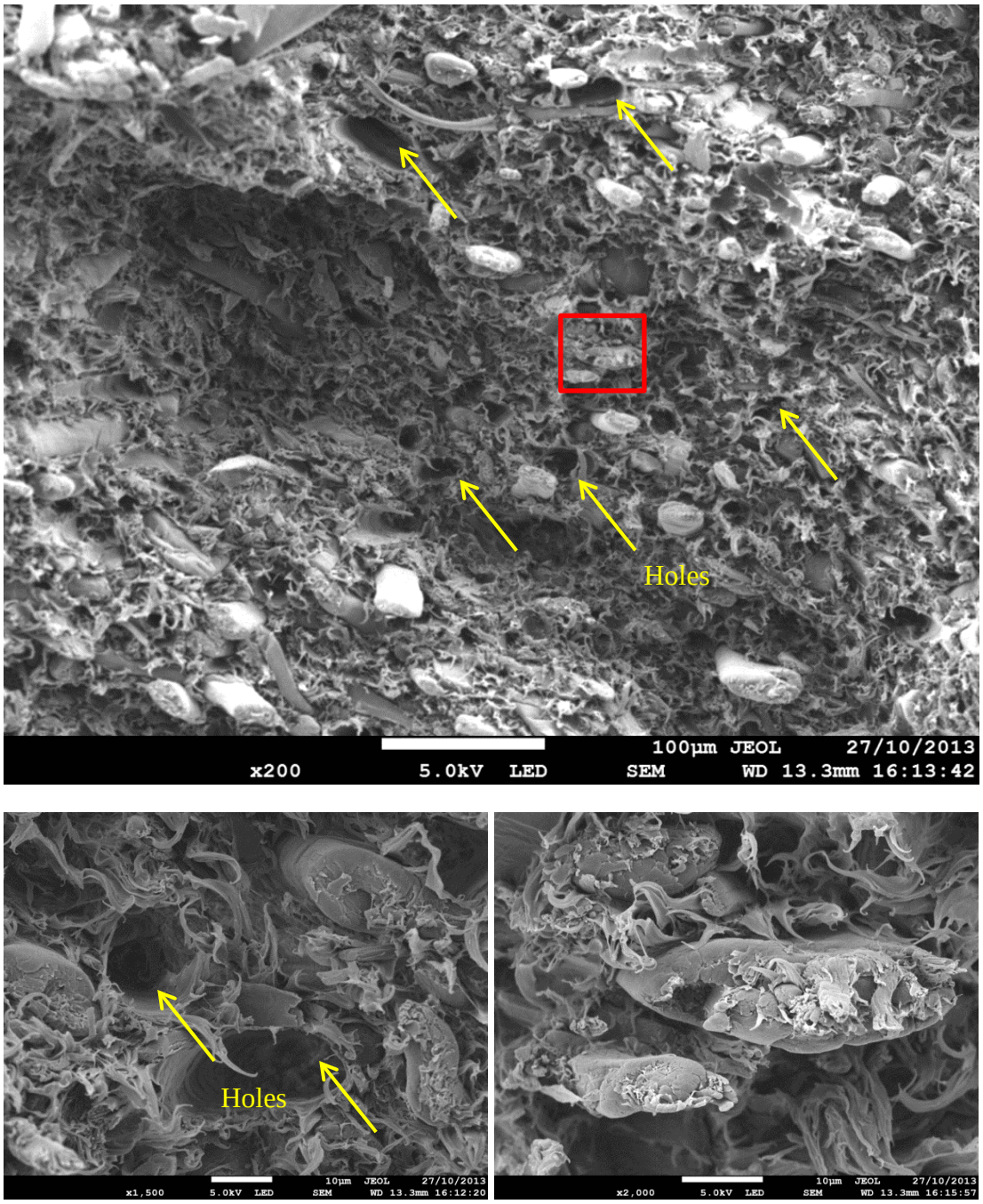

Figure 6.4 (continued)

The tensile strength of the composite with 60 wt% hemp content was the lowest among all samples. The lower tensile strength of the composite with 60 wt% hemp content occurred not only due to the low interfacial adhesion but also due to the voids formed. Figure 6.5 shows some typical voids observed in the microstructure of the composite. Since fibre addition increases the viscosity of the mixture, the voids are more likely to occur, as observed with the mixture with 60 wt% hemp fibre which is too viscous to effectively fill the mould.

To conclude, poor interfacial adhesion between fibres and matrices is one of the main reasons resulting in poor tensile properties. Besides that, the addition of short fibres to the matrix brought about a decline in composite strength due to the extremely higher viscosity of the fibre/matrix blend at higher fibre content. However, voids could happen even if the fibre content is low but it is more likely to happen by increase of viscosity due to fibre addition.

It also should be noted that in spite of reduced tensile strength, the Young's modulus of the composites increased linearly with an increase of fibre content. Although tensile strength and Young's modulus are different material properties, they can be obtained from a stress-strain curve. It should be noted that composite modulus are determined at low strains where the fibre/matrix interface is still intact. As the composite strain increases, interfacial debonding limits stress transfer of fibre/matrix interface which reduces the tensile strengths of the composite in the case of low bonding adhesion (Facca et al., 2007).

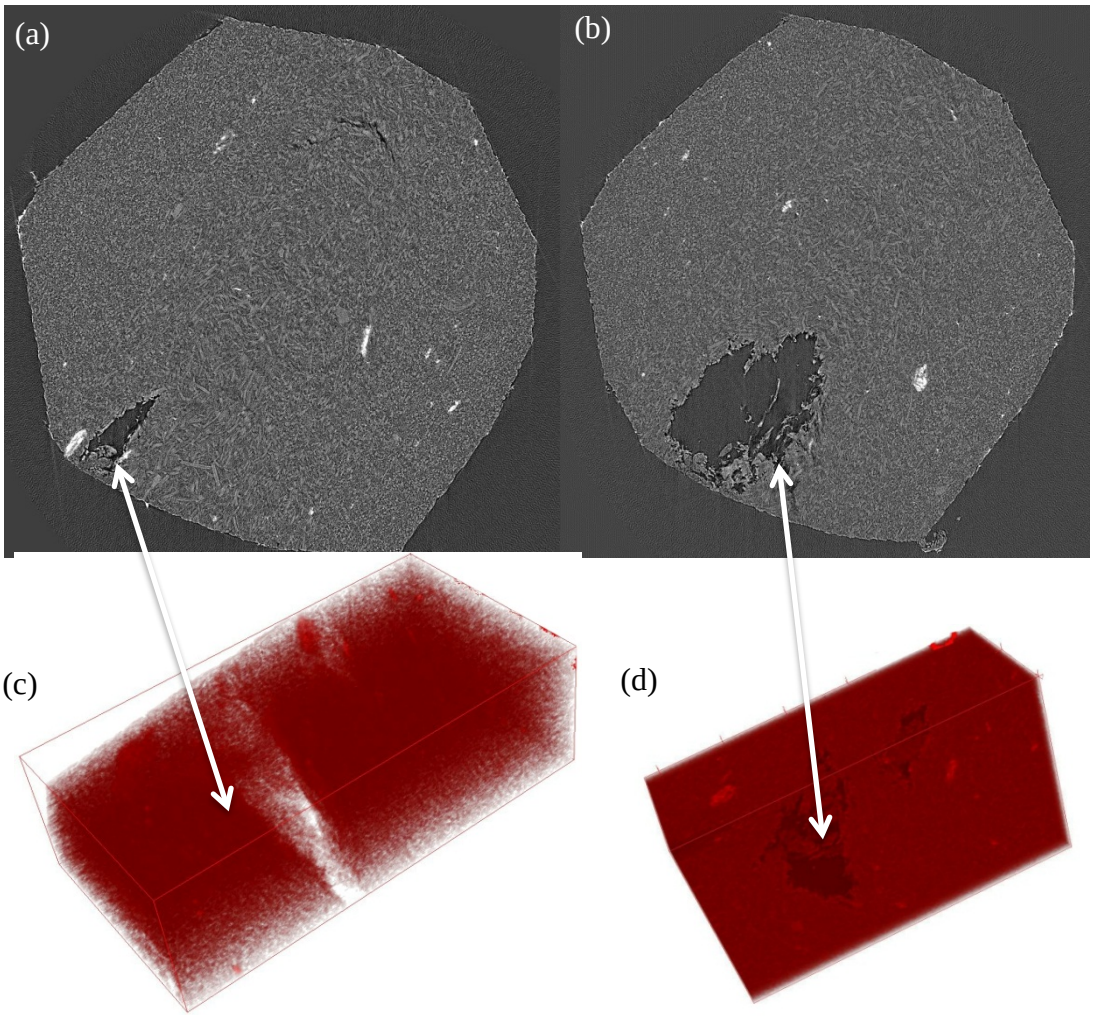

Figure 6.5: (a&b):Typical reconstructed x-ray micro-tomography images of the composite with 60 wt% hemp fibre, which shows voids, (c&d): 3D views of associated voids in the composites.

6.1.2 Effects of the Coupling Agent Addition

In general, when a coupling agent was added, the tensile strength of the composites should be improved. Figure 6.6 illustrates the influence of MAPP and MAPOE on the tensile strength with 30 wt% and 40 wt% noil hemp fibre. It can be seen that for the composite with 30 wt% hemp fibre, there was a slight difference between incorporation of 2.5 wt% and 5 wt% MAPP. While, for the composite with 40 wt% hemp fibre, the addition of 5 wt% MAPP caused the greatest improvement among the composites due to the higher availability of the fibre surface area. In other words, at

30 wt% fibre content, most of the fibre surface could be covered by addition of 2.5 wt% MAPP and addition of more MAPP did not have significant impact. However, at 40 wt% fibre content, 2.5 wt% MAPP did not seem to be adequate to cover all fibre surfaces and more amount of MAPP could increase tensile strength of the composites.

This figure indicates that addition of 5 wt% MAPP into 40 wt% hemp fibre improved the tensile strength (approx. 40%). Young's modulus (by approx. 15%) of the composites was also increased in comparison with uncoupled composites. In addition, it can be seen that the addition of MAPP had a stronger impact to enhance the tensile strength than MAPOE. This conclusion can be confirmed by a comparison between SEM micrographs illustrated in Figure 6.7 and Figure 6.8. Although MAPOE addition partially improved the interfacial adhesion, the evidence of pull-out can still be observed in Figure 6.7. On the other hand, there was almost no evidence of fibre pull-out when MAPP was added. The micro-fibrils marked in Figure 6.8 indicate that composite failure occurred mainly due to the fracture of the cellulose fibres.

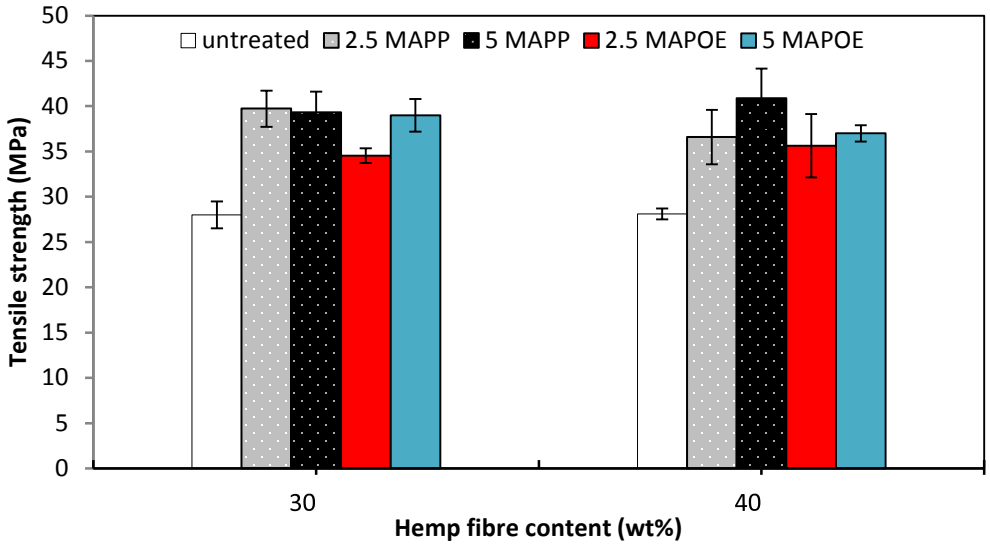

Figure 6.6: The influence of coupling agent type and their content on tensile strength of the noil hemp fibre reinforced polypropylene composites.

Figure 6.7: SEM micrographs of fractured surface for the 40 wt% hemp fibre polypropylene composite with 5 wt% MAPOE coupling agent.

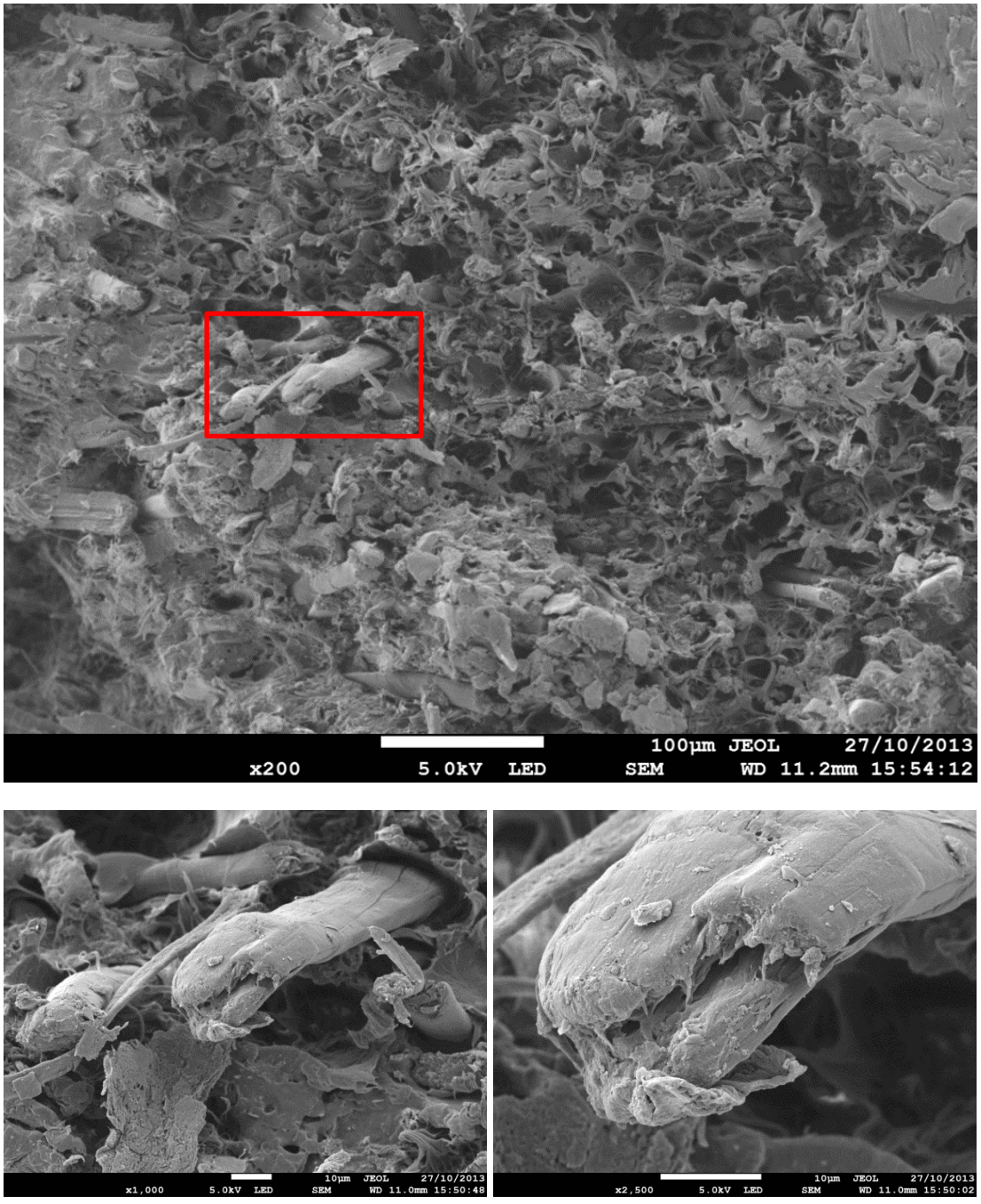

Figure 6.7: (continued)

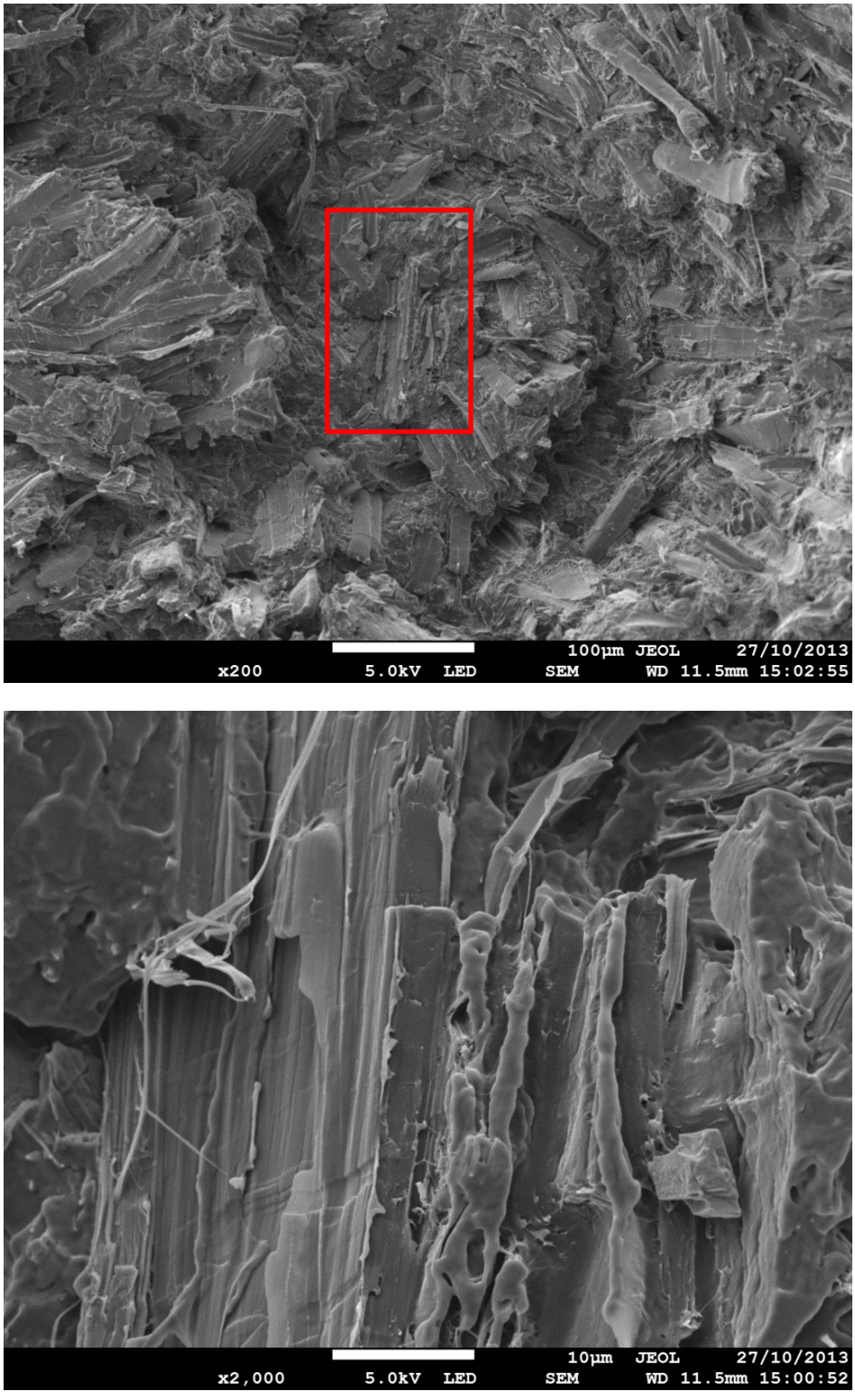

Figure 6.8: SEM micrographs of fractured surface for the 30 wt% hemp fibre polypropylene composite with 2.5 wt% MAPP coupling agent.

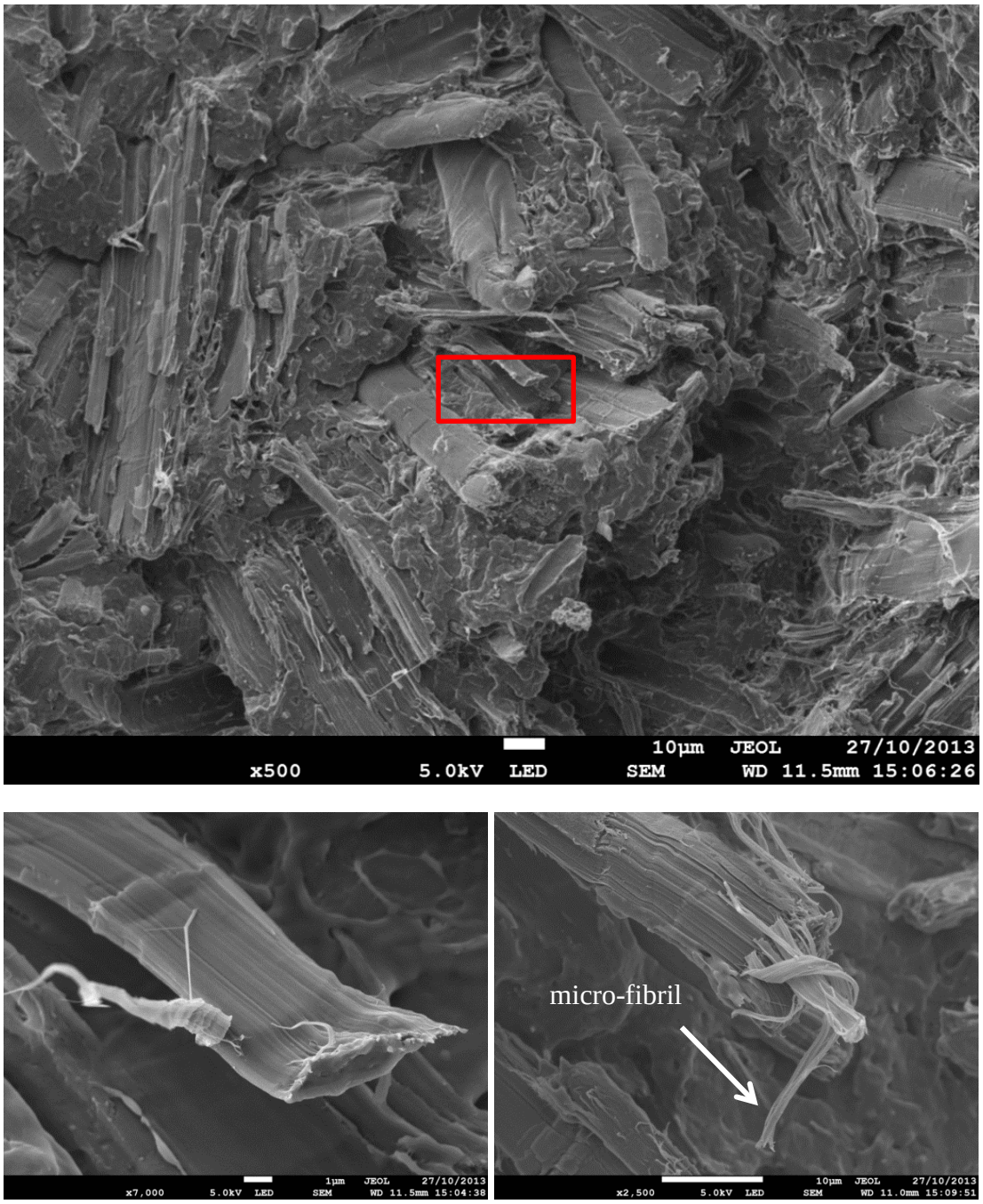

Figure 6.8 (continued)

6.1.3 Interfacial Adhesion

6.1.3.1 Introduction

Investigations on the use of natural fibres as reinforcement in fibre reinforced thermoplastics have introduced further applications in the automotive and construction industries. The mechanical properties of a composite are determined by mechanical properties of the constituent materials (fibre and matrix), their microstructures and their interfacial bonding. Incompatibility between natural fibres and polymers lead to poor properties of the composites. Thus, improving interfacial bonding between the fibres and the matrices is an essential effort which can be done by fibre treatment and/or matrix modification methods (Niu et al., 2011, Sawpan et al., 2011, Kabir et al., 2012a) .

Knowledge on interfacial adhesion is of fundamental importance in designing engineered fibre composites. The interfacial adhesion can be described by interfacial shear strength (IFSS). There are a number of methods to determine IFSS. It can be investigated in molecular, micro, meso and macro levels. The first two levels were considered mostly in the literature (Qiu and Schwartz, 1991, Morlin and Czigany, 2012, Zhandarov and Mäder, 2005). Molecular aspects are often discussed for interface formation, while micromechanical ones are mentioned almost for interfacial failure. Thus, from an engineering point of view, which deals with stress transfer efficiency, the micro level is more important than the molecular model (Zhandarov and Mäder, 2005). In the micro-mechanical approach, interfacial shear strength (IFSS) is determined via two main methods. In one group of methods, an external load is applied directly to a single fibre (such as fibre pull-out and push-out tests) while the

second group involves applying a load to the matrix (such as single fibre fragmentation test and the compression test) (Zhandarov and Mäder, 2005, Le Duigou et al., 2010, Qiu and Schwartz, 1991, Morlin and Czigany, 2012, Park et al., 2006). But the IFSSs determined from these tests cannot provide accurate values of an interfacial bonding between the fibres and matrix in an environment similar to that in a real composite (Li et al., 2009). Alternative methods produce conflicting results. This makes it a controversial issue to find out which method is more appropriate to be used. Besides, at the micro level only the interaction between one single fibre and the matrix is considered. Therefore, IFSS determined from the micro level approach cannot be extended completely to bulk composite due to the inconsistency of natural fibres in terms of geometry and property. Nevertheless, a macro property of a bulk composite such as tensile strength can be used to evaluate effective IFSS of the composite. Thus, the modified Bowyer and Bader model can be used for interfacial shear strength (IFSS) determination. Generally, the Bowyer-Bader model is used (Li et al., 2000) to predict the composite tensile stress as below:

$$\sigma_c = \eta \left\{ \sum_i \left[\frac{V_i \sigma_f L_i}{2 l_c} \right] + \sum_j \left[V_j \sigma_f \left(1 - \frac{L_c}{2 l_j} \right) \right] \right\} + V_m \sigma_m \qquad (6.1)$$

where σ_c is the composite tensile strength; η is the fibre orientation factor; σ_f and σ_m are applying stresses on the fibres and the matrix; V_i and V_j are the volume fractions of the sub-critical and super-critical fibre lengths; l_i and l_j are the sub-critical and super-critical fibre lengths and L_c is the critical fibre length which can be obtained from the Kelly and Tyson model as:

$$L_c = \frac{\sigma_f D}{2 \tau} \qquad (6.2)$$

where τ is the interfacial shear strength of either the matrix or the interface whichever is the smaller and, D is the average fibre diameter. The critical fibre length determines if there is sufficient fibre surface area for the fibres to be completely stressed and to be fractured during composite loading (Facca et al., 2007). In other words, if the fibre length is shorter than L_c then failure occurs at the fibre/matrix interface rather than in the fibre (Nystrom et al., 2007). This section aims to use this model with some modifications to predict the IFSS of natural fibre composites with and without 5 wt% MAPP.

6.1.3.2 Interfacial Shear Strength (IFSS) Estimation

The tensile properties of single hemp noil fibres were evaluated according to the procedure mentioned in section 3.6.1 at different gauge lengths. The stress vs. strain curves of the noil hemp fibres were almost linear until fracture. It has been shown that fibre strength depends on gauge length (Asloun et al., 1989, Beckermann and Pickering, 2009). Thus, several fibre gauge lengths were tested under tensile loading. Asloun et al.(Asloun et al., 1989) showed a logarithmic dependence of tensile strength on gauge length for carbon fibres while Beckerman et al. (Beckermann and Pickering, 2009) used a linear relationship between tensile strength and gauge length for hemp fibres. Figure 6.9 shows fibre strength vs. gauge length plot including a linear trend line with R^2 value of 0.98.

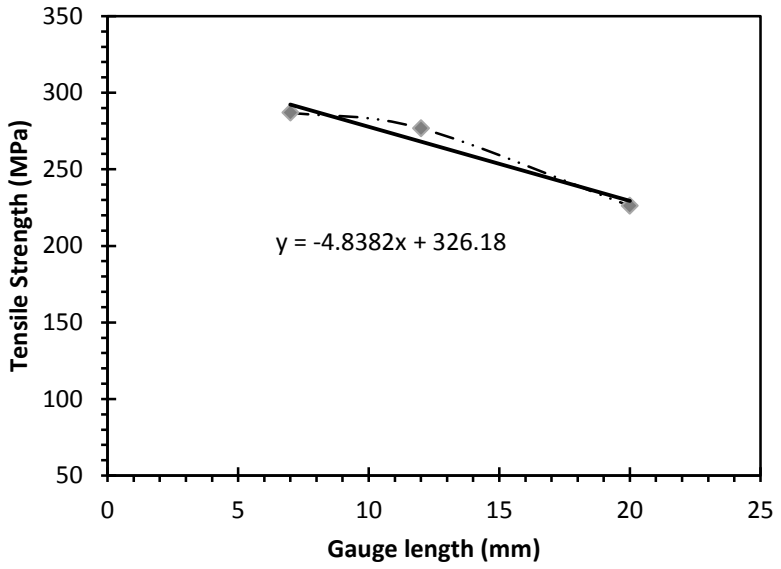

Figure 6.9: Average tensile strength of noil hemp fibres vs. gauge length.

Fibre aspect ratios were extracted for each fibre using the method mentioned in section 3.3.3. A two-parameter Weibull distribution was employed to describe the aspect ratio distribution of the fibres in the composites. The Weibull distribution density function is given by:

$$f(x) = \frac{\alpha}{\beta}\left(\frac{x}{\beta}\right)^{\alpha-1} \exp\left\{-\left(\frac{x}{\beta}\right)^{\alpha}\right\},\ x > 0,\ \alpha > 0\ and\ \beta > 0 \tag{6.3}$$

where α is the shape parameter and β is the scale parameter (Bhattacharya, 2011). In order to determine the shape and scale parameter of each sample, the Maximum Likelihood Estimator method was used and the Eq. 6.4 was solved.

$$\frac{\sum_{i=1}^{n} x_i^{\alpha}\ ln\, x_i}{\sum_{i=1}^{n} x_i^{\alpha}} - \frac{1}{\alpha} - \frac{\sum_{i=1}^{n} x_i^{\alpha}}{n} = 0 \tag{6.4}$$

where n is the number of random variables (x). This equation was solved using Newton-Raphson method for each sample. Once α was determined, β would be estimated using Eq. 6.5 as:

$$\beta = \frac{\sum_{i=1}^{n} x_i^{\alpha}}{n} \tag{6.5}$$

The calculated Weibull distribution parameters are shown in Table 6.2.

Table 6.2: Calculated Weibull aspect ratio distribution parameters.

Samples	Shape parameter (α)	Scale parameter (β)
10H	3.18	6.32
20H	2.68	6.76
30H	3.87	5.45
40H	3.68	5.58
30H5MAPP	3.77	5.76
40H5MAPP	5.06	5.08

Some modifications are applied to Eq. 6.1 and Eq. 6.2 in order to adapt the model for natural fibres. First, since natural fibres, especially noil hemp fibres, do not have consistent diameter due to their nature, instead of average diameter, aspect ratio of each fibre reinforcing the matrix (Eq. 6.6) was introduced. Therefore, Eq. (6.1) can be revised to Eq. 6.7 as:

$$S = \frac{\sigma_f}{2\,\tau} \tag{6.6}$$

$$\sigma_c = \eta \left\{ \sum_i [V_i S_i\, \tau] + \sum_j \left[V_j\, \sigma_f \left(1 - \frac{\sigma_f}{4\, S_j} \right) \right] \right\} + V_m\, \sigma_m \tag{6.7}$$

where S_i and S_j are the sub-critical and super-critical fibre aspect ratio. V_i and V_j are the product of aspect ratio density function and V_f (fibre volume fraction). Subscripts i and j here refer to the sub-critical and super-critical aspect ratios.

The related Cox–Krenchel model, including a theoretical orientation factor for in-plane random fibre orientations (η=3/8) can be used for random short-fibre composites (Thomason et al., 1996). However, Shao-Yun et al. (Fu and Lauke, 1996) have considered an additional efficiency factor (*K*) to account for the fibre length, strength and orientation distribution in the random short-fibre composites. The *K* factor can provide insight into the mechanical behaviour of the composite (Garkhail et al., 2000). For example, comparing the *K*-values of composites manufactured by different processing methods and/or containing different types of reinforcements illuminates the efficiency of those processing methods and reinforcements (Garkhail et al., 2000). In the case of natural fibre composites, even more factors can be added to this model. Natural fibres, especially hemp fibres, are susceptible to be bent in the matrix. Therefore, a bending factor can be suggested for this model as well, which makes the model more complicated. To simplify the model, the η' factor is introduced which is a product of all possible factors. Then:

$$\sigma_c = \eta' \left\{ \sum_i [V_i S_i \tau] + \sum_j \left[V_j \sigma_f \left(1 - \frac{\sigma_f}{4 S_j} \right) \right] \right\} + V_m \sigma_m \qquad (6.8)$$

When the composite strain is increased more than its yield point, the ROM equation (Eq. 2.2) is not applicable because composite failure is generally characterised by a critical local event rather than by average phenomena as assumed in the elastic region. In other words, we can assume that failure of the fibres triggers composite failure. Therefore, considering that $\varepsilon_c = \varepsilon_f$, Eq. 6.8 can be revised as:

$$\sigma_c = \eta' \left\{ \sum_i [V_i S_i \tau] + \sum_j \left[V_j E_f \varepsilon_C \left(1 - \frac{E_f \varepsilon_c}{4 S_j} \right) \right] \right\} + V_m \sigma_m \qquad (6.9)$$

All parameters of Eq. 6.9 were experimentally obtained except η' and τ parameters which were not generally known. However, values for those factors can be obtained if two points of (ε_1, σ_1) and (ε_2, σ_2) of the composite's tensile stress–strain curve are known (Figure 6.10). Then, IFSS of the composite can be calculated using Eqs. 6.10-6.12:

$$\sigma_1 = \eta' \left\{ \sum_i [V_i S_i \tau] + \sum_j \left[V_j \, E_f \, \varepsilon_1 \left(1 - \frac{E_f \, \varepsilon_1}{4 \, S_j} \right) \right] \right\} + V_m \, \sigma_{m1} \tag{6.10}$$

$$\sigma_2 = \eta' \left\{ \sum_i [V_i S_i \tau] + \sum_j \left[V_j \, E_f \, \varepsilon_2 \left(1 - \frac{E_f \, \varepsilon_2}{4 \, S_j} \right) \right] \right\} + V_m \, \sigma_{m2} \tag{6.11}$$

$$\frac{\sigma_1 - V_m \, \sigma_{m1}}{\sigma_2 - V_m \, \sigma_{m1}} = \frac{\left\{ \sum_i [V_i S_i \ \tau] + \sum_j \left[V_j \, E_f \, \varepsilon_1 \left(1 - \frac{E_f \, \varepsilon_1}{4 \, S_j} \right) \right] \right\}}{\left\{ \sum_i [V_i S_i \ \tau] + \sum_j \left[V_j \, E_f \, \varepsilon_2 \left(1 - \frac{E_f \, \varepsilon_2}{4 \, S_j} \right) \right] \right\}} \tag{6.12}$$

where σ_{m1} and σ_{m2} are stresses applied on the matrix at strain of ε_1 and ε_2, respectively, in elastic region. The η' also can be calculated using Eq. 6.10 or 6.11 when IFSS of the composite is determined.

Values of two strains of ε_1=0.2 % and ε_2 = 1 % were selected and the corresponding stresses (σ_1 and σ_2) were determined from the tensile stress–strain curves of the composites. σ_{m1} and σ_{m2} were obtained from tensile stress–strain curve of the pure PP sample at strains ε_1 and ε_2 respectively. Finally, IFSS(s) and η' were calculated for each composite using Eqs. 6.10-6.12. Table 6.3 presents σ_1, σ_2, IFSS and η' for each composite. The IFSS's between fibre and matrix as a function of fibre weight are shown for both coupled and uncoupled composites in Figure 6.11.

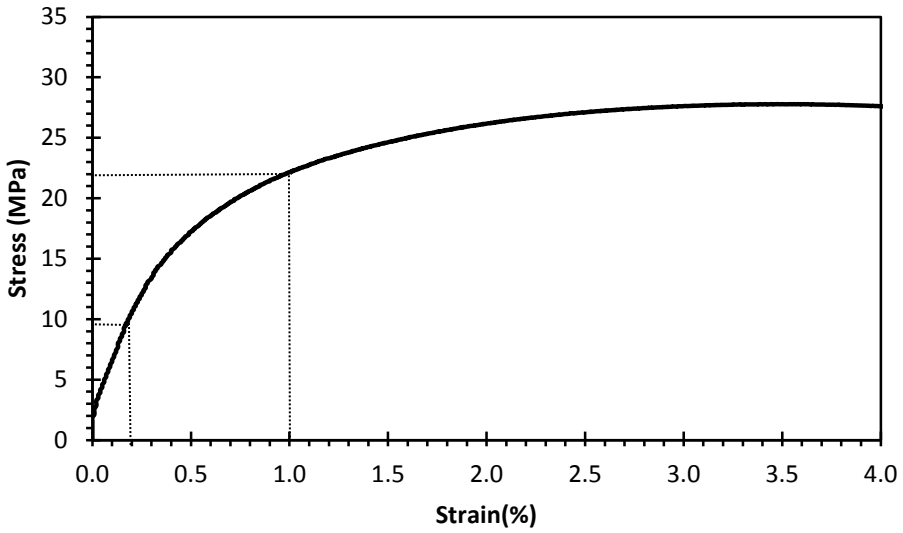

Figure 6.10: A typical stress-strain curve of 40H sample illustrating two extracted points.

Table 6.3: Obtained and predicted parameters

Samples	stress at strain of		η‘	IFSS (MPa)	Predicted tensile Strength (MPa)	Error (%)
	ε= 0.2%	ε= 1%				
Pure PP	3.50	12.00	-	-	-	-
10H	4.60	14.40	0.21	9.73	28.34	6.16
20H	5.36	16.16	0.20	9.50	29.47	1.97
30H	7.63	18.89	0.25	8.67	29.03	3.67
40H	10.46	22.16	0.30	7.25	28.86	2.71
30H5MAP	8.17	24.56	0.26	13.60	36.39	7.41
40H5MAP	10.86	29.59	0.38	12.40	42.76	6.90

As can be noted, IFSS of uncoupled composites were almost unchanged up to 20 wt% and then decreased as the fibre volume fraction further increased. This might happen due to: (1) the poor bonding between fibres when close to each other; (2) shear stress

concentration in the matrix between neighbouring fibres; and (3) possible change in matrix properties which alters the failure mechanism from interfacial debonding to a mixture of interfacial debonding and matrix failure (Qiu and Schwartz, 1991). It can also be seen that IFSS for composites with MAPP is considerable higher than for those without MAPP, supporting improved interfacial bonding between the matrix and fibres. Although the IFSS of the coupled composite with 10 wt% was not evaluated in this paper, it can roughly be estimated using extrapolation of the IFSS-fibre weight content curve for coupled composites. The IFSS of the coupled composite with 10 wt% hemp fibres can be estimated to be less than 15 MPa.

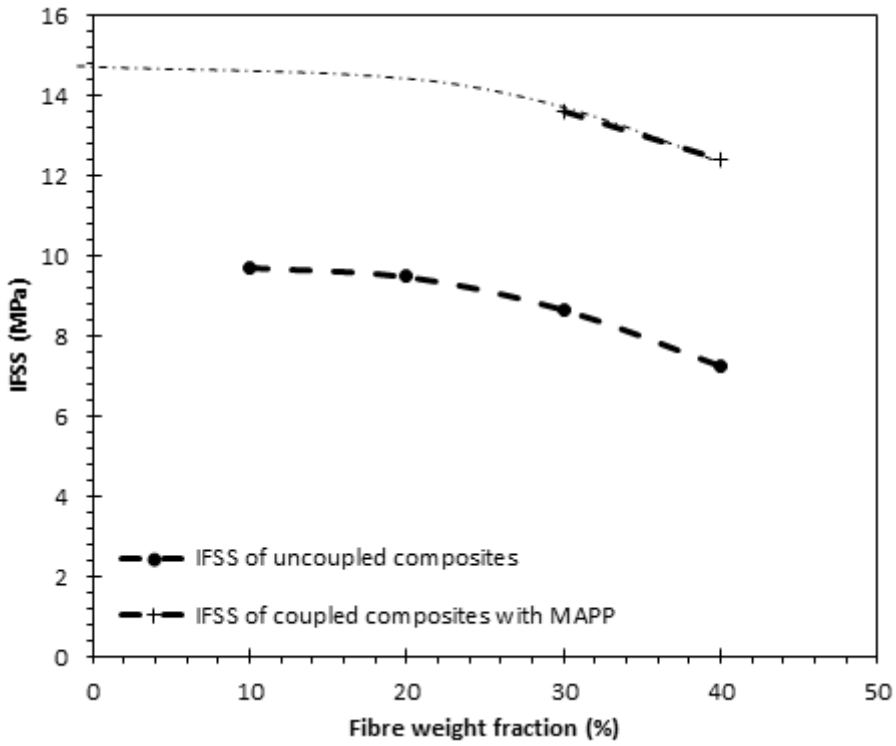

Figure 6.11: Effect of fibre content on interfacial shear strength of uncoupled and coupled noil hemp fibre polypropylene composites.

Referring to the literature, the interfacial shear strength between hemp fibre and polypropylene determined from micro droplet or pull-out tests are varying from 4 to 6

MPa depending on MAPP content or fibre treatment parameters (Li et al., 2009, Park et al., 2006). Also, the determined IFSS using single fibre fragmentation test for alkali treated hemp fibre reinforced polypropylene composite including 4% MAPP as compatibiliser was measured as 15.4 MPa (Beckermann and Pickering, 2009). Thus, calculated IFSS values using modified Bowyer and Bader model in this project are considerably higher than outcomes of micro droplet or pull-out tests and, almost the same as the results from single fibre fragmentation test.

In the case of the single fibre pull out and micro droplet tests, the fibre is subjected to an axial force resulting in a Poisson contraction in the radial direction. It leads to a reduction in the fibre cross sectional area. This phenomenon declines frictional component of the interfacial strength, which finally results in reduced IFSSs. Besides, the load in the pull-out test is axial and, it is assumed that there is a constant shear stress at the fibre–matrix. However, non-linear shear stress occurs because the fibres in real composites are not oriented parallel to the applied loads and they are not completely straight.

6.1.3.3 IFSS Verification

One of the significances of the IFSS values is that they can be used to predict the tensile strength of the noil hemp fibre reinforced polypropylene composites using modified Bowyer and Bader model, Eq. 6.8. The linear relationship shown in Figure 6.9 was used to estimate the tensile strength of the fibres. Stress applied on the matrix (σ_m) at strain failure of the composite was also determined using the stress-strain curve of pure PP. Figure 6.12 illustrates the comparison between the experimental and predicted results. A very good agreement between the experimental and predicted values was reached. The high correlation factor (R^2) in the linear regression implies the acceptable fitting of predicted values to the experimental data. Also, the average errors of 4.8% shows that the developed model has an excellent capability in predicting the tensile strength of noil hemp fibre reinforced polypropylene composites.

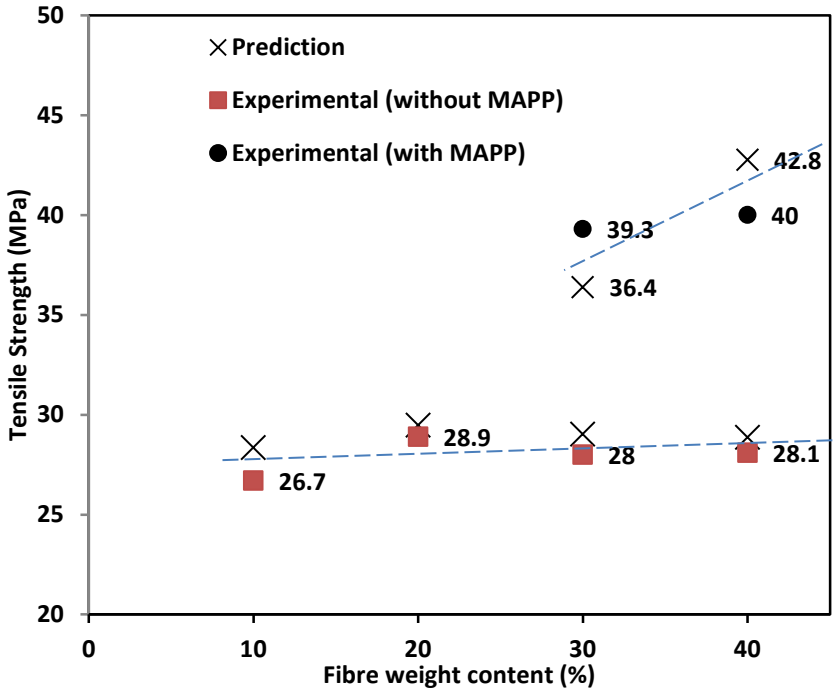

Figure 6.12: Predicted vs. measured tensile strength of the composites.

6.1.3.4 Predictions using the Developed Model

Many investigations have attempted to improve the interfacial strength of the fibre by modifying the fibre's surface or the matrix. The maximum interfacial shear strength is the shear strength of the matrix. The developed model can also be used for predicting the tensile strength of the composites using the shear strength of the matrix. The shear strength of the matrix is difficult to measure and very little data exists in the literature (Liu and Piggott, 1995). Assuming an isotropic matrix, the shear strength can be estimated by the von Mises criterion from the tensile strength of the pure matrix as:

$$\tau_m = {}^{\sigma_m}/_{\sqrt{3}} \qquad (6.13)$$

Therefore, the maximum shear strength for these composites is 17.9 MPa. Figure 6.13 illustrates the tensile strengths as a function of fibre weight content predicted by

Eq.6.8 at maximum theoretical IFSS (17.9 MPa). Even with assumption that maximum theoretical IFSS does not decrease with increase of fibre content, referring to this figure, the highest composite tensile strength can be achieved with 40 wt% fibre is less than 50 MPa, which is still much lower than the common tensile strength of short glass fibre composites.

Another factor to consider is the tensile strength of the fibre. As mentioned earlier, noil hemp fibres have lower mechanical properties than normal hemp fibres. Generally, the tensile strength of the fibres greatly influence the tensile strength of the composites. However, Figure 6.14a shows that once the fibres had a tensile strength more than 200 MPa, further increase in the fibre strength would not affect the tensile strength of the injection moulded composites. It might be due to the fact that higher tensile strength causes a higher critical aspect ratio referring to Eq. 6.6. In other words, the fibre aspect ratio then becomes the dominant factor.

Figure 6.14b presents the influences of scale parameter of aspect ratio from weibull distribution on tensile strength of the noil hemp fibre reinforced composite with 40 wt% hemp fibres. This figure implies that the fibre aspect ratio is of great importance for improving the composite strength. Nevertheless, severe fibre breakage happens during compounding and injection moulding processes, which reduce the aspect ratio of fibres. A most likely reason for this phenomenon is the poor lateral strength of the natural fibres (Davies and Bruce, 1998). Natural fibres exhibit composite-like structure. They consist of cellulose microfibrils with diameters in the order of a couple of nanometres. They are bound together by amorphous cellulose, hemicellulose and pectin which form together so-called elementary fibres of 10-20

μm. The elementary fibres are bound together by weak pectin forming the technical fibre with a diameter of around of 40-100 μm. Thus, due to the existence of the pectin, hemicellulose and amorphous cellulose, the lateral strength of the fibres is poor and natural fibres undergo a high level of fibre breakage during compounding and injection moulding (Davies and Bruce, 1998).

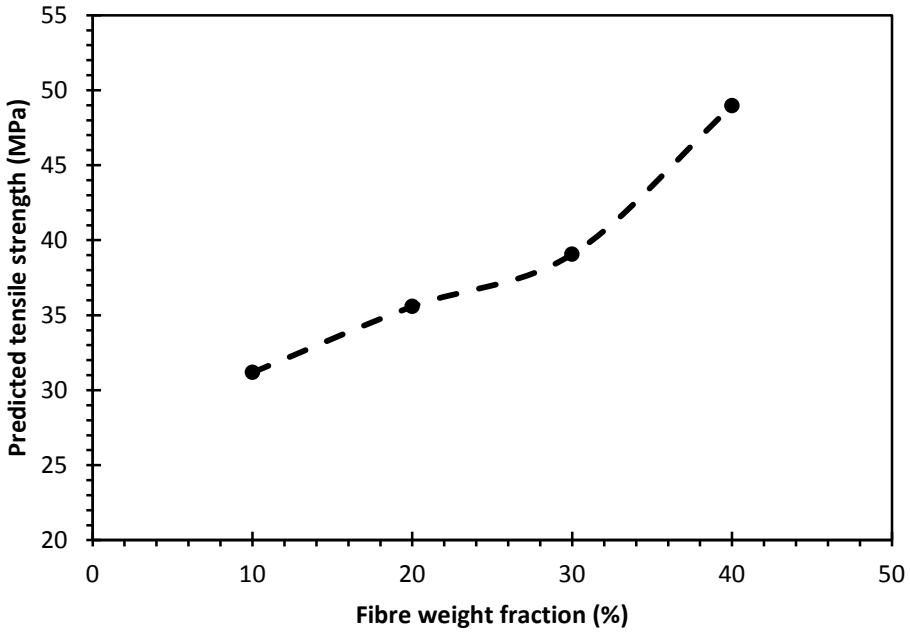

Figure 6.13: Predicted Tensile Strengths at Maximum Theoretical IFSS vs. Fibre Weight Content.

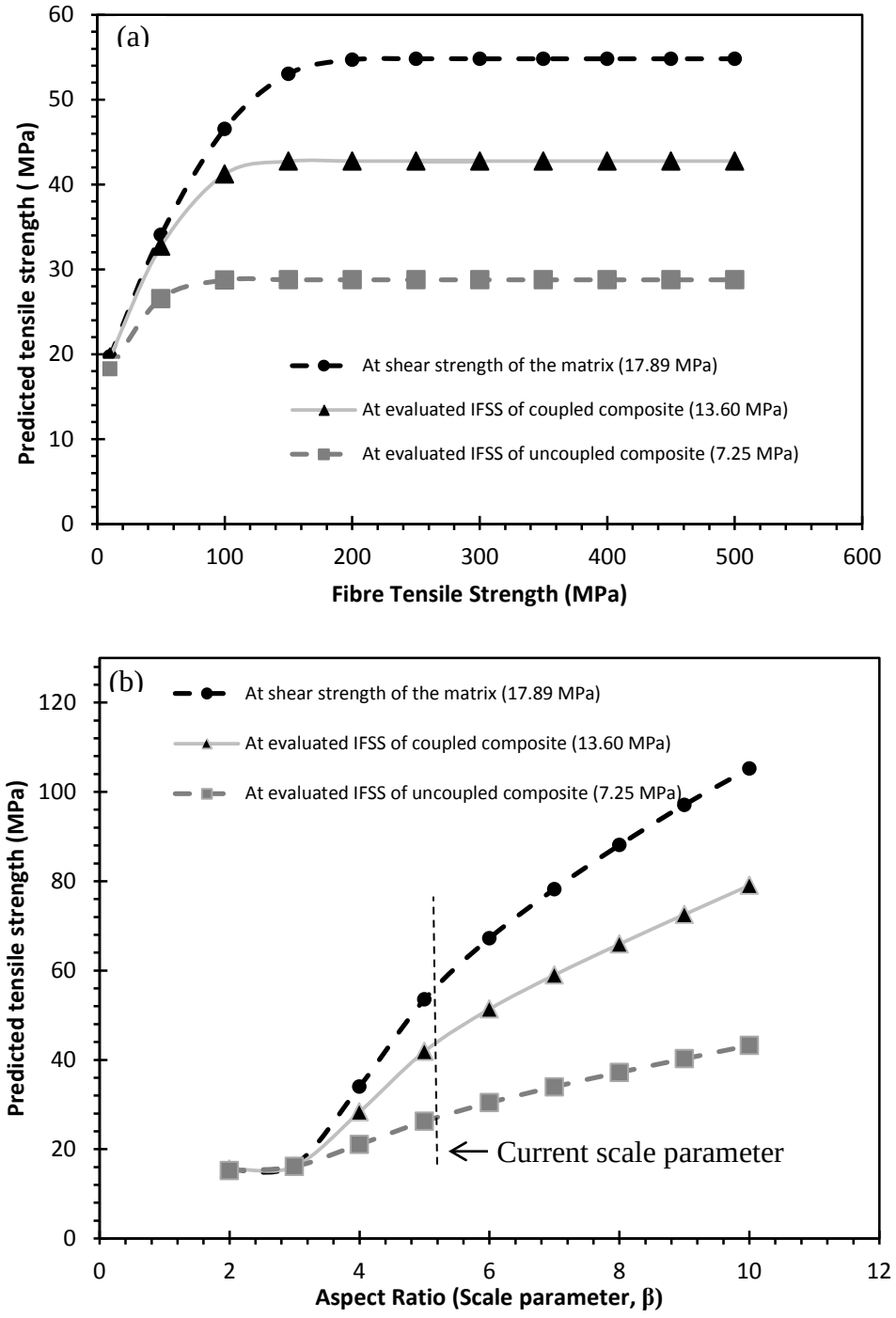

Figure 6.14: Predicted tensile strengths of 40 wt% noil hemp fibre reinforced polypropylene vs. (a) tensile strength of the fibre and (b) scale parameter (β) of aspect ratio Weibull distribution

6.2 Vibration Damping Characteristics

6.2.1 Free Vibration

Figure 6.15 shows the free vibration time histories of pure polypropylene and 40 wt% noil hemp fibres reinforced polypropylene with and without 5 wt% MAPOE coupling agent.

A comparison between Figure 6.15a and Figure 6.15b shows a considerably faster decaying (about 7 times faster) of the vibration acceleration with the addition of 40 wt% noil hemp fibres. Since damping defines the energy dissipation capability of a material (Yan, 2012), this figures implies a higher damping capacity of the 40H composite than that of neat polypropylene. However, as shown in Figure 6.15c, it took a longer time to dampen the vibration when 5 wt% MAPOE is added to the 40 wt% noil hemp fibres composite. However, vibration decayed 2 times faster than pure polypropylene.

The average damping ratios and natural frequencies of the composites, calculated according to section 3.6.5, are given in Table 6.4. Incorporation of fibres into polypropylene increased the natural frequency of the samples from approx. 10.5 Hz to approx. 12 Hz. Not much sensible difference was observed between natural frequencies of the uncoupled and coupled composites. However, roughly speaking, coupled composites showed a slightly higher (7%) natural frequency compared to the uncoupled ones. This will be elaborated upon later.

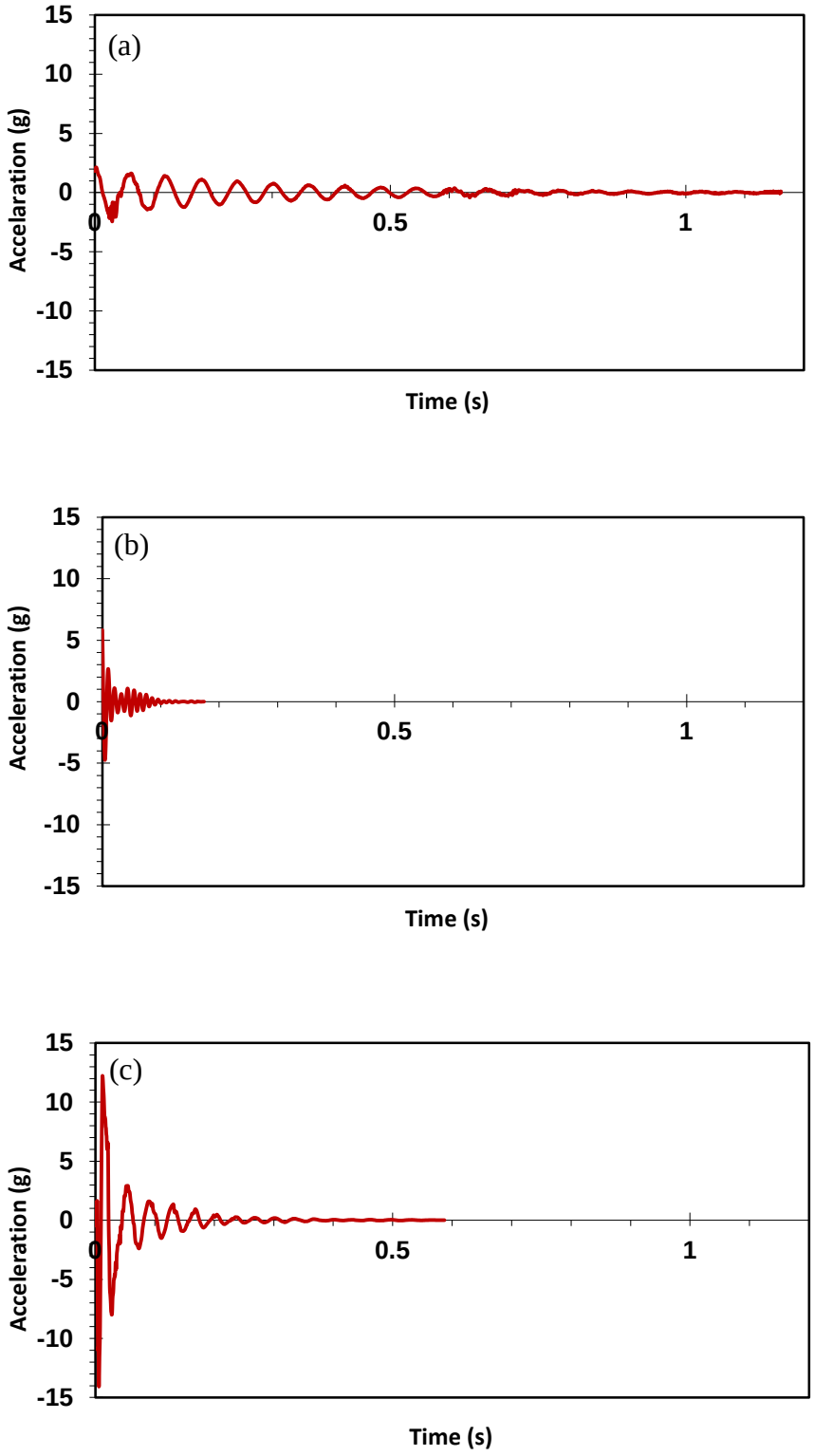

Figure 6.15: Vibration time-history of: (a) pure polypropylene, (b) 40 wt% noil hemp fibre composite without coupling agent and (c) 40 wt% noil hemp fibre composite with 5 wt% MAPOE.

Figure 6.16 plots damping ratio vs. hemp fibre content for uncoupled composites. It can be seen that the calculated damping ratio of the composites (calculated using Eq. 3.2) has been increased with addition of 10 wt% noil hemp fibres. This indicates a higher damping capabilities of the 10H composite compared to neat polypropylene. The same trend is observed by adding more fibre up to 30 wt%. The addition of fibre content above 40 wt% resulted in a sudden decrease in the damping ratios of the composites. Compared to the composite with 30 wt% fibres, a slight decrease of the damping ratio can be observed for the composite with 40 wt%, whereas 50 wt% and 60 wt% hemp fibres in the composites resulted in significantly lower damping ratios.

The hemp fibre and polypropylene have elastic and viscoelastic behaviours, respectively. Considering the nature of the materials, it was expected that as the fibre content increased, the composites behaviour would be shifted from viscoelastic to

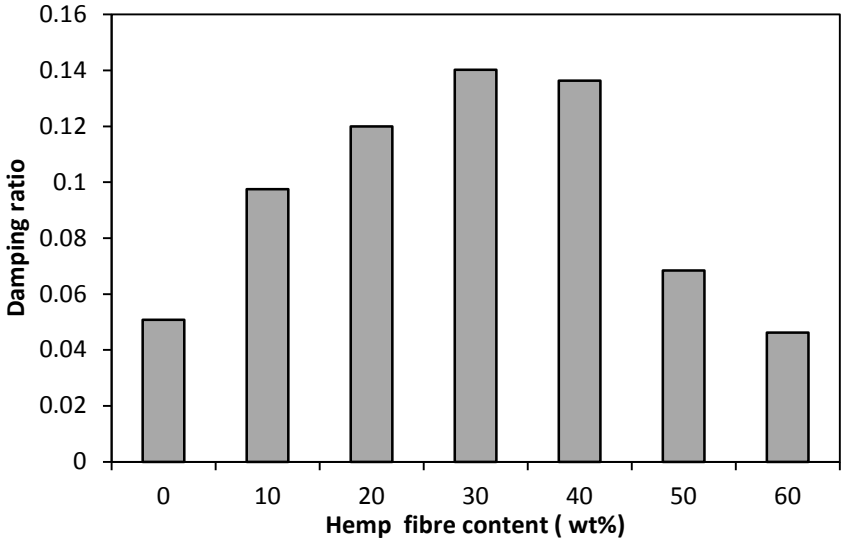

Figure 6.16: Damping ratio vs. hemp fibre content of uncoupled composites.

Table 6.4: Calculated natural frequency and damping ratio. Three specimens were tested for each composite sample.

Samples	Natural frequency (Hz)		Damping ratio	
PP	10.50	(±0.39)	0.053	(±0.002)
10H	12.52	(±0.16)	0.097	(±0.012)
20H	12.66	(±0.13)	0.120	(±0.009)
30H	11.68	(±0.41)	0.140	(±0.006)
40H	11.60	(±0.35)	0.136	(±0.015)
50H	11.11	(±0.56)	0.068	(±0.001)
60H	11.81	(±0.10)	0.046	(±0.003)
30H2.5MAPP	11.72	(±0.15)	0.083	(±0.006)
40H2.5MAPP	13.21	(±0.26)	0.053	(±0.017)
30H5MAPP	13.88	(±0.18)	0.055	(±0.008)
40H5MAPP	13.30	(±0.11)	0.049	(±0.015)
30H2.5MAPOE	12.47	(±0.27)	0.064	(±0.009)
40H2.5MAPOE	12.19	(±0.01)	0.053	(±0.015)
30H5MAPOE	12.50	(±0.34)	0.052	(±0.010)
40H5MAPOE	12.53	(±0.26)	0.052	(±0.016)

elastic behaviour and the damping ratio of the composite would be reduced. However, as mentioned earlier, damping ratios initially increased for fibre content up to 30 wt%, then reduced as the fibre content increased further. Our previous work (Etaati et al., 2013) on these composites revealed that the final fabricated composites include very short fibres and very low bonding adhesion between the short noil hemp fibres and the matrix in the absence of a compatibiliser. The interphase, a region next to the fibre surface all along the fibre length, possesses considerable thickness and its properties are different from those of the embedded fibres and matrix (Chandra et al., 2003) . Therefore, the presence of very short hemp fibres in the uncoupled matrix creates a high amount of fibre-matrix interfacial area in the composites where energy can be dissipated. Thus, more energy can be dissipated during vibration due to the internal friction between the fibres and the matrices when a high number of fibre/matrix interfaces are involved and the fibre/matrix bonding is low. Ultimately, this leads to larger damping ratios of the composites.

To summarise, the damping property of the composites is mainly comprised of two different damping mechanisms: the damping capabilities of (1) the PP matrix and (2) the interphase. Thus, although decrease in PP content can have a negative impact on damping capabilities of the matrix, it was evident that the damping ratio of the composites were increased with increasing content of noil hemp fibres. As the volume fraction of noil hemp fibre was increased from 0 to 30 wt%, more fibre–matrix interfacial area was created and more energy could be dissipated by the poor fibre–matrix interface. Therefore, “damping due to interphase” is the dominant damping mechanism if the noil hemp fibre content is less than 30 wt%. In higher fibre contents, the dominant damping mechanism gradually changes from “damping due to

interphase" to "damping due to the viscoelastic nature of PP". As can be seen in Figure 6.16, damping ratios of the composites with 60 wt% noil hemp fibre are even lower than that of pure PP because of the low amount of viscoelastic PP.

Figure 6.17 shows the impact of the matrix modification on damping ratio of noil hemp fibre reinforced polypropylene. Generally speaking, the damping ratio of the coupled composites is lower than that of the uncoupled composites. It is worth noting that unlike damping ratio, tensile strength of NFRC can be improved by compatibilisation (Etaati et al., 2013, Ku et al., 2011, Mohanty et al., 2001). In the presence of a compatibiliser, the fibre/matrix interfacial adhesion is improved due to the higher wettability of the matrix. It has been reported that there are visible voids and gaps between the adjacent fibres and the matrices without compatibilisers, which indicates a poor fibre/matrix interfacial adhesion (Yan, 2012, Mohanty et al., 2006). Under vibration, these gaps result in the dissipation of energy by fibre/matrix friction. On the other hand, with a coupling agent addition, the fibre/matrix interfacial adhesion is improved and the gaps at the fibre/matrix interfaces are narrowed resulting in less dissipation of energy during the vibration.

A comparison between Figure 6.17a and Figure 6.17b points the fact that coupled composites reinforced with 30 wt% noil hemp fibres have relatively higher damping ratios than the composite having 40 wt% fibres. Referring to Figure 6.16 and Figure 6.17, composites coupled with 2.5 wt% of either of the coupling agents demonstrate higher damping ratio than composites coupled with 5 wt%. The composite reinforced with 30 wt% noil hemp fibre and coupled with 2.5 wt% maleic anhydride grafted polypropylene (MAPP) coupling agent has the highest damping ratio among coupled

composites, although this is a 42% decrease in damping ratio of the uncoupled composite. The decrease in damping ratio is about 60% for all coupled composites having 40 wt% fibres, compared to the uncoupled one.

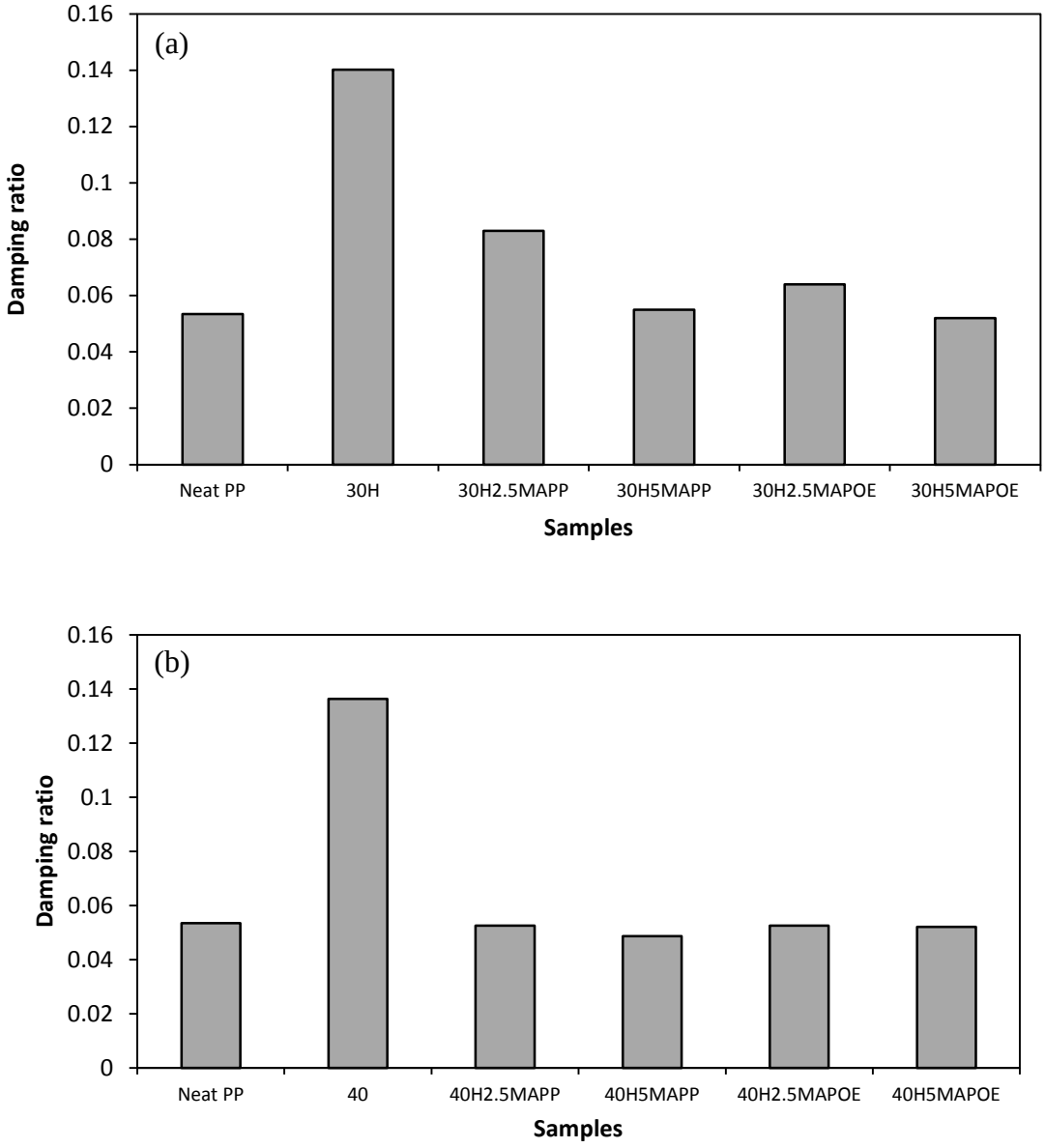

Figure 6.17: Effect of coupling agents on damping ratio of the composites reinforced with (a): 30 wt% and (b): 40 wt% noil hemp fibres.

6.2.2 Dynamic Vibration

The damping behaviour of the material is dependent on the temperature and frequency parameters that influence the tan δ (damping ratio) of the composites (Romanzini et al., 2012). In this work, the influence of frequency at room temperature of 25°C was investigated. Figure 6.18 presents the results obtained from the dynamic mechanical analysis at room temperature (single cantilever mode) as a function of frequency.

As can be viewed in Figure 6.18, the addition of noil hemp fibres up to 30 wt% hemp fibre content could increase the tan δ of the composites. However, further addition of fibres reduced the tan δ of composites. Finally, tan δ values of 50H and 60H samples were even lower than that of pure polypropylene. This is consistent with the results observed from the free vibration testing.

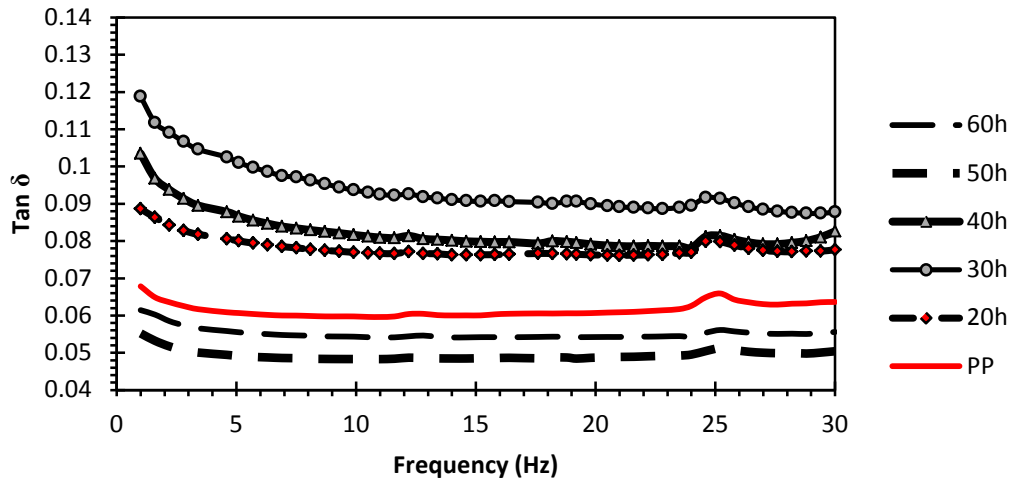

Figure 6.18: Tan δ values of uncoupled noil hemp fibre reinforced composites as a function of frequency.

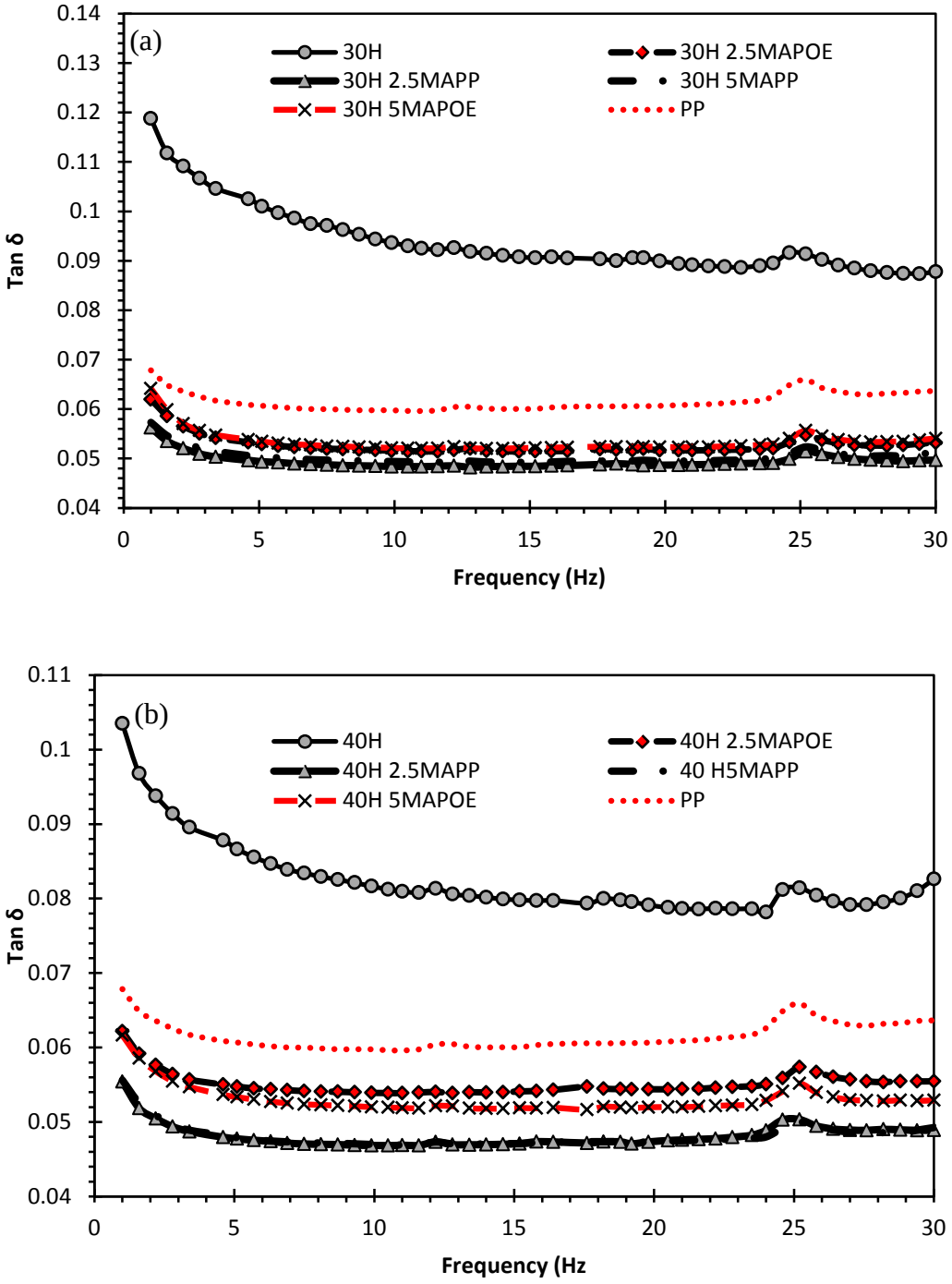

Figure 6.19: Effect of compatibiliser addition on tan δ of (a) 30wt% and (b) 40wt% noil hemp fibre reinforced composites.

As mentioned previously, two main mechanisms determine the damping capacity of composites. Composites with up to 30 wt% hemp content, frictional damping is the dominant mechanism that occurs due to the slip in the poor bonding regions between fibres and matrix interface. This mechanism improves damping capacity with increase of short fibres up to 30 wt%, whereas further increase of short fibre content changes the dominant damping mechanism to viscoelastic nature of the matrix and/or fibre. Since addition of short noil hemp fibres reduces the content of viscoelastic matrix, the damping capacity of the investigated composites with high fibre declined to the values even less than that of pure polypropylene.

Figure 6.19a and Figure 6.19b show the variations of the tan δ of modified short noil hemp fibre composites having 30 wt% and 40 wt% fibre content, respectively. Incorporating the compatibilisers in the 30H or 40H composites decreased tan δ to the levels less than that of pure PP. It happened due to the stronger interfacial adhesion between the fibre and coupled matrix, which reduces frictional damping in the interphases (Etaati et al., 2013, Ku et al., 2011, Bengtsson et al., 2007).

As observed in Figure 6.18 to Figure 6.19, tan δ values of polypropylene and the composites showed very little dependency on frequency below 30 Hz at room temperature. An initial small decrease in tan δ values was observed as the frequency increased to about 5 Hz. Despite initial variations, all values are relatively constant over the frequency range tested.

The values at about 12 and 25 Hz are the exceptions to this behaviour. The first natural frequency (12 Hz) observed in DMA curves is in correlation with the natural frequency calculated in free vibration testing. As such, these conditions have been

observed in the literature (Menard, 1999, Placet and Foltête, 2010) when the material-instrument system began to resonate at certain frequencies. These frequencies are either the natural resonance frequencies of the sample-instrument system or one of its harmonics. (Placet and Foltête, 2010)

The influence of frequency at room temperature is more noticeable at higher frequencies as presented in Figure 6.20. The figure shows the dependency of mechanical and damping properties on fibre content of the composites at a frequency range between 1 Hz to 200 Hz. Referring to Figure 6.20, the natural frequencies have been shifted by an increase of hemp fibre content in the matrix. Eq. 6.14 shows the relationship between natural frequency, stiffness and mass as:

$$f = \frac{1}{2\pi} \times \sqrt{\frac{E}{m}} \tag{6.14}$$

where f is natural frequency, m is composite mass and E is the composite's stiffness. Therefore, the natural frequency of a composite with higher amount of noil hemp reinforcing fibres is expected to increase because composites with higher content of noil hemp fibres have considerably higher stiffness. It is worth noting that the density of noil hemp fibres is slightly higher than that of polypropylene. However, the effect of fibre addition on the composite's mass is negligible.

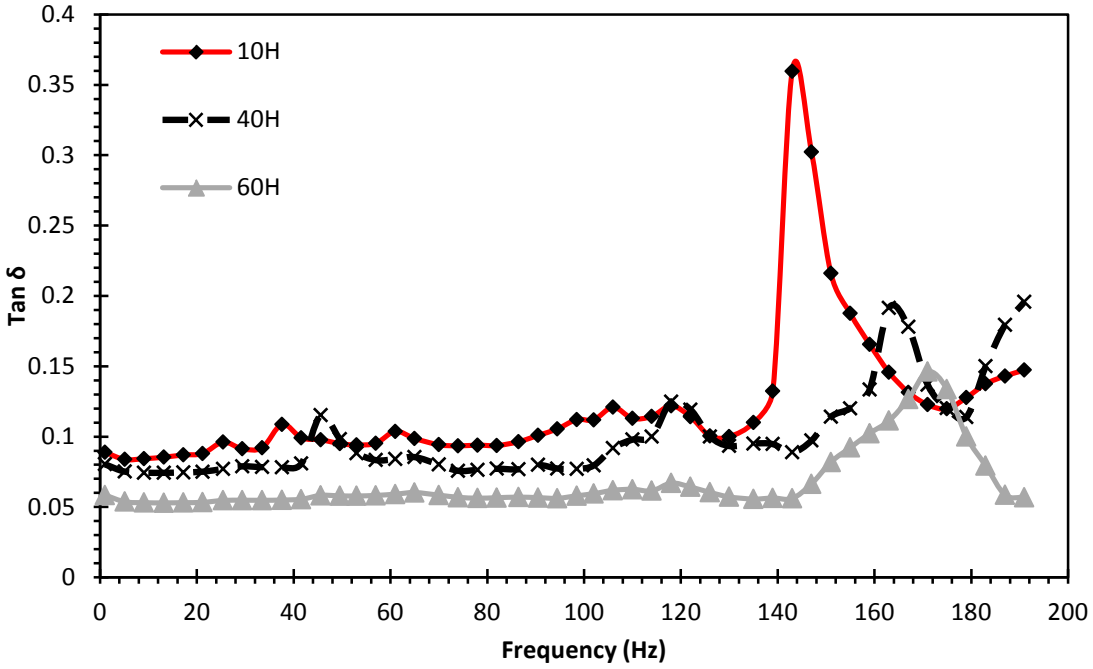

Figure 6.20: Tan δ values of uncoupled noil hemp fibre reinforced composites as a function of frequency.

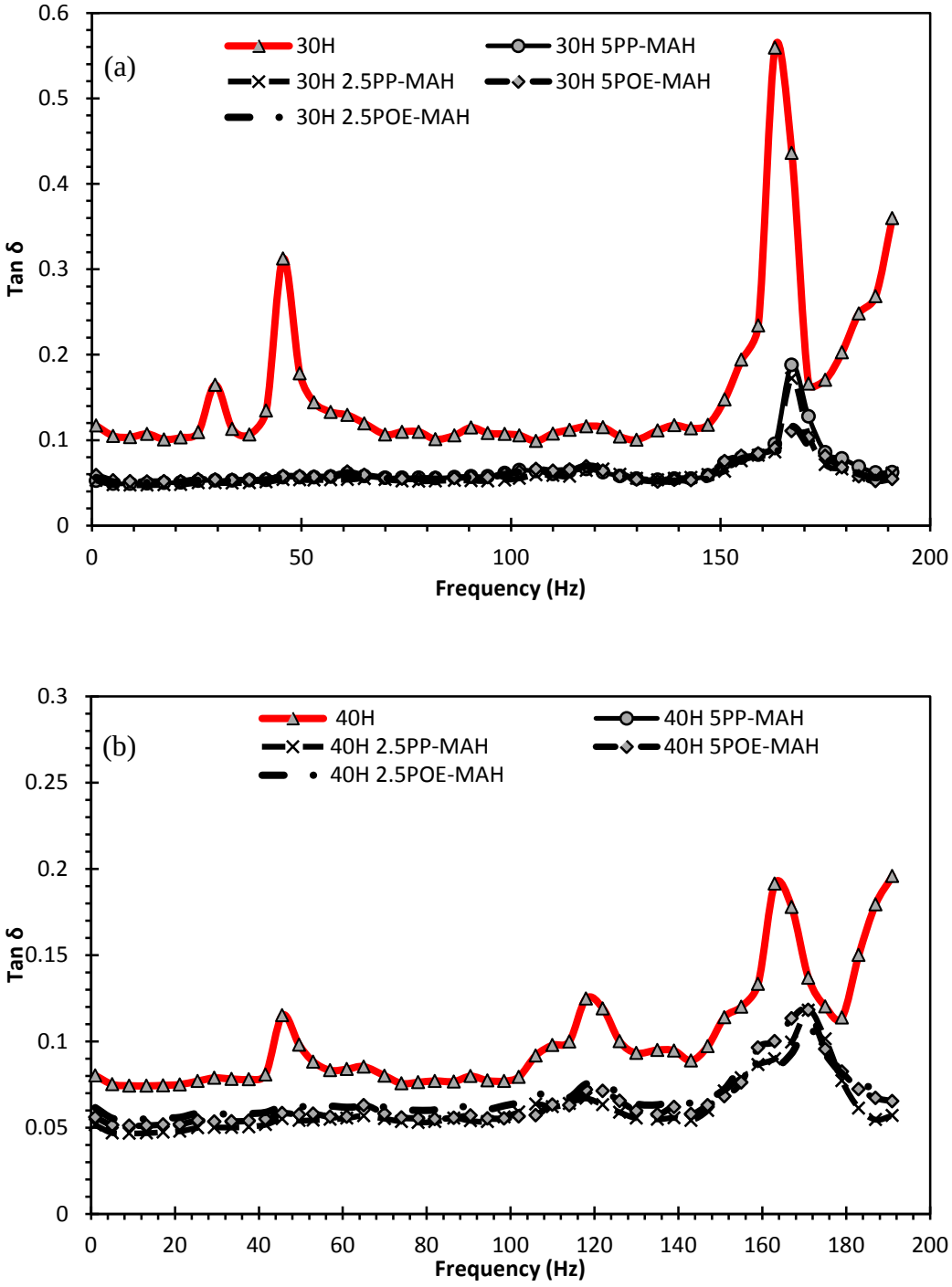

Figure 6.21: Effect of compatibiliser addition on tan δ of (a) 30wt% and (b) 40wt% noil hemp fibre reinforced composites.

Figure 6.21 presents the influence of compatibilisation on tan δ values of the composites in the frequency range up to 200 Hz. All coupled composites illustrated almost similar behaviours as the frequency increased.

Regardless of the amount and type of coupling agents, sharp peaks, which can be obvious in the tan δ-frequency curves of uncoupled composites, were weakened or even disappeared after compatibilisation. This implies that the addition of coupling agent improved the response of the composites at their natural frequencies, whereas compatibilisation decreased the damping ratio of the composites.

6.3 Dynamic Mechanical Analysis

6.3.1 Effect of fibre content

The storage modulus (E′) is the contribution of the elastic component of the composites. The variation of storage modulus as a function of temperature at different fibre contents under DMA frequency of 1 Hz is given in Figure 6.22. In comparison with the pure polypropylene, it can be seen that the storage modulus of the composites increases with increase in hemp contents over the entire temperature range. The modulus of polypropylene is determined primarily by the strength of the intermolecular forces and by the way the polymer chains are packed (Romanzini et al., 2012). However, when fibres are added into the polypropylene matrix, the increase in the modulus is attributed to the stiffness imposed by the fibres. Furthermore, a large fall can be observed in storage moduli of all composites with increasing temperature. The reinforcing effects of fibres in different temperatures can be evaluated by the effectiveness coefficient C. The effectiveness coefficient C is the ratio between the composite storage modulus (E′) in two different regions, such as

glassy and rubbery regions, in relation to the neat resin and can be calculated using *Eq. 6.15* (Romanzini et al., 2012):

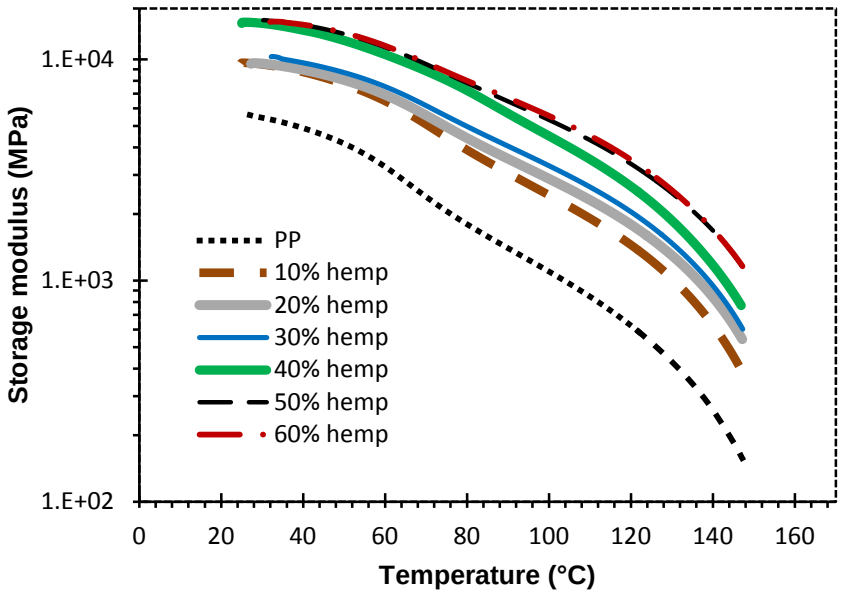

Figure 6.22: Storage modulus of uncoupled noil hemp fibre reinforced composites as a function of temperature under DMA loading frequency of 1Hz.

$$C = \frac{{E'_g}/{E'_r}\ composite}{{E'_g}/{E'_r}\ resin} \tag{6.15}$$

where E_g' and E_r' are the storage moduli in the glassy and rubbery regions, respectively. The higher the value of the constant C, the lower the effectiveness of the filler (Romanzini et al., 2012, Idicula et al., 2005). Table 6.5 shows the effectiveness coefficient C of the composites at four different elevated temperatures. All effectiveness coefficients C were calculated using *Eq. 6.15* based on the properties at the temperature of 45°C.

General speaking, as the temperature increases, the coefficient C value of the composites decreases. This indicates that the incorporation of fibres imposes a better

Table 6.5: Effectiveness Coefficient C as a function of noil hemp fibre content

Fibre content (wt%)	C (90°C)	C (110°C)	C (130°C)	C (150°C)
10	0.80	0.77	0.73	0.70
20	0.69	0.64	0.60	0.51
30	0.65	0.61	0.55	0.49
40	0.66	0.64	0.62	0.55
50	0.60	0.54	0.48	0.37
60	0.57	0.51	0.45	0.37

reinforcing effect at higher temperatures. In addition, increasing the fibre content decreases the coefficient C value. Hence, the effectiveness of the composite is higher at higher fibre content. The variation of loss modulus and tan δ with temperature for different fibre content is shown in Figure 6.23. Loss modulus (E'') is the contribution of the viscous component and is a measure of the energy dissipated in the materials. It can be seen in Figure 6.23a that the loss modulus increases with the increase of fibre content over the entire temperature range tested. The increase in loss modulus with increase in fibre content is attributed to the increase in energy absorption with increasing fibre content. The presence of very short hemp fibres in the matrix created a high amount of fibre-matrix interfacial area in the composites where energy could be dissipated. A stronger interface is characterised by lower energy dissipation. Thus, higher loss modulus values in the composites imply lower interfacial adhesion between fibres and the matrix. This can be studied in more detail by studying the damping ratio (tan δ) of the composites.

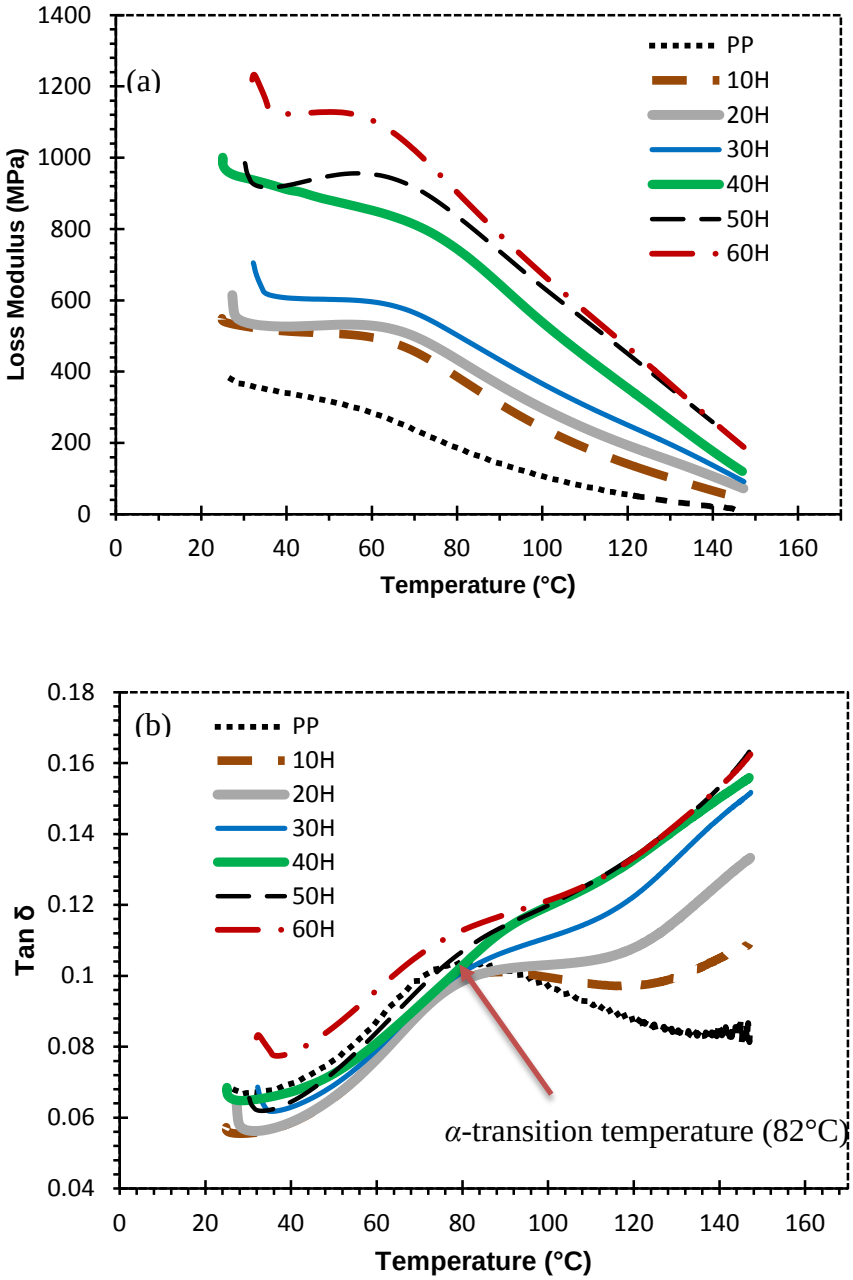

Figure 6.23: (a) Loss Modulus and (b) Damping Ratio of uncoupled noil hemp fibre reinforced composites as a function of temperature under DMA loading frequency of 1Hz.

Tan δ (loss factor/damping ratio) is defined as the ratio of the loss modulus to the storage modulus. It is the ratio of the energy dissipated to the energy stored during a dynamic loading cycle. The contribution to damping in a composite is due to: the nature of the matrix and/or fibre materials; friction generated from the slip in the matrix/fibre interface; energy dissipation at cracks and delaminations produced at

damaged locations; and viscoplastic and thermoelastic damping (John and Anandjiwala, 2009). Figure 6.23b shows the variation of tan δ with temperature for different fibre contents. For the polypropylene, as the temperature increased, the tan δ value initially increased until it reached a peak at its α-transition temperature and then decreased. The position of the peak can represent the α-relaxation temperature of 82°C for the polypropylene sample. It was also observed that the addition of noil hemp fibres does not cause significant changes in α-relaxation temperatures of the composites. This is in agreement with the literature (John and Anandjiwala, 2009, Jacob et al., 2006), in which the position of α-relaxation was not significantly altered upon incorporation of short fibres.

Studying the viscoelastic behaviour of the composites is more complicated than pure polypropylene. Total energy dissipation in the composites depends on the nature of the individual components, their fractions in the composite and the interfacial adhesion between the matrix and the fibre. To simplify the study of the viscoelastic behaviour, two elements will be considered: the damping ratio of the composites and the complex modulus. The relationship of the damping ratio can be stated as (Chauhan et al., 2009):

$$\tan \delta_C = \tan \delta_S + \tan \delta_{in} \tag{6.16}$$

where tan δ_C, tan δ_S *and* tan δ_{in} are damping ratios of the composite, the system/materials (fibre and matrix) and the interface respectively. The damping ratio of the system can be obtained from the complex modulus of the fibre and the matrix.

The tan δ_S can be calculated as (Chauhan et al., 2009):

$$\tan \delta_S = \frac{\tan \delta_f E'_f V_f}{E'_C} + \frac{\tan \delta_m E'_m V_m}{E'_C} \quad (6.17)$$

Therefore, the total system damping (tan δ_s) can be estimated from the storage modulus, damping ratio and volume fraction of the individual components (fibre and matrix) and storage modulus of the composite (Chauhan et al., 2009). Hence from *Eq. 6.16*, the interface damping (tan δ_{in}) can also be estimated by subtracting the system/material damping ratio (tan δ_s) from the total composite damping ratio (tan δ_c).

For a composite material consisting of solid elastic fibres and viscoelastic polymeric matrix, $\tan \delta_f$ would be almost zero (Chauhan et al., 2009) and thus $\frac{\tan \delta_f E'_f V_f}{E'_C} \approx 0$. Therefore, the total system damping (tan δ_s) is determined only by damping ratio and storage modulus of the matrix and the storage modulus of the composite.

However, in the case of natural fibre reinforced polymers the problem is more intricate. Unlike inorganic fibres, the lingo-cellulosic fibres are composed of amorphous (lignin, hemicellulose) and semicrystalline (cellulose) ingredients. Hence, the behaviour of the natural fibres must be considered as viscoelastic. Many researchers have studied the behaviour of cellulose and lingo-cellulosic materials (Montes et al., 1997, Roig et al., 2011, Placet, 2009). Referring to the literature, four temperature transition modes have been reported for hemp fibre. Two transition modes (γ and β) were observed below 0°C while the rest (α_1 and α_2) were observed above 0°C. The α_1 and α_2 transitions are attributed to the polymer chain movement of lignin and carbohydrate components (hemicelluloses and cellulose), respectively (Kelley et al., 1987, Jafarpour et al., 2008, Obataya et al., 2001) .

The transition modes and damping behaviour of hemp fibres are strongly affected by the fibre's moisture content and its composition. It has been reported by Placet et al. (Placet, 2009) that the viscoelastic behaviour of dry hemp fibre is similar to that of wood and its damping ratio (tan δ) is about 0.03 from room temperature to 150°C. Considering a damping ratio of 0.03, the tan δ_s and the tan δ_{in} of the composites were calculated and plotted (Figure 6.24)

Figure 6.24a presents the system/material damping ratio of the composites as a function of temperature. It can be seen that the material damping (tan δs) dropped significantly with the introduction of 10 wt% hemp fibre into the polypropylene matrix. This is associated with the fact that there is a physical difference between the matrix surrounding the fibres and the rest of the matrix. A shell of immobilised polymer surrounds the fibres and immobilised matrix hinders the molecular motion during the relaxation process. Therefore, the height of the peak declined as the 10 wt% hemp fibre was added into polypropylene matrix. Further addition of the hemp fibre decreased the damping ratio levels and flattened the curves, to the extent that there is no recognisable peak in tan δs curves of the composites with high fibre content.

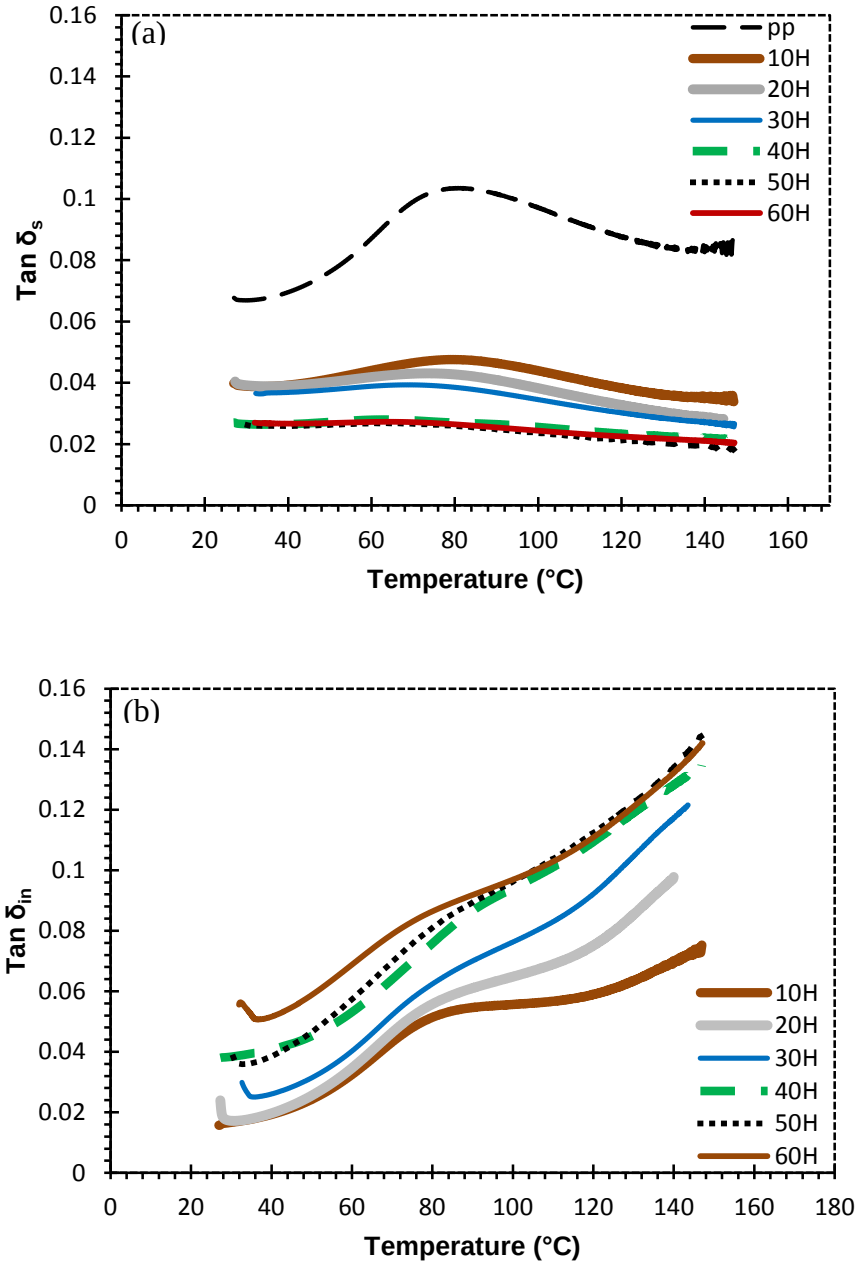

Figure 6.24: (a) System and (b) Interphase Damping Ratio of uncoupled noil hemp fibre reinforced composites as a function of temperature under DMA loading frequency of 1Hz.

Figure 6.24b shows the interphase-damping ratio of the composites as a function of temperature. In an ideal interface, the interface does not contribute to the damping. Practically, the interface region dissipates energy and contributes to the damping. As can be seen in Figure 6.24b, the interface damping in composites was found to increase with the increase in fibre content. Considering that for a weak interface, more energy is dissipated (Afaghi-Khatibi and Mai, 2002), the increase in the interface damping can be attributed to two reasons: (1) increase in fibre content results in a larger amount of energy dissipation sites and also (2) lower interfacial adhesion between fibre and matrix occurs as fibre content increases. In those composites with higher fibre content, lower interfacial adhesion between fibre and matrix can occur due to: (1) the poor bonding between fibres that are close to each other; (2) shear stress concentration in the matrix between neighbouring fibres; and (3) possible change in matrix properties which alters the failure mechanism from interfacial debonding to a mixture of interfacial debonding and matrix failure (Qiu and Schwartz, 1991).

It can be seen in Figure 6.24b that as the temperature increases, the interface damping (tan δ_{in}) increases. This results from lower interfacial adhesion between the fibres and the matrix at elevated temperatures. It is also worth mentioning that small peaks can be observed in the tan δ_{in}-temperature curves at α-transition temperature where the polymer's molecular motion occurs. The chain rotation of polymers leads to higher amounts of deformation/friction between fibres and the matrix, which increases damping at the interphases.

6.3.2 The effects of compatibiliser

Figure 6.25 illustrates the effects of coupling agent addition on storage modulus values of 30 wt% noil hemp fibre polypropylene composites. It can be seen that the storage modulus values of composites were greatly improved by the addition of the coupling agents into the PP matrix, which result from the enhancement of interfacial adhesion between the fibre and polypropylene matrix. Maleic anhydride coupling agents improve the bonding between fibre and matrix by chemically bonding to available OH groups on the fibre surface and then adhering to the matrix through molecular chain entanglement. It is interesting that the greatest improvements in E′ were achieved by the addition of 2.5 wt% of either coupling agents and, higher coupling agent content reduced the E′ values of the composite. Table 6.6 also confirms that 30 wt% noil hemp composite coupled with 2.5 wt% MAPP has the lowest effectiveness coefficient C (highest reinforcing effect) in the investigated temperature range.

As far as the bonding between the fibre and the matrix is concerned, tan δ is a better indicator than storage or loss modulus, as its value is not dependent on sample geometry (Tajvidi et al., 2010). Thus, in order to evaluate the effects of coupling agent on the composites, their effects on the polypropylene matrix and the matrix/fibre interphase was studied separately. In this regard, tan δ_S and tan δ_{in} of the coupled composites were also calculated using *Eq. 6.16* and *Eq. 6.17* and then plotted in Figure 6.26a and Figure 6.26b, respectively. Referring to Figure 6.26a, reduction in tan δ_s of the composites implies that the polypropylene matrix became more elastic as coupling agents were added.

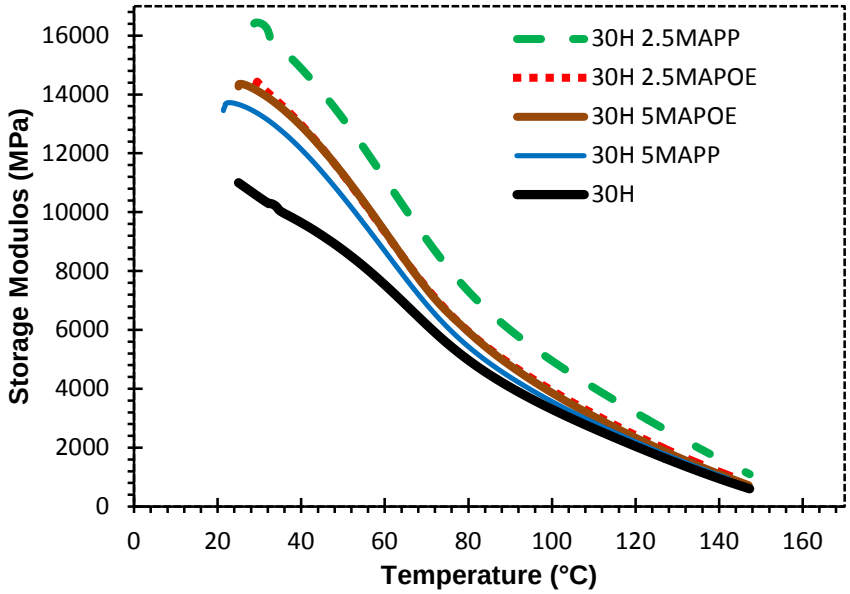

Figure 6.25: Influence of coupling agent addition on storage modulus values of 30wt% hemp sample.

At constant fibre content, the damping term can be used to evaluate the interfacial properties between the fibre and the matrix. Figure 6.26b shows the effects of coupling agent addition on the interphase damping of the composite with 30 wt% hemp fibre. General speaking, the addition of coupling agents significantly reduced the interphase damping (improvement in interfacial bonding).

It is worth noting that the effect of coupling agents appears to become more prominent at temperatures below the transition temperature than above it. Also, compared with MAPOE, MAPP coupling agent caused lower interphase damping ratio. This implies that bonding between the fibre and the matrix resulted from MAPP addition is considerably stronger than that resulted from MAPOE addition.

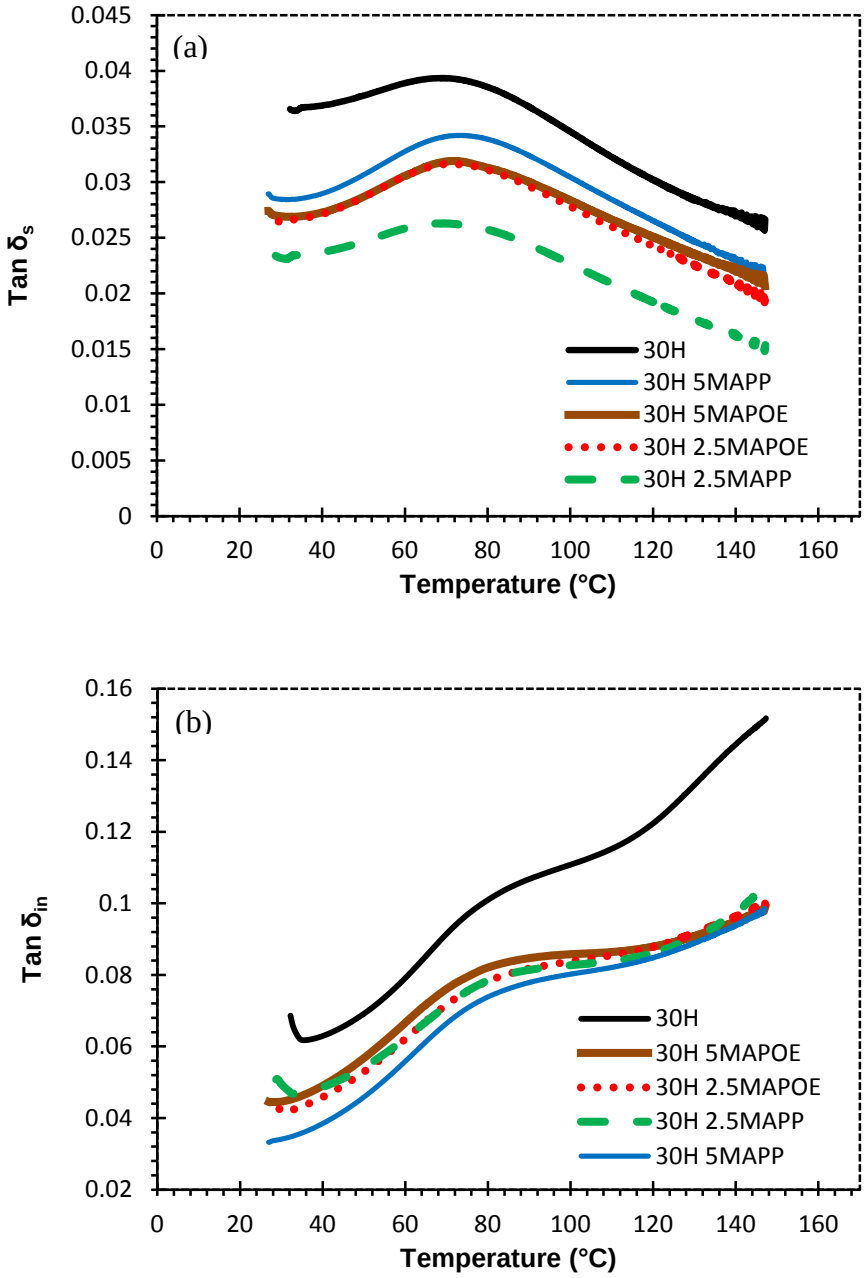

Figure 6.26: (a) System and (b) Interphase Damping Ratio of noil hemp fibre reinforced composites as a function of temperature under DMA loading frequency of 1Hz.

On the other hand, at high temperatures (above the transition temperature), the interphase damping ratios were almost at the same level for all coupled composites. It can also be seen that increase of coupling agent content from 2.5 to 5 wt% MAPP reduced the δ_{in} of the composite, which then improved the interfacial bonding between the fibre and the matrix. This occurred due to higher probability of the MAPP groups to bond to OH groups on the fibre surface.

Table 6.6: Influence of coupling agent addition on effectiveness coefficient C of 30 wt% noil hemp composite.

Coupling agent	Content (wt%)	C (90°C)	C (110°C)	C (130°C)	C (150°C)
MAPP	2.5	0.72	0.64	0.55	0.44
MAPP	5	0.79	0.74	0.66	0.55
MAPOE	2.5	0.77	0.72	0.64	0.53
MAPOE	5	0.78	0.73	0.68	0.58

7. Initial Fibre Length On Mechanical Properties

7.1 Introduction

It is well known that compounding and injection moulding of composites can damage fibres and also reduce the final fibre length. In a research work (Gupta et al., 1989) investigating commercial glass fibre reinforced polypropylene (PP) in extrusion and injection moulding, it was shown that forces on the fibre, mainly in the melting zone, break fibres into lengths of approximately 0.5 mm. Guo et al. compounded and injection moulded a range of natural fibres including wood pulps, bast fibres and wood flour (Guo et al., 2010). It was reported that after injection moulding all fibre types were reduced to fibre lengths of approximately 0.25 mm. Our previous work revealed that original fibre length of approximately 15 mm was shortened to less than 0.4 mm due to fibre breakage during the compounding and injection moulding processes. The average of the final length was approximately 0.2 mm, which was dependent on the fibre content and the compatibilisation addition (Etaati et al., 2013, Etaati et al., 2014). In addition, long initial fibres (1.5 cm) resulted in a high level of fibre agglomeration in the composite, which consequently degraded the mechanical properties of the composites, especially in high fibre loadings.

Longer fibres are generally preferred for achieving better mechanical properties of fibre reinforced composites. However, longer fibres can cause a higher level of fibre agglomeration. Agglomeration of the fibres declined the mechanical properties of the materials.

As the final fibre length is less than approximately 0.4 mm, the question then raised was what if ground fibres (powders/fillers) are used instead of longer fibres (1.5 cm) which can reduce the fibre agglomeration in the composites. Therefore, the fibres were ground into different lengths of 0.2, 0.5, 1 and 2 mm, composites containing 40 wt% short hemp fibre and 5 wt% maleic anhydride grafted polypropylene (MAPP) were fabricated using a twin-screw extruder and an injection moulding machine and then the effects of initial fibre length on mechanical properties of hemp fibre polypropylene composites were investigated in this chapter. It must be noted that the PP type used in this chapter is different from that used earlier. The mechanical properties of the samples are as below:

7.2 Tensile properties

The tensile strengths of the pure polypropylene and their composites with 40 wt% fibre content with various initial fibre lengths are illustrated in Figure 7.1 and Table 7.1. It can be seen that the addition of 40 wt% noil hemp fibre with an initial length of 0.2 mm into the pure PP increased the tensile strength of the samples from 16.9 MPa to 32.8 MPa.

Table 7.1: Tensile properties of the noil hemp fibre and hemp fibre composites with varying initial fibre lengths

Fibre length (mm)	Noil hemp fibre			Hemp fibre		
	Tensile strength (MPa)	Young's modulus (GPa)	Strain at break (%)	Tensile strength (MPa)	Young's modulus (GPa)	Strain at break (%)
0.20	32.85 ±0.67	3.57 ±0.29	3.06 ±0.32	33.61 ±1.35	3.77 ±0.31	3.09 ±0.61
0.50	31.83 ±1.96	3.29 ±0.29	3.29 ±0.88	32.86 ±0.36	3.38 ±0.67	3.35 ±0.36
1.00	27.90 ±2.76	3.03 ±0.07	2.51 ±1.3	31.53 ±2.23	3.55 ±0.88	2.53 ±0.41
2.00	31.18 ±2.47	3.32 ±0.30	2.76 ±1.25	29.64 ±1.78	3.03 ±0.52	2.48 ±0.71

In addition, it can be noted in Figure 7.1 that as the initial fibre length increased, the tensile strength of the samples decreased gradually. However, the difference between composites with 0.2 mm and 0.5 mm is insignificant.

This implies the fact that homogeneity (distribution) of fibre in the matrix is more important when final lengths of the fibres are below the respective critical fibre length. In other words, feeding of long fibres into compounding and injection moulding machines not only cannot improve the tensile properties of the composites but also can degrade their properties due to the formation of fibre agglomerations and consequently heterogeneous dispersion of the fibres.

Young's modulus of the samples followed the similar trend (Figure 7.2). It increased from 1 GPa for pure PP to 3.6 GPa for composite with 0.2 mm long fibres. Then it decreased gradually as the fibre length increased.

It is also worth mentioning that the increase of fibre length also reduced the strain at break of the composites. It was approximately 3 % for the composites with initial

fibre length of 0.2 mm and 0.5 mm, but only declined to approximately 2.5% for the initial fibre length of 1 and 2 mm (Figure 7.3).

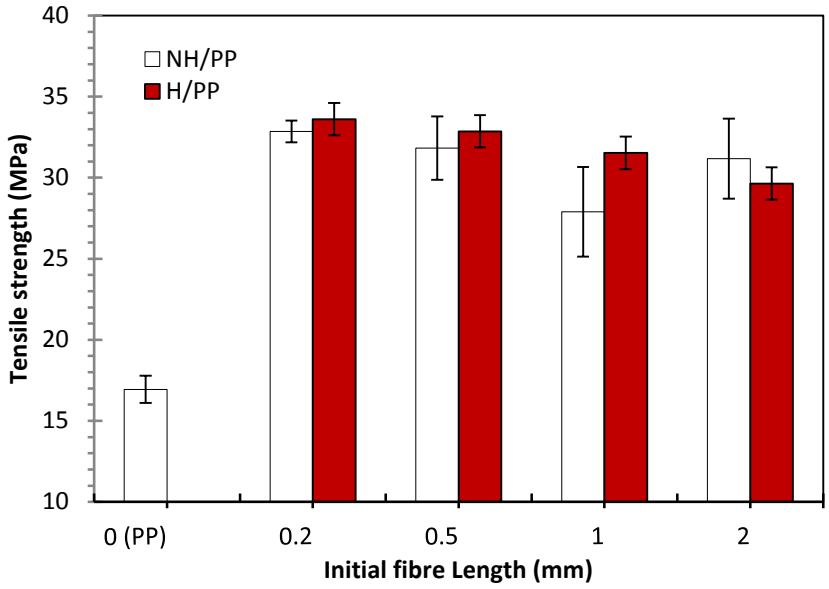

Figure 7.1: The influence of the initial fibre length on tensile strength of the noil (white) and hemp (Red) fibre reinforced polypropylene composites.

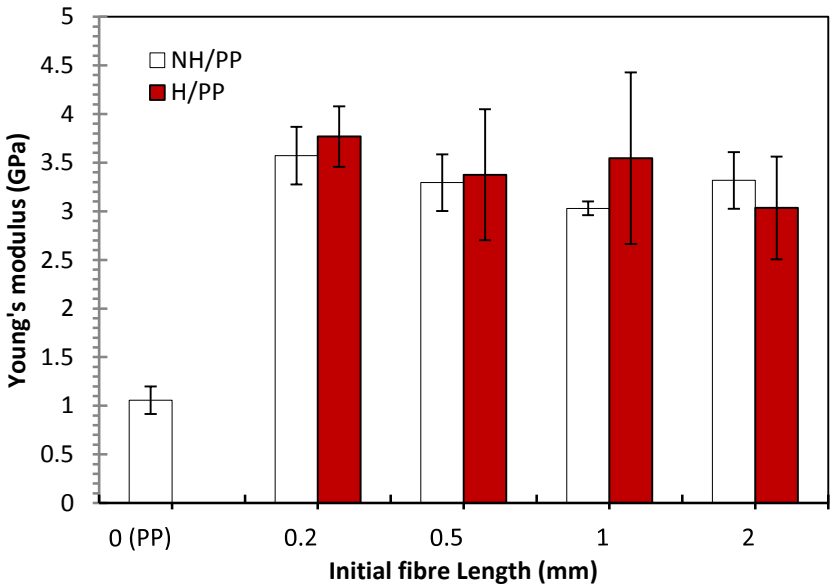

Figure 7.2: The influence of the initial fibre length on Young's Modulus of the noil (white) and hemp (Red) fibre reinforced polypropylene composites.

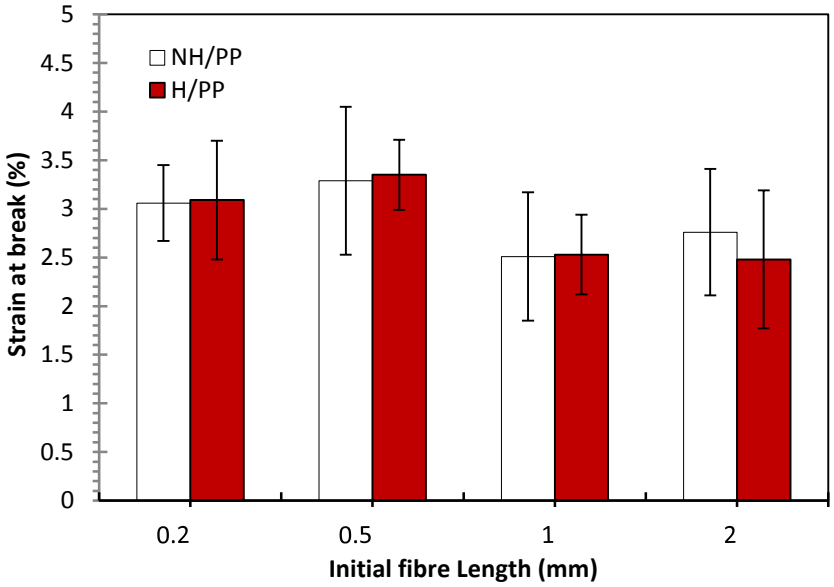

Figure 7.3: The influence of the initial fibre length on strain at break of the noil (white) and hemp (Red) fibre reinforced polypropylene composites.

A comparison between the tensile properties of alkali treated hemp fibre composites and noil fibre composites shown in Figure 7.1 and Figure 7.2 reveals that noil hemp fibres resulted insubstantially lower tensile strength and Young's modulus. As discussed earlier in section 4.4, this might be due to the lower tensile strength of noil fibres as a result of the degumming process which causes a higher level of defects (micro cracks) in the noil fibres.

7.3 Flexural properties

Flexural properties of composites were investigated via conventional three-point bending tests. In the flexural tests, firstly, the loading nose touches the upper surface of the specimen. Load is transferred from the elastic matrix to the fibres. The fibres then start to bend and strain into the matrix. Bent fibres generate further strains to neighbouring fibres and cause them to bend. This causes fibre-matrix interface instability and generates extremely high stresses on the matrix. Finally, the matrix is

shifted from elastic to plastic deformation and this initiates damage of the composites (Kabir, 2012, Huang, 2004).

During flexural testing, there is a combination of tensile and compressive stresses. Compressive stresses are applied to the top of the specimen. Compressive stresses produced large longitudinal tensile stresses on the lower surfaces of the specimen. The combination of vertical compressive stress and longitudinal tensile stress produced shear stresses. Also Figure 7.4 shows flexural failure modes of ground hemp fibre composite sample.

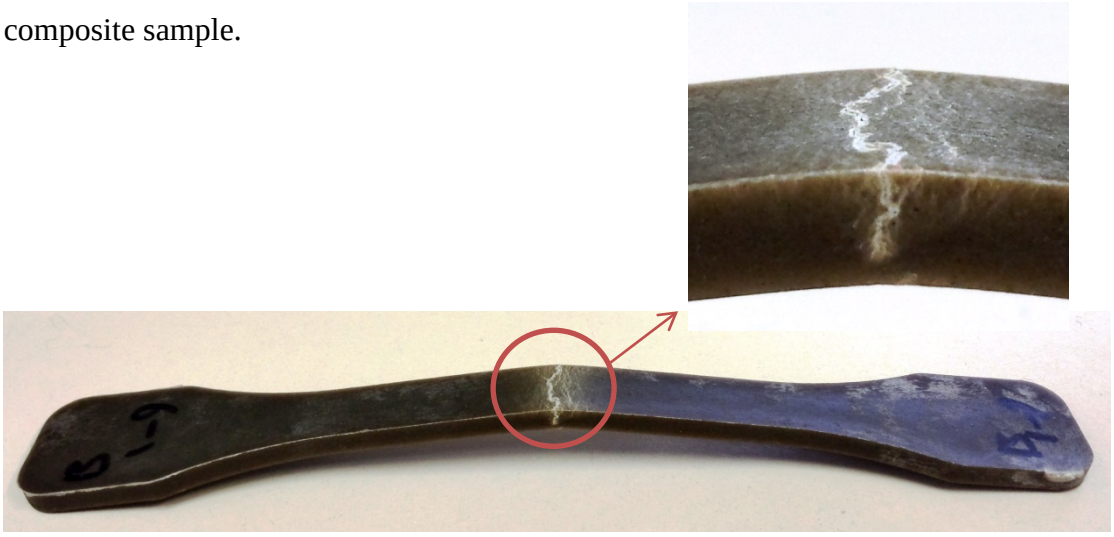

Figure 7.4: Flexural failure of ground hemp fibre composite sample

Typical flexural stress-strain curves for noil hemp fibre composites are presented in Figure 7.5. It can be seen that the curves show initially a linear portion, followed by a non-linear region prior to the maximum flexural stress. Once the maximum stress is reached, the stress decreases just slightly until the fracture happens.

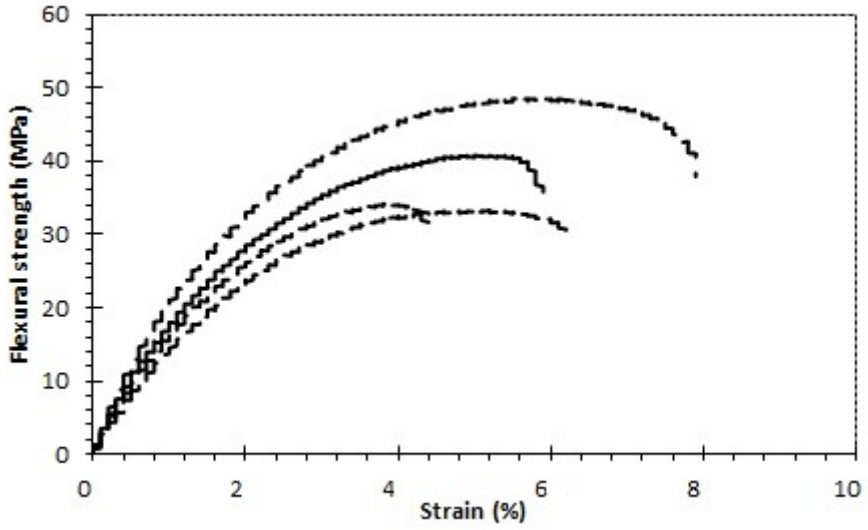

Figure 7.5: Flexural stress-strain curves for 40 wt% noil hemp fibre composite with initial fibre length of 2 mm

The average flexural strength and flexural modulus of the noil hemp fibre polypropylene (NH/PP) and hemp fibre polypropylene (H/PP) composites as a function of initial fibre length are shown in Table 7.2, Figure 7.6 and Figure 7.7. As can be seen in Figure 7.6, the flexural strength increased with the addition of 40 wt% short fibres into the pure polypropylene. The average flexural strength increased with addition of 0.2 mm short fibres from 12.4 MPa for pure polypropylene to 55.65 MPa for NH/PP and 51.19 MPa for H/PP. Likewise, the flexural modulus of the composites was increased from approximately 0.5 GPa for polypropyelne to higher than 3 GPa for the composites with fibre length of 0.2 mm. Similar to the tensile strength and Young's modulus findings, the flexural strength and flexural modulus of both composites were decreased as fibres longer than 0.2 mm were used to fabricate the composites.

Table 7.2: Flexural properties of composites with different fibre lengths

Fibre length (mm)	Noil hemp fibre composite			Hemp fibre composite		
	Flexural strength (MPa)	Flexural modulus (GPa)	Strain at break (%)	Flexural strength (MPa)	Flexural modulus (GPa)	Strain at break (%)
0.20	55.65 ±0.98	3.31 ±0.14	6.39 ±0.32	51.19 ±4.21	3.11 ±0.22	5.16 ±0.16
0.50	53.25 ±4.11	3.04 ±0.07	7.85 ±0.88	51.18 ±5.01	3.06 ±0.13	7.03 ±0.81
1.00	44.05 ±4.00	2.76 ±0.37	6.50 ±1.3	39.63 ±0.95	1.95 ±0.16	6.08 ±0.37
2.00	39.91 ±6.77	2.14 ±0.43	6.49 ±1.25	40.26 ±4.01	2.32 ±0.27	6.67 ±0.97

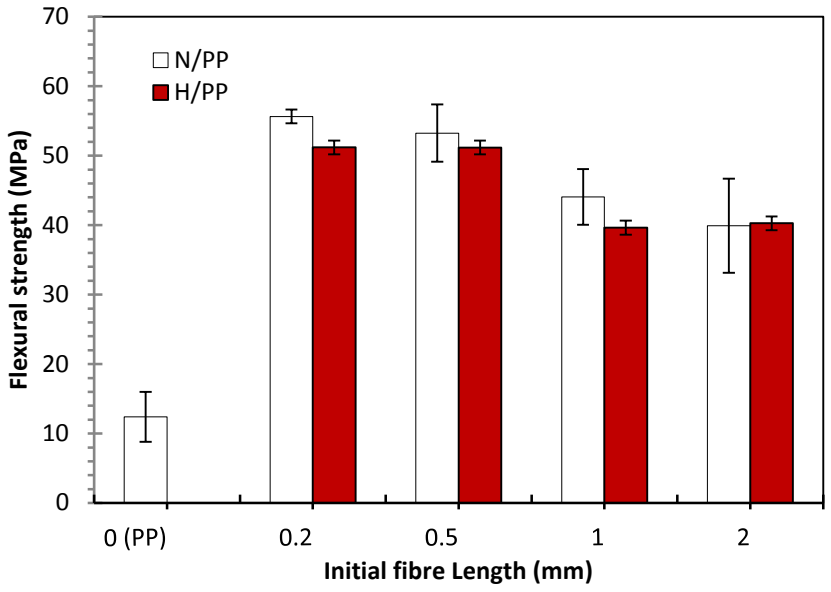

Figure 7.6: The influence of initial fibre length on flexural strength the noil (white) and hemp (Red) fibre reinforced polypropylene composites.

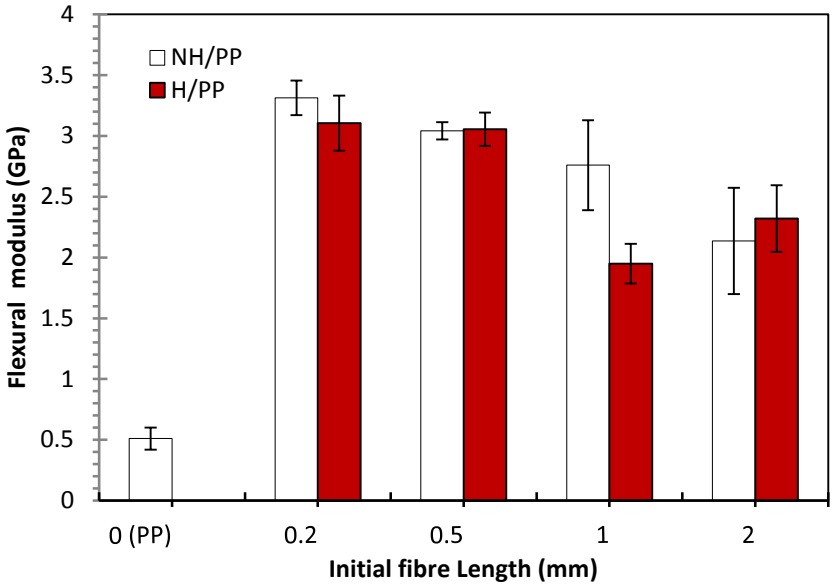

Figure 7.7: The influence of the initial fibre length on flexural modulus of the noil (white) and hemp (Red) fibre reinforced polypropylene composites.

7.4 Impact Strength

It has been concluded so far in this chapter that reinforcing fibres with an initial length of 0.2 mm can provide the highest tensile and flexural properties among all investigating noil hemp fibre and hemp fibre polypropylene composites. In order to extend the results, the effect of fibre lengths on impact toughness of the composite samples has been investigated using impact tests. The impact toughness of a composite is the amount of energy absorbed before fracture happens. Therefore, a study on impact properties of the composites can be of great importance when the reinforcing fibres are very short, as short fibres create stress concentration sites in the matrix, which might reduce impact toughness of the materials. The impact tests were carried out according to section 3.6.4. Typical impact force-time and impact energy-time curves are shown in Figure 7.8.

The Energy-Time curve, shown in Figure 7.8 was plotted using the calculation of the total area under the force–time curve. Then, the amount of total energy required to damage the composite can be extracted using the Energy-Time curve.

Belingardi and Vadori (Belingardi et al., 1998) introduced the damage degree (DD) to account for damage accumulation. It was defined as the ratio between the absorbed energy Ea and the impact energy Ei (Ea/Ei).

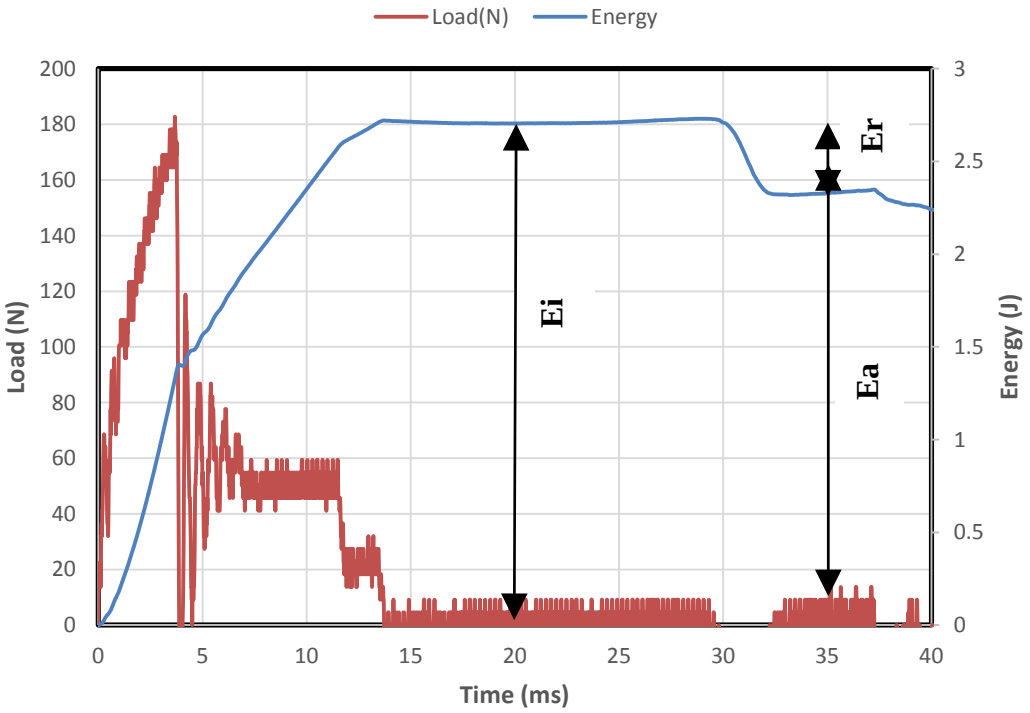

Figure 7.8: Load and energy history curves of a noil hemp fibre polypropylene composite specimen reinforced with 0.2 mm noil fibres.

Once the impact energy (E_i) is high enough, the composite failure eventually can happen. If the specimen does not completely fail, the projectile bounces back from the specimen. The energy created when the projectile bounces back is known as rebounded energy (E_r). When the specimen completely fails, the projectile does not

rebound and the rebound energy (Er) is zero. In this case, complete failure of the specimen happens and the DD value becomes 1.

The impact force (F_m), maximum impact energy (E_m), absorbed energy (E_a) rebounded energy (E_r) of the specimens were extracted from corresponding impact force-time and impact energy-time curves of the composites and then summarised in Table 7.3 and Table 7.4.

Moreover, the changes in impact force, absorbed energy, impact energy and Damage Degree as a function of initial fibre length are presented in Figure 7.9 and Figure 7.10.

Table 7.3: Impact properties of polypropylene sample

	F_m(N)	E_m(J)	E_a(J)	E_r(J)	DD
PP sample	118.50 ±0.75	3.05 ±0.43	2.41 ±0.52	0.64 ±0.12	0.79 ±0.08

Table 7.4: Impact properties of composites with different fibre length

Fibre length (mm)	Noil hemp fibre composite					Hemp fibre composite				
	F_m(N)	E_m(J)	E_a(J)	E_r(J)	DD	F_m(N)	E_m(J)	E_a(J)	E_r(J)	DD
0.2	191.70 ±8.6	2.99 ±0.22	2.57 ±0.21	0.42 ±0.02	0.86 ±0.01	175.50 ±2.20	2.71 ±0.01	2.25 ±0.04	0.46 ±0.04	0.83 ±0.01
0.5	177.24 ±3.16	2.80 ±0.17	2.43 ±0.12	0.37 ±0.01	0.87 ±0.01	173.30 ±3.12	2.64 ±0.08	2.24 ±0.07	0.40 ±0.01	0.85 ±0.01
1	164.40 ±2.31	2.64 ±0.25	2.32 ±0.26	0.32 ±0.08	0.88 ±0.02	173.67 ±3.83	2.75 ±0.13	2.37 ±0.12	0.38 ±0.01	0.86 ±0.00
2	150.00 ±5.65	2.45 ±0.63	2.30 ±0.51	0.15 ±0.06	0.94 ±0.01	159.65 ±4.55	2.38 ±0.06	2.11 ±0.18	0.34 ±0.06	0.86 ±0.02

A comparison between the pure PP sample and the composites shows that the Er and DD of the pure PP are higher and lower respectively. In other words, addition of fibres/fillers into the pure PP reduces the impact properties as expected.

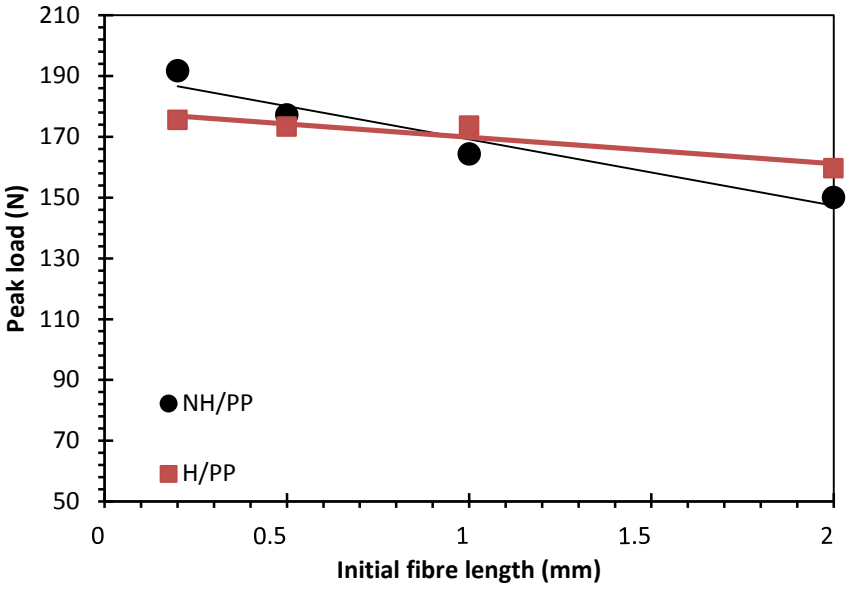

Figure 7.9: Effect of initial fibre length on peak load of noil hemp fibre and hemp fibre composites.

From Figure 7.9, it can be observed that as fibre length increased the peak load of the composites reduced. Peak load, also known as impact load, corresponds to the onset of material damage or complete failure. Therefore, the composite with 0.2 mm initial fibre showed better impact resistance among all other samples. During impact, compressive, shear and tensile loadings are applied on the composite samples simultaneously. As aforementioned, fibre agglomerations are more likely to form in composites with longer fibres. Then fibres are not properly wet up in agglomeration sites and cracks can be initiated from fibre/matrix interface in the agglomeration sites. As a result, poor dispersion of fibres reduces the composite's impact resistance during compression, shear and tensile loads by the reduction of interface bonding between the fibre and matrix in agglomeration sites.

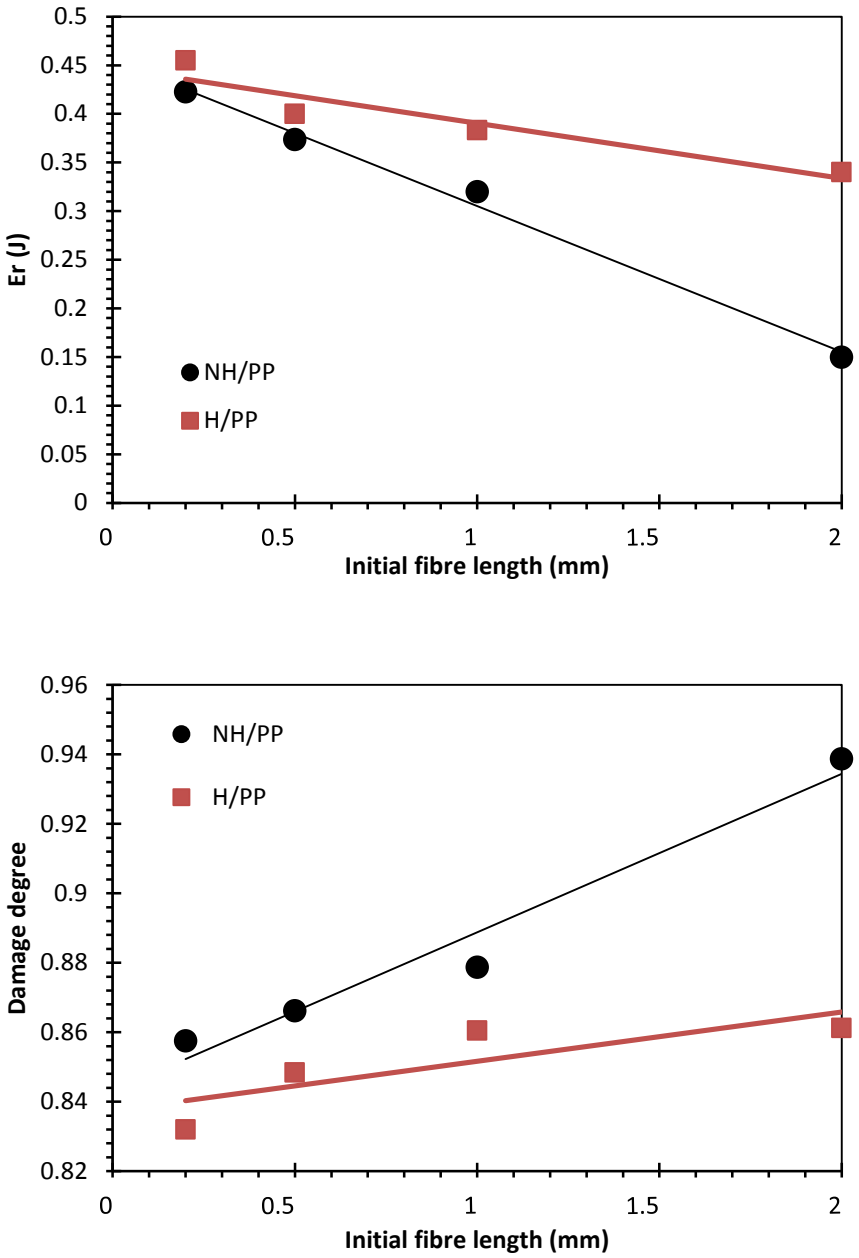

Figure 7.10: Effect of Initial fibre length on impact properties of noil hemp fibre and Hemp fibre composites (a) Impact Energy and (b) Damage Degree.

Likewise, Figure 7.10 (a) shows the higher E_r values for composites with shorter initial fibres. This indicates that better fibre dispersion and subsequently strong interfaces in the composites with shorter fibres prevented the impactor from penetrating the samples and thus more rebounded energy were observed. Also, the

lower DD values shown in Figure 7.10(b) indicated that the extent of impact damage was less for composites with shorter fibres.

Both noil hemp fibre composites and hemp fibre composites provided almost the same values of impact energy at different initial fibre lengths. However, as Figure 7.10 shows, the Damage Degree (DD) values of the noil hemp fibre composites are significantly higher than those of normal hemp fibre due to the fibre weakness (defects / cracks) caused by the degumming process. The impact results observed here is in correlation with their tensile and flexural properties as discussed earlier.

Therefore, the impact test results show that increase in the initial fibre length of the composites decreases the maximum load and rebounded energy but increases the damage degree (DD) of the composites. In addition, noil hemp fibres composite shows lower impact properties than hemp fibre composites.

In a nutshell, three common mechanical testing methods, i.e. tensile, flexural and impact tests, were carried out to investigate the effects of initial fibre length on relevant properties of the composites. Unlike the common understanding which prefers longer fibres to have higher reinforcing fibres in the composites, the results of this chapter specified that when it comes to injection moulded composites with very short fibres (powder), initial length only can slightly change the final mechanical properties while even shorter fibres could result in higher mechanical properties. According to the experimental data, it was seen, as the initial noil hemp fibre length decreased from 2 mm to 0.2 mm, the tensile strength of the composites increased from 31.1 to 32.9 MPa, Young's modulus from 3.3 to 3.6 GPa, flexural strength from 39.9

to 55.6 MPa, flexural modulus from 2.1 to 3.3 GPA and impact peak load from 150.0 to 191.7 N.

Although longer fibre is generally required to have higher reinforcing effects, shorter fibres can result in higher tensile, flexural and impact properties due less fibre agglomerations, better fibre dispersion and higher uniformity of the injection moulded composites with very short initial fibres (powder).

8. Conclusions and Recommendations

8.1 Conclusions

- **Fibres and Fibre Treatment**

Microstructural, thermal, chemical and tensile properties of alkali treated and untreated fibres were investigated using scanning electron microscopy (SEM), Thermogravimetric Analysis (TGA) and Differential Scanning Calorimetry (DSC), fourier transform infrared analysis (FTIR) and Dynamic Mechanical Analyser (DMA).

Higher thermal stability of alkali treated hemp fibres and noil hemp fibres than that of untreated fibres were observed due to the removal of the cementing materials especially hemicellulose and pectin, which are thermally unstable. Alkali treatment of normal hemp fibres could remove cementing materials (pectin, hemicellulose and lignin) partially or completely from the surface of the fibres.

Moreover, removal of the lignin, pectin and hemicellulose changed the morphology of the hemp fibre and improved tensile property of the treated hemp fibres. Unlike the untreated fibres, the treated fibres were clean but rough. The roughness could enhance mechanical interlocking bonding mechanisms between fibre and the matrix. The clean surfaces were supposed to create stronger bonding between OH groups of the fibre and the matrix by addition of the coupling agent.

Referring to the SEM images, the cleanliness and small thickness of the as-received noil hemp fibre bundle (technical fibre) implied that cementing materials were already

removed during the degumming processes in the textile industry. Noil hemp fibre contained almost the same type of chemical components as treated hemp fibres. Therefore, noil hemp fibres did not require any chemical treatments to remove the lignocellulosic amorphous materials.

However, the noil hemp fibres delivered lower tensile properties than both untreated and treated hemp fibres due to the cellulose degradations and micro-cracks, which occurred because of over-treatment in textile processing. Micro cracks were observed mostly on the surface of the noil hemp fibres.

- **Injection Moulded short noil Hemp fibre Composites**

Noil hemp fibre reinforced polypropylene composites with and without coupling agents were fabricated using melt mixing and injection moulding machines. The average length of fibres were reduced from 14 mm to around 200 μm during the processing of the composite with 10 wt% hemp fibre due to severe fibre breakage during compounding and injection moulding processes. While, composites with higher fibre content were exposed to more severe breakage due to higher fibre-fibre interactions. The fibre-fibre interaction mechanism was seen to be more considerable in composites with more than 30 wt% noil hemp fibre because at fibre content higher than 30 wt%, fibre–matrix interaction mechanism is also accelerated and caused more fibre breakage. However, the addition of coupling agents to the matrix decreased fibre breakage as it reduced the fibre-fibre interactions due to better fibre dispersion because of better wettability of the matrix on fibres.

Although addition of noil hemp fibres into the polypropylenes reduced tensile strength of the composites due to incompatibility between the fibres and the matrix, tensile strengths and storage moduli of the composites can be improved by the addition of either MAPP or MAPOE coupling agents because of the enhancement of interfacial adhesion between the fibre and polypropylene matrix and also reduction of fibre breakage. 2.5 wt% MAPP seemed to be adequate for enhancing the tensile properties of the composite with 30 wt% hemp fibre. While 5 wt% MAPP is required for the composite with 40 wt% fibres.

Although the noil hemp fibres have lower tensile properties than untreated hemp fibres due to the cellulose degradation, both composites delivered almost the same tensile strength. It was confirmed by the modified Bowyer and Bader model that tensile performance of the injection moulded composites is dependent on tensile strength of the reinforcing fibre only if fibre strength is less than a critical value (200 MPa in this specific study).

The IFSS obtained from the modified Bowyer and Bader model is in agreement with those in literature resulted from the single fibre fragmentation method. The evaluated IFSSs using the modified Bowyer and Bader model decreased from 9.7 to 7.2 MPa as the fibre content increased from 10 wt% to 40 wt% and the evaluated IFSS for composites with MAPP is approximately 60% higher than those without MAPP.

Although poor bonding between natural fibres and polymeric matrix needs to be modified, a low aspect ratio of fibres in injection-moulded composites limits the composite tensile properties to lower levels. Referring to the modified Bowyer and

Bader model, it was calculated that a slight increase in the final fibre's aspect ratio can considerably improve the composite tensile properties.

On the other hand, compatibilization reduced the damping properties of the composites as the composites having lower interfacial bonding between fibres and the matrix have higher energy dissipation capacity.

The storage moduli of the composites were increased with increases in short hemp fibre content up to 40 wt% because further increases in fibre content result in fibre agglomerations and/or voids. The addition of either MAPOE or MAPP increased the storage modulus of the composites again due to better interfacial adhesion between the fibre and polypropylene matrix. However, MAPP addition caused lower interphase damping ratio and hence stronger bonding strength in comparison with MAPOE addition.

- **Ground fibres as reinforcement**

In this project, ground alkali-treated hemp fibre composites and ground noil hemp fibre composites were also fabricated with various initial fibre lengths. The fibres were ground into different lengths of 0.2, 0.5, 1 and 2 mm. Composites containing 40 wt% short hemp fibre and 5 wt% maleic anhydride grafted polypropylene (MAPP) were produced by means of a twin-screw extruder and an injection moulding machine.

It can be concluded that the addition of 40 wt% ground noil hemp fibre (0.2 mm long) increased the tensile strength of the polypropylene from approximately 17 MPa to

approximately 33 MPa. However, as the initial fibre length increased from 0.2 mm to 2 mm, the tensile strength of the samples decreased gradually from 33 to 30 MPa.

The same trend was observed for Young's modulus of the samples. Young's modulus of the composites was increased from 1 GPa for pure PP to 3.6 GPa for composites with 0.2 mm long fibres. Then it decreased gradually to approximately 3 GPa as the fibre length increased to 2 mm.

Likewise, the average flexural strength increased with addition of 0.2 mm ground fibres from 12.4 MPa for pure polypropylene to 55.65 MPa for NH/PP and 51.19 MPa for H/PP. The flexural modulus of the composites rose from approximately 0.5 GPa for Polypropylene to higher than 3 GPa for the composites with fibre length of 0.2 mm. As the fibre length increased from 0.2 mm to 2 mm, the flexural strength and flexural modulus of composites gradually decreased to 40 MPa and 2.3 GPa.

All these phenomena happened because a better dispersion of the fibres was achieved with initial fibre length of 0.2 and thus more homogenous structure could be formed. The results were also confirmed by studying the impact strength of the composites, where the composite with 0.2 mm initial fibres showed the best impact resistance among all other samples.

8.2 Recommendations for Future Work

Some recommendations for future work have been proposed:

- I suggest future work should emphasize on characterising the fracture toughness of these composites and evaluate the associated toughening mechanisms.

- It is proposed that biodegradable polymers, such as PLA can be used as matrices instead of petroleum-derived polymers to result in 100% bio-composites.

- The use of coupling agents other than MAPP or MAPOE might be investigated. Their effects on fibre-matrix interfacial adhesion and also fibre dispersion can be studied.

- It is advised to measure the fibre length (aspect ratio) after each composite processing step, such as extrusion and injection moulding. This will identify the step which imposes the highest fibre breakage in the composites. Then, further considerations should be carried out to decrease the fibre breakage in that specific step.
- The average aspect ratios of fibres in injection moulded composites were below the critical aspect ratio. It was also found that the aspect ratio is the dominant factor controlling the tensile properties. Thus, it is proposed that an investigation be carried out to increase the aspect ratios of fibres by optimizing the manufacturing parameters such as screw speeds, mixing time and temperatures.

- The current study has not investigated thermal stability and moisture absorption properties of the composites. It is proposed to study the effects of the initial fibre length on thermal stability and moisture absorption properties.
- The current project has not measured the final fibre length using x-ray micro tomography in chapter 7. It is suggested a study should be done on the influences of initial fibre length on final fibre length in detail.

References

AFAGHI-KHATIBI, A. & MAI, Y. W. 2002. Characterisation of fibre/matrix interfacial degradation under cyclic fatigue loading using dynamic mechanical analysis. Composites Part a-Applied Science and Manufacturing, 33, 1585-1592.

AGRAWAL, R., SAXENA, N. S., SHARMA, K. B., THOMAS, S. & SREEKALA, M. S. 2000. Activation energy and crystallization kinetics of untreated and treated oil palm fibre reinforced phenol formaldehyde composites. Materials Science and Engineering a-Structural Materials Properties Microstructure and Processing, 277, 77-82.

AHMAD, I., BAHARUM, A. & ABDULLAH, I. 2006. Effect of extrusion rate and fiber loading on mechanical properties of twaron fiber-thermoplastic natural rubber (TPNR) composites. Journal of Reinforced Plastics and Composites, 25, 957-965.

AJI, I. S., SAPUAN, S. M., ZAINUDIN, E. S. & ABDAN, K. 2009. KENAF FIBRES AS REINFORCEMENT FOR POLYMERIC COMPOSITES: A REVIEW.

ALEMDAR, A., ZHANG, H., SAIN, M., CESCUTTI, G. & MUESSIG, J. 2008. Determination of fiber size distributions of injection moulded polypropylene/natural fibers using X-ray microtomography. Advanced Engineering Materials, 10, 126-130.

ARBELAIZ, A., CANTERO, G., FERNANDEZ, B., MONDRAGON, I., GANAN, P. & KENNY, J. M. 2005. Flax fiber surface modifications: Effects on fiber physico mechanical and flax/polypropylene interface properties. Polymer Composites, 26, 324-332.

ASLOUN, E. M., DONNET, J. B., GUILPAIN, G., NARDIN, M. & SCHULTZ, J. 1989. ON THE ESTIMATION OF THE TENSILE-STRENGTH OF CARBON-FIBERS AT SHORT LENGTHS. Journal of Materials Science, 24, 3504-3510.

ATAOLLAHI, S., TAHER, S. T., ESHKOOR, R. A., ARIFFIN, A. K. & AZHARI, C. H. 2012. Energy absorption and failure response of silk/epoxy composite square tubes: Experimental. Composites Part B-Engineering, 43, 542-548.

AZIZ, S. H., ANSELL, M. P., CLARKE, S. J. & PANTENY, S. R. 2005. Modified polyester resins for natural fibre composites. Composites Science and Technology, 65, 525-535.

BALEY, C. 2004. Influence of kink bands on the tensile strength of flax fibers. Journal of Materials Science, 39, 331-334.

BECKERMANN, G. W. & PICKERING, K. L. 2008. Engineering and evaluation of hemp fibre reinforced polypropylene composites: Fibre treatment and matrix modification. Composites Part a-Applied Science and Manufacturing, 39, 979-988.

BECKERMANN, G. W. & PICKERING, K. L. 2009. Engineering and evaluation of hemp fibre reinforced polypropylene composites: Micro-mechanics and strength prediction modelling. Composites Part a-Applied Science and Manufacturing, 40, 210-217.

BELINGARDI, G., GRASSO, F. & VADORI, R. 1998. Energy absorption and damage degree in impact testing of composite materials.

BENGTSSON, M., LE BAILLIF, M. & OKSMAN, K. 2007. Extrusion and mechanical properties of highly filled cellulose fibre-polypropylene composites. Composites Part a-Applied Science and Manufacturing, 38, 1922-1931.

BERNASCONI, A., DAVOLI, P., BASILE, A. & FILIPPI, A. 2007. Effect of fibre orientation on the fatigue behaviour of a short glass fibre reinforced polyamide-6. International Journal of Fatigue, 29, 199-208.

BHATTACHARYA, P. 2011. Weibull Distribution for Estimating the Parameters, InTech.

BLEDZKI, A. K., REIHMANE, S. & GASSAN, J. 1996. Properties and modification methods for vegetable fibers for natural fiber composites. Journal of Applied Polymer Science, 59, 1329-1336.

BOLTE, S. & CORDELIÈRES, F. P. 2006. A guided tour into subcellular colocalization analysis in light microscopy. Journal of Microscopy, 224, 213-232.

BOS, H. L., MUESSIG, J. & VAN DEN OEVER, M. J. A. 2006. Mechanical properties of short-flax-fibre reinforced compounds. Composites Part a-Applied Science and Manufacturing, 37, 1591-1604.

BULL, S. J., DAVIDSON, R. I., FISHER, E. H., MCCABE, A. R. & JONES, A. M. 2000. A simulation test for the selection of coatings and surface treatments for plastics injection moulding machines. Surface and Coatings Technology, 130, 257-265.

BYUNG S, H., BYUNG S, K., JUNG H, L., JOON H, B. & JONG M, P. Physical parameters and mechanical properties improvement for jute fiber/polypropylene composites by maleic anhydride coupler. 16TH INTERNATIONAL CONFERENCE ON COMPOSITE MATERIALS, 2007 Kyoto, Japan.

CERVENKA, A. 1999. Advantages and disadvantages of thermoset and thermoplastic matrices for continuous fibre composites. In: SOARES, C. A. M., SOARES, C. M. M. & FREITAS, M. J. M. (eds.) Mechanics of Composite Materials and Structures. Dordrecht: Springer.

CHANDRA, R., SINGH, S. P. & GUPTA, K. 1999. Damping studies in fiber-reinforced composites - a review. Composite Structures, 46, 41-51.

CHANDRA, R., SINGH, S. P. & GUPTA, K. 2003. A study of damping in fiber-reinforced composites. Journal of Sound and Vibration, 262, 475-496.

CHAUHAN, S., KARMARKAR, A. & AGGARWAL, P. 2009. Damping Behavior of Wood Filled Polypropylene Composites. Journal of Applied Polymer Science, 114, 2421-2426.

CLEMONS, C. M., CAULFIELD, D. F. & GIACOMIN, A. J. 1999. Dynamic fracture toughness of cellulose-fiber-reinforced polypropylene: Preliminary investigation of microstructural effects. Journal of Elastomers and Plastics, 31, 367-378.

CREDOU, J. & BERTHELOT, T. 2014. Cellulose: from biocompatible to bioactive material. Journal of Materials Chemistry B, 2, 4767-4788.

DAI, D. & FAN, M. 2010. Characteristic and Performance of Elementary Hemp Fibre. Materials Sciences and Applications, 1, 336-342.

DAVIES, G. C. & BRUCE, D. M. 1998. Effect of environmental relative humidity and damage on the tensile properties of flax and nettle fibers. Textile Research Journal, 68, 623-629.

DENN, M. M. 2008. Polymer Melt Processing - Foundations in Fluid Mechanics and Heat Transfer. November 2008 ed.: Cambridge Series in Chemical Engineering.

DI LANDRO, L. & LORENZI, W. 2009a. Mechanical Properties and Dynamic Mechanical Analysis of Thermoplastic-Natural Fiber/Glass Reinforced Composites. Macromolecular Symposia, 286, 145-155.

DI LANDRO, L. & LORENZI, W. 2009b. Static and Dynamic Properties of Thermoplastic Matrix/Natural Fiber Composites. Journal of Biobased Materials and Bioenergy, 3, 238-244.

DUC, A. L., VERGNES, B. & BUDTOVA, T. 2011. Polypropylene/natural fibres composites: Analysis of fibre dimensions after compounding and observations of fibre rupture by rheo-optics. Composites Part A: Applied Science and Manufacturing, 42, 1727-1737.

ETAATI, A., PATHER, S., FANG, Z. & WANG, H. 2014. The study of fibre/matrix bond strength in short hemp polypropylene composites from dynamic mechanical analysis. Composites Part B: Engineering, 62, 19-28.

ETAATI, A., WANG, H., PATHER, S., YAN, Z. & ABDANAN MEHDIZADEH, S. 2013. 3D X-ray microtomography study on fibre breakage in noil hemp fibre reinforced polypropylene composites. Composites Part B: Engineering, 50, 239-246.

EVANS, R., WEARNE, R. H. & WALLIS, A. F. A. 1989. MOLECULAR-WEIGHT DISTRIBUTION OF CELLULOSE AS ITS TRICARBANILATE BY HIGH-PERFORMANCE SIZE EXCLUSION CHROMATOGRAPHY. Journal of Applied Polymer Science, 37, 3291-3303.

FACCA, A. G., KORTSCHOT, M. T. & YAN, N. 2006. Predicting the elastic modulus of natural fibre reinforced thermoplastics. Composites Part a-Applied Science and Manufacturing, 37, 1660-1671.

FACCA, A. G., KORTSCHOT, M. T. & YAN, N. 2007. Predicting the tensile strength of natural fibre reinforced thermoplastics. Composites Science and Technology, 67, 2454-2466.

FARA, S. & PAVAN, A. 2004. Fibre orientation effects on the fracture of short fibre polymer composites: on the existence of a critical fibre orientation on varying internal material variables. Journal of Materials Science, 39, 3619-3628.

FITZGERALD, E. R., FERRY, J. D. & FITZGERALD, R. E. 1999. Dynamic mechanical measurements on 21 polymer systems reviewed for vibration damping applications; complex shear compliance, modulus, and loss tangent data transferred to computer disk for use in analysis and damping material design.

FOTOUH, A., WOLODKO, J. D. & LIPSETT, M. G. 2014. A review of aspects affecting performance and modeling of short-natural-fiber-reinforced polymers under monotonic and cyclic loading conditions. Polymer Composites, n/a-n/a.

FU, S. Y. & LAUKE, B. 1996. Effects of fiber length and fiber orientation distributions on the tensile strength of short-fiber-reinforced polymers. Composites Science and Technology, 56, 1179-1190.

GARCIA-JALDON, C., DUPEYRE, D. & VIGNON, M. R. 1998. Fibres from semi-retted hemp bundles by steam explosion treatment. Biomass & Bioenergy, 14, 251-260.

GARKHAIL, S. K., HEIJENRATH, R. W. H. & PEIJS, T. 2000. Mechanical properties of natural-fibre-mat-reinforced thermoplastics based on flax fibres and polypropylene. Applied Composite Materials, 7, 351-372.

GENC, G., EL HAFIDI, A. & GNING, P. B. 2012. Comparison of the mechanical properties of flax and glass fiber composite materials. Journal of Vibroengineering, 14, 572-581.

GEORGE, J., SREEKALA, M. S. & THOMAS, S. 2001. A review on interface modification and characterization of natural fiber reinforced plastic composites. Polymer Engineering and Science, 41, 1471-1485.

GIBSON, L. J. 2012. The hierarchical structure and mechanics of plant materials. Journal of the Royal Society Interface, 9, 2749-2766.

GREGOROVÁ, A., KOŠÍKOVÁ, B. & MORAVČÍK, R. 2006. Stabilization effect of lignin in natural rubber. Polymer Degradation and Stability, 91, 229-233.

GUO, Q. P., CHENG, B., KORTSCHOT, M., SAIN, M., KNUDSON, R., DENG, J. & ALEMDAR, A. 2010. Performance of long Canadian natural fibers as reinforcements in polymers. Journal of Reinforced Plastics and Composites, 29, 3197-3207.

GUPTA, V. B., MITTAL, R. K., SHARMA, P. K., MENNIG, G. & WOLTERS, J. 1989. Some studies on glass fiber-reinforced polypropylene. Part I: Reduction in fiber length during processing. Polymer Composites, 10, 8-15.

HALDAR, A. K., SINGH, S. & PRINCE 2011. Vibration Characteristics of Thermoplastic Composite. In: PATEL, R. B. & SINGH, B. P. (eds.) 2nd International Conference on Methods and Models in Science and Technology. Melville: Amer Inst Physics.

HARGITAI, H., RACZ, I. & ANANDJIWALA, R. D. 2008. Development of HEMP fiber reinforced polypropylene composites. Journal of Thermoplastic Composite Materials, 21, 165-174.

HERMAN, G. T. 1980. Image Reconstruction from Projections: The Fundamentals of Computerized Tomography, Academic Press.

HERRERA-FRANCO, P. J. & VALADEZ-GONZÁLEZ, A. 2005. A study of the mechanical properties of short natural-fiber reinforced composites. Composites Part B: Engineering, 36, 597-608.

HU, W., TON-THAT, M.-T., PERRIN-SARAZIN, F. & DENAULT, J. New advancements on single fiber tensile test of natural fibers. May 2-4, 2010 2010a Toronto, Ontario.

HU, W., TON-THAT, M. T., PERRIN-SARAZIN, F. & DENAULT, J. 2010b. An Improved Method for Single Fiber Tensile Test of Natural Fibers. Polymer Engineering and Science, 50, 819-825.

HUANG, Z. M. 2004. Progressive flexural failure analysis of laminated composites with knitted fabric reinforcement. Mechanics of Materials, 36, 239-260.

IANNUCCELLI, E., MOMPART, F., GELLIN, J., LAHBIB-MANSAIS, Y., YERLE, M. & BOUDIER, T. 2010. NEMO: a tool for analyzing gene and chromosome territory distributions from 3D-FISH experiments. Bioinformatics, 26, 696-697.

IDICULA, M., MALHOTRA, S. K., JOSEPH, K. & THOMAS, S. 2005. Dynamic mechanical analysis of randomly oriented intimately mixed short banana/sisal hybrid fibre reinforced polyester composites. Composites Science and Technology, 65, 1077-1087.

JACOB, M., FRANCIS, B., VARUGHESE, K. T. & THOMAS, S. 2006. The effect of silane coupling agents on the viscoelastic properties of rubber biocomposites. Macromolecular Materials and Engineering, 291, 1119-1126.

JACOB, M., THOMAS, S. & VARUGHESE, K. T. 2004. Mechanical properties of sisal/oil palm hybrid fiber reinforced natural rubber composites. Composites Science and Technology, 64, 955-965.

JACQUET, N., QUIEVY, N., VANDERGHEM, C., JANAS, S., BLECKER, C., WATHELET, B., DEVAUX, J. & PAQUOT, M. 2011. Influence of steam explosion on the thermal stability of cellulose fibres. Polymer Degradation and Stability, 96, 1582-1588.

JAFARPOUR, G., DANTRAS, E., BOUDET, A. & LACABANNE, C. 2008. Molecular mobility of poplar cell wall polymers studied by dielectric techniques. Journal of Non-Crystalline Solids, 354, 3207-3214.

JARMAN, C. 1998. Plant Fibre Processing: A Handbook, UK, Intermediate Technology Publications.

JOHN, M. J. & ANANDJIWALA, R. D. 2009. Chemical modification of flax reinforced polypropylene composites. Composites Part a-Applied Science and Manufacturing, 40, 442-448.

JOSEPH, P. V., JOSEPH, K. & THOMAS, S. 1999. Effect of processing variables on the mechanical properties of sisal-fiber-reinforced polypropylene composites. Composites Science and Technology, 59, 1625-1640.

KABIR, M. M. 2012. Effects of Chemical Treatments on Hemp Fibre Reinforced Polyester Composites. DOCTOR OF PHILOSOPHY, University of Southern Queensland.

KABIR, M. M., WANG, H., LAU, K. T. & CARDONA, F. 2012a. Chemical treatments on plant-based natural fibre reinforced polymer composites: An overview. Composites Part B-Engineering, 43, 2883-2892.

KABIR, M. M., WANG, H., LAU, K. T. & CARDONA, F. 2013. Effects of chemical treatments on hemp fibre structure. Applied Surface Science, 276, 13-23.

KABIR, M. M., WANG, H., LAU, K. T., CARDONA, F. & ARAVINTHAN, T. 2012b. Mechanical properties of chemically-treated hemp fibre reinforced sandwich composites. Composites Part B-Engineering, 43, 159-169.

KARUS, M. & KAUP, M. 2002. Natural Fibres in the European Automotive Industry. Journal of Industrial Hemp, 7, 119-131.

KARUS, M., ORTMANN, S., CHRISTIAN, G. & PENDAROVSKI, C. 2006. Use of natural fibres in composites for the German automotive production from 1999 till 2005.

KASUGA, T., OTA, Y., NOGAMI, M. & ABE, Y. 2001. Preparation and mechanical properties of polylactic acid composites containing hydroxyapatite fibers. Biomaterials, 22, 19-23.

KELLEY, S. S., RIALS, T. G. & GLASSER, W. G. 1987. RELAXATION BEHAVIOR OF THE AMORPHOUS COMPONENTS OF WOOD. Journal of Materials Science, 22, 617-624.

KHAN, S. U., LI, C. Y., SIDDIQUI, N. A. & KIM, J.-K. 2011. Vibration damping characteristics of carbon fiber-reinforced composites containing multi-walled carbon nanotubes. Composites Science and Technology, 71, 1486-1494.

KHOATHANE, M. C., VORSTER, O. C. & SADIKU, E. R. 2008. Hemp fiber-reinforced 1-pentene/polypropylene copolymer: The effect of fiber loading on the mechanical and thermal characteristics of the composites. Journal of Reinforced Plastics and Composites, 27, 1533-1544.

KIFANI-SAHBAN, F., KIFANI, A., BELKBIR, L., BOUHLASSA, S., ZOULALIAN, A., ARAUZO, J. & CORDERO, T. 1997. Dimensional variations accompanying thermal treatment of cellulose in an inert atmosphere. Thermochimica Acta, 307, 135-141.

KIM, H.-J. & EOM, Y.-G. 2001. Thermogravimetric analysis of rice husk flour for a new raw material of lignocellulosic fiber thermoplastic polymer composites. Journal of the Korean wood science and technology, 29, 59-67.

KONTTURI, E. J. 2005. Surface chemistry of cellulose: from natural fibres to model surfaces. PhD, Eindhoven University of Technology.

KORONIS, G., SILVA, A. & FONTUL, M. 2013. Green composites: A review of adequate materials for automotive applications. Composites Part B: Engineering, 44, 120-127.

KORTE, S. & STAIGER, M. P. 2008. Effect of processing route on the composition and properties of hemp fibre. Fibers and Polymers, 9, 593-603.

KU, H., WANG, H., PATTARACHAIYAKOOP, N. & TRADA, M. 2011. A review on the tensile properties of natural fiber reinforced polymer composites. Composites Part B: Engineering, 42, 856-873.

LAIARINANDRASANA, L., MORGENEYER, T. F., PROUDHON, H. & REGRAIN, C. 2010. Damage of Semicrystalline Polyamide 6 Assessed by 3D X-Ray Tomography: From Microstructural Evolution to Constitutive Modeling. Journal of Polymer Science Part B-Polymer Physics, 48, 1516-1525.

LANDIS, E. N. & KEANE, D. T. 2010. X-ray microtomography. Materials Characterization, 61, 1305-1316.

LE DUIGOU, A., DAVIES, P. & BALEY, C. 2010. Interfacial bonding of Flax fibre/Poly(L-lactide) bio-composites. Composites Science and Technology, 70, 231-239.

LE TROEDEC, M., PEYRATOUT, C. S., SMITH, A. & CHOTARD, T. 2009. Influence of various chemical treatments on the interactions between hemp fibres and a lime matrix. Journal of the European Ceramic Society, 29, 1861-1868.

LEE, B. H., KIM, H. J. & YU, W. R. 2009. Fabrication of long and discontinuous natural fiber reinforced polypropylene biocomposites and their mechanical properties. Fibers and Polymers, 10, 83-90.

LI, S. C., JARVELA, P. K. & JARVELA, P. A. 1999a. Melt rheological properties of polypropylene-maleated polypropylene blends. I. Steady flow by capillary. Journal of Applied Polymer Science, 71, 1641-1648.

LI, S. C., JARVELA, P. K. & JARVELA, P. A. 1999b. Melt rheological properties of polypropylene-maleated polypropylene blends. II. Dynamic viscoelastic properties. Journal of Applied Polymer Science, 71, 1649-1656.

LI, X., TABIL, L. G. & PANIGRAHI, S. 2007. Chemical treatments of natural fiber for use in natural fiber-reinforced composites: A review. Journal of Polymers and the Environment, 15, 25-33.

LI, Y., MAI, Y.-W. & YE, L. 2000. Sisal fibre and its composites: a review of recent developments. Composites Science and Technology, 60, 2037-2055.

LI, Y., PICKERING, K. L. & FARRELL, R. L. 2009. Determination of interfacial shear strength of white rot fungi treated hemp fibre reinforced polypropylene. Composites Science and Technology, 69, 1165-1171.

LIPS, S. J. J., DE HEREDIA, G. M. I., DEN KAMP, R. G. M. O. & VAN DAM, J. E. G. 2009. Water absorption characteristics of kenaf core to use as animal bedding material. Industrial Crops and Products, 29, 73-79.

LIU, H. L., YOU, L. L., JIN, H. B. & YU, W. D. 2013. Influence of alkali treatment on the structure and properties of hemp fibers. Fibers and Polymers, 14, 389-395.

LIU, K. & PIGGOTT, M. R. 1995. SHEAR-STRENGTH OF POLYMERS AND FIBER COMPOSITES .1. THERMOPLASTIC AND THERMOSET POLYMERS. Composites, 26, 829-840.

LU, N. & OZA, S. 2013. A comparative study of the mechanical properties of hemp fiber with virgin and recycled high density polyethylene matrix. Composites Part B: Engineering, 45, 1651-1656.

LUCIU, I., MITU, B., SATULU, V., MATEI, A., DINESCU, G. & IEEE 2008. Low and Atmospheric Pressure Plasma Treatment of Natural Textile Fibers. Isdeiv 2008: Proceedings of the Xxiiird International Symposium on Discharges and Electrical Insulation in Vacuum, Vols 1 and 2.

MALKAPURAM, R., KUMAR, V. & NEGI, Y. S. 2009. Recent Development in Natural Fiber Reinforced Polypropylene Composites. Journal of Reinforced Plastics and Composites, 28, 1169-1189.

MALLICK, P. K. 2007. Fiber-Reinforced Composites: Materials, Manufacturing, and Design, Third Edition, CRC Press

MEDINA, L., SCHLEDJEWSKI, R. & SCHLARB, A. K. 2009. Process related mechanical properties of press molded natural fiber reinforced polymers. Composites Science and Technology, 69, 1404-1411.

MENARD, K. P. 1999. Dynamic Mechanical Analysis: A Practical Introduction United States of America, CRC Press LCC.

MISHRA, S., MOHANTY, A. K., DRZAL, L. T., MISRA, M., PARIJA, S., NAYAK, S. K. & TRIPATHY, S. S. 2003. Studies on mechanical performance of biofibre/glass reinforced polyester hybrid composites. Composites Science and Technology, 63, 1377-1385.

MOGHADDAM, L. 2008. Vibrational spectroscopic investigation of polymer melt processing. PhD PhD, Queensland University of Technology, Australia

MOHANTY, A. K., MISRA, M. & DRZAL, L. T. 2001. Surface modifications of natural fibers and performance of the resulting biocomposites: An overview. Composite Interfaces, 8, 313-343.

MOHANTY, A. K., MISRA, M. & DRZAL, L. T. 2002. Sustainable bio-composites from renewable resources: Opportunities and challenges in the green materials world. Journal of Polymers and the Environment, 10, 19-26.

MOHANTY, S., VERMA, S. K. & NAYAK, S. K. 2006. Dynamic mechanical and thermal properties of MAPE treated jute/HDPE composites. Composites Science and Technology, 66, 538-547.

MONTES, H., MAZEAU, K. & CAVAILLE, J. Y. 1997. Secondary mechanical relaxations in amorphous cellulose. Macromolecules, 30, 6977-6984.

MORLIN, B. & CZIGANY, T. 2012. Cylinder test: Development of a new microbond method. Polymer Testing, 31, 164-170.

MORSHED, M. M., ALAM, M. M. & DANIELS, S. M. 2010. Plasma Treatment of Natural Jute Fibre by RIE 80 plus Plasma Tool. Plasma Science & Technology, 12, 325-329.

MUTJE, P., LOPEZ, A., VALLEJOS, M. E., LOPEZ, J. P. & VILASECA, F. 2007. Full exploitation of Cannabis sativa as reinforcement/filler of thermoplastic composite materials. Composites Part a-Applied Science and Manufacturing, 38, 369-377.

NAGHIPOUR, M., TAHERI, F. & ZOU, G. 2005. Evaluation of Vibration Damping of Glass-Reinforced-Polymer-Reinforced Glulam Composite Beams. Journal of Structural Engineering, 131, 1044-1050.

NIU, P., LIU, B., WEI, X., WANG, X. & YANG, J. 2011. Study on mechanical properties and thermal stability of polypropylene/hemp fiber composites. Journal of Reinforced Plastics and Composites, 30, 36-44.

NYKTER, M., KYMÄLÄINEN, H.-R., THOMSEN, A. B., LILHOLT, H., KOPONEN, H., SJÖBERG, A.-M. & THYGESEN, A. 2008. Effects of thermal and enzymatic treatments and harvesting time on the microbial quality and chemical composition of fibre hemp (Cannabis sativa L.). Biomass and Bioenergy, 32, 392-399.

NYSTROM, B., JOFFE, R. & LANGSTROM, R. 2007. Microstructure and strength of injection molded natural fiber composites. Journal of Reinforced Plastics and Composites, 26, 579-599.

OBATAYA, E., NORIMOTO, M. & TOMITA, B. 2001. Mechanical relaxation processes of wood in the low-temperature range. Journal of Applied Polymer Science, 81, 3338-3347.

PAKZAD, A., PARIKH, N., HEIDEN, P. A. & YASSAR, R. S. 2011. Revealing the 3D internal structure of natural polymer microcomposites using X-ray ultra microtomography. Journal of Microscopy, 243, 77-85.

PANAITESCU, D. M., VULUGA, Z., GHIUREA, M., IORGA, M., NICOLAE, C. & GABOR, R. 2015. Influence of compatibilizing system on morphology, thermal and mechanical properties of high flow polypropylene reinforced with short hemp fibers. Composites Part B: Engineering, 69, 286-295.

PANIGRAHY, B. S., RANA, A., PANIGRAHI, S. & CHANG, P. 2006. OVERVIEW OF FLAX FIBER REINFORCED THERMOPLASTIC COMPOSITES.

PANIGRAHY, J. F., S PANIGRAHI, A TRIPATHY, B RAJAKUMAR, A KAMAL 2006. Flax Fibre Based Composite Profiles For Construction Industries. CSBE/SCGAB. Edmonton, Alberta: American Society of Agricultural and Biological Engineers.

PARK, J.-M., QUANG, S. T., HWANG, B.-S. & DEVRIES, K. L. 2006. Interfacial evaluation of modified Jute and Hemp fibers/polypropylene (PP)-maleic anhydride polypropylene copolymers (PP-MAPP) composites using micromechanical technique and nondestructive acoustic emission. Composites Science and Technology, 66, 2686-2699.

PICKERING, K. L., BECKERMANN, G. W., ALAM, S. N. & FOREMAN, N. J. 2007a. Optimising industrial hemp fibre for composites. Composites Part a-Applied Science and Manufacturing, 38, 461-468.

PICKERING, K. L., LI, Y., FARRELL, R. L. & LAY, M. 2007b. Interfacial modification of hemp fiber reinforced composites using fungal and alkali treatment. Journal of Biobased Materials and Bioenergy, 1, 109-117.

PLACET, V. 2009. Characterization of the thermo-mechanical behaviour of Hemp fibres intended for the manufacturing of high performance composites. Composites Part A: Applied Science and Manufacturing, 40, 1111-1118.

PLACET, V. & FOLTÊTE, E. 2010. Is Dynamic Mechanical Analysis (DMA) a non-resonance technique? EPJ Web of Conferences, 6, 41004.

POLETTO, M., ZATTERA, A. J. & PISTOR, V. 2013. Structural Characteristics and Thermal Properties of Native Cellulose.

POVOLO, F. & GOYANES, S. N. 1996. Amplitude dependent damping in vinyl polymers. Journal De Physique Iv, 6, 579-582.

PRASAD, B. M., SAIN, M. M. & ROY, D. N. 2005. Properties of ball milled thermally treated hemp fibers in an inert atmosphere for potential composite reinforcement. Journal of Materials Science, 40, 4271-4278.

QIU, Y. P. & SCHWARTZ, P. 1991. A NEW METHOD FOR STUDY OF THE FIBER MATRIX INTERFACE IN COMPOSITES - SINGLE FIBER PULL-OUT FROM A MICROCOMPOSITE. Journal of Adhesion Science and Technology, 5, 741-756.

RAABE, D. & HANGEN, U. 1995. Introduction of a modified linear rule of mixtures for the modelling of the yield strength of heavily wire drawn in situ composites. Composites Science and Technology, 55, 57-61.

RACHINI, A., LE TROEDEC, M., PEYRATOUT, C. & SMITH, A. 2009. Comparison of the Thermal Degradation of Natural, Alkali-Treated and Silane-Treated Hemp Fibers Under Air and an Inert Atmosphere. Journal of Applied Polymer Science, 112, 226-234.

RAMIAH, M. V. 1970. Thermogravimetric and differential thermal analysis of cellulose, hemicellulose, and lignin. Journal of Applied Polymer Science, 14, 1323-1337.

RANGARAJ, S. V. & SMITH, L. V. 2000. Effects of moisture on the durability of a wood/thermoplastic composite. Journal of Thermoplastic Composite Materials, 13, 140-161.

REQUENA, G., FIEDLER, G., SEISER, B., DEGISCHER, P., DI MICHIEL, M. & BUSLAPS, T. 2009. 3D-Quantification of the distribution of continuous fibres in unidirectionally reinforced composites. Composites Part a-Applied Science and Manufacturing, 40, 152-163.

REZADOUST, A. M. & ESFANDEH, M. 2005. Study of fiber breakage and length distribution during compounding glass-NBR-Phenolic composites. Polymer-Plastics Technology and Engineering, 44, 63-71.

ROIG, F., DANTRAS, E., DANDURAND, J. & LACABANNE, C. 2011. Influence of hydrogen bonds on glass transition and dielectric relaxations of cellulose. Journal of Physics D-Applied Physics, 44.

ROMANZINI, D., ORNAGHI, H. L., AMICO, S. C. & ZATTERA, A. J. 2012. Influence of fiber hybridization on the dynamic mechanical properties of glass/ramie fiber-reinforced polyester composites. Journal of Reinforced Plastics and Composites, 31, 1652-1661.

ROULSON, D., SAIN, M. & COUTURIER, M. 2006. Resin transfer molding of hemp fiber composites: optimization of the process and mechanical properties of the materials. Composites Science and Technology, 66, 895-906.

ROWEL, R. M., SANADI, A. R., CAULFIELD, D. F. & JACOBSON, R. E. 1997. Utilization of Natural Fibers in Plastic Composites: Problems and Opportunities. Lignocellulosic-Plastics Composites, 23-51.

SAWPAN, M. A., PICKERING, K. L. & FERNYHOUGH, A. 2011. Effect of fibre treatments on interfacial shear strength of hemp fibre reinforced polylactide and unsaturated polyester composites. Composites Part a-Applied Science and Manufacturing, 42, 1189-1196.

SCHINDELIN, J., ARGANDA-CARRERAS, I., FRISE, E., KAYNIG, V., LONGAIR, M., PIETZSCH, T., PREIBISCH, S., RUEDEN, C., SAALFELD, S., SCHMID, B., TINEVEZ, J.-Y., WHITE, D. J., HARTENSTEIN, V., ELICEIRI, K., TOMANCAK, P. & CARDONA, A. 2012. Fiji: an open-source platform for biological-image analysis. Nat Meth, 9, 676-682.

SEDAN, D., PAGNOUX, C., CHOTARD, T., SMITH, A., LEJOLLY, D., GLOAGUEN, V. & KRAUSZ, P. 2007. Effect of calcium rich and alkaline solutions on the chemical behaviour of hemp fibres. Journal of Materials Science, 42, 9336-9342.

SHUBHRA, Q. T. H., ALAM, A. K. M. M., GAFUR, M. A., SHAMSUDDIN, S. M., KHAN, M. A., SAHA, M., SAHA, D., QUAIYYUM, M. A., KHAN, J. A. & ASHADUZZAMAN, M. 2010. Characterization of Plant and Animal Based Natural Fibers Reinforced Polypropylene Composites and Their Comparative Study. Fibers and Polymers, 11, 725-731.

SINHA, E. & PANIGRAHI, S. 2009. Effect of Plasma Treatment on Structure, Wettability of Jute Fiber and Flexural Strength of its Composite. Journal of Composite Materials, 43, 1791-1802.

SONG, M., HOURSTON, D. J. & SCHAFER, F. U. 2001. Correlation between mechanical damping and interphase content in interpenetrating polymer networks. Journal of Applied Polymer Science, 81, 2439-2442.

SONIA, A. & DASAN, K. P. 2013. Chemical, morphology and thermal evaluation of cellulose microfibers obtained from Hibiscus sabdariffa. Carbohydrate Polymers, 92, 668-674.

SPERLING, L. H. 1990. Sound and Vibration Damping with Polymers. Sound and Vibration Damping with Polymers. American Chemical Society.

STARK, N. 2001. Influence of moisture absorption on mechanical properties of wood flour-polypropylene composites. Journal of Thermoplastic Composite Materials, 14, 421-432.

SUN, X., NASU, K., WU, C., LI, L., LIN, D. L. & GEORGE, T. F. 1992. FREQUENCY-DEPENDENCE OF 2-PHOTON RESONANCE AND DAMPING IN POLYMERS. Synthetic Metals, 49, 141-145.

SYMINGTON, M., BANKS, W. M., THOMASON, J. L., PETHRICK, R. A. & DAVID-WEST, O. 2011. KINK BANDS IN FLAX AND HEMP POLYESTER COMPOSITES. 18TH INTERNATIONAL CONFERENCE ON COMPOSITE MATERIALS. Korea.

TAJ, S., MUNAVAR, A. M. & KHAN, S. U. 2007. NATURAL FIBER-REINFORCED POLYMER COMPOSITES. Pakistan Academy of sciences, 44, 129-144.

TAJVIDI, M., MOTIE, N., RASSAM, G., FALK, R. H. & FELTON, C. 2010. Mechanical Performance of Hemp Fiber Polypropylene Composites at Different Operating Temperatures. Journal of Reinforced Plastics and Composites, 29, 664-674.

TAJVIDI, M. & TAKEMURA, A. 2010. Thermal Degradation of Natural Fiber-reinforced Polypropylene Composites. Journal of Thermoplastic Composite Materials, 23, 281-298.

TANAKA, T., UESUGI, K., TAKEUCHI, A., SUZUKI, Y. & IWATA, T. 2007. Analysis of inner structure in high-strength biodegradable fibers by X-ray microtomography using synchrotron radiation. Polymer, 48, 6145-6151.

TASDEMIR, M., BILTEKIN, H. & CANEBA, G. T. 2009. Preparation and Characterization of LDPE and PP-Wood Fiber Composites. Journal of Applied Polymer Science, 112, 3095-3102.

TESSIER, R., LAFRANCHE, E. & KRAWCZAK, P. 2012. Development of novel melt-compounded starch-grafted polypropylene/polypropylene-grafted maleic anhydride/organoclay ternary hybrids. eXPRESS Polymer Letters, 6, 937–952.

THOMAS , S. & POTHAN , L. A. 2009. Natural Fibre Reinforced Polymer Composites:

From Macro to Nanoscale.

THOMASON, J. L. 2002. The influence of fibre length and concentration on the properties of glass fibre reinforced polypropylene: 5. Injection moulded long and short fibre PP. Composites Part a-Applied Science and Manufacturing, 33, 1641-1652.

THOMASON, J. L., VLUG, M. A., SCHIPPER, G. & KRIKOR, H. 1996. Influence of fibre length and concentration on the properties of glass fibre-reinforced polypropylene .3. Strength and strain at failure. Composites Part a-Applied Science and Manufacturing, 27, 1075-1084.

THYGESEN, A., ODDERSHEDE, J., LILHOLT, H., THOMSEN, A. B. & STÅHL, K. 2005. On the determination of crystallinity and cellulose content in plant fibres. Cellulose, 12, 563-576.

THYGESEN, L. G., EDER, M. & BURGERT, I. 2007. Dislocations in single hemp fibres-investigations into the relationship of structural distortions and tensile properties at the cell wall level. Journal of Materials Science, 42, 558-564.

VIGNON, M. R. & GARCIAJALDON, C. 1994. FIBERS FROM UNDER-RETTED HEMP BUNDLES BY STEAM EXPLOSION TREATMENT. Abstracts of Papers of the American Chemical Society, 207, 70-CELL.

VOGT, D. 2010. EIHA: "Targets for bio-based composites and natural fibres" in the EU. [Online]. Available: http://www.eiha.org/attach/569/10-11-25_LMI_Bio-Composites_EIHA_PM.pdf.

WAMBUA, P., IVENS, J. & VERPOEST, I. 2003. Natural fibres: can they replace glass in fibre reinforced plastics? Composites Science and Technology, 63, 1259-1264.

WANG, W., SAIN, M. & COOPER, P. A. 2006. Study of moisture absorption in natural fiber plastic composites. Composites Science and Technology, 66, 379-386.

WANG, Z., LI, L. & GONG, M. 2012. Measurement of dynamic modulus of elasticity and damping ratio of wood-based composites using the cantilever beam vibration technique. Construction and Building Materials, 28, 831-834.

X LI, L G TABIL, S PANIGRAHI & CRERAR, W. J. 2006. The Influence of Fiber Content on Properties of Injection Molded Flax Fiber-HDPE Biocomposites. ASAE Annual Meeting.

YAMAMOTO, S. & MATSUOKA, T. 1995. DYNAMIC SIMULATION OF FLOW-INDUCED FIBER FRACTURE. Polymer Engineering and Science, 35, 1022-1030.

YAN, L., CHOUW, N. & YUAN, X. 2012. Improving the mechanical properties of natural fibre fabric reinforced epoxy composites by alkali treatment. Journal of Reinforced Plastics and Composites, 31, 425-437.

YAN, L. B. 2012. Effect of alkali treatment on vibration characteristics and mechanical properties of natural fabric reinforced composites. Journal of Reinforced Plastics and Composites, 31, 887-896.

YAN, Z. L., ZHANG, J. C., ZHANG, H. & WANG, H. 2013. Improvement of Mechanical Properties of Noil Hemp Fiber Reinforced Polypropylene Composites by Resin Modification and Fiber Treatment. Advances in Materials Science and Engineering.

YANG, H., YAN, R., CHEN, H., LEE, D. H. & ZHENG, C. 2007. Characteristics of hemicellulose, cellulose and lignin pyrolysis. Fuel, 86, 1781-1788.

YU, W. D., POSTLE, R. & YAN, H. J. 2003. Characterization of the weak link of wool fibers. Journal of Applied Polymer Science, 90, 1206-1212.

ZHANDAROV, S. & MÄDER, E. 2005. Characterization of fiber/matrix interface strength: applicability of different tests, approaches and parameters. Composites Science and Technology, 65, 149-160.

ZHOU, X., YU, Y., LIN, Q. & CHEN, L. 2013. Effects of Maleic Anhydride-Grafted Polypropylene (MAPP) on the Physico-Mechanical Properties and Rheological Behavior of Bamboo Powder-Polypropylene Foamed Composites.

Appendix 1- **Summary of mechanical Properties of the Composites**

Summary of Tensile Properties of the Composites

Fibre Type	Original Fibre Length (mm)	Fibre Treatment	Fibre Content (wt%)	Matrix Type	Coupling Agent type	Agent Content (wt%)	Composite Fabrication Method	Tensile Strength (MPa)	T.S. STD. DEV. (MPa)	Young's Modulus (GPa)	Y.M STD. DEV. (GPa)
noil hemp	20-30	-	10	PP1	-	-	M1	26.7	0.7	1.6	0.1
noil hemp	20-31	-	20	PP1	-	-	M1	28.9	0.9	2.3	0.2
noil hemp	20-32	-	30	PP1	-	-	M1	28.0	1.5	2.8	0.2
noil hemp	20-33	-	40	PP1	-	-	M1	28.1	0.6	3.6	0.2
noil hemp	20-34	-	50	PP1	-	-	M1	29.3	2.4	4.4	0.2
noil hemp	20-35	-	60	PP1	-	-	M1	24.8	4.0	3.6	0.4
noil hemp	20-36	-	30	PP1	MAPP	2.5	M1	39.7	2.0	4.0	0.2
noil hemp	20-37	-	30	PP1	MAPP	5.0	M1	39.3	2.3	3.3	0.2
noil hemp	20-38	-	40	PP1	MAPP	2.5	M1	36.5	3.0	3.0	0.2
noil hemp	20-39	-	40	PP1	MAPP	5.0	M1	40.8	3.3	4.3	0.2
noil hemp	20-40	-	30	PP1	MAPOE	2.5	M1	34.5	0.8	3.2	0.4
noil hemp	20-41	-	30	PP1	MAPOE	5.0	M1	39.0	1.8	3.0	0.1
noil hemp	20-42	-	40	PP1	MAPOE	2.5	M1	35.6	3.5	3.2	0.3
noil hemp	20-43	-	40	PP1	MAPOE	5.0	M1	37.0	0.9	2.7	0.1
Normal hemp	0.2	-	40	PP2	MAPP	5.0	M2	32.9	0.7	3.6	0.3
Normal hemp	0.5	-	40	PP2	MAPP	5.0	M2	31.8	2.0	3.3	0.29
Normal hemp	1	-	40	PP2	MAPP	5.0	M2	27.9	2.8	3.0	0.1
Normal hemp	2	-	40	PP2	MAPP	5.0	M2	31.2	2.5	3.3	0.3
Normal hemp	0.2	5 wt% Alkali	40	PP2	MAPP	5.0	M2	33.6	1.4	3.8	0.3
Normal hemp	0.5	5 wt% Alkali	40	PP2	MAPP	5.0	M2	32.9	0.4	3.4	0.7
Normal hemp	1	5 wt% Alkali	40	PP2	MAPP	5.0	M2	31.5	2.2	3.6	0.9
Normal hemp	2	5 wt% Alkali	40	PP2	MAPP	5.0	M2	29.6	1.8	3.0	0.5

Summary of Flexural Properties of the Composites

Fibre Type	Original Fibre Length (mm)	Fibre Treatment	Fibre Content (wt%)	Matrix Type	Coupling Agent type	Coupling Agent Content (wt%)	Composite Fabrication Method	Flexural Strength (MPa)	F.S. STD. DEV. (MPa)	Flexural Modulus (GPa)	F.M STD. DEV. (GPa)	Strain at break (%)	Strain STD. DEV. (GPa)
Normal hemp	0.2	-	40	PP2	MAPP	5.0	M2	55.7	1.0	3.3	0.1	6.4	0.3
Normal hemp	0.5	-	40	PP2	MAPP	5.0	M2	53.3	4.1	3.0	0.1	7.9	0.9
Normal hemp	1	-	40	PP2	MAPP	5.0	M2	44.1	4.0	2.8	0.4	6.5	1.3
Normal hemp	2	-	40	PP2	MAPP	5.0	M2	39.9	6.8	2.1	0.4	6.5	1.3
Normal hemp	0.2	5 wt% Alkali	40	PP2	MAPP	5.0	M2	51.2	4.2	3.1	0.2	5.2	0.2
Normal hemp	0.5	5 wt% Alkali	40	PP2	MAPP	5.0	M2	51.2	5.0	3.1	0.1	7.0	0.8
Normal hemp	1	5 wt% Alkali	40	PP2	MAPP	5.0	M2	39.6	1.0	2.0	0.2	6.1	0.4
Normal hemp	2	5 wt% Alkali	40	PP2	MAPP	5.0	M2	40.3	4.0	2.3	0.3	6.7	1.0

Summary of Impact Properties of the Composites

Fibre Type	Original Fibre Length (mm)	Fibre Treatment	Fibre Content (wt%)	Matrix Type	Coupling Agent type	Coupling Agent Content (wt%)	Composite Fabrication Method	Impact Force (N)	Impact Force STD. DEV. (N)	Max. Impact Energy (J)	Impact Energy STD. DEV. (J)	Damage Degree	Damage Degree STD. DEV.
Normal hemp	0.2	-	40	PP2	MAPP	5	M2	191.7	8.6	2.99	0.22	0.86	0.01
Normal hemp	0.5	-	40	PP2	MAPP	5	M2	177.24	3.16	2.8	0.17	0.87	0.01
Normal hemp	1	-	40	PP2	MAPP	5	M2	164.4	2.31	2.64	0.25	0.88	0.02
Normal hemp	2	-	40	PP2	MAPP	5	M2	150	5.65	2.45	0.63	0.94	0.01
Normal hemp	0.2	5 wt% Alkali	40	PP2	MAPP	5	M2	175.5	2.71	2.71	0.01	0.83	0.01
Normal hemp	0.5	5 wt% Alkali	40	PP2	MAPP	5	M2	173.3	2.64	2.64	0.08	0.85	0.01
Normal hemp	1	5 wt% Alkali	40	PP2	MAPP	5	M2	173.6	2.75	2.75	0.13	0.86	0.01
Normal hemp	2	5 wt% Alkali	40	PP2	MAPP	5	M2	159.65	2.38	2.38	0.06	0.86	0.02

Appendix 2- Datasheets of the polypropylene used

Moplen EP203N

Polypropylene, Impact Copolymer

Product Description

Basell Australias polypropylene grade EP203N is a medium/high flow impact copolymer with a modified molecular weight distribution and is formulated with a general-purpose additive package. EP203N is designed for injection moulding applications requiring excellent mould filling properties, good stiffness, outstanding impact strength and exceptional impact strength retention at low temperatures. End use products typically made from EP203N include crates, pails, pail lids, other industrial mouldings, domestic appliances and closures.

Product Characteristics

Status	Commercial: Active ISO
Test Method used Availability	Asia-Pacific, Australia/NZ
Features	Copolymer, Impact, Flow, High, Food Contact Acceptable, Impact Resistance, High, Impact Resistance, Low Temp., Moldability, Good, Stiffness, Good
Typical Customer Applications	Appliances, Crates, Caps & Closures, Other Industrial

Typical Properties	Method	Value	Unit
Physical			
Density (Method D)	ISO 1183	0.90	g/cm³
Melt flow rate (MFR) (230°C/2.16Kg)	ISO 1133	11	g/10 min
Mechanical			
Tensile Stress at Yield	ISO 527-1, -2	20.0	MPa
Flexural modulus	ISO 178	800	MPa
Impact			
Notched izod impact strength	ISO 180		
(-20 °C, Type 1, Notch A)		4.0	
(23 °C, Type 1, Notch A)		10	kJ/m² kJ/m²
(0 °C, Type 1, Notch A)		5.0	kJ/m²

Hardness		
Shore hardness (Shore D)	ISO 868	62

Thermal		
Heat deflection temperature B (0.45 MPa) Unannealed	ISO 75B-1, -2	65 °C
Heat deflection temperature A (1.80 MPa) Unannealed	ISO 75A-1, -2	50 °C
Vicat softening temperature (Method A)	ISO 306	140 °C

Notes

Typical properties; not to be construed as specifications.

Additional Properties

Falling Weight Impact Strength @-55°C, BS2782-306b: 11 J Suitable for the production of articles for food contact use. As supplied in natural form, meets the requirements of Australian Standard 2070 - 1999, “Plastics Materials for Food Contact Use“. The base polymer complies with the United States of America Food and Drug Administration (FDA) Code of Federal Regulations 21 CFR177.1520 (a)(3)(i) and (c)3.1a for conditions of use C through to H in CFR 176.170(c), table 2. All other components used in the formulation meet the relevant FDA requirements for use in food contact applications. Conformity with these requirements should not be assumed for other variants and should be investigated with the appropriate supply source.

Release Date: 28 Sep 2007

Sanren M800E

Polypropylene Random Copolymer

SINOPECShanghaiPetrochemicalCo.Ltd.

TechnicalData

General			
Material Status	• Commercial: Active		
Search for UL Yellow Card	• SINOPEC Shanghai Petrochemical Co. Ltd.		
Availability	• Asia Pacific		
Features	• Food Contact Acceptable • High Gloss • High Heat Resistance	• High Rigidity • High Strength • Low to No Odor	• Random Copolymer
Uses	• Food Packaging	• Insulation	• Thin-walled Packaging
Forms	• Pellets		
Processing Method	• Injection Molding		

Physical	Nominal ValueUnit	Test Method
Melt Mass-Flow Rate (MFR) (230°C/2.16 kg)	8.0g/10 min	ASTM D1238
Mechanical	**Nominal ValueUnit**	**Test Method**
Tensile Strength (Yield)	25.0MPa	ASTM D638
Flexural Modulus	850MPa	ASTM D790
Impact	**Nominal ValueUnit**	**Test Method**
Notched Izod Impact (23°C)	25J/m	ASTM D256
Optical	**Nominal ValueUnit**	**Test Method**
Yellowness Index	3.0YI	ASTM D1925

Additional Information
Cleanliness, GB 12670: <=11-20 piece/kg

Notes

[1] Typical properties: these are not to be construed as specifications.